THE ANALYSIS AND COMPUTER CONTROL OF AN INDUCTION MOTOR

CONTENTS

UNIVERSITY OF SOUTHAMPTON

ABSTRACT

FACULTY OF ENGINEERING AND APPLIED SCIENCE
ELECTRICAL ENGINEERING

Master of Philosophy

THE ANALYSIS AND COMPUTER CONTROL OF AN INDUCTION MOTOR

by Christopher Graham Bright

This thesis discusses popular electric drives and lays particular emphasis upon variable-speed induction motor drives. It continues by describing the construction of a variable speed induction motor drive which uses a variable-voltage-variable frequency supply derived from linear amplifiers to power the induction motor. A mathematical model of the drive is developed and experimental tests used to check the validity of the model are described.

This thesis also describes a control system used to produce speed control over a limited range of speeds and compares experimental tests on the control system with computer simulations.

ACKNOWLEDGEMENTS

The author would like to thank the University of Southampton, and in particular the Department of Electrical Engineering for providing facilities for this research and would also like to thank the Science and Engineering Research Council for their financial support.

The author is grateful for the help, advice and assistance given by Dr. D. J. Brown during his supervision of this research and during the preparation of this thesis. The author is also grateful for the assistance given by Mr D. Levitt, Mr M. Barkhoarder and Mr R. Christie at various stages of the research. The author would also like to thank Dr Huda (formerly with the Department of Mathematics, University of Southampton) for his help with the mathematical analysis of the induction motor drive described in this thesis.

The author would also like to record his thanks to his present employers, the South Western Electricity Board (S.W.E.B.) for their loan of a BBC micro-computer on which to develop many of the computer programs used in this research. In particular the author would like to thank Mr P. Morgan, Mr B. M. Riley and the staff of the Avonbank control room of S.W.E.B. for arranging such a loan. The author is grateful to Mr C. T. Marshall of S.W.E.B. for his assistance with aspects of the computer programming and is also grateful to Mr P. A. Hulbert, also of S.W.E.B., for his help in proof-reading the text of this thesis.

Finally, the author would like to express his gratitude to his parents, relatives, friends and colleagues at the University of Southampton and also at S.W.E.B. who encouraged him to persevere with this thesis and, "after you have done everything, to stand" (Ephesians 6:13).

LIST OF SYMBOLS

$\underline{A}$ the square matrix equal to $\underline{L}^{-1}\,\underline{R}$.

a(k,l) an element of matrix $\underline{A}$ (where $k_1l = 1,2,3,4$).

$\underline{B}$ the square matrix equal to $\underline{L}^{-1}G$.

b(k,l) an element of matrix $\underline{B}$ (where k, l = 1,2,3,4).

$\underline{C}$ the square matrix equal to $\underline{L}^{-1}$.

c(k,l) an element of matrix $\underline{C}$ (where k,l = 1,2,3,4).

cos power factor.

E_{AG} the E.M.F. generated in the armature of a D.C. generator.

E_m the back E.M.F. of a D.C. generator acting as a motor.

E_t the modified phase voltage of a supply to an induction motor.

E_x the excitation of a D.C. generator.

E'_x the excitation of a D.C. generator acting as a motor.

F_f the form factor of an A.C. waveform.

$f_1, f_2, f_3, f_4, f_5, f_6$ the functions which relate $\dot{x}_1, \dot{x}_2, \dot{x}_3, \dot{x}_4, \dot{x}_5, \dot{x}_6$ respectively to the state variables $x_1, x_2, x_3, x_4, x_5, x_6$.

$\underline{f}$ the function matrix containing f_1 to f_6.

$\underline{G}$ the matrix describing the effects of rotation in Kron's primitive machine.

h the step-length used in the Kutta Merson algorithm.

I_{AG} the armature current of a D.C. generator.

I_{AM} the maximum value of the armature current of a D.C. generator (load variation test).

I_1 the r.m.s. stator winding phase current of an induction motor.

I_2 the r.m.s. rotor winding phase current of an induction motor.

$\underline{I}$ the column matrix describing the current in Kron's primitive machine.

i_f, i_d, i_q, i_g the instantaneous currents in coils F, D, Q and G respectively, of Kron's primitive machine.

i_R, i_Y, i_B the instantaneous currents in the red, yellow and blue phases, respectively, of a three-phase winding.

i_z the zero-sequence current.

J the polar moment of inertia of the motor-generator set.

K_{AG} the armature constant of a D.C. machine.

K_1, K_2, K_3, K_4, K_5 the coefficients of the 5th order Kutta-Merson algorithm.

k_{ff} the fluid friction torque constant.

k_{MAG} the magnetic loss factor of a D.C. machine.

k_x the constant describing the change in magnetic loss factor with excitation.

L_{AG} the self-inductance of the armature of a D.C. generator.

L_{ff}, L_d, L_q, L_{gg} the self inductances of coils F, D, Q and G respectively, of Kron's primitive machine.

L_{df} the mutual inductance between coils D and F of Kron's primitive machine.

L_{qg} the mutual inductance between coils Q and G of Kron's primitive machine.

L_{rf}, L_{rd}, L_{rq}, L_{rg} the constants which descirbe voltages induced in Kron's primitive machine due to rotation.

$\underline{L}$ the matrix describing inductances of elements in Kron's primitive machine.

M the mutual inductance between rotor and stator coils of the same phase in an induction motor.

m the number of phases of an induction motor.

N_e the number of pulses produced by a shaft encoder per revolution.

N_F the frequency number (describing the frequency of the supply to an induction motor).

N_s the speed number.

N_{ST} the target speed number.

n_p the number of pole-pairs in an induction motor.

P_{e3} the power flow from the supply to an induction motor.

P_d the mechanical power developed in coil D of Kron's primitive machine.

P_k the mechanical power developed in the rotor of Kron's primitive machine.

P_{MAG} the magnetic power losses in a D.C. machine.

P_{MG} the mechanical power developed in the armature of a D.C. generator acting as a motor.

P_q the mechanical power developed in coil Q of Kron's primitive machine.

p the differential operator.

q the index describing the variation of the magnetic loss factor with excitation of a D.C. machine.

R_{AG} the resistance of the armature of a D.C. generator.

R_f, R_d, R_q, R_g the resistance of coils, F, D, Q and G of Kron's primitive machine.

R_{LG} the load resistance connected to the output of a D.C. generator.

R_m the resistance representing magnetising losses in an induction motor.

R_t the modified per-phase resistance of the stator winding of an induction motor.

R_1 the per-phase stator winding resistance of an induction motor.

R_2 the per-phase rotor winding resistance of an induction motor.

$\underline{R}$ the matrix describing the resistances of elements in Kron's primitive machine.

r_{mg} the resistance representing the magnetic losses caused by A.C. in the armature of a D.C. generator.

s the slip of an induction motor.

T the gross torque developed by an induction motor.

T_{AG} the torque extended by a D.C. generator due to electromechanical energy conversion in the armature winding.

T_b the bearing and brush friction torque.

T_{bd} the dynamic bearing and brush friction torque.

T_E the gross torque developed by an induction motor at speed ω_E.

T_{E1} the gross torque developed by an induction motor at speed ω_{E1}.

T_{ff} the fluid friction torque.

T_J the torque exerted by the inertia of the motor-generator set during a change in speed.

T_K the torque developed in the rotor of Kron's primitive machine.

T_L the torque exerted on the induction motor by elements of the motor-generator set.

T_{MAG} The torque exerted by the magnetic losses in a D.C. machine.

T_{mm} the maximum gross torque developed by an induction motor during motoring.

T_{mg} the maximum gross torque absorbed by an induction motor acting as an induction generator.

T_s the starting torque of an induction motor.

T_2 the torque output of a two-pole induction motor.

$T(N_F, N_{ST})$ the torque developed by the induction motor when operating at as speed corresponding to N_{ST} and from a 240v supply whose frequency corresponds to N_F.

$T_i (N_F, N_{ST})$ the equivalent integer to $T(N_F, N_{ST})$.

t time.

t' the simulation time at which the speed of the motor - generator set equals the average value of speed during the simulation of a load variation test.

t_c the simulation time during the simulation of a load variation test at which the inequality $\omega_{rb} \leq \omega_{AV} \leq \omega_{ra}$ applies.

t_{GD} the time taken for the motor-generator set to come to rest after the disconnection of all supplies.

t_i the simulation time reached at the end of the first part of the simulation of a load variation test.

t_m the counting period of the speed-measuring circuit.

t_n the simulation time during the n^{th} iteration in a computer simulation.

$\underline{U}$ the column matrix describing the voltages across the windings of Kron's primitive machine.

u_f, u_d, u_q, u_g the instantaneous voltages across coils F,D,Q and G respectively of Kron's primitive machine.

V the r.m.s. phase voltage of a supply to an induction motor.

V_{AC} the r.m.s. voltage of an A.C. waveform produced by a Class B amplifier.

V_{AG} the voltage at the armature terminals of a D.C. generator.

V_{AM} the voltage supplied to the armature of a D.C. generator acting as a motor.

V_{DC} the magnitude of the voltage of each supply rail of a Class B amplifier with respect to earth.

v_R, v_Y, v_B The instantaneous voltages across the red, yellow and blue phases, respectively, of a three-phase winding.

v_z the zero sequence voltage.

X_m the per-phase magnetising reactance of an induction motor.

X_t the modified per-phase stator winding leakage reactance.

X_1 the per-phase stator winding leakage reactance of an induction motor.

X_2 the per-phase rotor winding leakage reactance of an induction motor.

x_1, x_2, x_3, x_4 the state space variables representing, respectively, the currents in coils F,D,Q and G of Kron's primitive machine.

x_5 the state-space variable representing the rotor speed of Kron's primitive machine.

x_6 the state-space variable representing the armature current of the D.C. generator.

$\underline{x}$ the column matrix containing the above state-space variables.

$|x_1|_1$ the absolute value of x, calculated during the previous step of an iteration in a computer simulation.

$|x_1|_2$ the absolute value of x, calculated two steps before the present step of an iteration in a computer simulation.

$\underline{x}_o$ matrix $\underline{x}$ at time t = 0.

$\underline{x}_n$ matrix $\underline{x}$ at time $t = t_n$.

$\underline{x}_{n+1}$ matrix $\underline{x}$ at time $t = t_{n+1}$.

$\underline{Z}$ the matrix describing the impedances of various elements in Kron's primitive machine.

α frequency change phase angle or point-of wave of phase angle, depending on the stage reached in the computer simulation of a deceleration test.

α_i point-of-wave phase angle used in the first part of the computer simulation of a deceleration test.

α_l frequency change phase angle (deceleration test).

α_p point-of-wave phase angle (acceleration test).

γ magnetic loss index.

Φ magnetic flux in an induction motor.

Φ_G magnetic flux in a D.C. generator.

ϕ_e error in determining the phase shift between changes in speed and changes in D.C. generator armature current (load variation test).

ϕ_s the phase shift between changes in speed and changes in D.C. generator armature current (load variation test).

η_B the efficiency of Class B amplification.

the supply frequency.

ω_{AM} the frequency of the changes in armature current of a D.C. generator.

ω_{AV} the average speed of the motor-generator set during a load variation test.

ω_E the estimated steady-state speed of an induction motor.

ω_{E1} a better estimate of the steady-state speed of an induction motor.

ω_{GD} the speed of the motor-generator set just before all supplies were turned off.

ω_{max} the maximum value of ω_r during a load variation test.

ω_{min} the minimum value of ω_r during a load variation test.

ω_{mg} the speed at which an induction motor acting as a generator absorbs maximum gross torque.

ω_{mm} the speed at which an induction motor develops maximum gross torque.

ω_r the rotor speed of an induction motor (also used to represent the speed of the motor-generator set since the induction motor is directly coupled to the D.C. generator).

ω_r' the rotor speed of Kron's primitive machine.

ω_{ra} the value of ω_r calculated at the end of the present iteration in the simulation of a load variation test.

ω_{rb} the value of ω_r calculated at the end of the previous iteration in the simulation of a load variation test.

ω_{rc} target speed (closed-loop control test).

ω_{ss} the steady-state speed of an induction motor.

ω_o the synchronous speed of an A.C. motor.

ω_1 supply frequency used at the start of a closed-loop control test

ω_2 estimated supply frequency needed for the induction motor to run at the target speed whilst delivering the same torque as was delivered when operating from a supply of frequency ω_1 (closed-loop control test).

LIST OF ABBREVIATIONS

C.T.	Current transformer
G.T.O.	Gate turn-off
M.C.B.	Miniature circuit breaker
P.L.L.	Phase-locked loop
P.W.M.	Pulse-width modulated
Q.S.W.	Quasi-square wave
S.C.R.	Silicon controlled-rectifier
V.V.V.F.	Variable-voltage variable-frequency

LIST OF FIGURES

INTRODUCTION

The need for electric drives

Industry has often needed a reliable source of mechanical power. Historically, steam and water power have met this need but speed control has been coarse and crude and the transmission of mechanical power has been difficult.

The advent of reliable and cheap supplies of electricity during the late nineteenth and early twentieth centuries led to the development of electric motor drives. Electricity could be distributed around a factory far more easily than mechanical power and speed control of electric drives proved easier and more accurate than speed control of steam or water power.

Electric drives are not confined to factories, indeed they are extensively used in homes shops or offices where steam or water power is unavailable or inappropriate. Railways also use electric drives for traction and Kielgas and Nill [1] report that the advantages of electric traction has prompted research into new types of electric locomotive. Electric traction is also being used for road vehicles and Wakefield [2] points to the increasing competitiveness of electric traction against the internal combustion engine. Electric drives have become so widespread that it is estimated by Holmes [3] that induction motors alone consume about 30% of the electricity generated in the U.K.

The advantages of variable speed drives are:-

1) Many industrial processes need variable speed drives
2) Ease of starting of large drives. The acceleration of machinery from rest needs large forces to overcome friction and inertia and so the drives draw a high current from the mains during starting. The large forces result in stress and wear and the high currents can cause dips in the supply voltage. Shilston [4] reports how the use of variable speed drives overcomes this problem.
3) Savings in energy: Some industrial processes, like pumping and compressing use a constant speed drive with throttling to control the flow rate. The throttling wastes energy and the use of a variable speed drive instead can save energy and therefore be more economic.

Background to the research described in this thesis

The past fifteen years have seen a remarkable growth in the variety and use of variable speed drives due to the following factors:

1) The fall in cost of power electronics used to supply power to the motor.
2) The development of power electronics with faster switching times.
3) The increase in sophistication and fall in cost of electronic control circuitry in particular, and the advent of microprocessors and microcomputers.
4) The rising cost of energy which makes the energy saving feature of variable speed drives attractive.

Many industrial drives use cage rotor induction motors because they are of simple construction and therefore cheap and robust. They also self-start and are capable of good efficiency and power factor. Say [5] states that large induction motors, when fully loaded, can be over 80% efficient and operate at power factors typically between 0.8 and 0.9. An advantage of cage rotor induction motors is the absence of slip rings or commutators which wear and therefore need maintenance, and spark, creating a fire hazard unless flameproof construction is used. The advantages of cage rotor induction motors has led to their widespread use. Say [5] estimates that 80% of the world's A.C. motor drives (apart from fractional-kilowatt machines) are cage rotor induction motors (henceforth referred to as cage induction motors).

One important feature of the cage induction motor is that its speed depends upon the supply frequency and the motor runs at almost constant speed. Although this feature may be useful for certain applications it makes the speed control of induction motors difficult. Nevertheless, much effort has been spent in developing a variable speed drive using a cage induction motor in order to combine the advantages of such a motor with the advantages of a variable speed drive. However, a cheap, reliable and accurate variable speed cage induction motor drive capable of four-quadrant operation (full motoring and generating in either direction) over a wide range of speeds has yet to be developed.

Objective of this research

The objective of this research was to develop a cage induction motor drive capable of four-quadrant operation over a wide range of speed under the control of a small dedicated computer.

CHAPTER 1 A REVIEW OF POPULAR ELECTRIC DRIVES

1.1. Introduction

There are many varieties of electric drives used in industry. This Chapter reviews some of the more popular electric drives, D.C. and A.C., that are used in industry.

1.2. D.C. motor drives

1.2.1 Basic principles of D.C. motors

The books written by Fitzgerald and Kingsley [6], Steven [7] and Cotton [8] describe in detail the construction and operation of D.C. motors. Strictly speaking such devices are more accurately termed "D.C. machines" as they can generate when supplied with mechanical power.

Basically, a D.C. motor has an armature with current-carrying conductors in a magnetic field produced by D.C. in a field winding. These conductors experience a force due to the magnetic field and the armature rotates. The armature conductors are connected to a commutator which has two functions. Firstly, it maintains electrical contact between the D.C. supply and the moving armature. Secondly, it acts as a mechanical switch keeping the armature currents flowing in the correct directions necessary for continuous rotation.

The performance of the D.C. motor is affected markedly by different connections of the armature and field winding. These are described briefly below:

1.2.2 The separately - excited D.C. motor

As its name implies, the supplies to the armature and field windings are separate, as shown in Figure 1.1a. Steven [7] shows that for given armature and field supply voltages the torque-speed characteristic is of the form sketched in figure 1.1b. and shows the motor to be an almost constant-speed machine showing a small decrease in speed with load. Steven [7] also shows that raising the armature supply voltage or decreasing the field supply voltage increases the speed. Such changes in voltage are often achieved using resistances connected in series with the appropriate supplies, as shown in Figure 1.1a.

Figure 1.1: The Separately-Excited D.C. Motor.

a) Electrical Connections

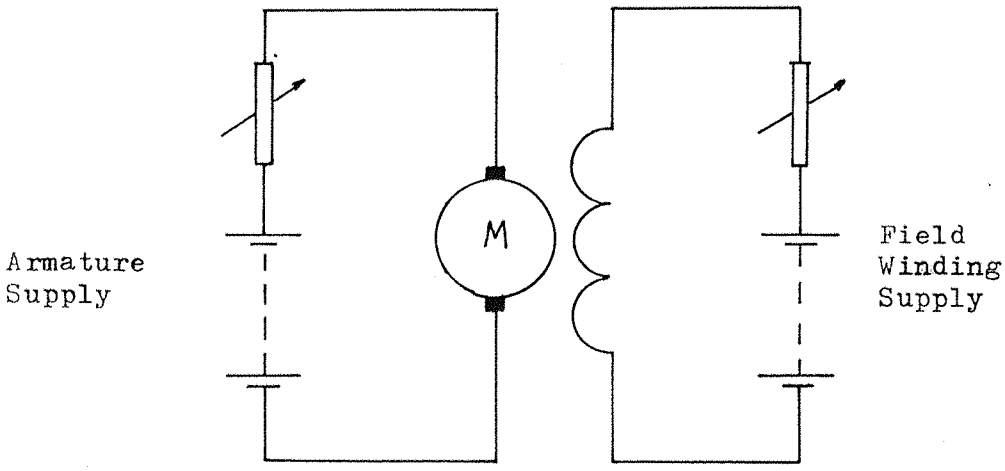

b) Torque-Speed Characteristic.

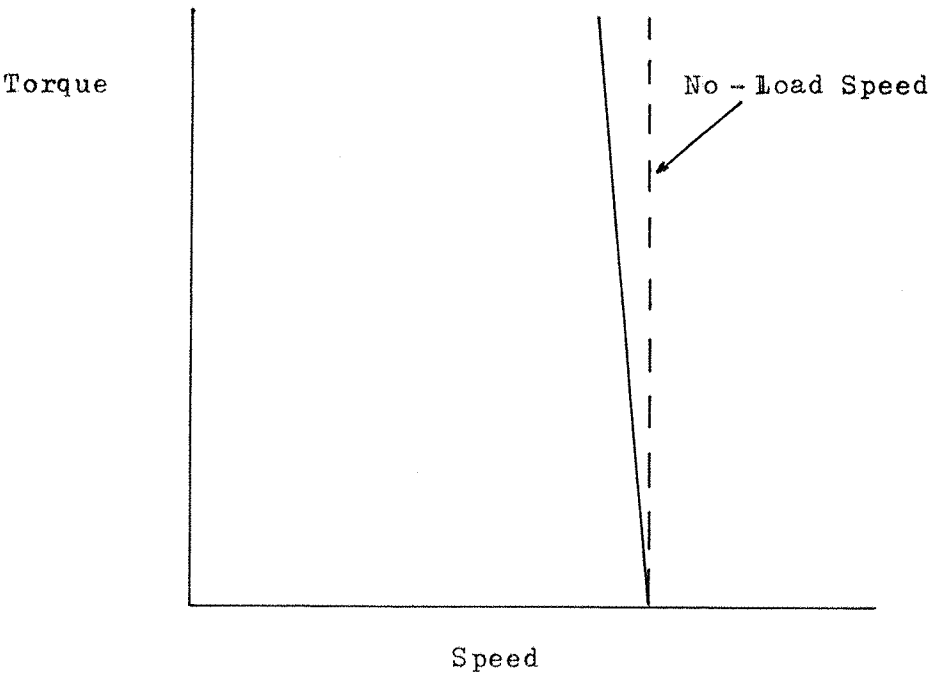

1.2.3 The shunt-wound D.C. motor

The shunt-wound D.C. motor has the field winding connected in parallel with the armature winding and therefore both field and armature windings have the same supply voltage. This motor may therefore be considered as a special case of the separately-excited motor in which both field and armature voltages are the same. Consequently the performance of both machines is similar and similar speed control may be achieved by using a resistance in series with the armature winding and a resistance in series with the field winding.

1.2.4 The series-wound D.C. motor

Figure 1.2 shows the connections and torque-speed characterisitic of this motor. The field and armature windings are connected in series and Steven [7] shows that the torque is approximately inversely proportional to the square of the speed. The torque is large at low speeds, explaining its popularity as a drive for electric traction where swift acceleration is needed. However, the motor can overspeed dangerously at light loads.

1.2.5 Reversal of direction of rotation of a D.C. motor

The direction of rotation of a D.C. machine of any type described previously may be achieved by reversing the connections to the field winding or the armature winding but not both. Reversal of the connections of both windings results in no change of direction or rotation.

1.2.6 The Ward-Leonard Control System

Such systems are described in detail by Fitzgerald and Kingsley [6] and Cotton [8] and figure 1.3 illustrates the general principle of their operation. A D.C. generator driven at constant speed by a motor supplies the armature of a D.C. motor. The D.C. motor has a constant field current and so altering the excitation of the generator alters its output voltage and therefore changes the speed of the D.C. motor. In effect the D.C. motor operates as a separately-excited motor with a variable armature supply voltage.

Closed loop speed control is possible using a D.C. tacho-generator to measure the speed of the D.C. motor and an amplifier to compare the output of the D.C. tacho-generator with a reference voltage and adjust the excitation of the D.C. generator accordingly. The amplifier adjusts the excitation to reduce the error between the tacho-generator and reference voltages, speed

Figure 1.2: The D.C. Series Motor.

a) Electrical Connections:

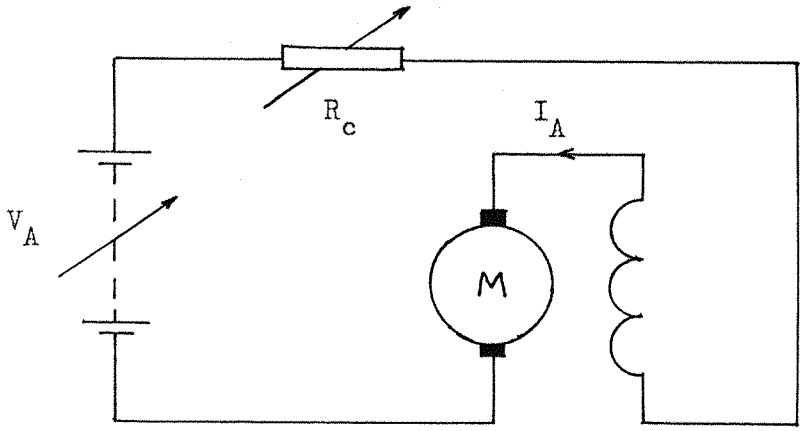

b) Torque-speed Characteristic.

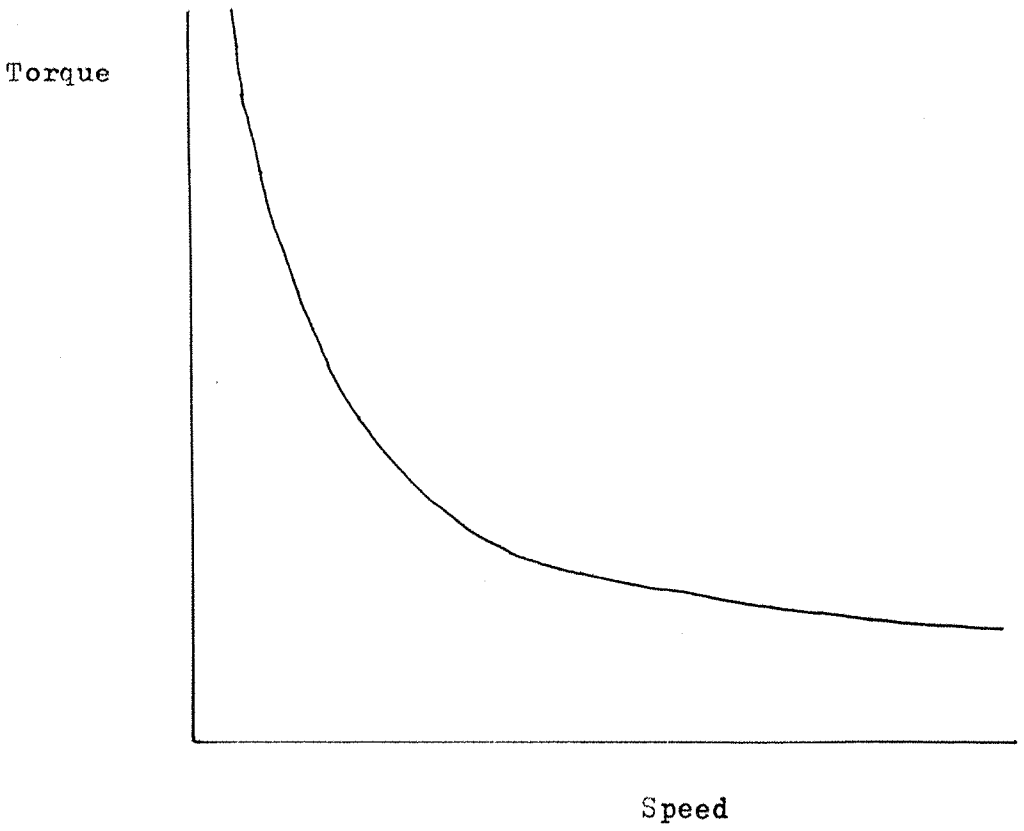

Figure 1.3: Ward-Leonard Control System.

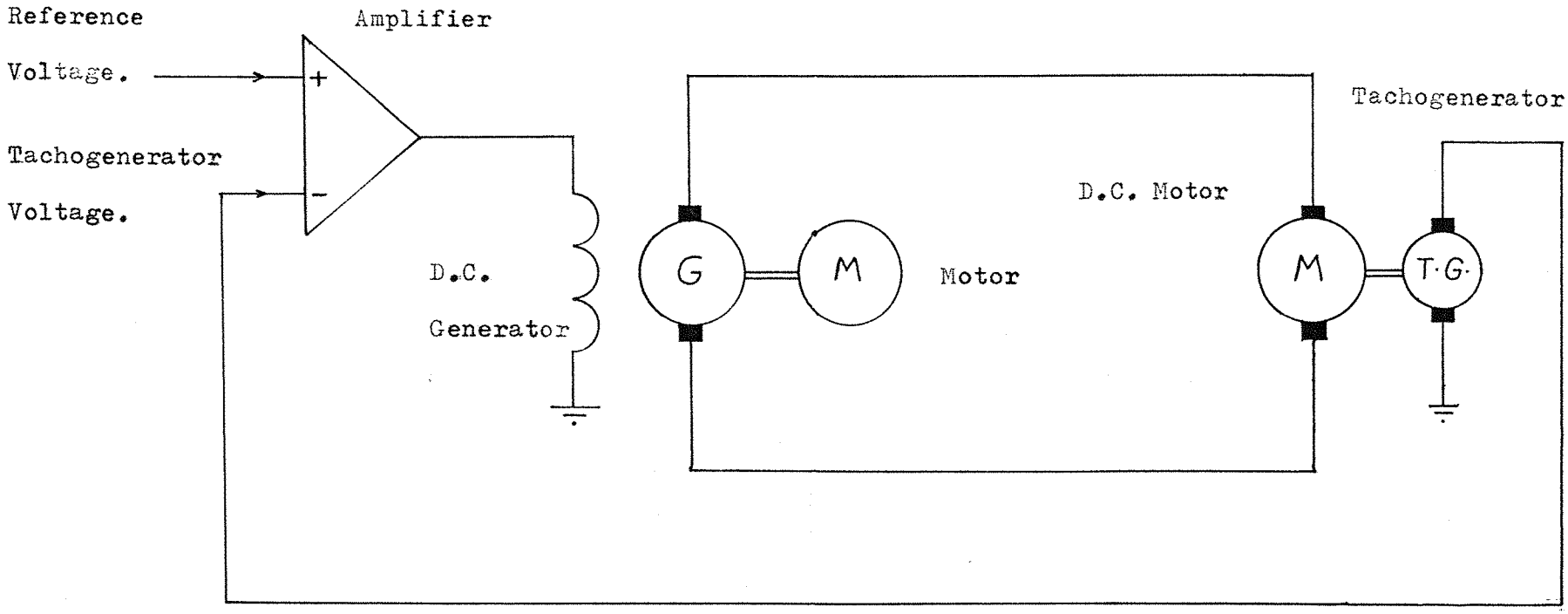

control being achieved by altering the reference voltage. Reversing the reference voltage achieves reversal of direction of rotation.

Historically, the amplifier has been a magnetic amplifier using rotating machines but the advent of power semiconductors has allowed more modern schemes to use electronic amplifiers.

The Ward Leonard control system is capable of fine speed control and has been used to drive rolling mills and lifts.

1.2.7 The suitability of D.C. motor drives

As stated previously, D.C. motors can operate in either forward or reverse and can also act as generators in either direction. They are therefore capable of four quadrant operation, and good speed control over a wide range of speeds is possible.

Recent advances in power semiconductor technology has allowed the construction of convertors of large capacity which can convert A.C. power to D.C. power and vice-versa. Such convertors are well able to drive D.C. motors and the bi-directional nature of the power flow in the convertor, together with its ability to change polarity of the D.C. supply to the motor produces an effective D.C. motor drive capable of four quadrant control. Joos and Barton [9] discuss some of the aspects of design of such drives and note how the drives are supplanting the Ward-Leonard drive.

The chief disadvantages of the D.C. motor lie with the commutator which wears and therefore needs frequent maintenance. Sparking at the commutator also poses a fire hazard hindering the use of D.C. motors in environments with explosive gases unless such motors are of flameproof construction.

1.3 A.C. motor drives

1.3.1 General principles of A.C. motor drives

A.C. motor drives above 1kVA rating normally operate from a polyphase supply. Since most polyphase supplies are three phase this thesis will only deal with A.C. motor drives operating from three phase supplies though many of the principles described apply to A.C. motor drives operating from other polyphase supplies.

In an A.C. motor the stator winding developes a rotating magnetic field in the motor and the interaction of the rotor with the rotating magnetic field develops torque in the rotor. The differences between types of A.C.

motor result mainly from the design of the rotor and the nature of its interaction with the magnetic field produced by the stator. Say [5], Fitzgerald and Kingsley [6], Steven [7] and Cotton [8] describe how the stator winding produces a rotating field and also describe the design of such stator windings.

The direction of rotation of a polyphase A.C. machine is reversed by reversing the phase sequence of the supply which reverses the direction of rotation of the magnetic field produced by the stator winding. The phase sequence of a three-phase supply may be reversed by changing-over any two phase connections.

1.3.2 The synchronous motor Say [5], Fitzgerald and Kingsley [6], Steven [7] and Cotton [8].

Figure 1.4 shows a simplified diagram of a three-phase two-role synchronous motor. The rotor is a D.C. electro-magnet which rotates in the rotating magnetic field produced by the stator winding. Because the rotor is magnetically polarized it experiences a torque due to magnetic forces tending to align the rotor with the rotating magnetic field and so during normal operation the rotor rotates in synchronism with the rotating magnetic field, hence the name "synchronous motor".

However the motor will not self-start since at standstill the relative motion between the rotor and the rotating field produced by the stator is too fast for the rotor to follow because of its inertia. For the motor to operate the rotor must be accelerated to its synchronous speed and then synchronised with the rotating magnetic field. Various methods of achieving this are described by Say [5], Fitzgerald and Kingsley [6], Steven [7] and Cotton [8].

The D.C. needed by the rotor for excitation can come either from an external supply via slip-rings or can be generated on the rotor itself using brushless excitation. Brushless excitation, described by Say [5] and Fitzgerald and Kingsley [6] avoids using slip rings which wear, increasing maintenance costs, and which spark, creating a fire hazard.

Say [5] shows that altering the excitation of the rotor can alter the power factor so that it is either unity, leading or lagging. Consequently synchronous motors are not only able to operate at unity power factor but are also able to correct the power factor of an electrical installation.

Say [5] also shows that a synchronous motor can generate when supplied with mechanical power: indeed, the vast majority of generators in power systems are synchronous generators and so the synchronous motor is

Figure 1.4: The Synchronous Machine.

(Rotor winding omitted for clarity)

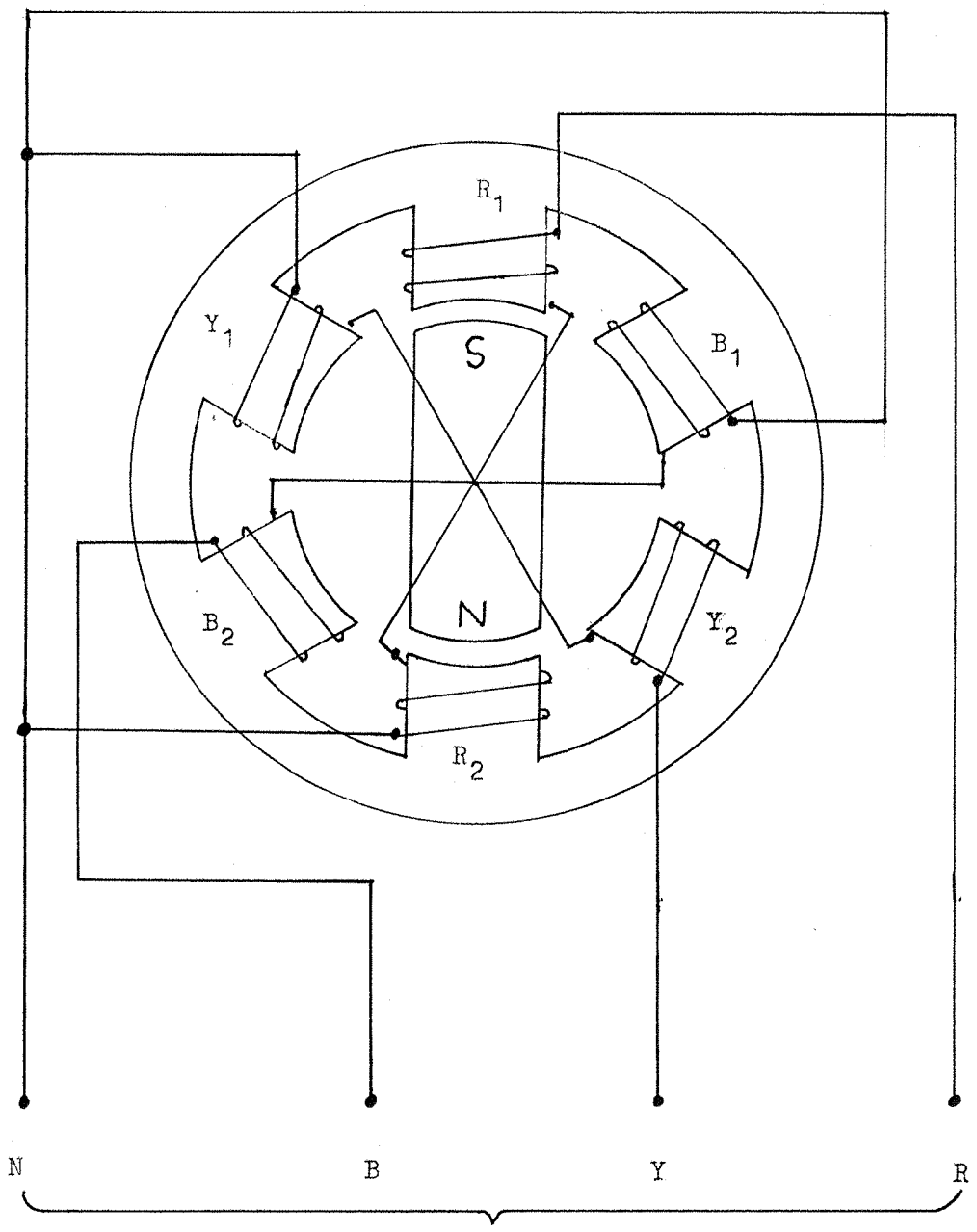

Three Phase Supply.

more accurately termed a synchronous machine. The ability of a synchronous machine to generate, together with its ability to rotate in either direction means that it is capable of four-quadrant operation.

1.3.1 The permanent-magnet synchronous machine

This machine is similar to the synchronous machine described earlier except that the permanent magnet synchronous machine has a permanent magnet rotor rather than an electro-magnetic rotor. Both kinds of machine have similar performance except that the power factor of the permanent magnet synchronous machine is not easily altered as it depends upon the fixed excitation provided by the permanent magnet. However the main advantage of a permanent magnet rotor is that it avoids D.C. excitation of the rotor, so producing a simpler machine and avoiding ohmic losses in the rotor. However, Say [5] states that a major problem of permanent magnet synchronous machines is demagnetisation of the rotor during starting or during some types of abnormal operation.

1.3.4 The reluctance motor Say [5]

The reluctance motor has many features in common with the synchronous motor : the rotors of both types of motor are polarized and both rotate in synchronism with the magnetic field produced by the stator winding. Unlike the synchronous motor in which the rotor is polarized by permanent or electro-magnetism, the rotor of a reluctance motor is polarized by the magnetic field produced by the stator. This is done by constructing the rotor so that it has a preferred axis (or axes) of magnetisation. During normal operation the rotor rotates in synchronism with the rotating magnetic field produced by the stator and experiences a torque due to magnetic forces tending to align the preferred axis of magnetisation with the axis of the rotating magnetic field. In these circumstances the rotor is magnetised along its preferred axis of rotation by the rotating magnetic field produced by the stator winding and the rotor rotates in synchronism with the rotating magnetic field.

Consequently, like the synchronous motor, the reluctance motor will not self-start but needs to be run up and synchronised. Unlike the synchronous motor, the power factor of the reluctance motor is not as readily controlled since the magnetisation of the rotor cannot be varied independently of the

magnetic field produced by the stator winding. Neverthless, Say [5] states that reluctance motors can operate at a power factor as good as 0.8.

Fitzgerald and Kingsley [6] state that a reluctance motor, like a synchronous motor, will operate as a generator when its shaft is supplied with mechanical power. Consequently, a reluctance motor or, more accurately a reluctance machine, is capable of four-quadrant operation.

1.3.5 The switched-reluctance motor

The switched-reluctance motor has many features in common with the ordinary reluctance motor. For example the rotors of each type of reluctance motors have a prefered axis (or axes) of magnetisation and are polarized by the magnetic field produced by the stator winding.

Figure 1.5 shows a simplified diagram of a switched-reluctance motor having four stator poles and two rotor poles, each stator pole carrying a coil. Unlike the ordinary reluctance motor, the switched-reluctance motor operates from a D.C. supply. Coils A_1 and A_2 are energised through switch S_A and coils B_1 and B_2 are energised through switch S_B.

The motor works on the well-known principle that soft iron is attracted to an electromagnet regardless of the polarity of the electromagnet. When coils A_1 and A_2 are energised and the rotor is in the position shown it experiences an anti-clockwise torque aligning it with the axis of coils A_1 and A_2. An electronic control system uses a shaft position sensor to detect when torque would be better produced by switching off coils A_1 and A_2 and energising coils B_1 and B_2. At such a time, appropriate signals are sent to the semiconductor switches S_1 and S_2. Continuous rotation of the rotor may be produced by appropriate switching of S_1 and S_2 in order to produce suitable excitation of the coils.

As may be deduced from the above description of the operation of the motor, the stator currents of the switched reluctance motor are pulses of D.C., unlike the stator currents of the ordinary reluctance motor which are A.C. Therefore, strictly speaking, the switched reluctance motor is a D.C. machine.

Davies [10] states that appropriate control of the semiconductor switches can produce forward and reverse direction of rotation, and that if the motor is supplied with mechanical power, the motor can act as a generator. Full four-quadrant operation is therefore possible. Davies [10] also states that in spite of power losses in the semiconductor switches, the overall

Figure 1.5: Simplified Diagram of a Switched Reluctance Motor.

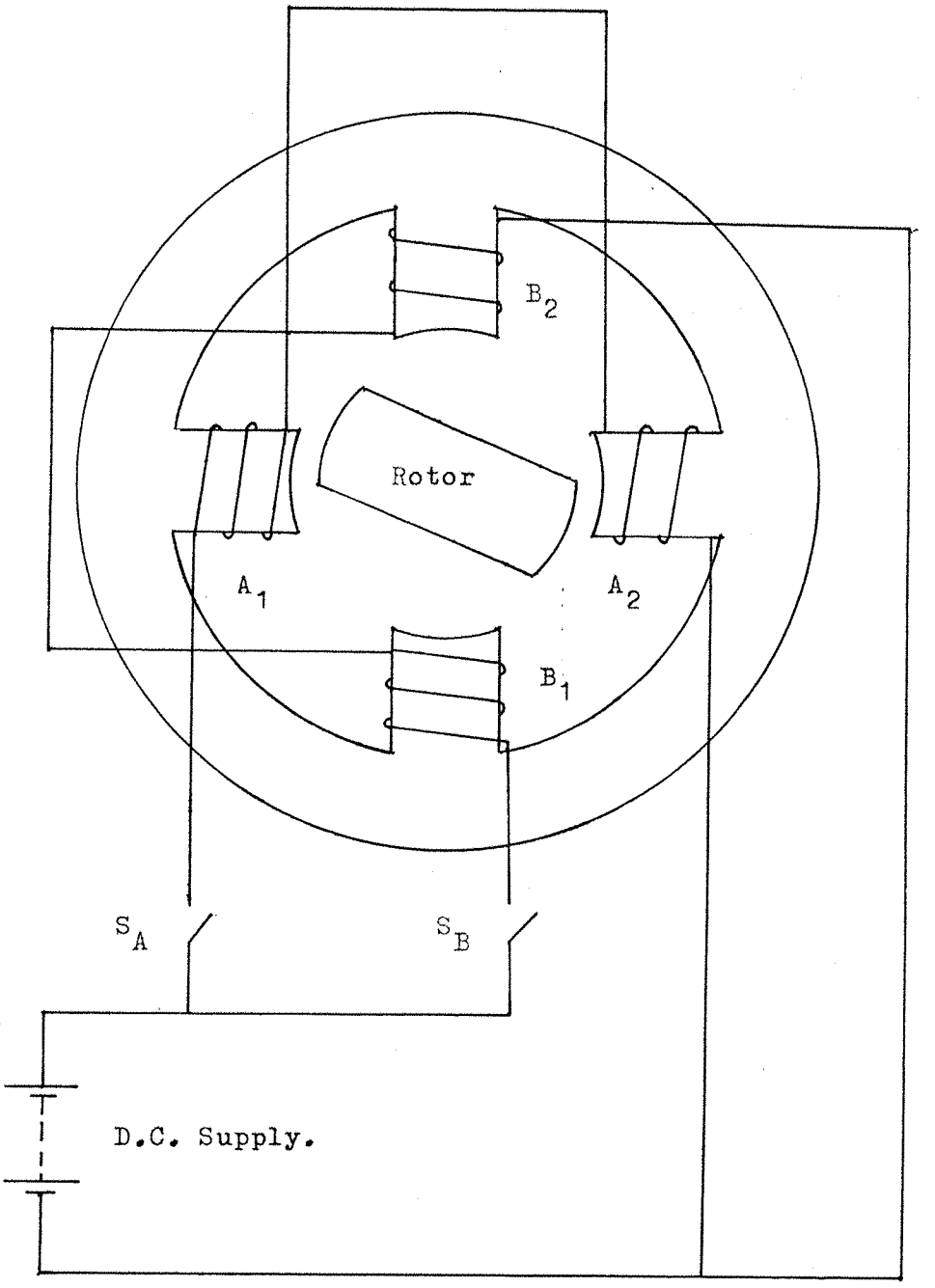

efficiency of a switched-reluctance motor drive is comparable to that of a polyphase induction motor operating from a sinusoidal supply. Furthermore, such performance is maintained at output powers as large as 50 kW.

Davies [10] also lists the constructional advantages of the switched-reluctance motor : it is brushless, has no rotor windings and consequently little heat is developed in the rotor. The stator winding is of simpler construction than in many motors because the coils can be bobbin-wound and inserted over the stator poles.

In view of the constructional simplicity and therefore cheapness of the motor and also its overall performance, it is likely that the switched reluctance motor will take a significant share of the market for variable-speed drives.

1.3.6 The induction motor Say [5], Fitzgerald and Kingsley [6], Steven [7], Cotton [8]

The rotor of an induction motor is a ferro-magnetic cylinder carrying conductors in which currents are induced by the rotating magnetic field produced by the stator. The interaction of these currents with the rotating magentic field produces a torque on the rotor which, by Lenz's law, is in the same direction as the direction of rotation of the magnetic field. If free to rotate, the rotor will accelerate reducing the relative speed between the rotor and the rotating magnetic field. Consequently the operation of the induction motor relies upon the induction of currents in the rotor windings - hence the name of the motor.

If the rotor rotates at synchronous speed and in the same direction as the rotating magnetic field there is no relative motion between the rotor conductors and the rotating magnetic field. In these circumstances there are therefore no rotor currents and no torque exerted upon the rotor, and so for the rotor to develop a torque it must rotate at a speed less than the synchronous speed. The amount by which the rotor speed-differs from the synchronous speed is termed the "slip" and is usually expressed as the fraction:

$$s = \frac{\omega_o - \omega_r}{\omega_o} \qquad (1.1)$$

Where s = the slip

ω_o = the synchronous speed (rads s^{-1})

ω_r = the rotor speed (rads s^{-1})

The synchronous speed equals the speed of the rotating field. is given by the following equation stated by Say [5]

$$\omega_o = \frac{\omega}{n_p} \tag{1.2}$$

where n_p = the number of pole-pairs of the stator winding

ω = the supply frequency (rad s^{-1})

During normal operation an increase in torque results in an increase in slip and therefore an increase in rotor current so that the motor can deliver the required torque. However, the slip needed to produce full load torque is usually small : Say [5] states that full load torque may result in 2kW induction motors operating at about 5% slip whereas a 1MW induction motor may operate at smaller slip, typically about 1%. Thus the induction motor is an almost constant speed motor whose speed falls slightly with load and in this respect the induction motor acts like a shunt-wound or separately-excited D.C. machine. Say [5] states that at full load large induction motors are capable of good efficiency and power factor : typical figures are 80% and 0.8 to 0.9 respectively.

Say [5] states that if an induction motor is supplied with mechanical energy so that it rotates above the synchronous speed the induction motor acts as a generator, and according to equation 1.1, operates at negative slip. Thus the induction motor is capable of four-quadrant operation.

Induction motors may be divided into two types according to the method of rotor construction described by Say [5].

1) **Cage rotor induction motors** Such motors have their rotor conductors in the form of a cylindrical cage : thick conductors are mounted in axial slots spaced equally around the rotor and a thick ring conductor at each end of the rotor connects the ends of the conductors in the slots. The resulting cage forms a crude but effective winding in which rotor currents flow. The simplicity of construction, together with the absence of slip rings, results in a motor which is cheaper and more robust than many other motors and is less of a fire hazard than motors which use slip rings or commutators which spark.

2) **Wound-rotor induction motors.** The rotors of these induction motors have a rotor winding comprising many turns of conductor. The resulting winding has the same number of phases and pole-pairs as the stator winding. The rotor winding is normally connected to slip-rings which allow access to the rotor circuit. Such access is not possible in cage motors since there are no slip rings. Consequently the wound rotor induction motor is generally easier to control than a cage induction motor.

An advantage that both types of induction motor have over synchronous motors and reluctance motors is that they self-start. This advantage together with the availability of polyphase electrical supplies and the cheap and robust form of construction of the cage rotor induction motor, has explained the overwhelming popularity of the cage rotor induction motor as an industrial drive.

1.3.7 The hysteresis motor (Say [5])

These motors have some resemblance to those operating on reluctance but the polarization of the rotor is produced in a different way. The rotor is an unwound cylinder of magnetically-hard material having high hysteresis loss independent of the axis of magnetisation. The material should also have a high resistivity in order to reduce eddy current loss. In order to further reduce eddy-current losses the rotor may be laminated, sintered or built up from alloy powder set in resin.

The operation of the motor is as follows: the rotating magnetic field produced by the stator winding produces a rotating magnetic field in the rotor. The axis of the magnetic field in the rotor is displaced from the axis of the magnetic field produced by the stator winding because of the hysteresis of the rotor. The displacement of these axes develops a torque in the rotor in the direction of rotation of the stator magnetic field. Thus the motor is able to self-start and can produce torque at speeds from standstill to synchronous speed. At synchronous speed the hysteresis of the rotor fixes the axis of the rotor flux with respect to the rotor and the motor operates synchronously in a manner resembling that of a reluctance motor.

Say [5] states that hysteresis motors can give an output no more than about one-quarter of an induction motor of similar dimensions and consequently hysteresis motors are usually made only in very small ratings.

1.3.8 Other polyphase A.C. drives

The A.C. drives described so far in this chapter constitute the most popular kinds of polyphase A.C. drives used in industry. Say [5] describes other A.C. drives which are used for special, though limited applications. These include low-power control devices such as selsyns and synchros which are usually used for accurate position control rather than high power A.C. drives.

1.3.9 Variable speed operation of polyphase A.C. drives

The A.C. drives described in this Chapter all operate at or close to synchronous speed, synchronous speed being fixed by the supply frequency and the number of pole-pairs of the stator winding according to equation 1.2. Conseqently variable speed operation of such drives presents problems.

A solution to the problem of driving a load at variable speed using a constant speed motor is to use a mechanical device to convert the motor speed to the speed required to drive the load. Devices such as gearboxes, pulleys and fluid couplings have not been outstandingly successful because of the problems of constructing a reliable mechanical system which will produce a wide range of variable speed ratios. A successful device is the eddy current coupling described by Shilston [4] and Bloxham and Wright [11]. The eddy current coupling uses electro-magnetic forces rather than a mechanical coupling to link the motor with the load. Although capable of good speed control the available range of load speeds is limited to between standstill and the constant speed of the A.C. motor.

In view of the limitations of the couplings described above many designers of variable speed A.C. drives have concentrated on varying the speed of the A.C. motor itself. Say [5] describes a number of variable speed A.C. motors which use commutators. Such motors, notably the Schrage motor and the doubly-fed motor enjoyed considerable success though interest in such motors has declined with more recent solutions to the problem of variable speed. One such solution is the use of variable voltage variable frequency (V.V.V.F.) supplies to power the A.C. motor. These supplies alter the frequency of the supply to the stator winding and therefore alter the speed of the A.C. motor. Bose [12] states that the speed of induction motors and synchronous motors may be varied in this manner and Say [5] states that similar speed control of reluctance motors is possible. V.V.V.F. supplies have become a popular way of achieving such speed control because of recent developments in power semiconductors. Four quadrant operation is possible in

such circumstances because V.V.V.F. supplies may be designed to accept power from a motor acting as a generator and can also be designed so that the phase sequence of the output may be reversed. Such supplies are described more fully in the next Chapter which discusses induction motor speed control.

1.4 Summary

D.C. machines have been, and still are a popular variable speed electric drive. They self-start and are capable of efficient four-quadrant operation over a wide range of speeds. The main disadvantage is the commutator which wears and also sparks, causing a fire hazard unless flame-proof construction is used.

The most popular A.C. motor used in drives above 1kVA is the induction motor. Other popular A.C. motors are the reluctance motor and the synchronous motor. All three types of motor offer good efficieny and power factor and are also capable of four-quadrant operation over a wide range of speeds when connected to a suitable V.V.V.F. supply.

A recently-developed drive is the switched-reluctance motor. Though strictly speaking it is a D.C. machine it shares many common features with the ordinary reluctance motor. Though in its infancy the switched reluctance motor shows much promise and may well capture a large share of the market for variable speed drives.

At present, however, the majority of industrial drives are cage induction motors operating from constant frequency supplies. Such drives are popular because unlike synchronous motors or reluctance motors induction motors are inherently self-starting. Furthermore, cage induction motors have a simple construction compared to many other motors and are therefore cheaper and more reliable. Consequently much effort and ingenuity has been employed to produce variable speed induction motor drives. The basic principles of the more common variable speed induction motor drives are described in the next Chapter.

CHAPTER 2 VARIABLE SPEED INDUCTION MOTOR DRIVES

2.1 Introduction

As stated in the previous chapter, the induction motor is a popular choice of drive and much work has been done to develop variable speed induction motor drives. This chapter begins by reviewing basic induction motor theory and continues by relating this theory to common methods of varying induction motor speed. Emphasis is placed upon the use of V.V.V.F. supplies since these enable four-quadrant operation of cage rotor induction motors over a wide range of speeds.

2.2 Basic induction motor theory

2.2.1 The equivalent circuit

Steven [7] describes how an induction motor may be represented by a per-phase equivalent circuit of the type shown in Figure 2.1. Although such a representation is only approximate it gives a fair description of the performance of the induction motor during steady-state operation provided that the motor operates from a balanced supply and each phase circuit of the motor is electrically identical. The elements of and currents and voltages in the equivalent circuit are listed below:

R_1 is the per-phase resistance of the stator winding.

R_2 is the per-phase resistance of the rotor winding referred to the stator winding.

X_1 is the per-phase leakage reactance of the stator winding and is caused by the portion of magnetic flux produced by currents in the stator winding but which does not link the rotor winding.

X_2 is the per-phase leakage reactance of the rotor winding referred to the stator winding. This reactance arises from the portion of magnetic flux produced by currents in the rotor winding but which does not link the stator winding.

R_m is the per-phase magnetising loss resistance which represents eddy current and hysterisis losses in the motor.

X_m is the per-phase magnetising reactance which represents the reactive power needed to magnetise the motor.

The values of these circuit elements for a particular induction motor may be estimated from two tests described by Steven [7] : the "light running" test and the "locked rotor" test.

Figure 2.1: The Equivalent Circuit of an Induction Motor.

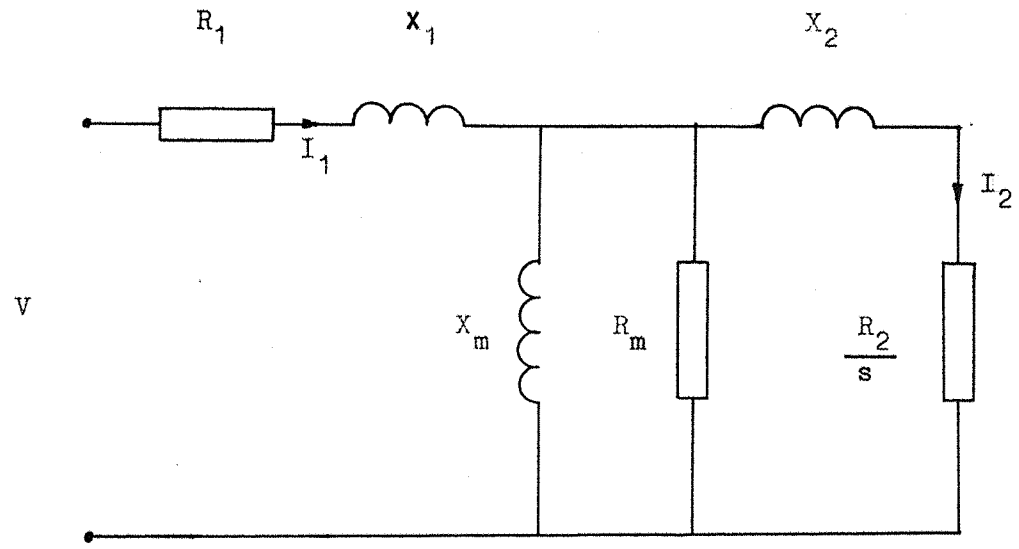

Figure 2.2: A Modified Equivalent Circuit of an Induction Motor.

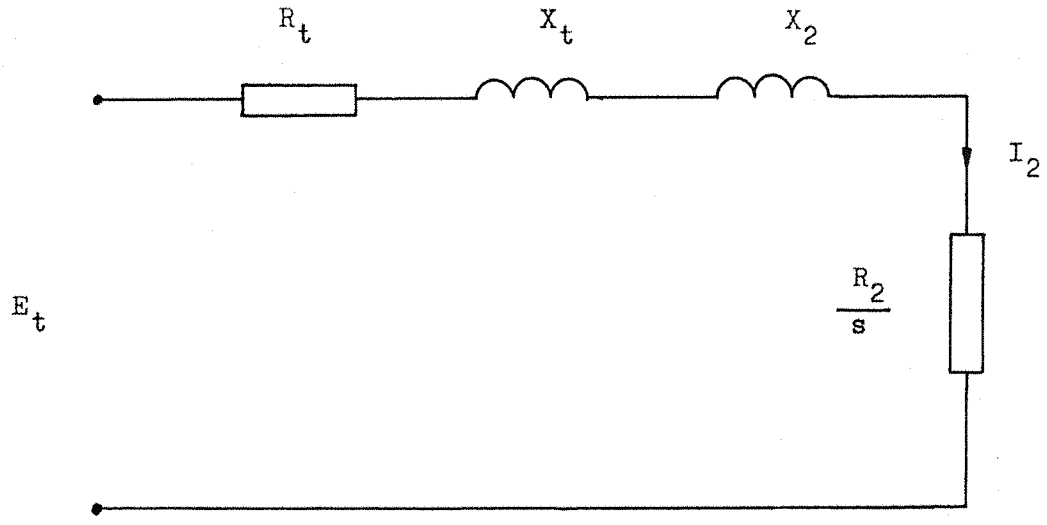

The voltages and currents in the equivalent circuit are as follows:

V = the supply phase voltage

I_1 = the stator winding phase current

I_2 = the rotor winding phase current referred to the stator winding.

The equivalent circuit and the basic induction motor theory relating to the equivalent circuit applies equally to wound rotor and cage rotor machines.

Stevens [7] suggests further simplification of the equivalent circuit as follows: It may be assumed that R_m may be removed and the losses it represents may be grouped with the friction and windage losses of the motor. The supply voltage V, the stator winding impedances R_1 and X_1 and the magnetising reactance X_m may be formed into an equivalent Thevenin voltage source, producing the modified equivalent circuit of the induction motor, shown in figure 2.2.

The Thevenin equivalent source voltage E_t is given by:

$$E_t = \frac{jX_m V}{R_1 + j(X_1 + X_2)} \qquad (2.1)$$

and the equivalent source impedance, represented by $R_t + jX_t$ is given by:

$$R_t + jX_t = \frac{jX_m(R_1 + jX_1)}{R_1 + j(X_1 + X_m)} \qquad (2.2)$$

R_t and X_t may be termed the modified per-phase resistance and leakage reactance of the stator winding, respectively and E_t may be termed the modified supply phase voltage.

2.3 The torque-speed characteristic of an induction motor

2.3.1 Equations describing the torque developed by an induction motor

Steven [7] shows how these equations may be derived from the modified equivalent circuit shown in figure 2.2. The equation relating the gross torque T to the induction motor slip is

$$T = \frac{mE_t^2 R_2}{s\omega_0\left(\left(R_t + \frac{R_2}{s}\right)^2 + (X_t + X_2)^2\right)} \tag{2.3}$$

where m is the number of phases of the induction motor. The gross torque is the torque developed in the rotor winding. The torque available to drive a load will be less than the gross torque becasue of friction and windage losses in the induction motor.

The equation relating the gross torque to the speed of the induction motor is

$$T = \frac{mE_t^2 R_2}{(\omega_0 - \omega_r)\left(\left(R_t + \frac{\omega_0 R_2}{\omega_0 - \omega_r}\right)^2 + (X_t + X_2)^2\right)} \tag{2.4}$$

This equation describes the torque-speed characteristic which is drawn in Figure 2.3.

2.3.2 The change in induction motor behaviour with speed

The torque-speed characteristic may be divided into three regions as illustrated in Figure 2.3:

Motoring region: If the rotor speed is between zero and synchronous speed the machine acts as a motor with the gross torque T being positive as indicated by equation 2.3. The "starting torque" T_s, ie, the torque developed at standstill, may be found by putting ω_r equal to zero in equation 2.4 to yield

$$T_s = \frac{mE_t^2 R_2}{\omega_0\left((R_t + R_2)^2 + (X_t + X_2)^2\right)} \tag{2.5}$$

From zero speed the gross torque rises with increasing speed until it reaches a maximum value T_{mm} known as the "pull-out" torque. The size of this torque and the speed ω_{mm} at which it occurs may be found by differentiating equation 2.4 to find the speed at which T has its most positive value. T_{mm} and ω_{mm} are given by:

$$T_{mm} = \frac{mE_t^2 (R_t^2 + (X_t + X_2)^2)^{\frac{1}{2}}}{2\omega_0((R_t^2 + (X_t + X_2)^2)^{\frac{1}{2}} + R_t)} \tag{2.6}$$

Figure 2.3: The Torque - Speed Characteristic of an Induction Motor.

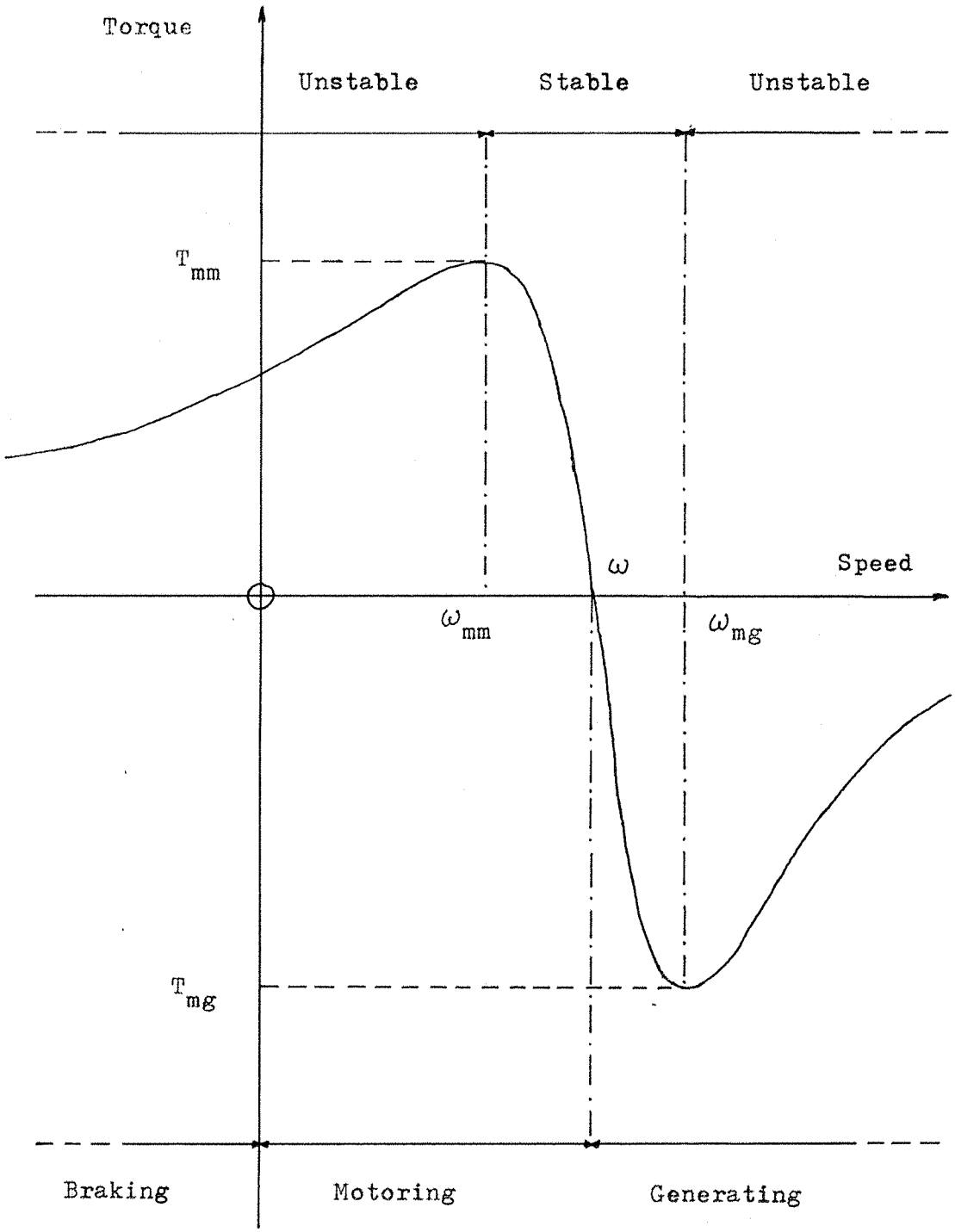

$$\omega_{mm} = \omega_o\left(1 - \left(\frac{R_2}{(R_t^2 + (X_t + X_2)^2)^{\frac{1}{2}}}\right)\right) \qquad (2.7)$$

As the speed rises past ω_{mm} the torque falls, reaching zero at synchronous speed.

The generating region

If an external source of mechanical power drives the rotor of an induction motor above its synchronous speed, the slip becomes negative as does T. The circuit element $\left(\frac{R_2}{s}\right)$ in the modified equivalent circuit becomes a negative resistance indicating that the motor is now acting as a generator converting some of the mechanical power supplied to the rotor to electrical power which is fed into the supply. Under such circumstances the induction motor is termed an "induction generator". Say [5] states that induction generators are of moderate efficiency and furthermore they need a supply of reactive power to magnetise the machine, such reactive power normally coming from the system to which the machine is connected. Consequently, induction generators have only found limited application.

Like the induction motor the induction generator also shows a maximum torque, T_{mg}. The size of this torque and the speed $_{mg}$ may be found in a similar manner to the way T_{mm} and ω_{mm} were found for the induction motor. T_{mm} and ω_{mg} are given by:

$$T_{mg} = -\frac{mE_t^2 (R_t^2 + (X_t + X_2)^2)^{\frac{1}{2}}}{2\omega_o (R_t^2 + (X_t + X_2)^2 - R_t (R_t^2 + (X_t + X_2)^2)^{\frac{1}{2}})} \qquad (2.8)$$

$$\omega_{mg} = \omega_o\left(1 + \left(\frac{R_2}{(R_t^2 + (X_t + X_2)^2)^{\frac{1}{2}}}\right)\right) \qquad (2.9)$$

During generation both T_{mg} and T are negative indicating that the machine is absorbing rather than generating mechanical power.

The braking region

If an external source of mechanical energy drives the rotor in the direction opposite to the rotating magnetic field produced by the stator, the

motor acts as a brake, converting the mechanical energy to heat in the windings of the machine. Say [5] states that this mode of operation is very useful in rapidly bringing an induction motor to rest. This is done by suddenly reversing the phase sequence of the supply to the induction motor and so reversing the direction of the rotating magnetic field produced by the stator winding. This method is called "plugging".

2.3.3 The stability of an induction motor

The torque speed characteristic may also be divided into regions of stable and unstable operation as shown in Figure 2.3. In regions of stability a change in load torque produces a change in speed which acts to reduce the change in load torque and in regions of instability a change in load torque produces a change in speed which acts to increase the change in load torque. Consequently at a point of stable operation the slope of the torque-speed characteristic is negative and vice versa. For example during stable motoring any increase in load torque will cause deceleration of the induction motor which in turn will cause it to develop more torque. Provided that the load-torque does not exceed the pull-out torque the induction motor will eventually run stably supplying the increased load torque at a lower speed. If the load torque exceeds the pull-out torque the induction motor will decelerate past mm into the region of unstable motoring, eventually coming to rest. This process is called "stalling".

2.4 The theoretical basis of some popular methods of altering induction motor speed

The operation of a variable speed induction motor drive may be considered in terms of controlling the induction motor so that it delivers a given torque at a particular speed. The speed, or speeds, at which an induction motor delivers a particular gross torque T may be found by re-arranging equation 2.4 and solving the resulting quadratic equation to yield:

$$\omega_r = \omega_o - \left(\frac{R_2}{2T\,(R_t^2 + (x_t + X_2)^2)} \right) (mE_t^2 - 2R_t\omega_o T \pm$$

$$(m^2E_t^4 - 4\omega_o T\,(R_t mE_t^2 + \omega_o T\,(X_t + X_2)^2))^{\frac{1}{2}}) \qquad (2.10)$$

The above equation indicates three possible types of solution, depending on the value of T.

1. If $T = T_{mm}$ then substituting equation 2.6 for T into equation 2.10 and comparing the result with equation 2.7 shows that the induction motor operates at speed $\omega_r = \omega_{mm}$. In other words there is one solution indicated by equation 2.10 and this corresponds to operation with the induction motor delivering pull-out torque. A similar situation occurs if $T = T_{mg}$ in which case the induction motor operates as a generator absorbing maximum pull-out torque at speed ω_{mg}.

2. If $T_{mg} < T < T_{mm}$ then equation 2.10 indicates two possible speeds: one corresponding to stable operation, the other to unstable operation.

3. If $T > T_{mm}$ then equation 2.10 indicates that ω_r has an imaginary component. Physically this corresponds to the induction motor being subject to a load torque greater than its pull out torque, causing it to stall. Similarly if $|T| > |T_{mg}|$ during operation as an induction generator, ω_r has an imaginary component. Phsycially this situation corresponds to the induction generator "running away" and overspeeding.

Equation 2.10 also indicates the following possible methods of altering the speed of an induction motor:

1. Altering the supply voltage. According to equations 2.1 and 2.10 this results in a change in E_t and therefore a change in speed.

2. Connecting an impedance in series with the supply and the stator winding. Such an impedance is therefore in series with the stator winding impedances R_1 and X_1 and the resulting induction motor performance may be analysed by including this series impedance in R_1 and X_1 in the equivalent circuit. Consequently according to equations 2.1 and 2.2 altering this series impedance will affect E_t, R_t, and X_t, which in turn will alter the motor speed according to equation 2.10.

3. Altering the rotor resistance. Such a method results in a change of speed according to equation 2.10 but is only applicable to wound-rotor machines where the rotor circuit is accessible via the slip rings.

4. Altering the synchronous speed of the induction motor. This can be done in two ways according to equation 1.2:

a) Altering the number of pole pairs n_p of the stator winding

b) Altering the supply frequency ω.

With the exception of speed control achieved by altering the rotor resistance of an induction motor, the methods of speed control which are listed above are described in greater detail below. Methods of speed control using changes in rotor resistance are only applicable to wound-rotor induction motors and are therefore not relevant to the speed control of cage induction motors which is the main subject of this thesis.

2.5 Altering induction motor speed by altering the supply voltage

2.5.1 Theoretical basis

Equations 2.1 and 2.4 show that the torque developed by an induction motor operating at a given speed is proportional to the square of the supply voltage. Figure 2.4 shows the effect of a reduction in supply voltage upon the torque-speed characteristic of an induction motor and the change in speed when the induction motor delivers a torque that is constant with speed. The effect of a reduction in supply voltage is to alter the scale of the torque-speed characteristic in the direction of the torque axis and the resulting change in speed may be estimated from the change in intersection of the torque-speed chracteristic with the line representing the load torque. A similar line of reasoning follows even if the load torque changes with speed : e.g. a fan.

2.5.2 Practical methods of altering the supply voltage

This can be done simply and cheaply if the induction motor uses an auto-transformer starter of a type described by Say [5] to reduce the voltage applied to the induction motor during starting. However, the starter must be rated to carry continuously the currents likely to arise during such speed control. A star-delta starter may be used in a similar manner as it produces a change in voltage across each coil and therefore produces an effect similar to a change in supply voltage. However a star-delta starter can only produce one such change in voltage across each coil and therefore only one such change in speed.

An alternative method uses electronic switches such as thyristors or triacs connected between the induction motor and the supply. These switches can conduct during all or part of the A.C. cycle, effectively altering the R.M.S. voltage supplied to the induction motor. Spooner [13] describes an example of such a method.

Figure 2·4 : The Effect of Reduced Supply Voltage upon the Torque - Speed Characteristic of the Induction Motor and the Running Speed of the Motor.

—.—.— Torque - speed characteristic at normal supply voltage voltage.

— — — — Torque - speed characteristic at reduced supply voltage.

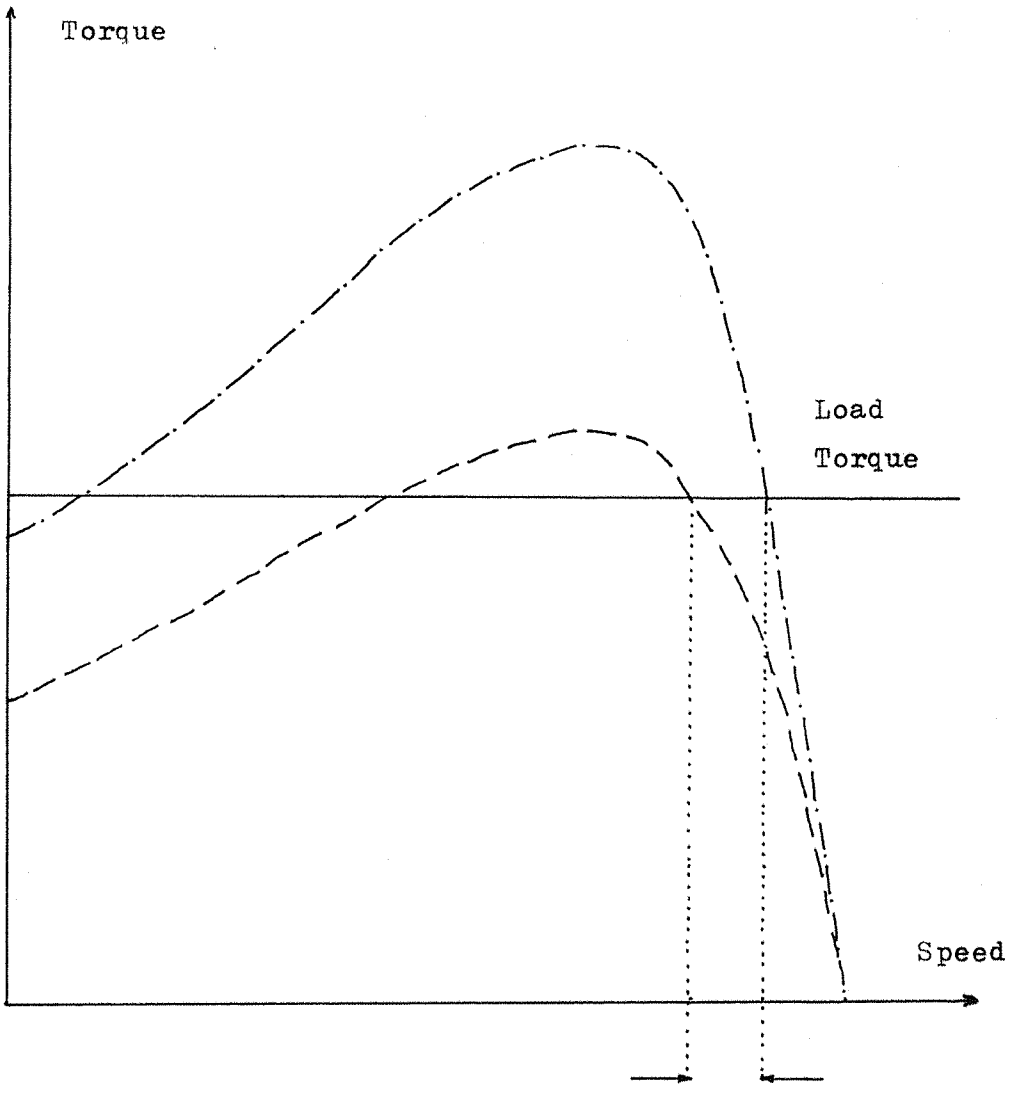

2.5.3 The viability of altering induction motor speed by altering the supply voltage

Although this method is a practical way of altering the speed of an induction motor it produces a limited range of speeds. This limited range arises for two main reasons:

1) The motor is only able to operate stably between synchronous speed and the speed at which pull out torque occurs. For a large induction motor this range of speeds is typically a small fraction of the range of speeds between zero and synchronous speed.

2) Such speed control is only possible when the motor is delivering less than its full-load torque. An attempt to make the induction motor deliver full-load torque whilst operating from a reduced voltage supply can cause the induction motor current to rise above its full-load value. This is because the motor is delivering almost full output power, since the change in speed is small, and is therefore consuming almost full-load kVA. Consequently, a fall in supply voltage can cause a rise in current leading to possible overheating though the rise in current is somewhat reduced as the reduced supply voltage causes the induction motor to take less magnetising current.

Spooner [13] describes a method of induction motor speed control which uses electronic switching to reduce the supply voltage to the motor. An advantage of this method is that the available range of speeds is much greater than would be expected from considering the typical torque-speed characteristic of an induction motor. This is because the method of electronic switching used to alter the voltage of the supply to the induction motor produces harmonics in the supply. These harmonics affect the performance of the induction motor considerably, producing a torque-speed characteristic much different to the typical torque-speed characteristics illustrated in figures 2.3 and 2.4. Spooner [13] quotes possible speed ranges in the ratio 1.5 or 2 to 1 when this method is used to control the speed of an induction motor driving a fan or a pump. Although the circuitry needed to achieve such speed control is simple and therefore cheap the harmonics produced in the supply to the induction motor increase the iron and copper losses in the induction motor and can cause it to overheat. These losses, together with the tendency of the harmonics to produce torques which oppose the main torque mean that such a method of speed control reduces the efficiency of the induction motor. The electronic switching can also inject harmonics into the power system supplying

the drive and these harmonics can adversely affect other equipment connected to the power system.

Therefore although the harmonics are advantageous from the point-of-view of increasing the available range of speeds they are disadvantageous from the points-of-view of efficiency and interference with other equipment.

As can be seen from equation 2.6 reduced supply voltage reduces the pull-out torque of the induction motor. Consequently when designing a drive based on the method of induction motor speed control by alteration of supply voltage, care must be taken to ensure that the load torque never exceeds the pull-out torque, otherwise the induction motor will stall.

2.5.4 An overall assessment of the method of altering induction motor speed by altering the supply voltage

Although this method is a practical way of altering the speed of an induction motor the available speeds are limited and are all below the synchronous speed of the induction motor. This method also reduces the pull-out torque of the induction motor. Consequently this method of speed control has found limited application.

2.6 Altering induction motor speed by using impedances in series with the supply and the induction motor

The voltage drop across the series impedance effectively reduces the voltage of the supply to the induction motor and this method of induction motor speed control therefore shares many similarities with the method of speed control using variation of the supply voltage. The resulting reduction in supply voltage is current-dependent and therefore load-dependent, complicating the control of such an induction motor drive. The use of series resistances produce an ohmic power loss which reduces the efficiency of the drive. If series inductances are used to avoid ohmic losses these inductances can worsen the power factor of the drive. In any case, whatever the type of impedances used they must be rated to carry the currents resulting from such a method of speed control. The available range of speeds and the problems caused by reduced pull out torque are similar to those resulting from the control of supply voltage. In view of the current rating of the series impedances and their effect on the efficiency and power factor of the drive and also in view of the limited speed and pull-out torque available the method of induction motor speed control using series impedances is uncommon. Say

[5] states that such a method tends to be limited to induction motors with ratings less than 1kW.

2.7 Alteration of induction motor speed by alteration of the number of pole-pairs of the stator winding

2.7.1 Theoretical basis

Since induction motors normally run at speeds close to their synchronous speed, any change in the synchronous speed will alter the speed at which an induction motor delivers a given load torque. According to equation 1.2 the synchronous speed may be altered by altering the number of pole-pairs of the stator winding.

2.7.2 Methods of altering the number of pole-pairs of the stator winding

One method is to wind an induction motor with two more than one stator winding, the windings having different numbers of pole pairs. Switching the supply from one winding to another changes the induction motor speed. Rawcliffe, Burbidge and Fong [14] report that such induction motors have been made for two-speed operation of fans in power stations. However, providing more than one stator winding adds to the size and cost of the induction motor and so methods of changing the number of pole pairs of a single winding have been developed.

Two methods of changing the number of pole pairs of a single stator winding are: pole-changing, described by Rawcliffe and Jayawant [15] and pole-amplitude modulation, described by Rawcliffe, Burbidge and Fong [14]. Both methods use switches to reverse the connections of some conductors in the stator windings and so alter the number of pole-pairs and therefore the speed of the motor.

2.7.3 The viability of alteration of induction motor speed by altering the number of pole-pairs

The methods described above all offer good efficiency and power factor and speed control may be simply achieved by appropriate switching. Say [5] states that a properly-designed cage rotor will respond satisfactorily to any number of pole-pairs of the stator winding but the rotor winding of a wound-rotor induction motor must be altered in a similar manner to the stator winding so that the polarities of both windings correspond.

However Rawcliffe, Burbidge and Fong [14] and Rawcliffe and Jayawant [15] report that pole-changing and pole-amplitude modulation can increase the leakage reactance of the induction motor and can also increase the harmonics present in the magnetic field produced by the stator winding. This is because both pole-changing and pole-amplitude modulation produce a considerable change in the pattern of the magnetic field within the induction motor. Increased leakage reactance results in poorer power factor while an increase in harmonics can reduce the efficiency and overall performance of the motor.

The chief disadvantage of altering induction motor speed by altering the number of pole-pairs of the stator winding is that this method produces only a few different speeds. Furthermore all speeds produced cannot be greater than the synchronous speed of a two-pole machine connected to the same supply.

2.7.4 An assessment of the method of varying induction motor speed by varying the number of pole-pairs of the stator winding

This method generally offers good efficiency and power factor but can only produce a few different speeds, none of which can be above the synchronous speed of a two-pole induction motor connected to the same supply.

2.8 Alteration of induction motor speed by alteration of the supply frequency

2.8.1 Theroretical basis

Equation 1.2 quoted in Chapter 1 shows that altering the supply frequency alters the synchronous speed of the induction motor. This results in an almost proportional change in induction motor speed as induction motors normally operate close to synchronous speed. However magnetic saturation can arise at reduced supply frequency because the magnetic flux Φ in the induction motor is given approximately by the relationship

$$\Phi \propto \frac{V}{\omega} \tag{2.11}$$

This relationship shows that Φ increases as ω decreases and in such circumstances the supply voltage is reduced to avoid magnetic saturation. Magnetic saturation is undesirable as it causes excessive magnetising currents

and can cause harmonic magnetic fields in the induction motor which affect its performance.

Consequently most schemes which control induction motor speed by altering the supply frequency also control the supply voltage to avoid magnetic saturation. The supply to the induction motor is therefore a variable-voltage variable-frequency (V.V.V.F.) supply. The different types of V.V.V.F. suppy in common use are listed below:

1) Motor-Generator sets.

2) Cycloconvertors.

3) D.C. link inverters.

These are described in greater detail below:

2.8.2 Motor-Generator sets

A variable-speed motor may be used to drive an A.C. generator to produce a V.V.V.F. supply suitable for induction motor speed control. Such motor-generator sets tend to be noisy and bulky and require frequent maintenance. Furthermore, when using such a system the problem of controlling the speed of an induction motor becomes one of controlling the speed of the motor driving the motor-generator set, which may also cause problems. Consequently V.V.V.F. supplies based on motor-generator sets have been largely superseded by V.V.V.F. supplies such as cycloconverters and D.C. link inverters which use power electronics.

2.8.3 Cycloconverters

Say [5] describes the construction and operation of a three-phase to three-phase cycloconverter which converts a three phase input from one frequency to a three phase output of a much lower frequency, typically less than a third of the frequency of the three-phase input. If the output frequency exceeds about one third of the input frequency the output waveform becomes intolerably distorted. Consequently the limited frequency output means that the speed of an induction motor drive based on such a cycloconverter can only vary between zero and one-third of the synchronous speed at which the induction motor would operate if connected to the same supply powering the cycloconverter. Consequently cycloconverters have found only limited application in variable speed induction motor drives. However cycloconverters are able to change frequency in either direction, so allowing regeneration, and the output voltage may be varied by controlling the power electronics used in

their construction. Suitable control of the power electronics can also reverse the phase sequence of the output, and so reverse the direction of an induction motor connnected to the output.

2.8.4 D.C. link inverters

General Principles

A D.C. link inverter rectifies input A.C. power to D.C. power and then inverts the D.C. power to A.C. power. An inverter may be designed and operated so that its output differs in voltage, frequency and number of phases from the input. Inverters also exist which produce A.C. power from a D.C. source such as a battery or a D.C. generator. Wakefield [2] describes such a battery-powered inverter used in an induction motor drive for an electric vehicle. Strictly speaking inversion describes the conversion from D.C. to A.C. although Kirk and Leppard [16] report that devices using rectification and inversion to alter the voltage frequency and number of phases of A.C. power are often called "inverters" despite their A.C. input/output characteristics.

Figure 2.5 shows the circuit diagram of a typical three-phase to three-phase inverter. A three-phase bridge rectifier using thyristors rectifies the input A.C. power to D.C. and a three-phase bridge circuit, also using thyristors inverts the D.C. power to three phase A.C. power. Many such inverters similar to the types described by Bose [12] and Turnbull and Lipo [17] use low-pass filters in the D.C. link to smooth the D.C. output of the rectifier. For clarity, Figure 2.5 does not show such a filter.

Although D.C. link inverters may be designed having a diode bridge rectifier producing D.C., thyristors are preferred because the rectifying action of a thyristor may be controlled. Such control allows variation of the output voltage of the inverter, and also allows bi-directional power flow where the rectifier and inverter exchange functions. Bi-directional power flow and variable voltage operation will be discussed later.

A thyristor behaves as a controllable diode - indeed another name for a thyristor is a "silicon controlled - rectifier" or SCR. The construction and operation of thyristors is described by Green [18] and the main points relevant to D.C. link inverters are as follows: A thyristor is a three-terminal device, two terminals of which are the anode and cathode which are similar to those of an ordinary diode. The third terminal is called the "gate" and is used to control the thyristor. A thyristor behaves like a diode except that it only conducts when forward biased and when triggered by an electrical pulse at the

Figure 2·5 : D.C. Link Inverter.

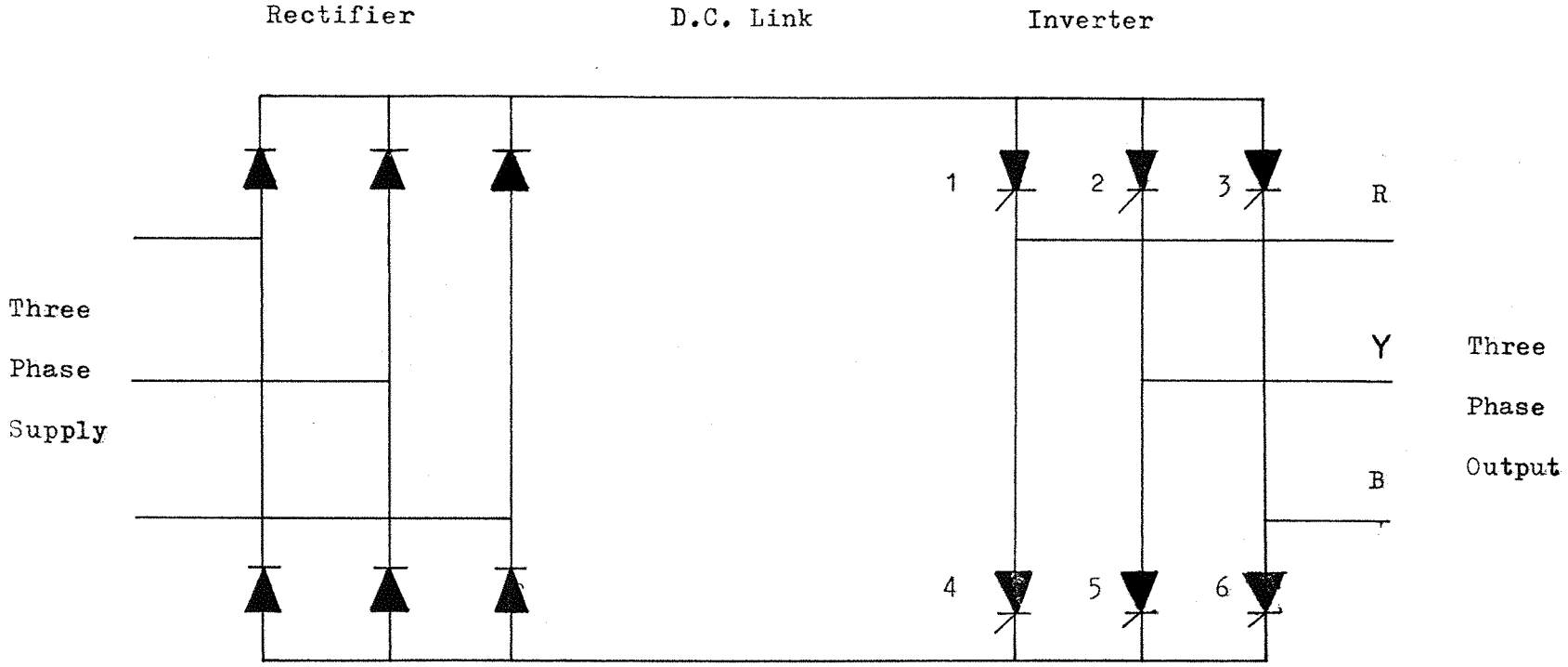

gate. Once triggered the thyristor conducts whilst forward biased regardless of whether or not triggering pulses are present at the gate. Like a diode a thyristor does not conduct when reverse-biased.

Turning off a thyristor is called "commutation", and can only happen when the current flowing through the thyristor falls below a certain value called the "holding" current, or is reverse-biased. Commutation may be either "natural" or "forced". Natural commutation occurs when the voltage across the thyristor naturally reverses, for example during an A.C. cycle. Forced commutation occurs when an auxiliary circuit called a "commutating" circuit momentarily reduces the current through the thyristor to zero and reverse-biases the thyristor. For clarity Figure 2.5 does not show the triggering and commutation circuits necessary to control the thyristors. Taylor [19] describes the recent development of the "gate turn-off" thyristor or G.T.O. thyristor which behaves in a similar way to an ordinary thyristor except that it may be turned off by an electrical pulse of appropriate polarity at the gate. Consequently a G.T.O. thyristor does not need a commutation circuit.

Inverters may be classified according to their output waveforms. There are two types of inverter : quasi-square wave inverters (Q.S.W.) and pulse-width modulated inverters (P.W.M.).

Quasi-square wave inverters

Phillips [20] and Lipo and Turnbull [17] describe the construction as an operation of Q.S.W. inverters. These inverters are so called because their output waveforms typically resemble square waves. Figure 2.6 shows an example of an output waveform of one phase. The production of this waveform may be understood by considering the operation of thyristors 1 and 4 in the output of the red phase of the circuit shown in figure 2.5. These thyristors conduct alternately producing positive and negative pulses whose amplitudes equal, respectively, the voltages of the positive and negative supply rails of the D.C. link. In a similar manner, thyristors 2 and 5 produce the yellow phase waveform and the thyristors 3 and 6 produce the blue phase waveform with the conduction sequences of the thyristors being set to give the appropriate phase displacements.

Pulse-width modulated inverters

A P.W.M. inverter produces a high-frequency rectangular waveform similar to that shown in figure 2.7. This waveform has a variable mark-to-

Figure 2·6 : The Output Waveform of a QSW Inverter based upon the Circuit shown in Figure 2·5

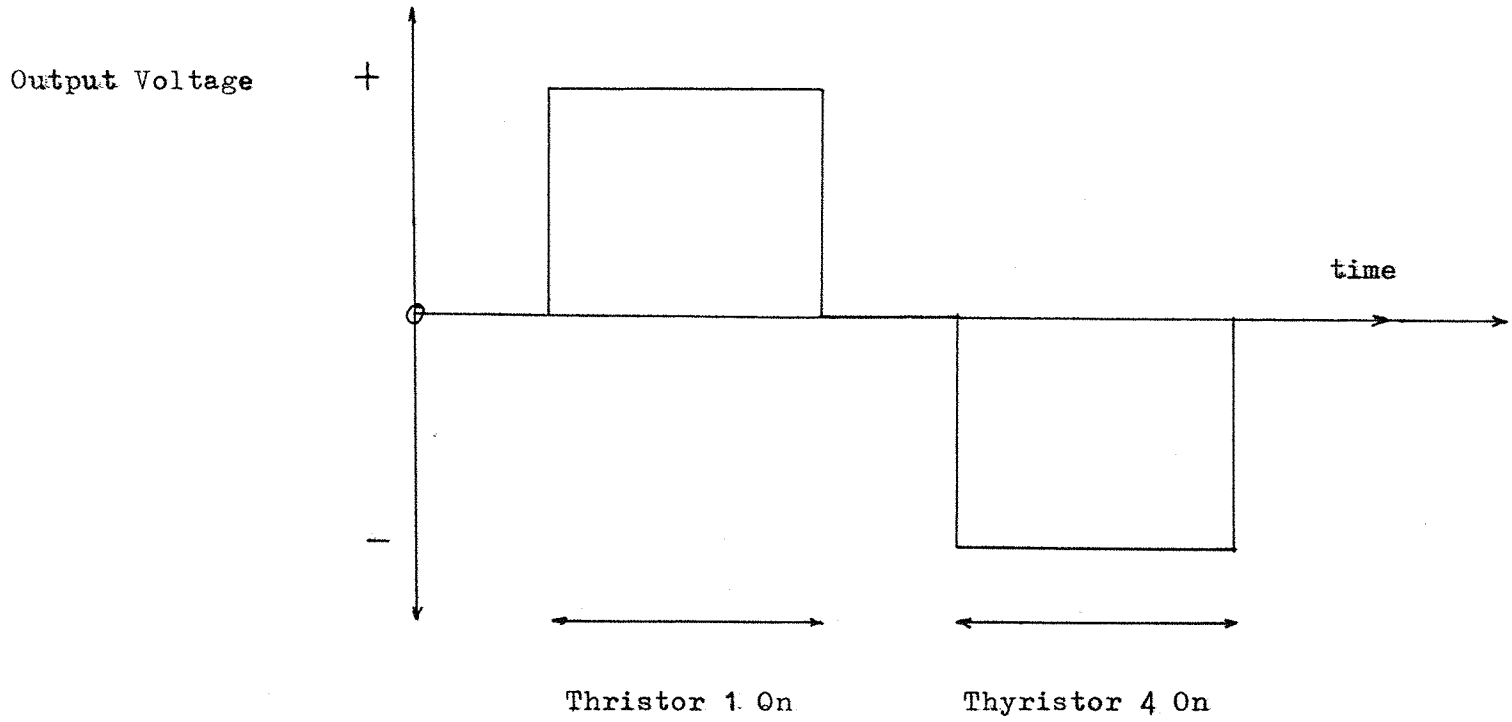

Figure 2.7: A Typical Output Waveform of a P.W.M. Inverter.

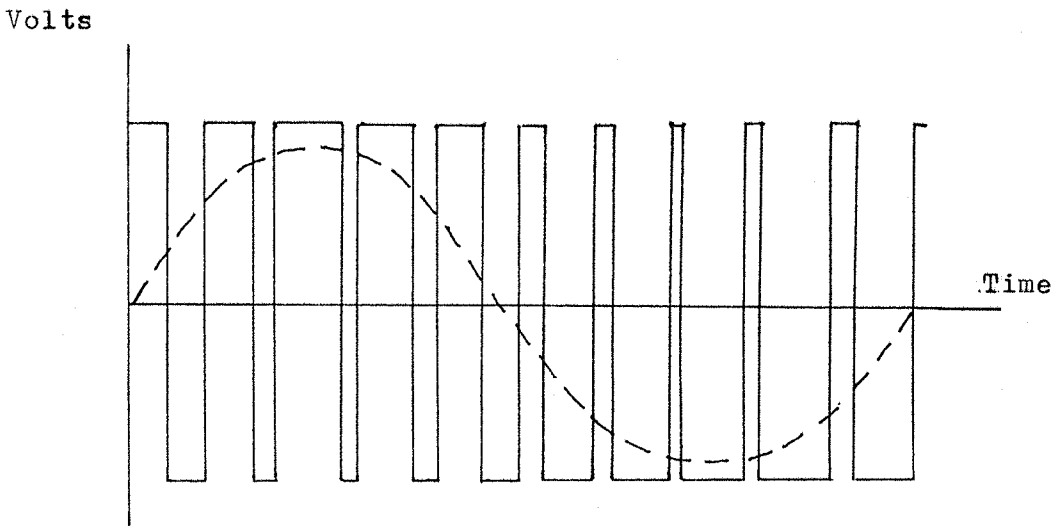

— — — — Low Frequency A.C. Component.

space ratio which produces a low frequency A.C. component (shown dotted in figure 2.7) in the output. In the circuit shown in figure 2.5 such an output waveform of the red phase would be produced by rapid alternative conduction of thyristors 1 and 4. Thyristors 2 and 5 generate the yellow phase waveform and thyristors 3 and 6 generate the blue phase waveform with appropriate phase-shifting of the conduction pattern of each pair of thyristors in order to give the appropriate phase displacements. Nayak and Hoft [21] describe ways of generating a P.W.M. waveform.

The outputs of both types of inverter are markedly non-sinusoidal and therefore rich in harmonics. Say [5] reports that induction motors will act satisfactorily from Q.S.W inverters although the performance of an induction motor in such circumstances is poorer than when it operates from a sinusoidal supply. Poorer performance results because the harmonics in the output of the Q.S.W. invertor increase the iron and copper losses in the induction motor and also cause parasitic torques which oppose the main torque. Kirk and Leppard [16] and Grant and Barton [22] state that P.W.M. inverters are better in this respect because of their improved waveform synthesis. However P.W.M. inverters need power electronics with faster swithcing times.

Variable-voltage operation of an inverter

The three most common ways of achieving this are as follows:

1) Altering the output voltage of the rectifier. Bose [12] states that this may be done by controlling the thyristors of the rectifier so that the portion of A.C. cycle during which they conduct can be varied. However, Weedy [23] states that such a method can produce harmonics in the mains supply to the rectifier and also poor power factor. This is because reduced voltage operation requires the thyristors to conduct later in the A.C. cycle resulting in the inverter taking a non-sinusoidal current whose phase lags that of the supply voltage.

2) Using a D.C. chopper in the D.C. link: Kirk and Leppard [16] describe how a D.C. chopper operating with a variable mark-to-space ratio may be used to alter the output voltage of an inverter.

3) Alteration of the mark-to-space ratio of the output voltage waveform, as described by Bose [12]. This is, of course, only application to P.W.M. inverters which use a variable mark-to-space ratio waveform.

Reversal of rotation of the induction motor

This may be achieved by reversal of the phase sequence of the output of the inverter. If the inverter has a three-phase output the phase sequence of

the output may be reversed by exchanging the switching sequence of the thyristors controlling one phase with the switching sequence of the thyristors controlling any other phase.

Regeneration

From figure 2.5 it may be seen that, apart from the polarities of the thyristors, the circuits of the rectifier and the inverter are the same. Consequently, suitable control of the thyristors can result in the rectifier and the inverter exchanging roles, as described by Weedy [23]. This allows regeneration, that is, the induction motor is able to operate as a generator, delivering power to the mains via the inverter. Both Q.S.W. and P.W.M. inverters may be designed to allow regeneration, as described by Phillips [20] and Plunkett and Plette [24], respectively.

The suitability of D.C. link inverters as a way of altering induction motor speed

D.C. link inverters can produce a wide range of output frequencies and voltages and induction motor drives using such inverters are therefore capable of a wide range of speeds. Consequently, unlike previously-described methods of altering induction motor speed, a D.C. link inverter can allow a cage induction motor to operate well above its rated synchronous speed. D.C. link inverters can be designed to allow regeneration and are also capable of reversing the direction of rotation of the induction motor. Therefore, full four quadrant operation is possible.

An advantage of D.C. link inverters is that the number of input phases need not be the same as the number of output phases. This can, for example, allow the operation of polyphase motors where only single-phase supplies are available.

The main disadvantages of D.C. link inverters are poor power factor produced in certain circumstances and harmonics produced in the mains supply and the output of the inverter. If necessary, the power factor may be corrected by suitable methods, and the harmonics removed by filtering.

The advantages described above account for the widespread popularity of induction motor drives using D.C. link inverters. In view of their popularity the next section describes some of the common methods of controlling such drives.

2.9 The control of induction motor drives which use D.C. link inverters

2.9.1 Open loop control

Many applications of variable speed induction motor drives such as drives for fans or pumps do not need accurate speed control. Open-loop control is sufficient and the control system simply alters the speed of the induction motor by altering the output frequency and voltage of the inverter. The small change in speed with load of a typical induction motor is considered unimportant.

2.9.2. Closed-loop speed control

Applications demanding more accurate speed control than is possible with open loop control use closed-loop speed control. In its basic form, closed loop speed control compares the actual speed of the induction motor with a desired speed and the difference between the two speeds is used to control the output frequency of the inverter. Phillips [20] and Moffat et al [25] describe examples of such systems. The system described by Moffat et al [25] uses a phase-locked loop to control the induction motor and excellent speed regulation of 0.002% has been achieved.

2.9.3. Current control

Phillips [20] states that a disadvantage of some control systems which use open loop speed control or closed loop speed control alone is that unusual load variations can cause a shutdown of, or even damage to, the drive. Consequently current source inverters have been developed which can produce a constant current output whose magnitude can be controlled. Current control is normally achieved by controlling the firing angles of the thyristors in the rectifier of an inverter and by using a choke in the D.C. link. Phillips [20] describes the operation of such a current source inverter. One main advantage of a current source inverter is that it can limit the current available to the motor and can therefore protect against current overload. Other advantages are the control of torque and the control of flux.

2.9.4 The control of torque

Many speed control schemes use torque control as part of the overall control system. A good example described by Plunkett and Pleete [24] is electric traction where good torque control of the motors regulates the

acceleration of the vehicle and gives the occupants a smooth ride. Torque may be regulated by the following methods:-

Regulation of torque using slip-current control.

Cotton [8] shows that the gross torque developed by an induction motor is given by the relationship

$$T \propto \frac{I_2^2}{\omega s} \tag{2.12}$$

which shows that torque may be regulated by suitable control of I_2 in response to ωs. ωs is a quantity often called the "slip frequency" and is the product of the supply frequency and the motor slip (quantities which are easily measured using appropriate transducers). I_2 is controlled by using a current source inverter which regulates the stator current I_1 of the induction motor in response to ωs. This achieves suitable control of I_2 provided that allowance is made for the magnetising current of the induction motor. Control systems which regulate induction motor torque by controlling current in response to slip and freqency are termed "slip-current" systems. Plunkett and Lipo [26] and Abbondanti and Brennan [27] give examples of such systems together with methods of allowing for magnetising current when controlling the stator current.

Regulation of torque using flux-slip control

Plunkett and Plette [24] describe flux-slip control as an alternative method of torque regulation and quote the following formulae which describe, approximately, the relationships between current, flux, supply voltage and frequency and torque of an induction motor operating at low slip:

$$T \propto \Phi I_2 \tag{2.13}$$

$$\Phi \propto \frac{V}{\omega} \tag{2.14}$$

$$I_2 \propto \Phi \omega s \tag{2.15}$$

From the above equation it may be shown that

$$T \quad \left(\frac{V}{\omega}\right)^2 \omega s \tag{2.16}$$

Since the induction motor is operating at low slip, its speed is approximately proportional to the supply frequency. Plunkett and Plette [24] describe three distinct modes of operation.

1) Constant Torque : if the output voltage and freqency of the inverter are controlled to give constant flux (V/ω) and slip frequency ωs, constant torque operation results.

2) Constant power: As can be seen from equations 2.14 and 2.15 constant motor current and therefore constant power operation results if the output voltage of the inverter is kept constant and the output frequency is controlled so that the slip frequency is proportional to the supply frequency.

3) Torque inversely proportional to the square of the speed: as can be seen from equation 2.16 this may be achieved by maintaining constant inverter voltage and controlling the output frequency so that the slip frequency remains constant. The torque is therefore inversely proportional to the square of the supply frequency and therefore approximately proportional to the square of the speed. In this mode the induction motor behaves like a series-wound D.C. motor.

An advantage of flux-slip control is that a current source inverter is not needed, current control being achieved by appropriate control of slip frequency and supply voltage and frequency according to equations 2.14 and 2.15.

Plunkett [28] states that many induction motor control systems regulate the torque of the motor by controlling the flux and the stator current in a manner according to equation 2.13. This method of torque control is similar in many ways to the torque control of a D.C. machine in which torque is proportional to the flux in the D.C. machine and the armature current. Most induction motor control systems which regulate torque by controlling flux and current assume the flux to be proportional to the voltage divided by the supply frequency and control these quantities accordingly. Current is controlled by a current source inverter.

2.9.5 The computer control of variable speed induction motor drives

The control schemes described in this section have often been implemented by hard-wired logic circuits and discrete components. Recent advances in microprocesor technology has meant that many of these control

systems can now be implemented using microprocessors which promises the advantage of flexibility. Such systems are more flexible than systems using hard-wired logic and discrete components because microprocessor-based systems can implement the control system in software. If it is necessary to change the characteristic of the drive, this can be done by changing the software, with little or no alteration to the hardware.

Sen, Tresize and Sack [29] describe an induction motor drive which uses a microprocessor to achieve current-slip control for torque regualtion. As described previously accurate regulation of torque requires that allowance should be made for magnetising current when controlling the stator current in response to the slip frequency. This resulting relationship between slip frequency and stator current is non-linear and is therefore difficult to implement using hard-wired logic. However, the system described by Sen, Tresize and Sack [29] overcomes this difficulty by storing the relationship in a look-up table in the memory of the microprocessor control system.

Another example of the versatility of microprocessor-based control systems is a phase-locked loop control system described by Harashima and Haneyoshi [30]. This system uses a microprocessor to perform the functions of a P.L.L. to achieve excellent speed control.

An advantage of computer-based speed control systems is that they offer a completely digital system, apart from the transducers. They are therefore substantially free from the drift and offset errors which are inherent in conventional analogue systems. Computer-controlled variable speed induction motor drives are likely to become more common-place due to recent advances in microprocessor technology.

2.10 Summary

This chapter has reviewed the common methods of altering the speed of a cage rotor induction motor. Of all the methods reviewed only D.C. link inversion is capable of four-quadrant control over a wide range of speeds both above and below the rated synchronous speed of the induction motor.

Speed control using D.C. link inversion is efficient and practical and suitable control of the inverter can regulate the torque of the induction motor and can protect the drive against overload. Such speed control is readily suited to a computer and many computer-controlled induction motor drives have been developed.

CHAPTER 3 EQUIPMENT USED IN THIS STUDY

3.1 Introduction

This chapter describes the variable speed induction motor drive built by the author and also describes the equipment used to control the drive. This chapter also describes test and measurement apparatus used in the study of the drive.

3.2 The general form of the variable speed induction motor drive

The variable speed induction motor drive, hereafter referred to as "the drive" used a cage induction motor powered from a V.V.V.F. supply. Figure 3.1 shows a diagram of the drive. The V.V.V.F. supply was derived from powerful linear amplifiers and transformers which produced sinusoidal output waveforms. This was preferred to Q.S.W. or P.W.M. inversion because the resulting V.V.V.F. supply was free from harmonics. Such harmonics were undesirable because they would spoil the performance of the induction motor and also because it is more difficult to analyse an induction motor operating from a non-sinusoidal supply than from a sinusoidal supply.

An alternative to linear amplification would be the use of Q.S.W. or P.W.M. inversion with suitable filtering. However, King [31] lists the following disadvantages of such filters:

1) They tend to be bulky and expensive because they must cope with the full output voltage and current of the inverter.
2) Resistance in the circuit elements of the filters cause power loss.
3) The reactive circuit elements of the filters can produce bad transient voltages and currents during changes in voltage, frequency and load.

Linear amplification tends to be less efficient than Q.S.W. or P.W.M. inversion but work done by King [31] and outlined in Appendix A suggests that linear amplification can produce a sinusoidal three-phase supply with efficiencies comparable with Q.S.W. or P.W.M. inversion. This is achieved by supplying the amplifiers with a waveform comprising the fundamental and the third harmonic of the desired supply frequency. The nature of this waveform, hereafter termed the "high efficiency waveform" is described in Appendix A.

In the drive described in this chapter, digital waveform synthesis was used to produce the high efficiency waveform. Appendix B describes this

Figure 3.1: The Induction Motor Drive

(Single solid lines indicate three-phase connections.)

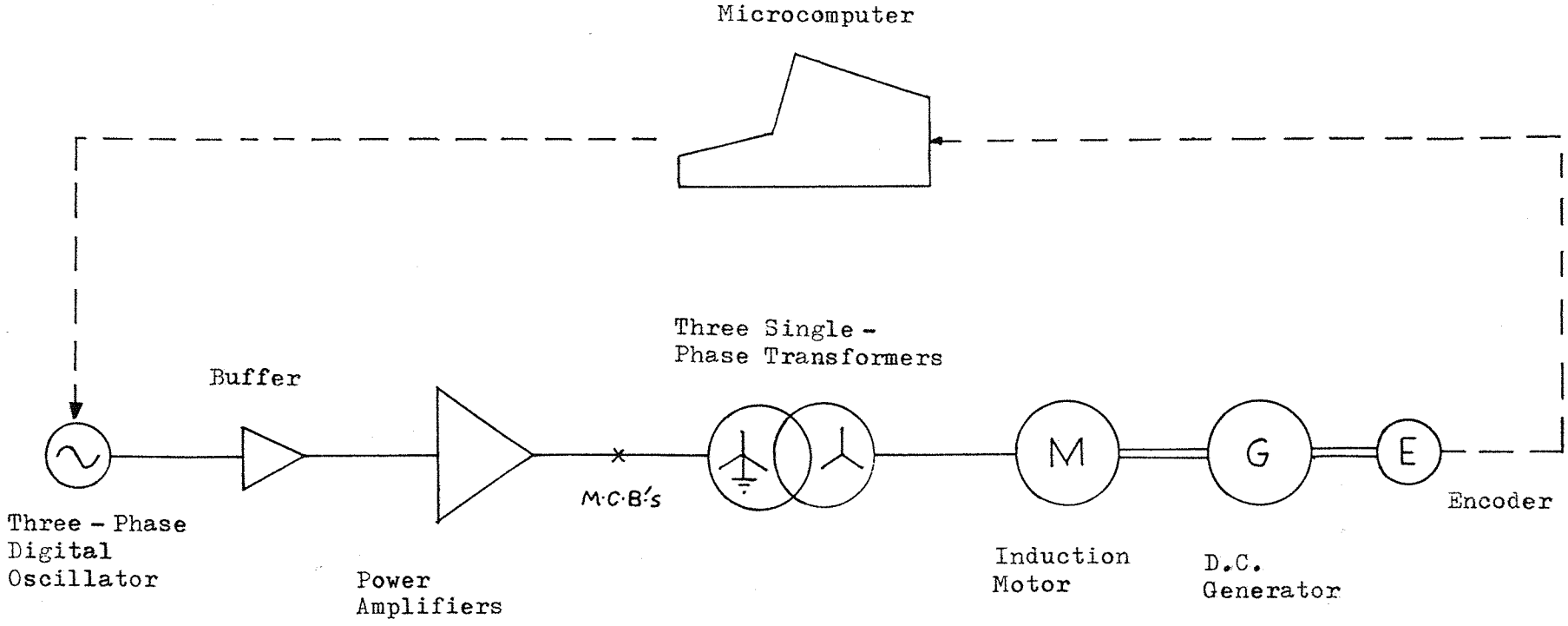

method of synthesis. The presence of the third harmonic in the high efficiency waveform was needed to increase the efficiency of the linear amplification but was not needed in the supply to the induction motor. A suitable connection of the transformers linking the motor to the amplifiers removed the third harmonic producing a sinusoidal supply to the motor.

The three-phase digital oscillator produced the input waveforms for the linear amplifiers. Altering the voltage and frequency of the oscillator altered the voltage and frequency of the supply to the motor and so altered its speed.

An important part of the study of the drive was its behaviour when subject to load. Consequently the induction motor was coupled to a D.C. generator to provide a simple way of loading the motor.

The remainder of this Chapter deals in greater detail with the components of the drive and with equipment used for control, measurement and test.

3.3 The Computer

The computer used to control the drive was an "Apple II" microcomputer which used an 8-bit microprocessor. The computer measured the motor speed by reading an 8-bit binary number produced by a circuit which measured the output frequency of the encoder, the size of the number being proportional to the motor speed. The computer controlled the motor speed by controlling the output frequency of the three-phase digital oscillator. The computer controlled the frequency by sending an 8-bit number along a ribbon cable to the oscillator, the size of the number determining the output frequency.

3.4 The three-phase digital oscillator

The three-phase digital oscillator was designed and built by Mr D. Levett and Mr M. Barkhordah of the Department of Electrical Engineering, the University of Southampton. Figure 3.2 shows a photograph of the outside of the oscillator and Figure 3.3 shows a photograph of the components used in the oscillator. The photographs include a fifty-pence coin to indicate the size of the objects in the photographs.

The oscillator was based upon an 8-bit microprocessor and used digital waveform synthesis to generate three phase voltages having the high

Figure 3.2: Photograph of the Three Phase Digital Oscillator.

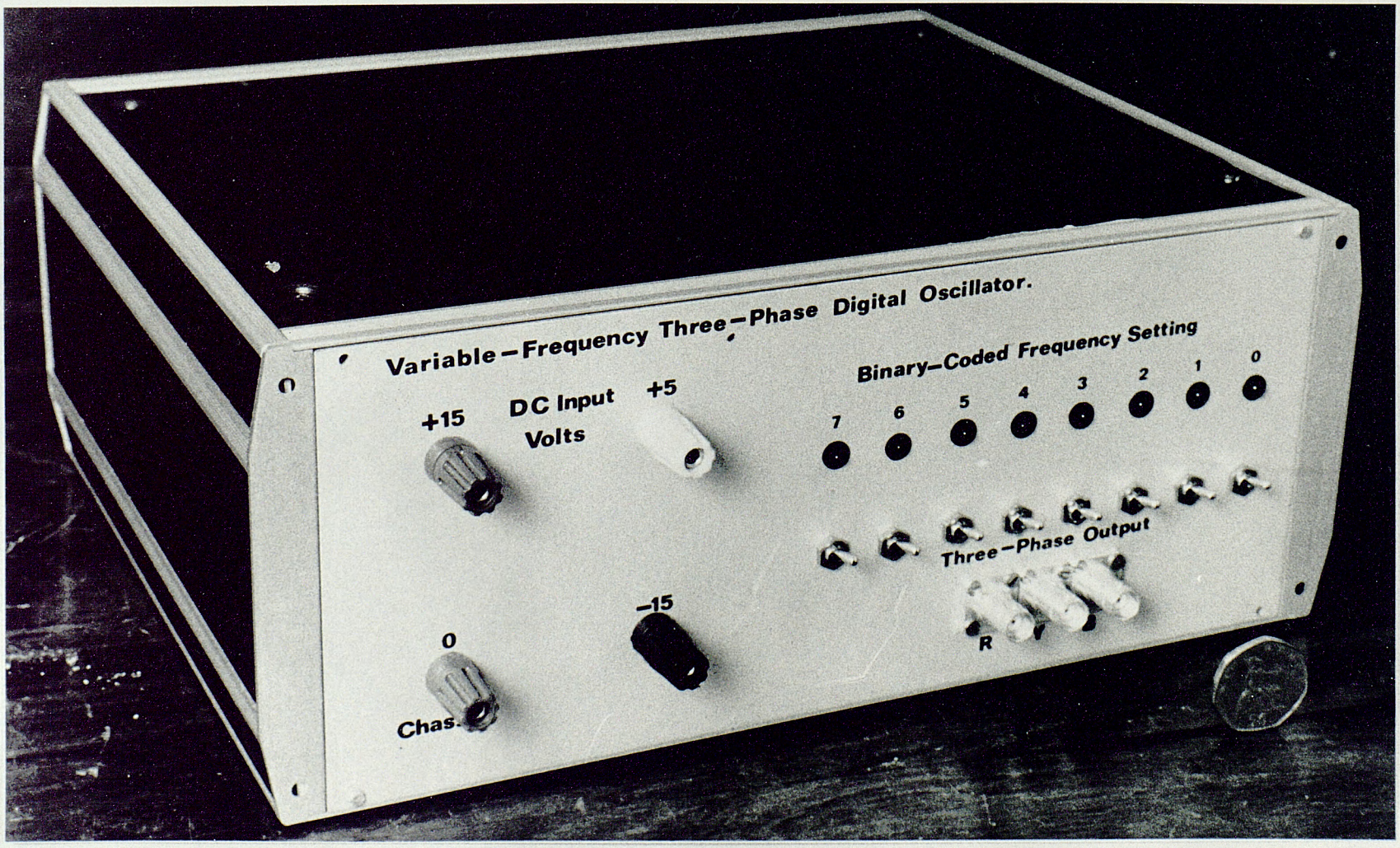

Figure 3.3: Photograph of the Components used in the Three-Phase Oscillator.

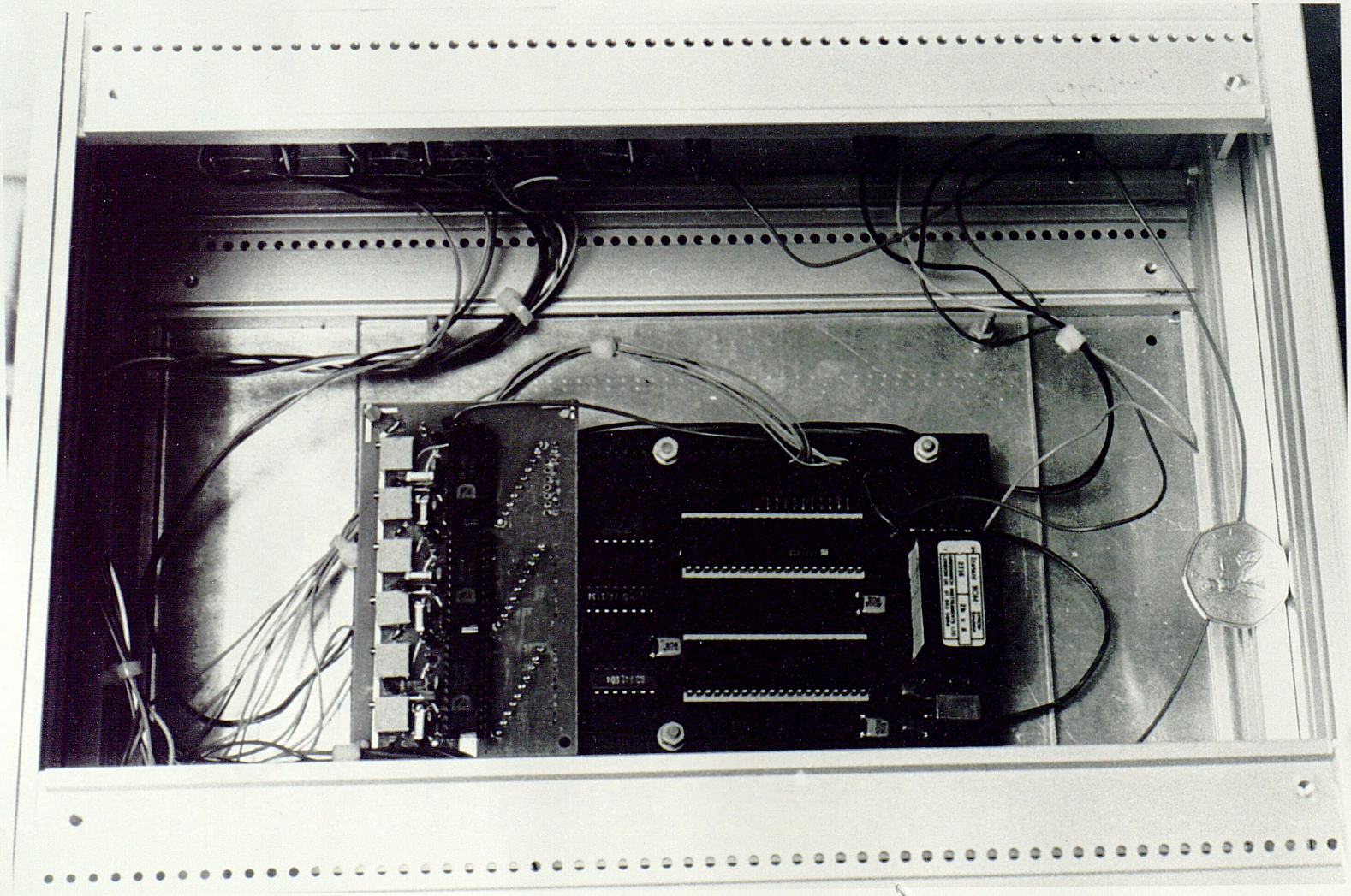

efficiency waveform described in Appendix A. Appendix B describes the principles of digital waveform synthesis and their use in the oscillator.

The oscillator could produce 64 different frequencies between 8.4Hz and 240.4Hz. The frequency could be controlled either by switches on the front of the oscillator or by an 8 bit number sent from the computer to the oscillator along a ribbon cable. A change-over switch selected the method of frequency control.

Each phase waveform had a 5 volt D.C. offset caused by the method of waveform synthesis. However, a buffer circuit between the oscillator and the power blocked the D.C. component preventing it reaching the amplifiers and producing large D.C. power flows in the transformers.

The A.C. component of each phase waveform had a maximum possible amplitude of 10 volts peak-to-peak. The amplitude was not independent of frequency but was controlled by the oscillator so that the amplitude varied with frequency in the following manner:

At frequencies above 50Hz the oscillator produced maximum amplitude. This produced rated voltage across the induction motor terminals. At frequencies below 50Hz the oscillator reduced the amplitude of the A.C. component so that the amplitude was proportional to frequency. This produced an amplifier output voltage proportional to frequency and kept the peak values of the magnetic fluxes in the transformers and the induction motor constant and avoided magnetic saturation. The ratio of amplitude of the A.C. component to frequency produced rated flux in the induction motor.

The operation of the induction motor at rated voltage, or operation at rated flux if the supply frequency is low enough for the rated voltage to cause saturation, results in a more efficient drive because the current needed to produce a given torque is minimized by such operation.

3.5 The buffer circuit

The buffer circuit had three functions:

1) To buffer the outputs of the three phase digital oscillator. The D/A units comprising the outputs could not supply enough current to directly drive the inputs of the power amplifiers.
2) To block the D.C. component of the outputs of the three-phase digital oscillator.
3) To reduce the amplitude of the A.C. component of the outputs of the three-phase digital oscillator. The maximum A.C. component was 10v

peak-to-peak but the maximum input voltage capable of linear amplification by the power amplifiers was 2v peak-to-peak. Therefore the buffer circuit was used to reduce the amplitude of the A.C. component to a fifth of its original value.

Each output phase of the three-phase digital oscillator was buffered by a 741 operational amplifier with associated feedback and input resistors set to give a gain of a fifth. The 741 operational amplifier also boosted the current available to the input of the power amplifier. A capacitor between the output phase and the input resistor connected to the input of the 741 operational amplifier blocked the D.C. component of the output waveform. The values of capacitors and resistors used in the buffer were chosen to that over the whole range of output frequencies there would be no change in amplitude or shape of the output waveform. In other words:

1. The gain of the buffer circuit would be constant with respect to frequency at both the fundamental frequency and the third harmonic frequency of the whole range of output frequencies.
2. The buffer circuit would preserve the phase relationship between the fundamental frequency and the third harmonic frequency over the whole range of output frequencies.

3.6 The power amplifiers

These were stereo power amplifiers, each taking a 240v 50Hz single phase supply. The induction motor drive used two such amplifiers so that four channels were available to power the motor. Only three channels were used for the three phase supply to the motor : one channel for each phase and the remaining channel was spare.

Each channel had a gain control independent of the other channels and had a maximum gain of 50. With maximum gain each channel was able to deliver its maximum A.C. output of 500 VA into a 2.5 Ohm load of any power factor. This corresponds to a maximum output current of 14A r.m.s. and output voltage of 35.5 V r.m.s.

Each amplifier channel featured full protection against thermal and current overload : either type of overload caused the output transistors to overheat which caused a temperature-sensitive device to switch off both channels of the affected amplifier. Each channel also had free-wheeling

diodes across the output transistors to protect against voltage spikes caused by inductive loads.

Manufacturer's data stated that the induction motor would take 2.7 amps, corresponding to 648 VA per phase, during a direct on line start at rated supply voltage and frequency. Since each amplifier channel is rated at 500 VA a direct-on-line start would cause an overload of approximately 30% though in practice this would be reduced because of the impedance of the transformers connecting the motor to the amplifier channels. It was therefore assumed that the amplifiers would tolerate such an overload since it was of short duration.

The manufacturers of the amplifiers advised against connecting the live terminal of any amplifier channel to any other amplifier or any equipment liable to feed power into the amplifier channel.

Each channel had a bandwidth from D.C. to 20kHz. However the channels showed a tendency to oscillate but connecting a small capacitor across the output terminals of each channel stopped the oscillations. Although this reduced the bandwidth of each channel, each was able to amplify faithfully the input waveform at all frequencies used in this study.

3.7 Overcurrent protection

Although each channel of the amplifiers was fully protected against overloads, miniature circuit-breakers (M.C.B.'s) connected as shown in figure 3.1 provided back-up protection. The M.C.B.'s were set to operate at 10 amps though their current-time characteristic allowed them to tolerate small overloads of short duration. This characteristic prevented "nuisance" operation during motor starting. Further protection was provided by a 10amp fuse (not shown in figure 3.1) connected in series with each M.C.B. Figure 3.4 shows a photograph of the box containing the overcurrent protection.

3.8 The transformers

These stepped up the output voltage of the power amplifiers to that needed to drive the induction motor. Three single-phase transformers were preferred against one three-phase transformer to avoid magnetic coupling between adjacent phase windings which could cause one amplifier channel to feed power into another. The low voltage windings were connected in earthed star rather than in delta or isolated star. Connection in isolated star or delta would cause the output currents of two channels to flow into the input of the third which could cause power flow into a channel : a situation against which

the manufacturers advise. Connection in earthed star avoids this situation as each channel supplies its own low voltage winding and cannot supply any other.

The high voltage windings were connected in star as a delta connection would allow large third harmonic currents to flow in the windings in response to the third harmonic component of the high efficiency waveform. Since the stator winding of the induction motor was connected in star and the star point was inaccessible, no connection existed between the star point of the motor winding and the star point of the high voltage winding of the transformer. Consequently no third harmonic current was able to flow in the motor : a necessary conditon for effective use of the high efficiency waveform (see appendix A). The presence or absence of an earth at the star point of the high voltage winding had no effect upon the performance of the induction motor and so the star point was unearthed so that the high and low voltage windings were electrically separate. It was thought that this would prevent any chance of high voltages from the motor circuit travelling along the earth connection common to high and low voltage windings and affecting the computer, buffer circuit and power amplifiers.

Each transformer was rated at 200 VA which produced a combined three phase rating of 600 VA for the three transformers. This rating was sufficient for the power demands of the motor when fully loaded and operating from a 415v 50Hz three phase supply. It was assumed that the transformers would tolerate short duration overloads such as would occur when the motor starts.

The theoretical analysis of the induction motor drive needed the values of elements in the equivalent circuit of the transformers. These values were found using open and short circuit tests and Appendix C lists these values.

For safety, the transformers were housed in a metal box. The connections to the windings were made through sockets on the outside of the box and the box was earthed through the earth pin of a 13-amp plug. Figure 3.4 shows a photograph of the box. A three-pole relay with an A.C. - operated coil connected the high voltage windings to the appropriate sockets on the outside of the box. This relay was supplied from the 13-amp plug through which the box was earthed, and was controlled by a switch on the front of the box. This arrangement allowed easy connection and disconnection of the high voltage windings and also ensured that the box was earthed when these windings were connected.

Figure 3.4: Photograph of the Boxes containing the Overcurrent Protection and the Transformers.

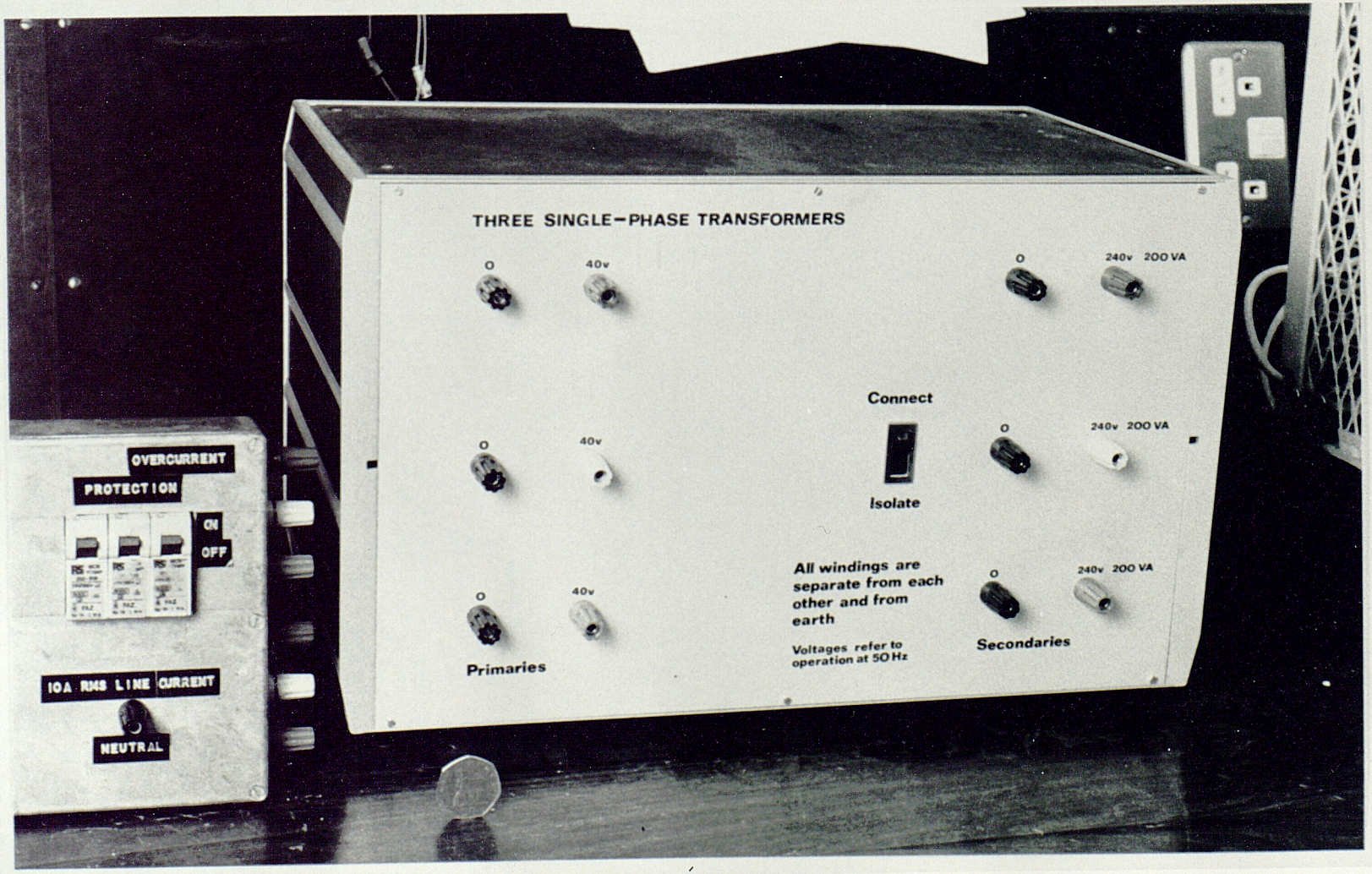

3.9 The motor-generator set

3.9.1 The general form of the motor-generator set

The motor generator set comprised a three phase induction motor directly coupled to a D.C. generator. An encoder measured the speed of both machines. Figure 3.5 shows photograph of the induction motor and the encoder at the side of the enclosure. The wire mesh enclosure prevented inadvertent contact with the rotating shafts of both machines and with the live terminals on each machine. The enclosure also contained a small rectifier which converted single phase 240V 50Hz A.C. from an ordinary 13 amp three pin plug to an unsmoothed D.C. supply suitable for exciting the generator or even driving the generator as a motor. Some of the tests described in Appendix C required the D.C. generator to run as a motor.

The same single phase A.C. supply also supplied the operating coil of a three pole relay inside the enclosure. This relay connnects the three phase supply to the motor when the coil is energised.

The enclosure also had a hinged lid which allowed access to the machines. When the lid was lifted it opened a microswitch which disconnected the A.C. supply to the rectifier and also to the operating coil of the three pole relay. Opening the lid therefore switches off the three phase supply to the motor and also switches off the D.C. supply in the enclosure and unless the D.C. generator was running as a motor from a D.C. supply other than that from the enclosure, both machines would stop. A toggle switch on the front of the enclosure was connected in series with the micro-switch so that operating the toggle switch could control the A.C. supply to the motor and could also control the D.C. supply in the enclosure.

However, opening the lid or operating the toggle switch still left live connections and terminals in the enclosure and care needed to be taken when gaining access to the machine. A future design of enclosure should include shrouding of live parts.

The enclosure was earthed by a connection to the earth conductor of the single phase A.C. supply used in the enclosure. This precaution avoided electric shock from the enclosure. This method of earthing ensured that the motor would not operate nor would the D.C. supply in the enclosure become alive unless the single phase A.C. supply was present, and the presence of the A.C. supply implied that the enclosure was earthed through the earth conductor of that supply.

Figure 3.5: Photograph showing the Motor–Generator Set in its Wire Mesh Enclosure and also showing an Induction Motor similar to that used in the Motor–Generator Set.

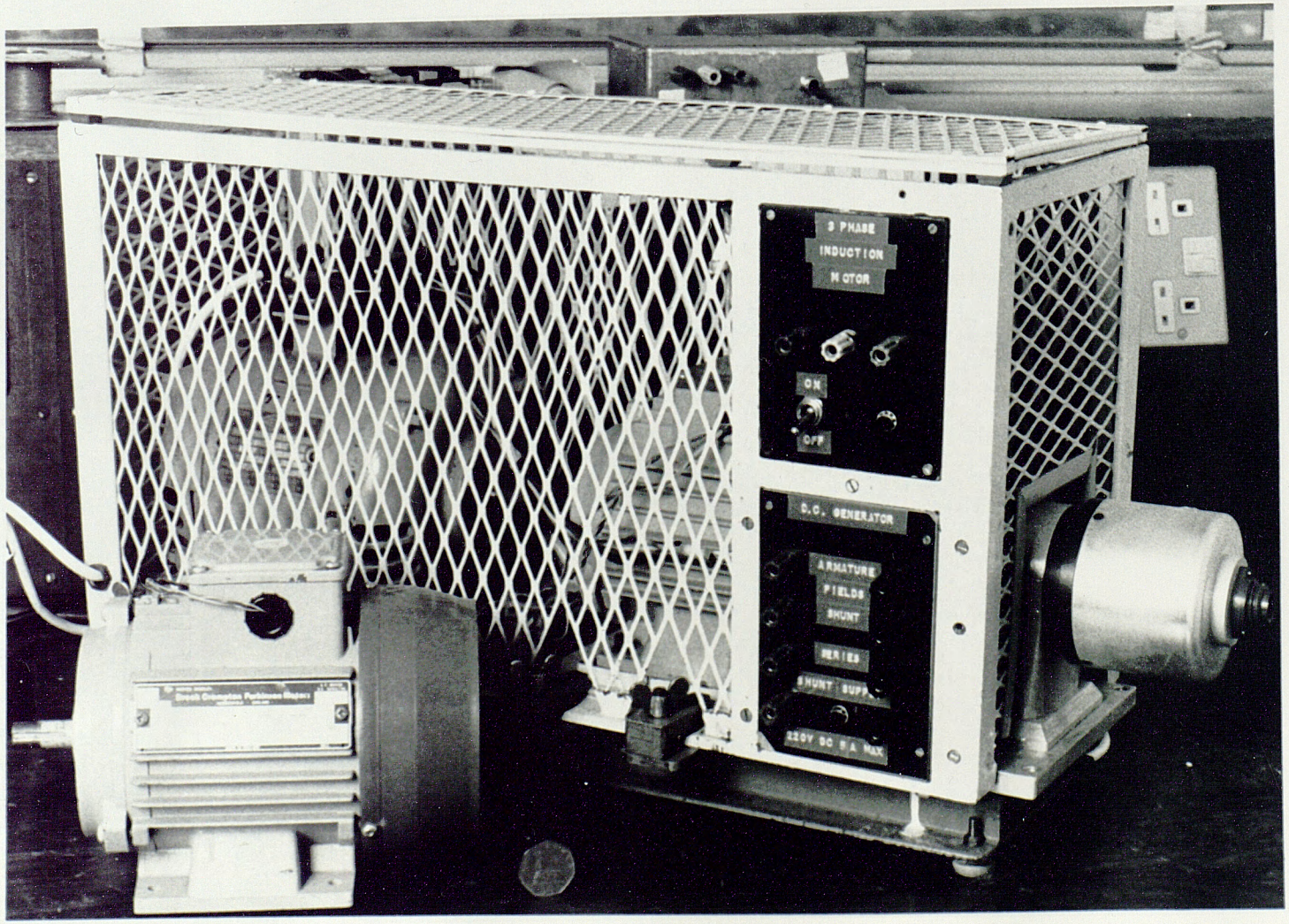

The connections to the machines and the D.C. supply were made to terminals on the front of the enclosure shown in Figure 3.5. Neon indicators on the front of the enclosure showed whether the single phase A.C. supply was present, and whether the D.C. supply was alive.

The encoder was a later addition to the motor generator set and was coupled to the motor in the position shown in Figure 3.5. Although the encoder was mounted outside the enclosure the position of the encoder prevented inadvertent contact with the encoder shaft.

3.9.2 The induction motor

The induction motor was a three-phase four-pole motor designed to run from a 415v 50Hz three-phase supply and therefore had a synchronous speed of 1500 r.p.m. Appendix C gives details about the motor, in particular the values of the elements in its equivalent circuit. These values will be used later in this thesis as part of a theoretical study of the behaviour and control of the induction motor drive.

3.9.3 The D.C. Generator

The D.C. generator was used to load the induction motor and its rated speed, 1400 r.p.m. closely matched the synchronous speed of the induction motor to which it was coupled. The generator had both series and shunt field windings though only the shunt winding was used in this study. Appendix C lists data about the generator, in particular the resistance and self inductance of the armature. These two impedances will be used later in this thesis as part of a theoretical study of the behaviour and control of the induction motor drive.

3.9.4 The encoder

The encoder was an optical shaft encoder which produced a T.T.L. - compatible square waveform whose frequency was proportional to the speed of the encoder shaft. The encoder produced 250 pulses per revolution of its shaft and its shaft was directly coupled to the rotor of the induction motor.

3.10 Measuring equipment

3.10.1 The digital speed-measuring circuit

This circuit measured the speed of the motor by counting the number of encoder pulses during a 15.5 ms period. The circuit represented the

number of pulses counted as an 8 bit binary number which was sent to the computer. At the end of the 15.5 ms period the computer read the number and the circuit was reset by the computer so that it counted the encoder pulses during another 15.5 ms.

The use of the 15.5 ms period arose because Mr D. Levitt originally made the circuit for use in his research. The circuit and its 15.5 ms period was satisfactory for the purposes of this research.

3.10.2 The frequency-to-voltage conversion circuit

This circuit was built by the author to produce a voltage proportional to the frequency of the encoder output and therefore motor speed. A potentiometer adjusted the conversion factor of the circuit.

3.10.3 The measurement of motor speed by a digital frequency meter

A multiply-by-four circuit multiplied the frequency of the encoder output and produced a T.T.L. - compatible square waveform having 1000 pulses per revolution of the encoder. A digital frequency meter calibrated in hertz and measuring the frequency of this waveform produced a display which gave the motor speed in revolutions per second when divided by 1000.

3.10.4 The use of a digital frequency meter to measure the frequency of the supply to the induction motor

This was achieved by measuring the output of an amplifier channel rather than measuring the frequency of the motor supply voltage directly because the motor supply voltage exceeded the rated voltage of the input to the digital frequency meter but the output voltage of an amplifier channel did not.

3.10.5 Measurement of voltage

Meters measured the phase voltages of the motor supply and also the output voltage of the armature of the D.C. generator . An oscilloscope measured the waveforms of voltages of interest and small step down transformers were used to allow the oscilloscope to measure A.C. voltages that would otherwise exceed the rating of the oscilloscope input.

3.10.6 Measurement of current

Meters measured the output currents of all amplifier channels contributing to the three phase supply, the phase currents of the motor and also the armature current of the D.C. generator.

The waveform of each phase current was measured by connecting an oscilloscope or a chart recorder to a resistance connected to the output of a current transformer measuring the phase current in question. Altering the resistance connected to the current transformer altered the amplitude of the trace displayed by the oscilloscope or the chart recorder. The current transformers used were small high quality current transformers suitable for use in measuring instruments.

3.10.7 The chart recorder

The chart recorder was an ultraviolet chart recorder which used mirror galvanometers to draw voltage against time graphs of voltages applied to the inputs of the chart recorder. The chart recorder had eight galvanometers and eight inputs allowing it to draw graphs of eight different inputs simultaneously. The chart recorder was used to measure the motor speed and the motor phase currents in the following way:

1) Measurement of the current of a motor phase : An input of the chart recorder measured the voltage across a resistor connected across the output terminals of a current transformer measuring the phase current in question. The sensitivities of the galvanometers were fixed but the amplitude of the trace could be varied by altering the resistance across the current transformer or by using a potential divider between the resistance and the input to the chart, or both.
2) Measurement of the motor speed. An input to the chart recorder measured the output voltage of the frequency-to-voltage converter which produced a voltage proportional to the motor speed. The amplitude of the trace could be altered by altering the conversion factor of the circuit or by using a potential divider between the output of the circuit and the input of the chart recorder, or both.

3.11 Commissioning the induction motor drive

The induction motor drive was run without computer control to check that the drive itself worked correctly. The drive operated safely and reliably over the whole range of available oscillator frequencies. Although the highest

output freqency, 59.3 Hz, caused the induction motor and D.C. generator to run about 20% above their rated speeds, this was not considered dangerous as such machines may be run safely well above their rated speeds. During commissioning, the following phenomena were observed:

3.11.1 The flow of third harmonic current in the drive

Checks using an oscilloscope showed that there was no third harmonic voltage in the line voltages and no third harmonic currents in the three phase supply to the induction motor. These findings bore out the predictions of Appendix A which also predicted no third harmonic current flow in the low voltage circuit connected to the transformers because there was no third harmonic current in the supply to the motor. However tests with an oscilloscope and a current transformer showed small third harmonic currents in the outputs of the amplifier channels and the neutral connections. It was assumed that these small currents resulted from the third harmonic component of the transformer flux density waveform produced by the third harmonic component of the outputs of each amplifier channel.

3.11.2 Regeneration

While the motor was running a sudden large fall in supply frequency could cause the motor to operate briefly at supersynchronous speed and generate forcing power back into the amplifiers. Although the amplifier channels were not designed to cope with power fed into their outputs, they coped safely with limited regeneration during deceleration. This phenomenon is examined more fully in Section 5.3 of Chapter 5.

3.11.3 Vibration

Vibration was a serious problem that affected the measurement of the speed of the motor. The main symptoms of vibration were:

1) Changes in the output frequency of the encoder. This was noticed as a sideways "jitter" of the encoder waveform when displayed on an oscilloscope. These changes in frequency in turn caused:
2) Changes in the eight bit binary number produced by the digital speed measuring circuit. These changes greatly affected the closed loop control of the drive.
3) Fluctuations in the output voltage of the frequency to voltage converter used to produce a D.C. voltage proportional to speed. These fluctuations

in turn caused undulations in the graph of speed against time drawn by the chart recorder.

An oscilloscope display of the output of the voltage to frequency converter showed that the size and nature of the vibration depended upon the motor speed. The vibration was largest when the motor speed was either close to 120 revolutions per second or 8 revolutions per second. Near such speeds the frequency of vibration was about 39 Hz although the exact frequency depended upon the motor speed.

At speeds greatly different to 20 or 8 revolutions per second the frequency of vibration was approximately equal to the motor speed in revolutions per second. This suggested that the coupled shafts of the motor, generator and encoder had a natural frequency of 39Hz. Likely sources of vibration were the bearings of the motor, generator and encoder, the brushes of the D.C. generator and eccentricity of the shafts. These last two sources would explain why the frequency of vibration depende upon motor speed. The observations described above suggested that the vibrations were causing torsional oscillations involving the shafts of the motor, the generator and the encoder, and the couplings linking the shafts. Furthermore, these oscillations had a natural frequency of about 39 Hz.

The problems of vibration and torsional oscillations were eased by using a more compliant coupling between the encoder and the motor generator set. Another possible solution to the problem of fluctuations in the output voltage of the frequency to voltage converter could be a filter but filtering was not used as a filter could mask or affect changes in output voltage caused by genuine changes in speed.

3.12 Summary

This chapter has described a variable speed induction motor drive based around a cage motor and using a three-phase digital oscillator and linear power amplifiers as V.V.V.F. three-phase supply to the motor. This chapter has drawn attention to the use of a high efficiency waveform to improve the efficiency of the amplifiers, and has also drawn attention to the problems of vibration and torsional oscillations of the motor-generator set.

CHAPTER 4 A MATHEMATICAL MODEL OF THE VARIABLE SPEED INDUCTION MOTOR DRIVE USED IN THIS STUDY

4.1 The purpose of the mathematical model

The mathematical model was to be the basis of a control strategy capable of accurate speed control during all likely operating conditions. In other words the model had to describe accurately the induction motor drive in the following circumstances:

1) Motoring, generating and braking.
2) Forward and reverse direction of rotation.
3) Steady - state and transient operation.

4.2 Mathematical modelling of the induction motor

4.2.1 The equivalent circuit of an induction motor

One of the simplest models of an induction motor is the equivalent circuit described in Section 2.2 of Chapter 2. The equivalent circuit gives a good description of the behaviour of an induction motor under steady state conditions. The equivalent circuit is based upon the assumption of balanced supply voltages and currents and as this assumption is likely to be invalid during transients the equivalent circuit would not be a good basis for a control strategy able to cope with operation during transients.

4.2.2 Representation of a three-phase induction motor by a three-phase machine

Adkins and Harley [32] describe the voltate equation of a three-phase machine. A three-phase machine has six circuits because each three-phase winding has three circuits and there are two three phase windings: one on the stator and one on the rotor. Consequently there are six voltage equations which describe the relationships between voltages and currents in the coils which comprise the windings of the three-phase machine.

The current flowing in a particular coil depends upon the voltage across the coil and also the following quantities:

1) The resistance of the coil
2) The self inductance of the coil
3) The mutual inductances between the coil and each of the other coils on the same member of the machine.
4) The mutual inductances between the coil and each coil on the other members of the machine.

The mutual inductances between the coils means that the current in each coil depends upon the current in the other coils in the machine. This interdependence makes analytical solution of the voltage equations of the three phase machine difficult. Analytical solution is made more difficult because changes in rotor position affect the orientation of the rotor coils with respect to the stator coils and consequently affect the mutual inductances between the stator and rotor coils. If the rotor has saliency, changes in rotor position affect the magnetic circuit of the machine and change the self inductances of coils and the mutual inductances between coils on the same member.

Transforming a three phase induction motor to an equivalent two-axis Kron primitive machine can simplify the voltage equations of the induction motor considerably.

4.2.3 **The two-axis Kron primitive machine** (Adkins and Harley [32]).

The two-axis Kron primitive machine is an idealized representation of a machine which is approximately equivalent to the practical machine. Figure 4.1 shows a diagram of a Kron primitive machine. The machine has two axes, the direct or D-axis and the quadrature or Q-axis. The machine has four coils, one on each axis on each member, that is with coils F and G on the stationary member and coils D and Q on the rotating member. The axes of coils D and F coincide with the D-axis of the machine and the axes of coils Q and G coincide with the Q-axis of the machine. Each coil produces a magnetic field sinusoidally distributed in space. Some machines may need fewer than four coils to represent them while other machines may need more.

The axes of coils D and Q remain fixed on the D and Q axes respectively despite motion of the rotating member. These coils are called "pseudo-stationary" coils and in order that the effects of rotation in a practical machine may be represented accurately, the coils have special properties. The properties are the same as those of a commutator winding, namely:

1) A current in a pseudo-stationary coil produces a field which is stationary in space.
2) Nevertheless a voltage can be induced in the coil by rotation of the moving member.

Figure 4.1: Kron's Primitive Machine.

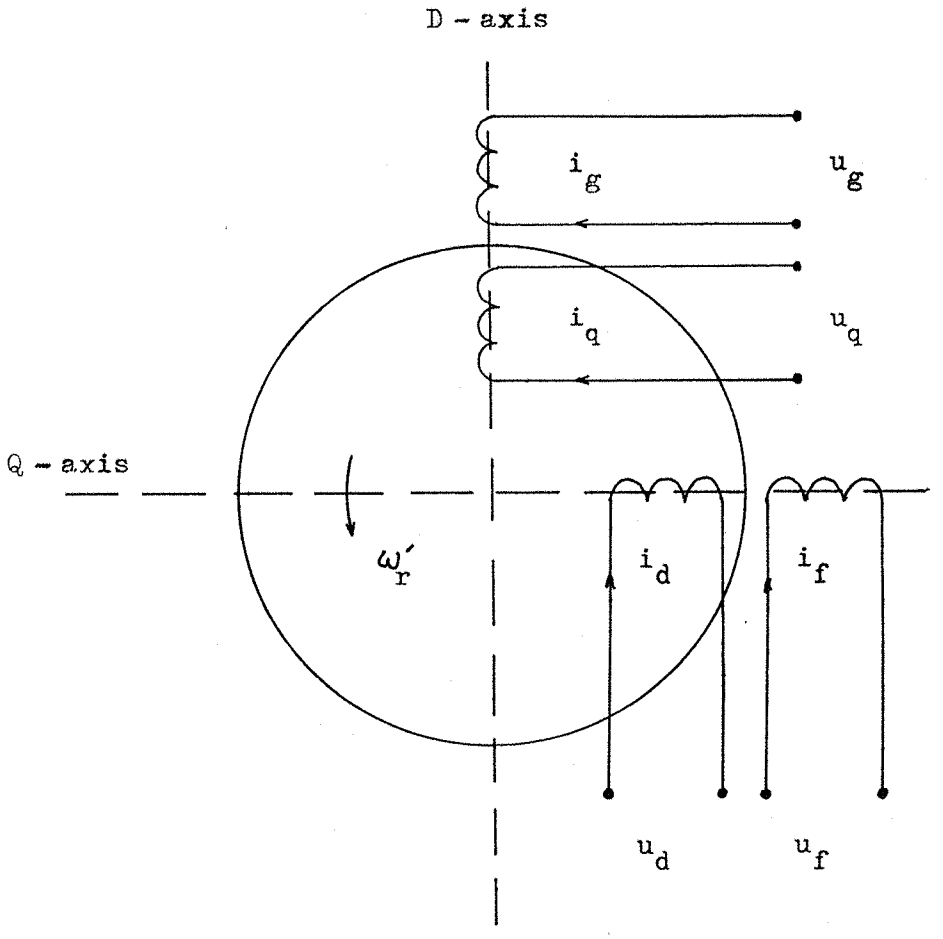

These properties give rise to the following matrix of voltage equations for the primitive machine

$$\begin{pmatrix} u_f \\ u_d \\ u_g \\ u_g \end{pmatrix} = \begin{pmatrix} R_f + pL_{ff} & pL_{df} & 0 & 0 \\ pL_{df} & R_d + pL_d & \omega_r' L_{rq} & \omega_r' L_{rg} \\ -\omega_r' L_{rf} & -\omega_r' L_{rd} & R_q + pL_q & pL_{qg} \\ 0 & 0 & pL_{qg} & R_g + pL_{gg} \end{pmatrix} \begin{pmatrix} i_f \\ i_d \\ i_q \\ i_g \end{pmatrix}$$

(equation 4.1)

where

ω_r' is the rotor speed of Kron's primitive machine

p is the differential operator

u_f, u_d, u_q and u_g are the instantaneous voltages across coils F, D, Q and G respectively.

i_f, i_d, i_q, i_g, are the instantaneous currents in coils F, D, Q and G respectively.

R_f, R_d, R_q, and R_g are the resistances of coils F, D, Q and G respectively.

L_{ff}, L_d, L_q, and L_{gg} are the self inductances of coils F, D, Q and G respectively.

L_{df} is the mutual inductance between coils D and F.

L_{qg} is the mutual inductance between coils Q and G.

L_{rf}, L_{rd}, L_{rq}, L_{rg} are constants similar in nature to inductances and determine the voltage induced in a rotor coil on one axis due to rotation in the magnetic field produced by a coil on the other axis.

Kron's primitive machine is simpler to analyse than a three phase machine for the following reasons:

1) Kron's primitive machine needs only four circuits to represent the three phase induction motor.
2) The mutual inductance between the rotor and stator coils does not change with rotor position because
   a) The axes of the stator coils and the pseudo-stationary rotor coils stay fixed regardless of rotor position.
   b) The magnetic fields produced by the stator coils and the pseudo-stationary rotor coils remain fixed in space regardless of rotor position.
3) Currents in a particular stator coil are unaffected by currents in coils on the other axis because the magnetic fields produced by these coils do not have a component along the axis of the stator coil in question since the D and Q axes are perpendicular. This results in less mutual inductance

terms in the voltage equations of Kron's primitive machine than in the voltage equations of the three-phase machine.

The following subsections describe how Kron's primitive machine can represent an induction motor.

4.2.4 The voltage equations of Kron's primitive machine when used to represent a three phase induction motor.

Adkins and Harley [32] show that provided some assumptions are made about a three-phase induction motor it may be represented by Kron's primitive machine. One assumption is that the motor windings are wound so that at any point in time each phase current produces an M.M.F. sinusoidally distriubted in space. This assumption is reasonable for the stator winding of an induction motor and the rotor winding of a wound rotor machine. Say [5] assumes that the currents in a cage rotor are sinusoidally distributed and Adkins and Harley [32] show that a cage winding can be treated as a two-phase winding for the purposes of analysis using Kron's primitive machine. Consequently it may be assumed that the cage winding produces an M.M.F. sinusoidally distributed in space.

Say [5] states that although the magnetic material of the motor is "semi-saturated" to economize on material costs, the air gap of the machine forms the major part of the reluctance of the magnetic circuit. It may therefore be assumed that the sinusoidal M.M.F.'s produced by each phase current produce add together produce a sinusoidally distributed flux density since the air gap of an induction motor is uniform and saturation may be neglected.

It should be emphasised that the above assumptions depend upon the construction of the motor and the nature of the magnetic material of the motor. Since the construction of the motor does not change during its operation the flux density may be assumed to be sinusoidally distributed during both steady state operation and operation during transients provided neither condition saturates the motor.

Adkins and Harley [32] show how Equation 4.1, the voltage equations of Kron's primitive machine, may be simplified and adapted to represent a three phase induction motor:

1) The assumption of a sinusoidal flux density distribution in the machine leads to the following simplifications

$L_{rd} = L_d$ (4.2) $L_{rf} = L_{df}$ (4.3)

$$L_{rq} = L_q \quad (4.4) \qquad L_{rg} = L_{qg} \quad (4.5)$$

2) If the electrical characteristics of each phase are the same then

$$R_f = R_g \quad (4.6) \qquad R_d = R_q \quad (4.7)$$

$$L_{ff} = L_{gg} \quad (4.8) \qquad L_d = L_q \quad (4.9)$$

$$L_{df} = L_{qg} \quad (4.10)$$

Adkins and Harley [32] also show that the above quantities are related to the circuit elements of the equivalent circuit according to the equations:

$$R_f = R_g = R_1 \quad (4.11) \qquad R_d = R_q = R_2 \quad (4.12)$$

$$L_{ff} = L_{gg} = L_1 \quad (4.13) \qquad L_d = L_q = L_2 \quad (4.14)$$

$$L_{df} = L_{qg} = M \quad (4.15)$$

Where:

M is the per-phase mutual inductance between the stator and rotor windings of the induction motor and is given by the equation:

$$M = \frac{X_m}{\omega} \quad (4.16)$$

and

$$L_1 = M + \frac{X_1}{\omega} \quad (4.17) \text{ and}$$

$$L_2 = M + \frac{X_2}{\omega} \quad (4.18)$$

3) A cage rotor has a short-circuited winding and so

$$u_d = u_q = 0 \quad (4.19)$$

Substituting equations 4.2 to 4.15 and equation 4.19 into equation 4.1 yields the voltage equation of Kron's primitive machine representing a three-phase induction motor :

$$\begin{pmatrix} u_f \\ 0 \\ 0 \\ u_g \end{pmatrix} = \begin{pmatrix} R_1 + pL_1 & pM & 0 & 0 \\ pM & R_2 + pL_2 & \omega_r' L_2 & \omega_r' M \\ -\omega_r' M & -\omega_r' L_2 & R_2+pL_2 & pM \\ 0 & 0 & pM & R_1 + pL_1 \end{pmatrix} \begin{pmatrix} i_f \\ i_d \\ i_q \\ i_g \end{pmatrix} \quad (4.20)$$

There are two important points to note about the above equation:

1) Kron's primitive machine model of an induction motor does not include the resistance R_m which represents the magnetising losses of the induction motor. This is not a serious omission as it is commonly

assumed that R_m has little effect on the performance of the induction motor, and so the mathematical model developed in this Chapter to model the induction motor drive ignores R_m.

2) It should be noted that ω_r', the speed of the rotor of Kron's primitive machine representation of the induction motor, is the rotor speed of a two-pole motor (Adkins and Harley [32]).

4.2.5 The torque equation of Kron's primitive machine

The torque equation of Kron's primitive machine can be derived by considering the voltages in coils D and Q of the rotor. In the D coil:

1) pMi_f is the voltage induced in coil D by the current i_f in coil F and the mutual inductance between coils D and F.

2) $(R_2 + pL_2)\, i_d$ is the voltage drop across the resistance and self-inductance of coil D.

3) $\omega_r' L_2\, i_q$ is the voltage induced in coil D by its rotation in the magnetic field produced by current i_q flowing through coil Q.

4) $\omega_r' M\, i_g$ is the voltage induced in coil D by its rotation in the magnetic field of coil G.

The last two voltages represent the conversion of electrical power to mechanical power by the current i_d. The mechanical power P_d developed in coil D is given by the product of i_d and the sum of those two voltages :

$$P_d = i_d \omega_r' (L_2 i_q + M i_g) \tag{4.21}$$

By symmetry the mechanical power P_q developed in coil Q is given by

$$P_q = - i_q \omega_r' (M i_f + L_2 i_g) \tag{4.22}$$

The total mechanical power P_k developed in the rotor is the sum of the mechanical powers developed in each coil and is given by

$$P_k = P_d + P_q \tag{4.23}$$

substituting equations 4.21 and 4.22 for P_d and P_q in equation 4.23 and dividing by ω_r' yields the torque T_k developed by Kron's machine:

$$T_k = M (i_d i_g - i_f i_q) \tag{4.24}$$

4.2.6 The relationship between currents and voltages in a three phase induction motor and its equivalent Kron's primitive machine (Adkins and Harley [32])

Stator winding voltages and currents: Kron's primitive machine represents a three phase stator winding by an equivalent two phase winding. The following three-phase to two-phase transformation gives the relationship between the currents in both windings.

$$\begin{pmatrix} i_f \\ i_g \\ i_z \end{pmatrix} = \frac{2}{3} \begin{pmatrix} 1 & -\frac{1}{2} & -\frac{1}{2} \\ 0 & -\frac{\sqrt{3}}{2} & \frac{\sqrt{3}}{2} \\ \frac{1}{2} & \frac{1}{2} & \frac{1}{2} \end{pmatrix} \begin{pmatrix} i_R \\ i_Y \\ i_B \end{pmatrix} \tag{4.25}$$

where i_R, i_Y and i_B are the instantaneous currents in the red, yellow and blue phases respectively.

i_z is called the "zero sequence" current, a term adopted from symmetrical component theory, and is defined by

$$i_z = \frac{1}{3} (i_R + i_Y + i_B) \tag{4.26}$$

and represents an instantaneous value of current which may vary with time in any manner. It may be visualized physically as the magnitude of each of a set of equal currents flowing in all three phases and therefore producing no resultant M.M.F.

In a delta connected winding, or a star connected winding whose star pointed is isolated from the neutral of the three phase supply, by Kirchoff's laws, $i_R + i_Y + i_B$ equals zero since the current in one phase equals the sum of the currents in the other two phases. According to equation 4.26 i_z, therefore, equals zero in such windings.

The corresponding two-phase to three phase transformation also exists and is the inverse of equation 4.25:

$$\begin{pmatrix} i_R \\ i_Y \\ i_B \end{pmatrix} = \begin{pmatrix} 1 & 0 & 1 \\ -\frac{1}{2} & -\frac{\sqrt{3}}{2} & 1 \\ -\frac{1}{2} & \frac{\sqrt{3}}{2} & 1 \end{pmatrix} \begin{pmatrix} i_f \\ i_g \\ i_z \end{pmatrix} \tag{4.27}$$

Similar equations to equations 4.25, 4.26 and 4.27 relate the voltages u_f and u_g of the two phase stator winding of Kron's primitive machine with the three phase voltages of a three phase stator winding:

$$\begin{pmatrix} u_f \\ u_g \\ u_z \end{pmatrix} = \frac{2}{3} \begin{pmatrix} 1 & -\frac{1}{2} & -\frac{1}{2} \\ 0 & -\frac{\sqrt{3}}{2} & \frac{\sqrt{3}}{2} \\ \frac{1}{2} & \frac{1}{2} & \frac{1}{2} \end{pmatrix} \begin{pmatrix} v_R \\ v_Y \\ v_B \end{pmatrix} \tag{4.28}$$

and

$$\begin{pmatrix} v_R \\ v_Y \\ v_B \end{pmatrix} = \begin{pmatrix} 1 & 0 & 1 \\ -\frac{1}{2} & -\frac{\sqrt{3}}{2} & 1 \\ -\frac{1}{2} & \frac{\sqrt{3}}{2} & 1 \end{pmatrix} \begin{pmatrix} u_f \\ u_g \\ u_z \end{pmatrix} \qquad (4.29)$$

where v_R, v_Y and v_B are the instantaneous red, yellow and blue phase voltages u_z is the "zero sequence" phase voltage, the concept of which is similar to the zero sequence current i_z.

u_z is defined by

$$u_z = \frac{1}{3}(v_R + v_Y + v_B) \qquad (4.30)$$

These voltage equations can be used to transform a three phase supply having balanced voltages to an equivalent two-phase supply. Consider such a three phase supply having red-yellow-blue phase rotation and having the following voltage equations:

$$v_R = \sqrt{2}\ V \cos \omega t \qquad (4.31)$$

$$v_Y = \sqrt{2}\ V \cos (\omega t + 120^\circ) \qquad (4.32)$$

$$v_B = \sqrt{2}\ V \cos (\omega t - 120^\circ) \qquad (4.33)$$

substituting these equations into equation 4.28 yields

$$u_f = \sqrt{2}\ V \cos \omega t \qquad (4.34)$$

$$u_g = \sqrt{2}\ V \sin \omega t \qquad (4.35)$$

and the zero sequence voltage u_z equals zero. Thus the equivalent two phase supply has two phases 90° apart in phase but having the same phase voltage as the three phase supply. The equivalent two phase supply is also balanced and has no zero sequence component.

Rotor winding currents.

The rotor circuit of a cage motor is inaccessible and consequently the rotor currents are unavailable for measurement or control. Therefore the relationship between the actual rotor currents in a cage rotor induction motor and currents in the rotor of the equivalent Kron's primitive machine are not of direct relevance to this study. The relationship, called Park's transformation, is described by Adkins and Harley [32].

4.2.7 The relationship between the torque developed in a three-phase induction motor and the torque developed in the equivalent Kron's primitive machine.

Equation 4.24 states that the torque T_k developed in the equivalent Kron primitive machine is given by

$$T_k = M (i_d i_g - i_f i_q) \tag{4.24}$$

However, this is not the same as the torque developed by the equivalent three phase motor. This difference arises because of the nature of the three phase to two phase transformation of equation 4.25. Adkins and Harley [32] describe in detail the effect of the transformation upon the relationship between the torque developed in both machines and state that

$$T_2 = \frac{3}{2} T_k \tag{4.36}$$

where T_2 is the torque developed in an equivalent three-phase two-pole induction motor.

4.2.8 Summary of the advantages and use of Kron's primitive machine as a mathematical model of an induction motor.

The chief advantage of Kron's primitive machine is that it avoids the difficulty of solving equation which contain coefficients which vary with rotor position, namely the mutual inductances between the rotor and stator coils. The use of Kron's primitive machine reduces the number of voltage equations of the motor since Kron's primitive machine has less phases than the equivalent three-phase machine. The use of Kron's primitive machine also eliminates the effect of mutual inductances between stator phases.

Consequently when studying the behaviour of the induction motor it is easier to use the voltage equations of Kron's primitive machine and the transformations between three phase and two phase systems, rather than use the voltage equations of a three phase induction motor.

The next section uses Kron's primitive machine to develop state-space equations of the induction motor.

4.3 The differential equations describing the induction motor drive.

4.3.1 The differential equations of the Kron primitive machine used to represent the induction motor

Equation 4.20 may be written as

$$\underline{U} = \underline{Z}\,\underline{I} \tag{4.37}$$

where

$\underline{U}$ is a four element column matrix describing the voltages across the coils of the primitive machine, and $\underline{I}$ is a four element column matrix describing the currents in the coils of the primitive machine. The elements of $\underline{U}$ and $\underline{I}$ are

$$\underline{U} = \begin{pmatrix} u_f \\ 0 \\ 0 \\ u_g \end{pmatrix} \quad (4.38) \qquad \text{and} \qquad \underline{I} = \begin{pmatrix} i_f \\ i_d \\ i_q \\ i_g \end{pmatrix} \tag{4.39}$$

$\underline{Z}$ is a four-by-four square matrix whose elements are the various resistances and inductances of the Kron primitive machine used to represent the induction motor.

$$\underline{Z} = \begin{pmatrix} R_1 + pL_1 & pM & 0 & 0 \\ pM & R_2 + pL_2 & \omega'_r L_2 & \omega'_r M \\ -\omega'_r M & -\omega'_r L_2 & R_2 + pL_2 & pM \\ 0 & 0 & pM & R_1 + pL_1 \end{pmatrix} \tag{4.40}$$

$\underline{Z}$ may be expressed in terms of three four-by-four square matrices, $\underline{R}$, $\underline{L}$ and $\underline{G}$, the rotor speed of the Kron primitive machine ω'_r and the differential operator p:

$$\underline{Z} = \underline{R} + p\,\underline{L} + \omega'_r \underline{G} \tag{4.41}$$

where

$$\underline{R} = \begin{pmatrix} R_1 & 0 & 0 & 0 \\ 0 & R_2 & 0 & 0 \\ 0 & 0 & R_2 & 0 \\ 0 & 0 & 0 & R_1 \end{pmatrix} \quad (4.42) \qquad L = \begin{pmatrix} L_1 & M & 0 & 0 \\ M & L_2 & 0 & 0 \\ 0 & 0 & L_2 & M \\ 0 & 0 & M & L_1 \end{pmatrix} \tag{4.43}$$

and

$$\underline{G} = \begin{pmatrix} 0 & 0 & 0 & 0 \\ 0 & 0 & L_2 & M \\ -M & -L_2 & 0 & 0 \\ 0 & 0 & 0 & 0 \end{pmatrix} \tag{4.44}$$

Substituting equation 4.41 for $\underline{Z}$ in equation 4.37, rearranging and using dot notation instead of the differential operator p yields

$$\dot{\underline{I}} = \underline{L}^{-1}\,(\underline{U} - \underline{R}\,\underline{I} - \omega'_r\,\underline{G}\,\underline{I}) \tag{4.45}$$

which is the matrix form of the state-space equations which describe the voltages and currents in Kron's primitive machine representing the three-phase induction motor.

Manipulation of equation 4.45 is made easier by substituting:

$$\underline{A} = \underline{L}^{-1}\underline{R} \qquad (4.46)$$

$$\underline{B} = \underline{L}^{-1}\underline{G} \qquad (4.47)$$

$$\underline{C} = \underline{L}^{-1} \qquad (4.48)$$

in equation 4.45 to yield:

$$\dot{\underline{I}} = \underline{C}\,\underline{U} - \underline{A}\,\underline{I} - \omega_r'\,\underline{B}\,\underline{I} \qquad (4.49)$$

The above expression shows that the currents in Kron's primitive machine depend upon the rotor speed of the primitive machine. The next two subsections describe how the torques exerted in the motor generator set affect ω_r', the rotor speed of the Kron's primitive machine representation of the induction motor.

4.3.2 The torques in the motor-generator set

Throughout the following analysis, the symbol ω_r, which has been used to represent the speed of the rotor of an induction motor will be used to represent the speed of both the rotor of the induction motor and the armature of the D.C. generator since the shafts of both machines are directly coupled. ω_r will therefore be termed the speed of the motor-generator set.

Figure 4.2 shows a diagrammatic representation of the motor-generator set which shows elements representing the different torques exerted in the motor-generator set. These different elements and the torques exerted by them are described below:

Kron's primitive machine and the torque multiplication factor.

The torque multiplication factor multiplies the torque output of Kron's primitive machine by $1\frac{1}{2}$ as that it equals the torque output of the equivalent two pole machine represented by the primitive machine. The torque output of the two pole machine is given by equation 4.36:

$$T_2 = \frac{3}{2} T_k \qquad (4.36)$$

The ideal gearbox

The use of Kron's primitive machine to represent the induction motor is based upon a two-pole motor whereas the induction motor used in the drive had four poles. The ideal gearbox has a ratio of $n_p : 1$ where n_p is the number of pole-pairs of the induction motor used in the drive (in this case, $n_p = 2$).

Figure 4.2: A Diagrammatic Representation of the Motor-Generator Set.

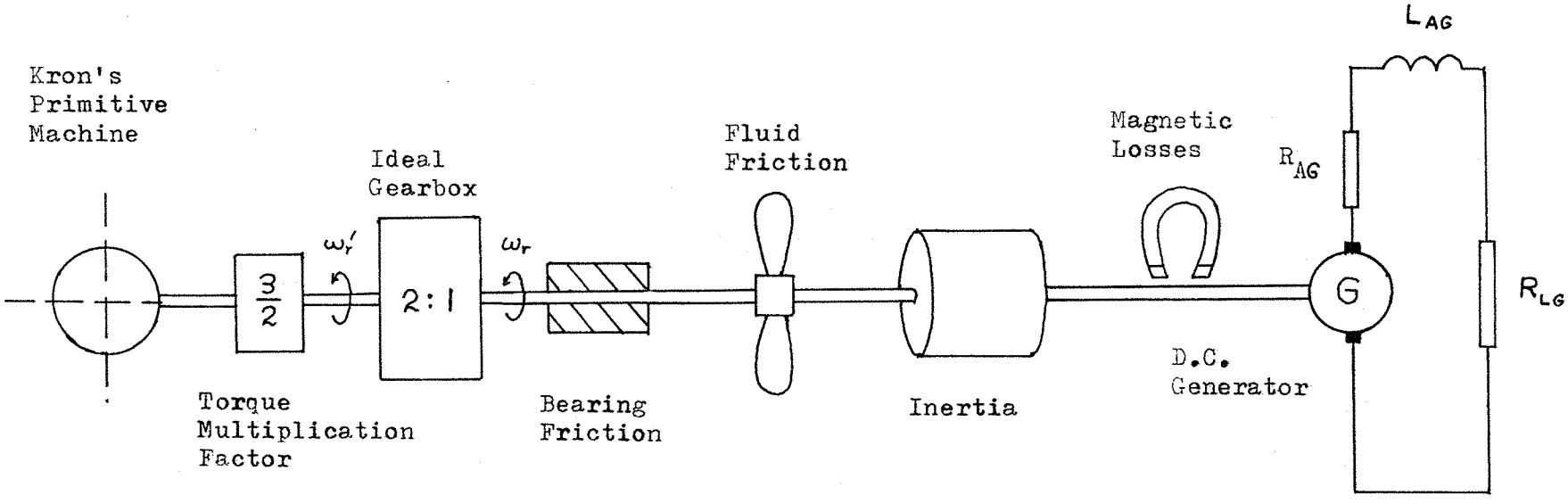

The ideal gearbox converts the torque and speed of the two-pole motor upon which the Kron's primitive machine representation has been based, to the torque and speed of the four-pole motor used in this study. The conversion is according to the following expressions :

$$T = n_p T_2 \tag{4.50}$$

$$\omega_r = \frac{\omega'_r}{n_p} \tag{4.51}$$

The bearing and brush friction torque T_b

This torque represents the friction between surfaces in the bearings of the induction motor, the D.C. generator and the encoder, and also between the surfaces of the brushes and commutator segments of the D.C. generator. At standstill this torque equals the torque produced by the induction motor until the torque produced by the induction motor overcomes the static friction of the surfaces described above. When this situation is reached the shafts of the motor-generator set rotate and the bearing and brush torque is assumed to be constant regardless of speed and to act in a direction to oppose the rotation. The magnitude of this torque is called the dynamic bearing and brush frictional torque, T_{bd}, and represents the dynamic friction in the bearings and the brushes. Appendix C lists the value of T_{bd}.

The description of the behaviour of T_b may be summarized by the following statements

1) If $\omega_r > 0$, $T_b = T_{bd}$

2) If $\omega_r < 0$, $T_b = -T_{bd}$

3) If $\omega_r = 0$ and $|T| \leq T_{bd}$ then $T_b = \pm T$, the sign of T_b being such that T_b opposes T, the torque produced by the induction motor.

4) If $\omega_r = 0$ and $|T| > T_{bd}$ then $T_b = \pm T_{bd}$, the sign of T_b being such that it opposes T, the torque produced by the induction motor. In such a case, the difference between T and T_b causes the shafts of the motor-generator set to begin to rotate.

It should be noted that the torque needed to overcome the static friction and rotate the shafts of the motor generator set would be greater than T_{bd} because static friction is greater than dynamic friction. However, the difference between static and dynamic friction has been assumed to be insignificant for the purposes of this study.

The fluid friction torque T_{ff}

This represents the fluid friction torque of windage, and of lubricant in the bearings. The fluid friction torque is assumed to be proportional to the speed of the motor-generator set according to the equation:

$$T_{ff} = k_{ff}\ \omega_r \tag{4.52}$$

where k_{ff} is the fluid friction constant. Appendix C lists the value of k_{ff}.

The polar moment of inertia J.

J is the polar moment of inertia of the rotating parts of the motor-generator set about their common axis. These rotating parts exert a torque T_J upon the induction motor when ω_r changes. T_J is given by:

$$T_J = J\frac{d\omega_r}{dt} \tag{4.53}$$

Appendix C lists the value of J for the motor-generator set.

The D.C. Generator

Fitzgerald and Kingsley [6] show that the torque T_{AG} exerted by a D.C. generator as a result of electro-mechanical energy conversion in the armature is given by the following formula:

$$T_{AG} = \frac{E_{AG} I_{AG}}{\omega_r} \tag{4.54}$$

where

I_{AG} is the armature current.

E_{AG} is the E.M.F. generated in the armature winding. Fitzgerald and Kingsley [6] also show that E_{AG} is related to Φ_G, the magnetic flux in the D.C. generator according to the equation:

$$E_{AG} = K_{AG}\omega_r\ \Phi_G \tag{4.55}$$

where K_{AG} is the armature constant of the D.C. generator.

The excitation E_x of the D.C. generator may be defined as the voltage generated per unit speed and in which case E_x is given by the following equation:

$$E_x = \frac{E_{AG}}{\omega_r} \tag{4.56}$$

which by substituting equation 4.55 for E_{AG} into the above equation yields:

$$E_x = K_{AG}\ \Phi_G \tag{4.57}$$

Equations 4.55 and 4.56 show that E_{AG} and E_x depend upon Φ_G and are therefore limited by magnetic saturation which limits Φ_G.

Combining equations 4.54 and 4.56 yields

$$T_{AG} = E_x I_{AG} \tag{4.58}$$

Magnetic losses

These arise from eddy currents and hysterisis in the armature as it rotates in the magnetic field of the D.C. generator. Cotton [8] states that the following relationship gives a good estimate of P_{MAG}, the power loss produced by the magnetic losses

$$P_{MAG} = k_{MAG}\, \omega_r^{\gamma} \tag{4.59}$$

Where

γ is the magnetic loss index

k_{MAG} is the magnetic loss constant. Experimental tests described in Appendix C suggests that a good estimate of k_{MAG} is given by the relationship

$$k_{MAG} = k_x (E_x)^q \tag{4.60}$$

where k_x is a constant and q is an index which describe the variation of k_{MAG} with E_x.

Substituting equation 4.60 for k_{MAG} in equation 4.59 and dividing the result by ω_r gives an expression for the torque T_{MAG} exerted by the magnetic losses:

$$T_{MAG} = k_x (E_x)^q\, \omega_r(\gamma - 1) \tag{4.61}$$

Appendix C lists values of k_x and q found from experimental tests.

The following analysis shows how each of the elements illustrated in Figure 4.2 and described in the previous subsection affect the rotor speed wr of the Kron's primitive machine representation of the induction motor, and the armature current of the D.C. generator.

4.3.3 The differential equation describing ω_r

The torque T_L exerted upon the induction motor by elements of the motor-generator set comprise:

1) Torques due to rotational losses = T_b, T_{ff} and T_{MAG}
2) The torque T_J needed to accelerate or decelrate the inertia of the motor-generator set.
3) the torque T_{AG} exerted by the conversion of mechanical power to electrical power in the D.C. generator.

T_L is equal to the sum of the above torques and is given by

$$T_L = T_b + T_{ff} + T_{MAG} + T_J + T_{AG} \tag{4.62}$$

Substituting equations 4.52, 4.53, 4.54, 4.58 and 4.61 for T_{ff}, T_J, T_{AG} and T_{MAG} respectively yields:

$$T_L = T_b + k_{ff}\,\omega_r + k_x\,(E_x)^q\,\omega_r^{(\gamma-1)} + J\,\frac{d\omega_r}{dt} + E_x I_{AG} \qquad (4.63)$$

However, the torque T_L exerted upon the induction motor equals the torque T produced by the induction motor and therefore equation 4.61 may be re-written as:

$$T = T_b + k_{ff}\,\omega_r + k_x\,(E_x)^q\,\omega_r^{(\gamma-1)} + J\,\frac{d\omega_r}{dt} + E_x\,I_{AG} \qquad (4.64)$$

Using equations 4.36 and 4.50 to replace T in the above equation by T_k, and substituting equation 4.51 for ω_r in the above equation yields:

$$\frac{3}{2}n_p\;T_k = T_b + k_{ff}\,\frac{\omega_r'}{n_p} + k_x(E_x)^q\left(\frac{\omega_r'}{n_p}\right)^{(\gamma-1)} + \frac{J}{n_p}\,\frac{d\omega_r'}{dt} + E_x I_{AG} \qquad (4.65)$$

Rearranging the above equation and substituting equation 4.36 for T_K yields:

$$\frac{d\omega_r'}{dt} = \frac{1}{J}\left(\frac{3}{2}\,n_p{}^2 M(i_d i_g - i_f i_q) - n_p T_b - k_{ff}\omega_r' - k_x(E_x)^q n_p^{(2-\gamma)}\omega_r'^{(\gamma-1)} - n_p E_x I_{AG}\right) \qquad (4.66)$$

4.3.4 The differential equation describing I_{AG}, the armature current of the D.C. generator

This is derived from the equation of current flow in the D.C. generator armature circuit:

$$E_{AG} = I_{AG}\,(R_{AG} + R_{LG}) + L_{AG}\,\frac{dI_{AG}}{dt} \qquad (4.67)$$

where

r_{AG} is the resistance of the armature of the generator
R_{LG} is the load resistance connected to the generator output
L_{AG} is the self inductance of the D.C. generator armature
E_{AG} is the generated voltage in the generator armature

Rearranging equation 4.56 and substituting the resultant equation for E_{AG} into equation 4.57 and substituting equation 4.51 for ω_r in the resulting equation and rearranging yields:

$$\frac{dI_{AG}}{dt} = \frac{1}{L_{AG}}\left(\frac{E_x\omega_r}{n_p} - I_{AG}\,(R_{AG} + R_{LG})\right) \qquad (4.68)$$

4.4 Summary of the differential equations describing the induction motor drive.

The differential equations describing the currents in the Krons primitive machine representation of the induction motor are represented by the matrix equation

$$\dot{\underline{I}} = \underline{L}^{-1} (\underline{U} - \underline{R}\,\underline{I} - \omega_r' \underline{G}\,\underline{I}) \tag{4.45}$$

The differential equation describing ω_r', the rotor speed of the Kron's primitive machine representation of the induction motor is

$$\frac{d\omega_r'}{dt} = \frac{1}{J}\left(\frac{3}{2} n_p^2 M (i_d i_g - i_f i_g) - n_p T_b - k_{ff}\omega_r' - k_x (Ex)^q n_p^{(2-\gamma)} \omega_r^{(\gamma-1)} - n_p E_x I_{AG}\right) \tag{4.66}$$

The differential equation describing I_{AG}, the armature current of the generator is:

$$\frac{dI_{AG}}{dt} = \frac{1}{L_{AG}}\left(\frac{E_x \omega_r'}{n_p} - I_{AG}(R_{AG} + R_{LG})\right) \tag{4.68}$$

Appendix C gives values for some of the constants and indices in the equations above, and describes how these values were found. The constants and indices described in Appendix C are :

1) The circuit elements of the equivalent circuit of the induction motor.
2) Constants and indices describing the rotational losses in the motor generator set.
3) The moment of inertia of the motor-generator set.
4) The resistance and self inductance of the armature of the D.C. generator.

each phase of the equivalent three-phase voltage source equals the sum of the following:

1) The internal impedance of an amplifier channel referred to the high voltage winding of a transformer.
2) The resistance and leakage reactance of both windings of a transformer referred to the high voltage winding of a transformer.

This analysis assumes that the amplifier channels are similar to each other and also that the transformers are similar to each other.

The internal impedance of the equivalent Thevenin source is in series with the resistance and leakage reactance of the stator winding of the induction motor, and may therefore be included as extra stator winding resistance and leakage inductance in the voltage equations describing the induction motor. In other words, R_1 and L_1 are modified as follows:

L_1 = M , the per-phase mutual inductance between the rotor and stator windings of the induction motor, plus
The leakage reactances of both windings of a transformer referred to the high voltage winding, plus
The internal impedance of an amplifier channel referred to the high voltage winding of a transformer (4.69)

R_1=The per-phase resistance of the stator winding of the induction motor, plus
The resistances of both windings of a transformer referred to the high voltage winding, plus
The internal resistance of an amplifier channel referred to the high voltage winding of the transformer. (4.70)

Appendix C lists the values of the impedances of the transformers and the amplifier channels, each impedance being referred to the high voltage winding of the transformer. Appendix C also describes how these values were found.

4.6 The state-space equations of the induction motor drive

4.6.1 General form of the state-space equations

The general form of the state space equations of the induction motor drive is:

$$\frac{d\underline{x}}{dt} = \underline{f}(\underline{x}, \underline{U}) \tag{4.71}$$

where

$\underline{x}$ is a column matrix containing the variables which vary with time in the differential equations which describe the induction motor drive.

$\underline{U}$ is the voltage matrix described previously

$\underline{f}$ is a function matrix which describes the relationship between the elements of $\underline{U}$, $\underline{x}$ and $\frac{d\underline{x}}{dt}$

4.6.2 The conversion of the differential equations of the induction motor drive to state-space form

The conversion may be achieved by the following steps

$$x_1 = i_f \quad (4.72), \qquad x_2 = i_d \quad (4.73)$$

$$x_3 = i_q \quad (4.74), \qquad x_4 = i_g \quad (4.75)$$

$$x_5 = \omega'_r \quad (4.76), \qquad x_6 = I_{AG} \quad (4.77)$$

and define $\underline{x}$ as

$$\underline{x} = \begin{pmatrix} \underline{I} \\ \omega'_r \\ I_{AG} \end{pmatrix} = \begin{pmatrix} x_1 \\ x_2 \\ x_3 \\ x_4 \\ x_5 \\ x_6 \end{pmatrix} \tag{4.78}$$

and

$$\dot{\underline{x}} = \frac{d\underline{x}}{dt} = \begin{pmatrix} \dot{x}_1 \\ \dot{x}_2 \\ \dot{x}_3 \\ \dot{x}_4 \\ \dot{x}_5 \\ \dot{x}_6 \end{pmatrix} \tag{4.79}$$

where the dot notation denotes differentiation with respect to time.

Define

$$\underline{f} = \begin{pmatrix} f_1 \\ f_2 \\ f_3 \\ f_4 \\ f_5 \\ f_6 \end{pmatrix} \qquad (4.80)$$

where f_1, f_2 etc are functions which relate x_1, x_2 etc, respectively, to the state space variables x_1, x_2 etc and the elements of the voltage matrix $\underline{U}$.

Functions f_1 to f_6 are defined below:

Functions f_1 to f_4

These follow from considering the matrix equation 4.49. Define the elements of matrices A, B and C in the following ways:

Elements of A = a (k, l)

Elements of B = b (k, l)

Elements of C = c (k, l) where k, l = 1, 2, 3, 4.

Then from equations 4.49, 4.71, 4.80 and using equations 4.72, to 4.77 as substitutes for x_1 to x_6 yields

$$f_1 (\underline{x}, \underline{u}) = (a_{11} + b_{11} x_5)x_1 + (a_{12} + b_{12}x_5)x_2 + (a_{13} + b_{13}x_5)x_3 + (a_{14} + b_{14}x_5)x_4 + c_{11}u_f + c_{14} u_g \qquad (4.81)$$

$$f_2 (\underline{x}, \underline{U}), = (a_{21} + b_{21}x_5)x_1 + (a_{22} + b_{22}x_5)x_2 + (a_{23} + b_{23}x_5)x_3 + (a_{24} + b_{24}x_5)x_4 + c_{21}u_f + c_{24}u_g \qquad (4.81)$$

$$f_3(\underline{x}, \underline{U}) = (a_{31} + b_{31}x_5)x_1 + (a_{32} + b_{32}x_5)x_2 + (a_{33} + b_{33}x_5)x_3 + (a_{34} + b_{34}x_5)x_4 + c_{31} u_f + c_{34}u_g \qquad (4.83)$$

$$f_4(\underline{x}, \underline{U}) = (a_{41} + b_{41}x_5)x_1 + (a_{42} + b_{42}x_5)x_2 + (a_{43} + b_{43}x_5)x_3 + (a_{44} + b_{44}x_5)x_4 + c_{41} u_f + c_{44}u_g \qquad (4.84)$$

Function f_5

This is derived from equations 4.66, 4.71, 4.79 and 4.80 and equation 4.72 to 4.77 as substitutes for x_1 to x_6.

$$f_5 (\underline{x}, \underline{u}) = \frac{1}{J} \left(\frac{3}{2} n_p^2 M (x_2x_4 - x_1 x_3) - n_p T_b - k_{ff}x_5 - k_x (E_x)^q \; n_p^{(2-\delta)} \; x_5^{(\delta-1)} - n_p \; E_x \; x_6 \right) \qquad (4.85)$$

Function f_6

This is derived from equations 4.68, 4.71, 4.79 and 4.80 and equations 4.72 to 4.77 as substitutes for x_1 to x_6.

$$f_6(x, u) = \frac{1}{L_{AG}}\left(\frac{k_{AG}\, x_5}{n_p} - x_6 (R_{AG} + R_{LG})\right) \tag{4.86}$$

4.7 The solution of the state space equations

4.7.1 Iterative solution using the fifth order Kutta-Merson set of equations

The differential equations of 4.45, 4.66, and 4.68 which describe the induction motor have coefficients which vary with time. Particular examples include ω'_r, in equations 4.45 and 4.68 and I_{AG}, i_f, i_d, i_q and i_g in equation 4.66. This means that these differential equations and the resulting state space equations cannot be solved analytically and a numerical method must be used. The method chosen used step by step integration using the fifth order Kutta-Merson algorithm. This algorithm was chosen because it allowed a larger interval betwen the steps and yet offers good accuracy. Adkins and Harley [32] describe the fifth order Kutta-Merson algorithm.

5^{th} order Kutta-Merson algorithm

$$\underline{K}_1 = \frac{h}{3}\underline{f}\,(\underline{x}_n, t_n) \tag{4.87}$$

$$\underline{K}_2 = \frac{h}{3}\underline{f}\left(\underline{x}_n + \underline{K}_1, t + \frac{h}{3}\right) \tag{4.88}$$

$$\underline{K}_3 = \frac{h}{3}\underline{f}\left(\underline{x}_n + \frac{1}{2}(\underline{K}_1 + \underline{K}_2), t + \frac{h}{3}\right) \tag{4.89}$$

$$\underline{K}_4 = \frac{h}{3}\underline{f}\left(\underline{x}_n + \frac{1}{8}(3\,\underline{K}_1 + 9\,\underline{K}_3), t + \frac{h}{2}\right) \tag{4.90}$$

$$\underline{K}_5 = \frac{h}{3}\underline{f}\left(\underline{x}_n + \frac{1}{2}(3\,\underline{K}_1 - 9\underline{K}_3 + 12\underline{K}_4), t + h\right) \tag{4.91}$$

and $$\underline{x}_{n+1} = \underline{x}_n + \frac{1}{2}(\underline{K}_1 + \underline{K}_5) + 2\,\underline{K}_4 \tag{4.92}$$

where

$\underline{x}_n$ is the value of matrix $\underline{x}$ at time t_n during the algorithm,

h is the step-length

$\underline{x}_{n+1}$ is the value of matrix $\underline{x}$ at time $t_n + h$ (the time at which the next step in the algorithm occurs).

$\underline{K}_1$, $\underline{K}_2$, $\underline{K}_3$ $\underline{K}_4$ and $\underline{K}_5$ are termed coefficients of the fifth order Kutta-Merson algorithm and are six element column matrices.

4.7.2 Inputs to the fifth order Kutta-Merson algorithm.

The inputs are:

1) u_f and u_g, the supply voltages to the two-phase winding of Kron's primitive machine representing the induction motor. Equation 4.28 relates u_f and u_g to the supply to the three phase motor.
2) The initial conditions. These are the values of the elements $\underline{x}$ at time t = 0 in the algorithm. The matrix containing these values is denoted $\underline{x}_o$. The initial conditions depend upon the past history of the motor-generator set before the start of the algorithm, and with the set at rest with no currents flowing in the motor or generator, $\underline{x}_o = O$.

4.7.3 The calculation of the currents in the motor-generator set, and the speed of the motor - generator set

The solutions to the state-space equations are the rotor speed, the currents in the coils of Kron's primitive machine used to represent the induction motor, and the D.C. generator armature current. The speed and the phase current of the three-phase induction motor may be calculated from the following equations based upon the two-phase to three-phase voltage transformation of equation 4.29 and remembering that $i_f = x_1$ and $i_g = x_4$. Since the induction motor winding is connected in isolated star there is no zero sequence current and so:

$$i_R = x_1 \tag{4.93}$$

$$i_Y = -\tfrac{1}{2}(x_1 + \sqrt{3}\, x_4) \tag{4.94}$$

$$i_B = \tfrac{1}{2}(-x_1 + \sqrt{3}\, x_4) \tag{4.95}$$

The speed of the induction motor is derived from equations 4.76 and 4.51

$$\omega_r = \frac{x_5}{n_p} \tag{4.96}$$

4.8 The calculation of the steady-state speed of the motor -generator set

4.8.1 The equations which describe the steady-state speed of the motor-generator set

The state-space equations described in Section 4.6 are not essential for describing the steady-state speed : equations based upon the equivalent circuit of the induction motor are adequate.

Equation 2.4 of Chapter 2 describes the torque-speed characteristic of the induction motor in terms of the elements of the equivalent circuit.

$$T = \frac{mE_t^2 R_2}{(\omega_o - \omega_r)\left(\left(R_t + \frac{\omega_o R_2}{\omega_o - \omega_r}\right)^2 + (X_t + X_2)^2\right)} \qquad (2.4)$$

Equation 4.63 describes T_L, the torque exerted upon the induction motor. During steady-state operation, ω_r is constant and therefore $\frac{d\omega_r}{dt}$ equals zero. Therefore, during steady-state operation, equation 4.64 simplifies to

$$T_L = T_b + k_{ff}\omega_r + k_x(E_x)^q \omega_r^{(\gamma-1)} + E_x I_{AG} \qquad (4.97)$$

During steady state operation, I_{AG} is constant and E_{AG} may be expressed as

$$E_{AG} = (V_{AG} + I_{AG}R_{AG}) \qquad (4.98)$$

Where V_{AG} is the ouput voltage at the terminals of the armature of the D.C. generator.

From the above equation and the definition of excitation given in equation 4.56, the excitation E_x is given by:

$$E_x = \frac{V_{AG} + I_{AG}R_{AG}}{\omega_r} \qquad (4.99)$$

Substituting this equation for E_x in equation 4.96 yields

$$T_L = T_b + k_{ff}\omega_r + k_x\left(\frac{V_{AG} + I_{AG}R_{AG}}{\omega_r}\right)^q \omega_r^{(\gamma-1)} + \frac{(V_{AG} + I_{AG}R_{AG})\, I_{AG}}{\omega_r} \qquad (4.100)$$

This equation describes the torque T_L exerted upon the induction motor in terms of ω_r, the speed of the motor generator set, the armature current I_{AG}, the voltage V_{AG} at the armature terminals and the constants and indices which describe the rotational losses of the motor-generator set.

It may be shown, using equations 4.58, 4.59 and 4.99 that the term

$$k_x \left(\frac{(V_{AG} + I_{AG}R_{AG})}{\omega_r} \right)^q \omega_r{}^{(\gamma-1)}$$

equals T_{MAG}, the torque exerted by the magnetising losses and the term

$$\frac{(V_{AG} + I_{AG}R_{AG})I_{AG}}{\omega_r}$$

equals T_{AG}, the torque exerted by the conversion of mechanical power to electrical power in the armature of the D.C. generator.

Since the torque T produced by the induction motor equals T_L, the torque exerted upon the induction motor, equating equations 2.4 and 4.100 produces an equation which describes the steady-state speed of the motor-generator set:

$$\frac{mE_t{}^2R_2}{(\omega_o - \omega_r)\left(\left(R_t + \frac{\omega_o R_2}{\omega_o - \omega_r}\right)^2 + (X_t + X_2)^2\right)} =$$

$$= T_b + k_{ff}\omega_r + k_x\left(\frac{V_{AG} + I_{AG}R_{AG}}{\omega_r}\right)^q \omega_r^{(\gamma-1)} + \frac{(V_{AG} + I_{AG}R_{AG})\ I_{AG}}{\omega_r} \quad (4.101)$$

This equation is difficult to solve analytically. However, it may be solved numerically. The next two subsections describe the types of solutions to the above equation, and a numerical method of finding a value of ω_r which is near the synchronous speed of the induction motor and which satisfies the above equation.

4.8.2 A graphical description of possible solutions to the equation describing the steady-state speed of the motor-generator set

The equation may be solved numerically by considering the two equations from which it has been derived : equations 2.4 and 4.100. If graphs of T and T_L are plotted against ω_r, any intersection of the graphs will represent a solution to equation 4.101, the equation describing the steady-

state speed of the motor-generator set. The solution of the equation is considered under the following circumstances.

1) Operation with the D.C. generator loaded and excited.

2) Operation with the D.C. generator unloaded and unexcited.

Loaded, excited D.C. generator

Figure 4.3 shows graphs of T and T_L against ω_r. The graph of T against ω_r is a graph of equation 2.4 and is the torque-speed characteristic of the induction motor. The graph of T_L against ω_r is a graph of equation 4.100 in which V_{AG} and I_{AG} are both constant and equal to the values of V_{AG} and I_{AG}, respectively for which the solution of the equation describing the steady-state speed of the motor-generator set is required. Any intersection of these two graphs implies that $T = T_L$ and therefore represents a solution of the equation describing the steady-state speed of the motor-generator set.

The shape of the graph of T_L against ω_r has been derived in the following manner:

1) As ω_r tends to infinity, the term $k_{ff}\omega_r$ dominates and T_L increases with speed.

2) As ω_r tends to zero the terms representing the torques due to magnetic losses and electrical generation tend to infinity since the denominators of these terms contain positive powers of ω_r (remembering that Appendix C quotes $\gamma = 1.34$ and $q = 2.75$ for the motor generator set used in this study).

3) From the behaviour of T_L near $\omega_r = 0$ and ω_r = infinity there must be at least one minimum value of T_L between ω_r equals zero and ω_r equals plus infinity. The turning values of T_L may be found by differentiating equation 4.100 with respect to ω_r :

$$\frac{dT_L}{d\omega_r} = k_{ff} + k_x(\gamma-q-1)\left(\frac{V_{AG} + I_{AG}R_{AG}}{\omega_r}\right)^q \omega_r^{(\gamma-2)} - \frac{(V_{AG} + I_{AG}R_{AG})\, I_{AG}}{\omega_r^2} \qquad (4.102)$$

Further information about the turning values may be obtained by differentiating the above equation with respect to ω_r.

$$\frac{d^2T_L}{d\omega_r^2} = k_x(\gamma-q-1)(\gamma-q-2)\left(\frac{V_{AG} + I_{AG}\ R_{AG}}{\omega_r}\right)^q \omega_r^{(\gamma-3)} + \frac{2(V_{AG} + I_{AG}R_{AG})}{\omega_r^3} \qquad (4.103)$$

Figure 4.3: Graphs of T_L and T against ω_r for the Motor-Generator Set operating with the D.C. Generator loaded and delivering constant V_{AG} and constant I_{AG}

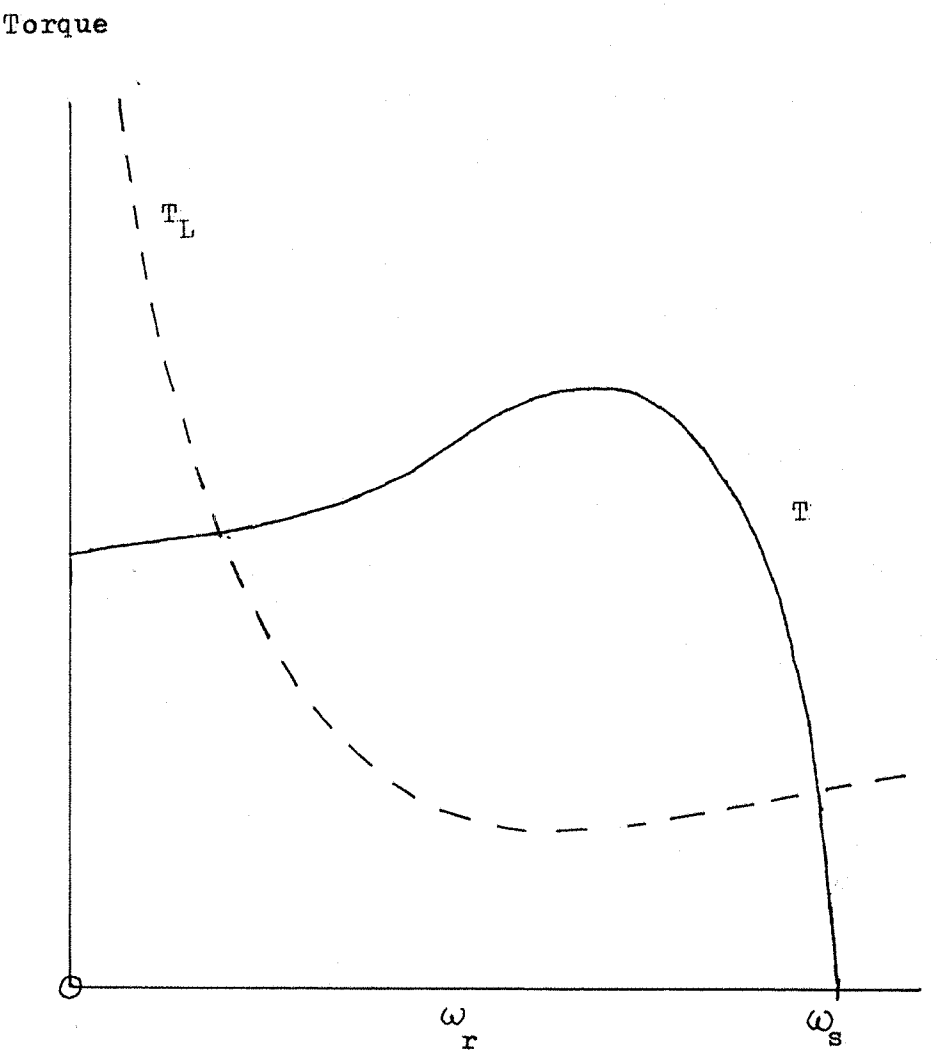

According to this equation $\frac{d^2T_L}{d\omega_{r2}}$ is always positive for values of ω_r between zero and plus infinity and therefore there is only one turning point in this range of ω_r and that turning point is a minimum.

The value of ω_r at which the minimum value of T_L occurs is that value which makes $\frac{dT_L}{d\omega_r} = 0$ in equation 4.102. Substituting this value of ω_r into equation 4.100 gives the minimum value of T_L. Equation 4.102 shows that the speed at which minimum T_L occurs depends upon V_{AG} and I_{AG}. Figure 4.3 shows this speed to be below that of the synchronous speed of the induction motor although a value above the synchronous speed is possible, depending on V_{AG} and I_{AG}.

It should be noted that although equation 4.99 suggests that T_L will tend to plus infinity as ω_r tends to zero, this will not happen in practice for the following reasons:

Equation 4.100 shows that an infinite value of T_L at $\omega_r = 0$ would require a non-zero value of V_{AG} and therefore infinite excitation would be needed, according to equation 4.99. Magnetic saturation limits the excitation of the D.C. generator, and consequently at very low speeds the D.C. generator will not be able to deliver the value of V_{AG} for which a solution to the equation describing the steady-state speed of the motor-generator set is required.

Figure 4.3 shows two intersections of the graphs of T and T_L against ω_r, indicating two possible solutions to the equation describing the steady-state speed of the motor-generator set. One solution corresponds to operation just below the synchronous speed of the induction motor. The other solution corresponds to operation at a very low speed, but this may not occur because of the problem of maintaining output voltage V_{AG} at very low speeds.

However, if the excitation of the D.C. generator is able to maintain V_{AG} at this low speed, the motor-generator set will operate stably because any increase in speed will, for a given excitation, cause a proportionate increase in E_{AG}, I_{AG} (assuming a fixed load resistance connected to the armature) and therefore V_{AG}. This will result in an almost proportional increase in T_L with speed. However, the torque-speed characteristic of the induction motor, shows that the torque produced by the induction motor does not increase with speed as fast as T_L. Therefore the motor-generator set will slow down and V_{AG}, I_{AG}, T, T_L and ω_r will settle back to their original values

given by the intersection of the graphs of T and T_L at a speed well below synchronous speed. By similar reasoning any slight decrease in speed will cause a difference between T and T_L which will act to restore the speed to that given by the intersection of the graphs.

It must be remembered that any changes in T_L produced by change in speed at a given excitation will not lie along the graph of T_L against ω_r in Figure 4.3 since this graph assumes constant values of V_{AG} and I_{AG} whereas any change in speed at a given excitation will cause a change in V_{AG} and I_{AG}.

Unloaded, unexcited D.C. generator

A special case exists if the D.C. generator is unloaded and unexcited. In this case, V_{AG} and I_{AG} equal zero and T_L is given by

$$T_L = T_b + k_{ff}\omega_r \qquad (4.104)$$

and so equation 4.101 which describes the steady state speed of the induction motor becomes:

$$\frac{mE_t^2R_2}{(\omega_0-\omega_r)\left(\left(R_t + \frac{\omega_0 R_2}{\omega_0-\omega_r}\right)^2 + (X_t + X_2)^2\right)} = T_b + k_{ff}\omega_r \qquad (4.105)$$

This solution of this equation is given by the intersection of the graph of T against ω_r, given by equation 2.4, with the graph of T_L against ω_r, given by equation 4.104. Equation 4.104 describes a straight line graph and the number and type of solutions to equation 4.101 depends upon the relationship of this graph to the shape of the graph of T against ω_r. Figure 4.4 shows four diagrams of graphs of T and T_L against ω_r and these diagrams of graphs show four possible relationships between the graphs and indicate the number and types of solution to equation 4.105.

Diagram (a) of Figure 4.4 shows a situation in which T is greater than T_L for most motor speeds. The intersection of the graphs of T and T_L against ω_r occur at point A in diagram (a) and represents operation at a speed just below the synchronous speed of the induction motor. Operation at this speed is stable for small changes in speed so these changes result in differences between T and T_L which act to oppose the change in speed.

If the frequency of the supply to the induction motor remains the same but the voltage is reduced from that which produced the graph of T against ω_r in diagram (a), the torque produced at any given speed decreases and it is possible to produce a graph of T against ω_r similar to that shown in

Figure 4.4: Graphs of T and T_L against ω_r for the motor-generator set operating with an unloaded unexcited D.C. generator. These graphs indicate possible solutions to the equation describing the steady-state speed of the motor-generator set.

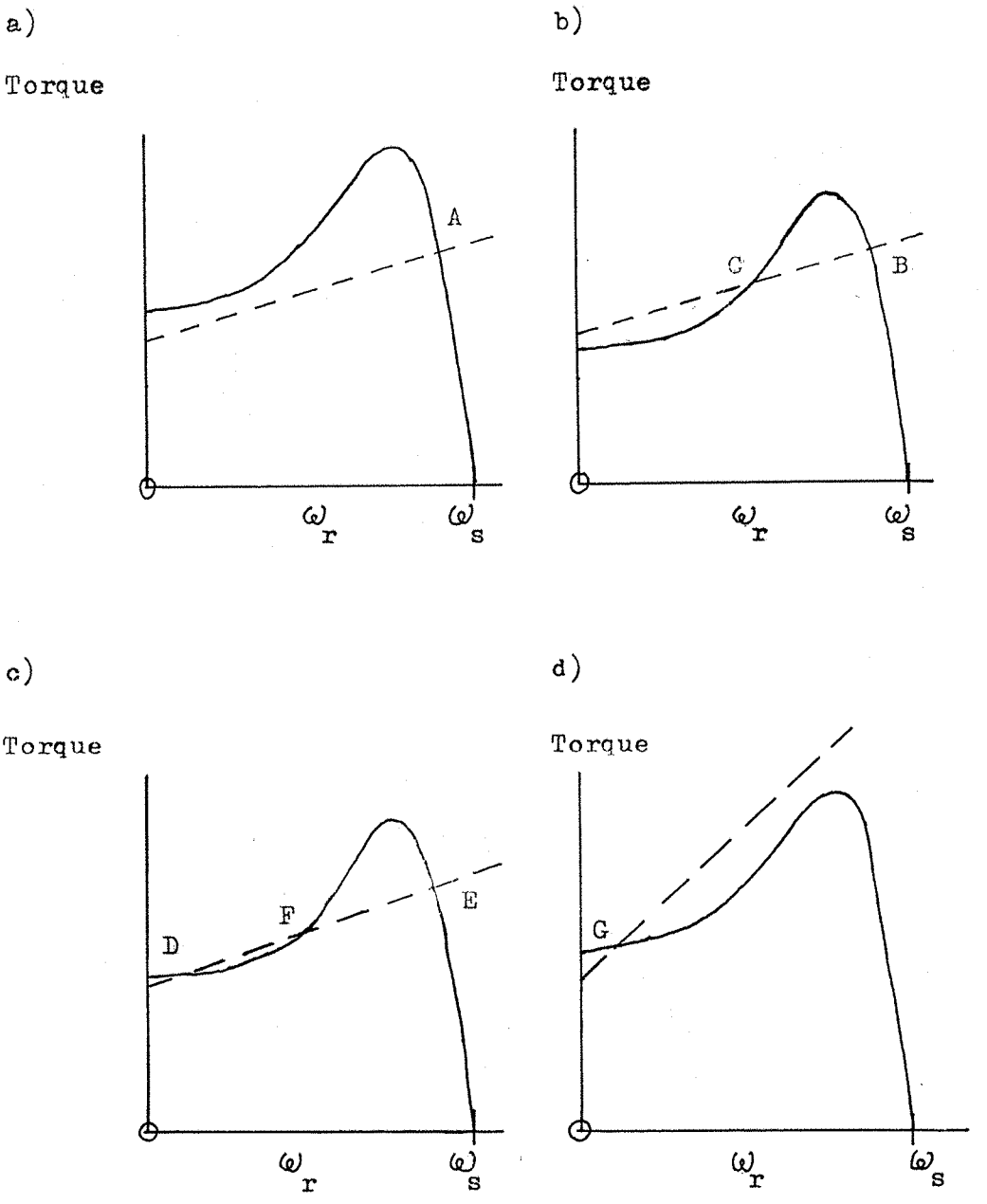

Key:

——— T — — — T_L

diagram (b). The graphs of T and T_L intersect at points B and C. Point B is similar to point A in diagram (a) and represents stable operation at a speed just below the synchronous speed of the induction motor. Point C also represents a speed which satisfies equation 4.101 but corresponds to unstable operation: any slight change in speed produces a difference between T and T_L which increases the speed change. The induction motor either stalls or operates stably at point B, depending upon the nature of the change in speed. However, at standstill, T_L is greater than T and the motor will not start. Stable operation at point B is only possible if the induction motor has been operating from a supply which allows it to run at a speed between that indicated by point C and the synchronous speed and if the induction motor has been running at such a speed.

The statement that, from diagram (b), T_L is greater than T at standstill does not mean that the induction motor will rotate backwards. At standstill $T_L = T_b$, but subsection 4.3.2 states that T_b can never be greater than T as it is a frictional torque that only exists in response to rotation or the torque exerted by the induction motor or both. The graphs of T_L against ω_r in all four diagrams of Figure 4.4 have been based upon the value of T_b appropriate to rotation whereas subsection 4.3.2 states that at standstill, T_b can be considerably less than this value.

If the voltage supplied to the induction motor is between the voltages supplied which produced the graphs of T against ω_r in diagrams (a) and (b), but the supply frequency is kept the same then it is possible for the graphs of T and T_L against ω_r to intersect at three points as shown in diagram (c). Under these conditions the induction motor will start, since at standstill T is greater than T_L, but it will run at a very low speed corresponding to the intersection of the graphs at point D. The other two points of intersection, E and F, correspond to points of stable and unstable operation respectively and are similar, respectively, to points B and C in diagram (b). In a similar manner to the previous description of operation at point B in diagram (b), operation of the motor-generator set at point D is only possible if the motor-generator set has been running at a speed between the synchronous speed of the induction motor and the speed indicated by point E and a change in supply voltage and frequency produces a graph of T against ω_r the same as that shown in diagram (b).

Diagram (d) shows the effect of a large fluid friction constant k_{ff} upon the graph of T_L against ω_r and the solution to the steady state speed of

the motor-generator set. The graph of T_L against ω_r climbs very steeply and only once intersects the graph of T against ω_r. The point of intersection, G, corresponds to operation at a very low speed, and is similar to point D in diagram (c).

4.8.3 The method of numerical solution used to solve the equation describing the steady-state speed of the motor-generator set.

During the investigations described in this thesis, all steady-state operation of the motor-generator set occurred at or near synchronous speed. Consequently the method of numerical solution described below assumes a solution at or near synchronous speed.

The method of solution is shown graphically in figure 4.5 which shows small portions of the graphs of T and T_L against ω_r and shows their intersection at a speed just below the synchronous speed of the induction motor. The intersection is the steady-state speed, labelled ω_{ss} in Figure 4.5.

The method begins with an estimate ω_E of the steady-state speed and calculates T_E and T_{LE}, the values of T and T_L at ω_E. The method assumes that the graph of T against ω_r between $\omega_r = \omega_o$ and $\omega_r = \omega_E$ may be represented, approximately, as a straight line passing through the points (ω_E, T_E) and (ω_o, O). Figure 4.5 shows that ω_{E1}, a better estimate of ω_{ss} than ω_E, is given by

$$\omega_{E1} = \omega_o - \frac{T_{LE}}{T_E} (\omega_{ss} - \omega_E) \qquad (4.106)$$

An even better estimate may be obtained by repeating the above procedure using ω_{E1} as the estimate of steady-state speed.

Figure 4.5 shows a graph of T_L which has positive slope in the region shown in Figure 4.5. However, the analysis described above is still valid, even if the slope is zero or negative in that region.

4.9 Conclusions

This chapter has described and developed a mathematical model which describes the behaviour of the induction motor drive during both steady-state and transient operation. The mathematical model is based on Kron's primitive machine and uses state-space equations to describe the behaviour of the drive. The state-space equations are non-linear and the fifth order Kutta-Merson algorithm is used for their solution. This chapter also describes how

Figure 4.5: The method of numerical solution used to solve the equation which describes the steady-state speed of the motor-generator set.

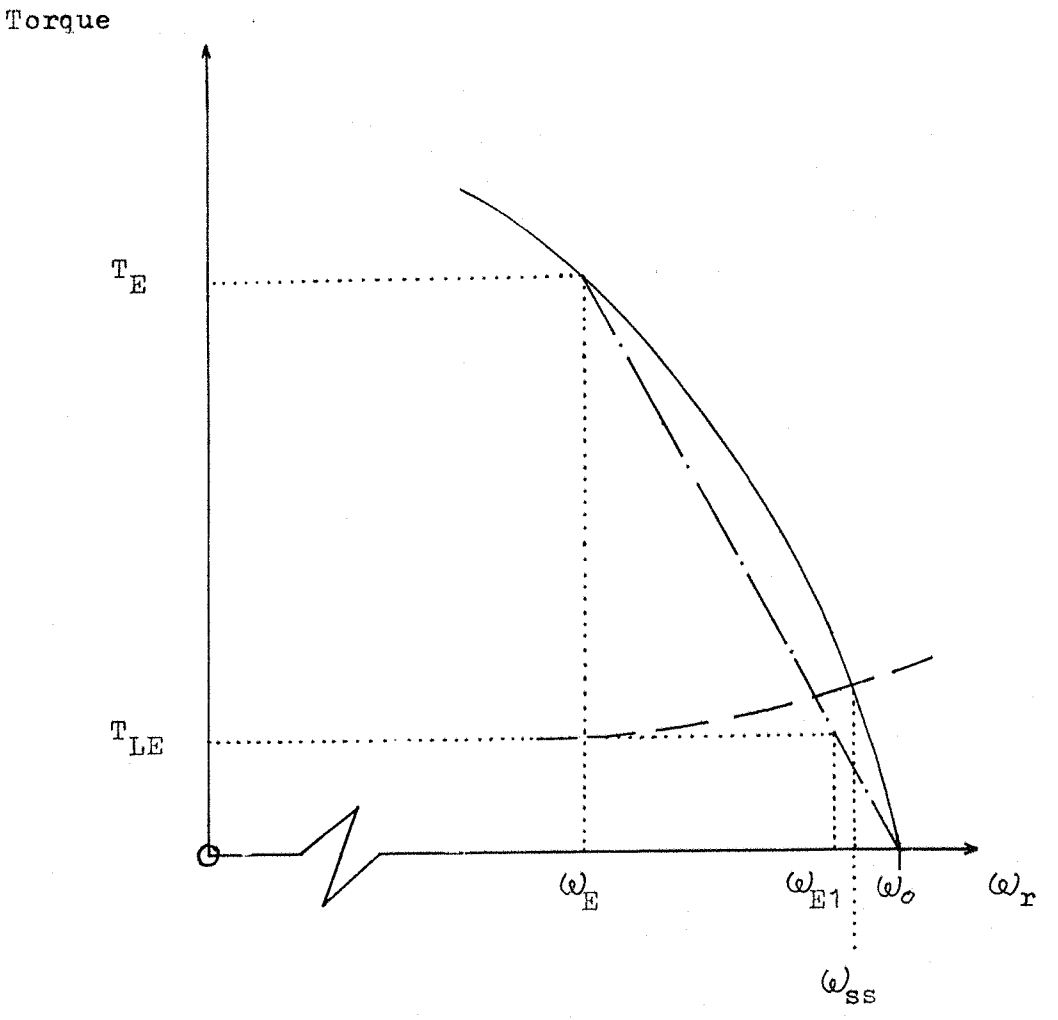

Key:

———— Graph of T against ω_r.

—.—.— Linear approximation to the graph of T against ω_r.

— — — Graph of T_L against ω_r.

the currents in the induction motor, the armature current of the D.C. generator, and the speed of the motor-generator set may be found from the solution of these equations.

The chapter ends by describing a method of finding the steady-state speed of the motor generator set. This method does not use Kron's primitive machine to describe the induction motor but uses the equivalent circuit instead.

The author would like to acknowledge the help of Dr. Huda (formerly with the Department of Mathematics, University of Southampton) in formulating the state-space equations described in this chapter.

CHAPTER 5 EXPERIMENTAL TESTS USED TO VERIFY THE VALIDITY OF THE MATHEMATICAL MODEL OF THE INDUCTION MOTOR DRIVE

5.1 Introduction

The previous chapter described a mathematical model designed to describe the behaviour of the induction motor drive during transients. This chapter describes three kinds of test designed to verify the validity of the model. The tests were:

1) Acceleration of the motor-generator set from rest to a steady-state speed : referred to henceforth as the "acceleration test".
2) Deceleration of the motor-generator set from a higher speed to a lower speed : referred to henceforth as the "deceleration test".
3) Load variation: the effect of a varying load upon the speed of the motor-generator set.

The results of these tests were compared with theoretical predictions made using the mathematical model.

5.2 Experimental procedure common to all three tests

5.2.1 Equipment used

The equipment used in the test described in this chapter is that described in Chapter 3 and illustrated in Figure 3.1 with the following exception: no closed loop feedback was used. Ammeters and voltmeters (not shown in Figure 3.1) measured the phase voltages and currents of the induction motor, and a chart recorder recorded graphs of the motor-generator set speed against time, and graphs of the current in one phase of the induction motor against time.

5.2.2 Adjustment of the voltage of the V.V.V.F. supply to the induction motor

Adjustments to the phase voltage of each phase of the V.V.V.F. supply were made by adjusting the gain of the appropriate amplifier channel. These adjustments were made while the induction motor was disconnected from the supply in order to avoid problems that could arise from large unbalanced currents flowing in the induction motor, transformers and amplifier channels during adjustment. The problems that could arise would be heating of the induction motor and possibly reverse power flow into one or more amplifier channels. Reverse power flow could result from unbalanced

voltages and currents causing one or more amplifier channels to feed power into other amplifier channels via the transformers and the induction motor. Disconnection of the induction motor from the V.V.V.F. supply removes the path available for possible reverse power flow into one or more channels.

5.2.3 Calibration of the chart recorder channel used to plot the phase current of the induction motor against time

Only one phase current was plotted in order to avoid a confusion of graphs which would arise if all three phase currents and the speed of the motor-generator set were all plotted on the same chart and were of sufficient size to show reasonable detail.

The motor-generator set was run at a steady speed, and the burden of the C.T. used to measure the phase current and the zero setting of the chart recorder were adjusted to give a graph of suitable size and position on the paper of the chart recorder. This was done with the paper feed mechanism disengaged in order to save paper. The size and position of the graph likely to be produced was estimated from the position and deflection of the spot of light used by the chart recorder channel to draw the graph. The channel was calibrated by comparing the deflection with the phase current measured by an ammeter.

5.2.4 Calibration of the chart recorder channel used to plot the speed of the motor-generator set against time

This consisted of measuring the deflection produced in a graph of speed against time by a change in speed, the speed being shown by a frequency meter which measured the output frequency of the encoder. If desired, the sensitivity of the chart recorder channel to changes in speed could be altered by methods described in Chapter 3.

Although this calibration was carried out during the series of load peturbation tests it was not carried out during the series of acceleration and deceleration tests because of an oversight of the author. Also, since no records were made of the steady-state speeds attained during the acceleration and deceleration tests, the graphs of speed against time cannot be scaled by comparing the steady-state speeds indicated by the graphs with steady state speeds measured during the tests.

However, the graphs can be scaled against steady-state speeds calculated from equations which describe the steady-state speed of the motor-

generator set (see section 4.8 of Chapter 4). If it is assumed that these equations are a good description of the motor-generator set then it may be assumed that the steady-state speeds calculated from these equations are close to those speeds obtained during experiment. Although it is therefore not possible to compare speeds obtained during tests with those predicted by the mathematical model, nevertheless the shapes of graphs produced during tests may be compared with the shapes of graphs produced by the mathematical model in order to check the validity of the mathematical model.

5.2.5 Supply frequencies used

In order to study the behaviour of the drive under conditions similar to those for which the induction motor was designed, many tests used supply frequencies close to 50Hz. Owing to the nature of the three-phase digital oscillator an output frequency exactly equal to 50Hz was not possible. The deceleration and load variation tests, which were performed earlier than the acceleration test, used a 50.2 Hz supply frequency when it was wished to study the behaviour of the drive under conditions similar to those for which the induction motor was designed. In those circumstances, 50.2 Hz was the closest available frequency to 50Hz.

However, after the deceleration and load variation tests the three-phase digital oscillator was re-programmed to allow it to produce higher output frequencies. This resulted in the nearest output frequency to 50Hz being 50.3 Hz and so the acceleration test used 50.3 Hz as the closest approximation to 50 Hz when it was wished to study the behaviour of the drive under conditions similar to those for which the induction motor was designed.

5.3 Acceleration Test

5.3.1 Experimental procedure

This test was repeated three times with the V.V.V.F. supply delivering rated voltage to the induction motor. Different supply frequencies were used. In two tests the D.C. generator was unloaded and unexcited and in the other test it was loaded and excited.

Before each repetition of the test the motor-generator set was run with the V.V.V.F. supply delivering the voltage and frequency to be used in the test. If the test involved loading the D.C. generator then the load and excitation were adjusted to the values needed for the test. A rheostat was used to load the D.C. generator and meters measured the output voltage and

current of the armature. The D.C. generator was shunt-wound and separately excited using a rheostat in series with the shunt winding and the 220v. D.C. supply housed in the cage containing the motor-generator set. This method of excitation ensured that the excitation would remain constant during a test. Constant excitation would not be possible using series or self-excitation.

Readings were taken of the open-circuit voltage of the armature of the D.C. generator and of the armature current that flowed upon connection of the load resistance. It is appreciated that the application of load to the D.C. generator caused the speed of the motor-generator to fall and therefore then caused the internal E.M.F. of the armature to fall. However, this was not realized at the time the test was performed. Allowance for this fall in E.M.F. has been made in the analysis of the results of this test. Section 5.3.4 describes how this allowance was made.

Whilst the motor-generator set was running the chart recorder channel used to measure current was adjusted as described in the previous section. The chart recorder channel and associated circuitry used to measure speed were adjusted so that the chart recorder would produce a graph of speed against time having a suitable size and position on the chart. The size and position of the graph were estimated from the size and position of the deflection of the spot of light used by the chart recorder channel to draw the graph. The deflection of interest was that produced by the change in speed from rest to steady state operation. The adjustments and calibrations described were made with the paper-feed mechanism disengaged in order to save paper.

When the chart recorder had been set up ready for measurement and the load and excitation of the D.C.-generator was set ready for the test, the toggle switch on the front panel of the enclosure containing the motor-generator set was opened, disconnecting the motor-generator set from all supplies.

When the motor-generator set had come to rest, the test began by engaging the paper feed mechanism of the chart recorder an then closing the toggle switch. Once the motor-generator set had reached a steady speed, which happened usually less than a second after closing the toggle switch, the paper feed mechanism was disengaged, and the toggle switch was opened. This marked the end of the test.

5.3.2 Computer simulation of the acceleration test

This simulation was based upon the mathematical model of the induction motor drive and was developed to see whether the mathematical model would accurately describe the behaviour of the drive during the acceleration of the motor generator set. A computer program was designed to solve the state space equations listed in section 4.6 of Chapter 4, using the 5th order Kutta-Merson algorithm described in section 4.7 of Chapter 4. The computer program needed the following data:

Input data

1) Parameters of the induction motor drive. These are listed in Table C.2 of Appendix C.

2) Supply voltage and frequency

The state space equations use voltages U_f and U_g to describe the two phase supply to a Kron primitive machine used to represent the three-phase induction motor. If the three-phase induction motor is supplied from a balanced three-phase supply of r.m.s. voltage V and frequency then if v_R, the red phase voltage of such a supply is described by the equation

$$v_R = \sqrt{2}\, V \cos \omega t \qquad (5.1)$$

then equations 4.34 and 4.35 Chapter 4 shows that u_f and u_g are given by

$$u_f = \sqrt{2}\, V \cos \omega t \qquad (4.34)$$

$$u_g = \sqrt{2}\, V \sin \omega t \qquad (4.35)$$

3) "Point of wave" phase angle

It was believed that the behaviour of the motor generator set during acceleration would be affected by "point of wave switching", that is the point on the supply voltage waveform at which the induction motor was connected to the supply. Accordingly equations 4.34 and 4.35 were modified to include p, the "point-of-wave" phase angle:

$$u_f = \sqrt{2}\, V \cos (\omega t + \alpha_p) \qquad (5.2)$$

$$u_g = \sqrt{2}\, V \sin (\omega t + \alpha_p) \qquad (5.3)$$

The computer simulation used time t = o to represent the instant at which the induction motor was connected to the supply and so α_p represented the phase angle between the instant at which the red phase voltage crossed the zero voltage axis and became positive, and the instant at which the induction motor was connected to the supply.

However, it must be noted that during the experimental tests the point on the supply voltage waveform at which the induction motor was connected to the V.V.V.F. was uncertain since the method of connection involved manually operating a switch to close a three-phase relay. Neverthless, the use of the computer simulation to study the effects of point-of-wave switching would ascertain whether any difference between experimental results and the computer simulation was due to the effects of point-of-wave switching.

4) The excitation of the D.C. generator

This quantity is only of interest if the acceleration test used a loaded and therefore excited D.C. generator. If the generator was unexcited then the excitation is made equal to zero in the state space equations.

During tests involving a loaded and excited D.C. generator measurements were not taken of the steady-state speed reached and so the values of excitation cannot be calculated from experimental data. However, the values of excitation can be estimated by solving the equations used to describe the steady-state speed of the induction motor, knowing V_{AG}, the voltage at the terminals of the armature of the D.C. generator and I_{AG}, the armature current used in the test. These equations and a method of their solution are described in Section 4.8 of Chapter 4. Once the steady-state speed reached during the test has been estimated, the excitation E_x can be estimated from equation 4.99.

5) The load resistance connected to the D.C. generator

This can be calculated from the values of armature current and voltage at the armature terminals used during the test. If the test did not involve a loaded generator, the value of load resistance used in the computer program was immaterial, since the value of excitation entered in such a case was zero. This resulted in the computer predicting zero armature current.

6) The initial conditions

The Kutta Merson algorithm requires initial values at t = o for the rotor and stator currents of the primitive machine, the speed of the rotor of the primitive machine, and the armature current. Since the computer program was simulating the acceleration from rest of the motor generator set when the induction motor was suddenly connected to the supply then the initial values of the above quantities are all zero.

7) Step length h

The Runge-Kutta algorithm solved the state-space equations using an iterative numerical method. The step-length h chosen was a compromise, between the following considerations: too large a step-length resulted in too few iteration steps per cycle of supply voltage causing a poor representation of the waveform of the supply voltage. Too large a step-length also caused the algorithm to be unstable. Too small a step-length resulted in a long time taken to execute the programme. The step length chosen was 0.5 ms which resulted in a stable iteration and resulted in 40 iteration steps per cycle of 50 Hz waveform. Shorter steps had little effect on the output of the computer program but greatly increased the execution time so steps shorter than 0.5 ms were not used.

Allowances made for the effects of the behaviour of bearing and brush torque Tb with speed ω_r

As stated in section 4.3 of Chapter 4, T_b obeys the following

If $\omega_r > 0$, $T_b = T_{bd}$,

If $\omega_r < 0$, $T_b = - T_{bd}$,

If $\omega_r = 0$ and $|T| \leq T_{bd}$ then $T_b = \pm T$,

If $\omega_r = 0$ and $|T| > T_{bd}$ then $T_b = \pm T_{bd}$

In both of the last two cases in which $\omega_r = 0$, the sign of T_b is such that it opposes the torque T developed by the induction motor.

Also, if the motor generator set is at rest ($\omega_r = 0$) then the shafts will not rotate unless $|T|$ exceeds T_{bd}.

In the computer program, allowances for these effects were made in the following way:

At the start of each step in the iteration, the value of x_5, the speed of the rotor of the Kron's primitive machine used to represent the induction motor, was tested. Equation 4.96 shows that the sign of x_5 is the same as that of ω_r, and if x_5 equals zero so does ω_r.

If x_5 was not equal to zero this implies rotation of the shafts of the motor-generator set, and the magnitude of T_b was made equal to T_{bd} and the sign of T_b was made that of x_5 for the duration of that step in the iteration.

If x_5 was equal to zero this implied that the motor-generator set was at rest. The value of T, the torque developed in the rotor of the induction was calculated using equation 4.24, 4.36, and 4.72 to 4.75 and the values of x_1 to

x_4 obtained from the previous step in the iteration. If the magnitude of T was greater than T_{bd} this implied that the induction motor was able to overcome the friction in the motor generator set. In such a case the magnitude of T_b was made equal to T_{bd} and the sign of T_b was made the same as that of T in order that T_b would be in the same sense to oppose the torque developed by the induction motor.

If x_5 was equal to zero but the magnitude of T was less than T_{bd} this implied that the induction motor could not overcome the friction in the motor generator set and the motor-generator set was unable to accelerate from rest. At the end of a step of the iteration in which these circumstances applied the computer program ensured that x_5 was made equal to zero so that ω_r would equal zero, implying that the motor-generator set was stationary. x_5 was made equal to zero in the following way:

During each step in the iteration, the computer program calculates the elements of the matrices K_1 to K_5 which are the coefficients of the 5th order Runge-Kutta algorithm. The elements of these matrices correspond to the state-space variables x_1 to x_6 in the manner described in section 4.6 of Chapter 4. It may be shown, using equation 4.92 of Chapter 4, that x_5 can be made equal to zero by taking all elements of the coefficients which correspond to x_5 and putting these elements equal to zero throughout the step of the iteration. In other words, function f_5 described by equation 4.85 in Chapter 4 is made equal to zero throughout the step in question.

The advantage of this method of putting x_5 equal to zero over a simpler method which would be to equate x_5 equal to zero at the end of the step, is that it ensured that the elements corresponding to x_5 would be equal to zero throughout the step in question. Since these elements represent change in x_5 calculated during the step, non-zero values would imply changes in speed ω_r of the motor-generator; a situation which would not arise if the rotor were at rest and unable to accelerate because the induction motor was unable to overcome the friction of the motor-generator set. Making such elements equal to zero during the step ensured that the calculations in the step were based upon a stationary motor-generator set. The method used to put x_5 equal to zero also avoided putting T_b equal to T in function f_5 since function f_5 was simply made equal to zero.

Output Data

The computer programme produced values of motor-generator speed and phase current against time for comparison with experimental results.

Speed of the motor-generator set (ω_r)

The computer programme produced values of ω_r against time every millisecond. The speed was calculated from x_5 and equation 4.96 of Chapter 4.

$$\omega_r = \frac{x_5}{n_p}$$

Phase current:

Any difference between the point-of-wave phase angle encountered in a test and the point-of-wave phase angle used during the computer simulation of that test will cause a difference in phase between the supply voltage used in the test and that used in the simulation. This, in turn, will cause a phase shift between the phase current waveform measured during a test and the phase current produced during a simulation. The problems of this phase shift are further complicated by the uncertainty of which phase current was measured during the test. This problem of phase shift prevents comparison between the shapes of cycles of phase current waveform produced during the test and those produced during the simulation. These difficulties arise because of the phase shift between corresponding points on the waveforms.

Instead, it was decided to compare the shapes of the envelopes of the current waveforms. It is appreciated that point-of-wave switching may have some effect upon the shape of the envelope, particularly at or near the time at which the induction motor is connected to the supply. It is possible for the computer program used for the simulation to produce current waveforms for all three phases by using x_1 and x_4, which represent, respectively, the d and q axis currents of the Kron's primitive machine used to represent the induction motor, and equations 4.93, 4.94 and 4.95. The choice of which phase current waveform to use for comparison purposes is unimportant since the uncertainty in the point-of-wave switching affects comparison between the phase current waveform produced during the test and any of the phase current waveforms produced by the computer simulation. The red phase current waveform produced by the computer simulation was chosen for comparison purposes since it is the easiest to calculate: equation 4.93 shows that the red phase current equals x_1.

It was decided to compare the envelopes by comparing the "average envelope" of each waveform, that is an envelope constructed from the average

of the positive and negative halves of the envelope of the waveform in question. This was done by plotting the absolute values of the peaks of the positive and negative half cycles against time and drawing a smooth curve to represent the average envelope. The use of the average envelope was intended to reduce the effects of point-of-wave switching on the comparison between the envelopes of phase current waveforms produced during the test and produced by the computer simulation.

The average envelope of the waveform of the phase current produced during the test was plotted from absolute values obtained by drawing and measurement. The average envelope of the phase current waveform produced by the computer was plotted from absolute values obtained in the following manner:

During each step in the algorithm used in the computer simulation to solve the state-space equations, the computer calculated $|x_1|$, the absolute value of x_1 and compared $|x_1|$ with:

$|x_1|_1$, the absolute value of x_1, calculated one step before the present step in the iteration, and

$|x_1|_2$ the value of x_1, which was calculated two steps before the present step.

The computer deduced that a positive or a negative peak value occurred during the step in the iteration before the present step if the following expression was satisfied:

$$|x_1|_2 \leq |x_1|_1 \geq |x_1| \tag{5.4}$$

The computer printed $|x_1|_1$, the absolute value of this peak value, and the simultation time at which it occurred. The time in question equals the simultation time corresponding to the end of the step in the iteration at which $|x_1|_1$, was calculated and equals the simulation time at the start of the step minus the step length h.

The ambiguity in estimation of simulation time that could occur on the rare occasions when $|x_1|_1 = |x_1|$ or $|x_1|_1 = |x_1|_2$ would result in a possible error in simulation time of half the step length, ie 0.25ms, which would be a small fraction of the periodic time of the current waveforms encountered during the tests and simulation. This error was considered small and therefore ignored. The situation in which $|x_1| = |x_1|_1 = |x_1|_2$ was unlikely to arise since the step length used allowed the instantaneous value of the phase current calculated during the simulation to change sufficiently to allow difference between at least two of three successive value of $|x_1|$.

At the end of each step in the iteration, $|x_1|_2$ was replaced by $|x_1|_1$ and $|x_1|_1$ by $|x_1|$ ready for the next step in the iteration.

5.3.4 The comparison between experimental results and computer simulations of the acceleration tests

Three tests were performed : two with the D.C. generator loaded and one with the D.C. generator unloaded. Figures 5.1 to 5.3 compare experimental graphs of speed and current envelope against time with similar graphs produced by computer simulation. As described previously in subsection 5.3.1 the experimental graphs are not scaled against steady-state speeds measured during the tests but are scaled against estimates of steady-state speed derived from the steady-state representation described in Section 3.8.

The conditions of each test are listed in table 5.1 below. The conditions include supply voltage and frequency and estimated steady-state speed. Where appropriate the conditions include the excitation of the D.C. generator and the load resistance. These were calculated using the steady state representation and the appropriate values of supply voltage and frequency. The excitation of the D.C. generator was calculated from the open-circuit E.M.F. of the armature. The resistance connected to the armature was calculated from the excitation and the armature current, and the steady-state speed under these conditions was also calculated from the steady-state representation. Such calculations allowed for the fall in internal E.M.F. of the armature caused by the fall in speed resulting from the connection of load to the armature.

Table 5.1 The conditions of the three accelations tests performed

Condition	Acceleration Test		
	1	2	3
Supply voltage volts	240	240	240
Supply frequency Hz	50.3	55.3	50.3
Estimated steady - state -state speed revs s^{-1}	25.03	27.355	22.949
DC Generator	Unloaded	Unloaded	Loaded
Excitation (Volts s^{-1} rad^{-1})	0	0	1.4668
Load resistance (Ohms)	-	-	211.5

The comparison between the experimental results and computer simulation of acceleration tests 1 to 3 are illustrated in Figures 5.1 to 5.3 respectively. The point-of-wave switching angle used in each of the simulations was zero.

From figures 5.1 to 5.3 the following phenomena can be seen:

1) The effects of vibrations and torsional oscillations

Section 3.11 of Chapter 3 describes vibration and torsional oscillations of the motor-generator set. The inertias of the shafts of the motor, D.C. generator and encoder, and the elasticity of the couplings between these three shafts formed a mechanically resonant system having a resonant frequency at about 39Hz. It is likely that during the starting of the induction motor, the large torques produced would excite this mechanically resonant system and would produce large torsional oscillations. These in turn would produce the large undulations observed in the speed against time graph at the start of each acceleration test. Support for this theory comes from the frequencies of these undulations which were about 39Hz: close to the resonant frequency observed previously. These oscillations decreased once the motor-generator set reached a steady state but did not die away completely. The small undulations observed were assumed to result from small torsional oscillations maintained by bearing and brush friction in the motor-generator set.

Consequently, comparisons between experimental results and computer simulation should be made with these oscillations in mind.

Figure 5.1: Acceleration test 1: Graphs of speed and average current envelope against time.

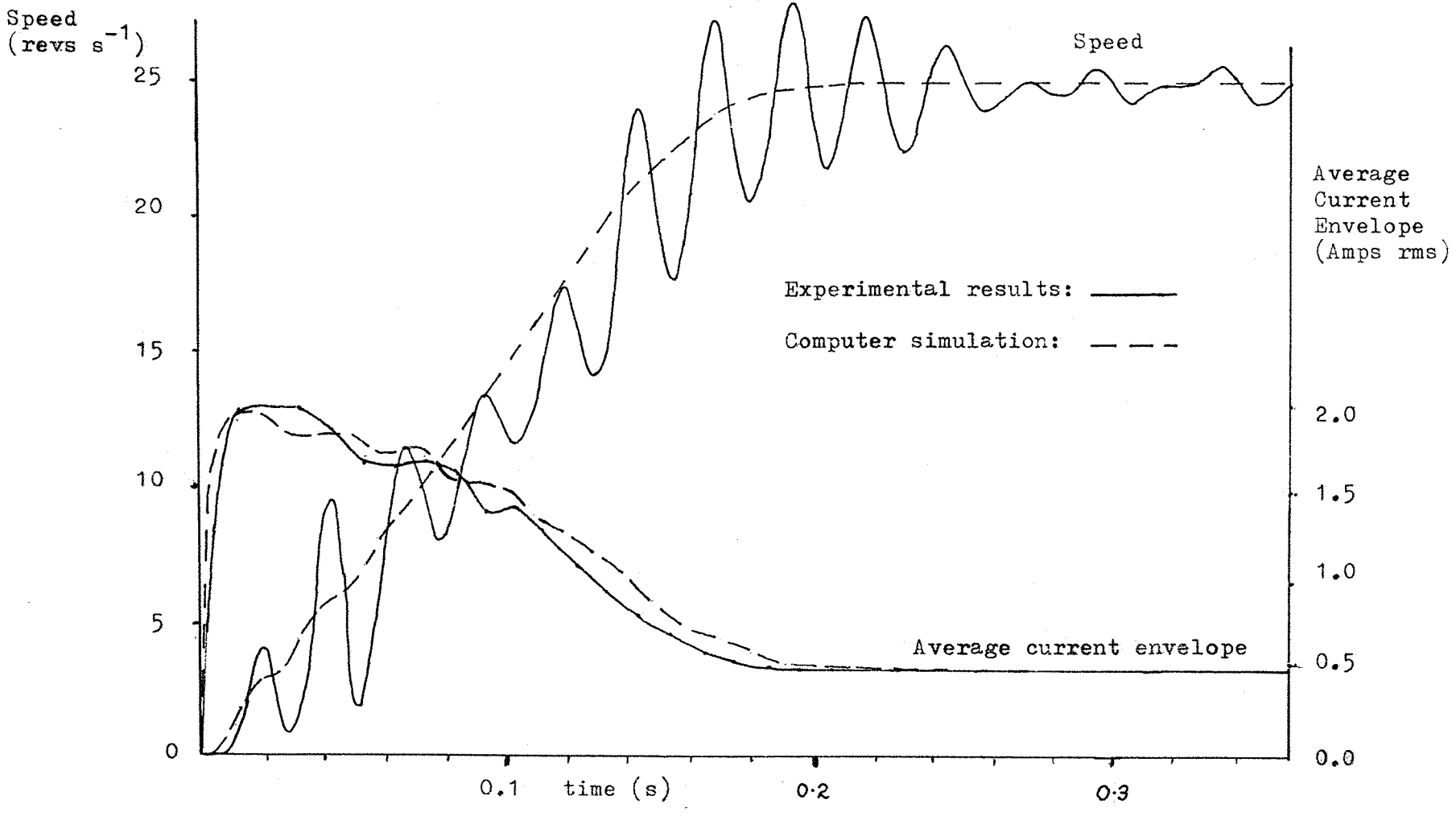

Figure 5.2: Acceleration test 2: Graphs of speed and average current envelope against time.

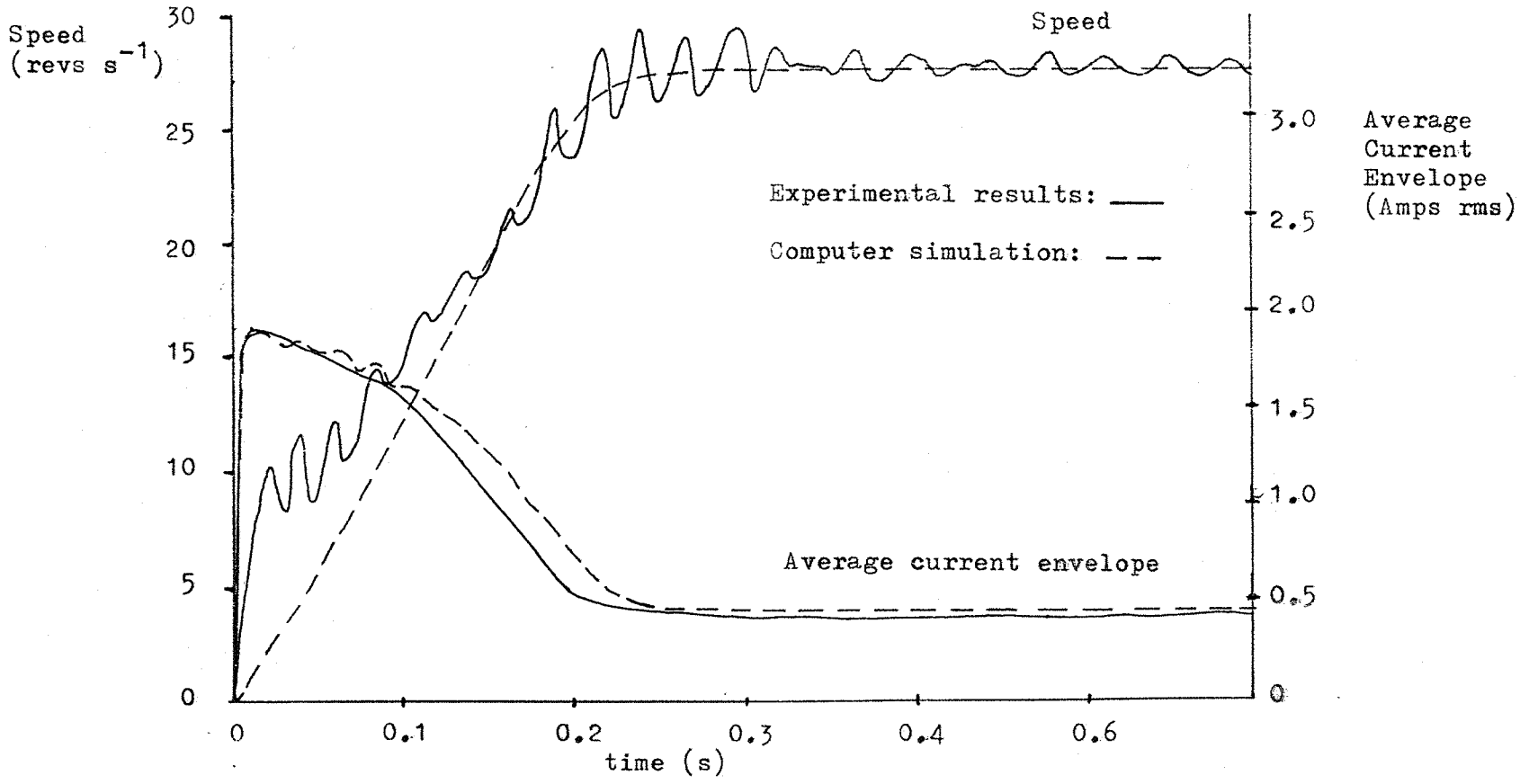

Figure 5.3: Acceleration test:3: Graphs of speed and average current envelope against time.

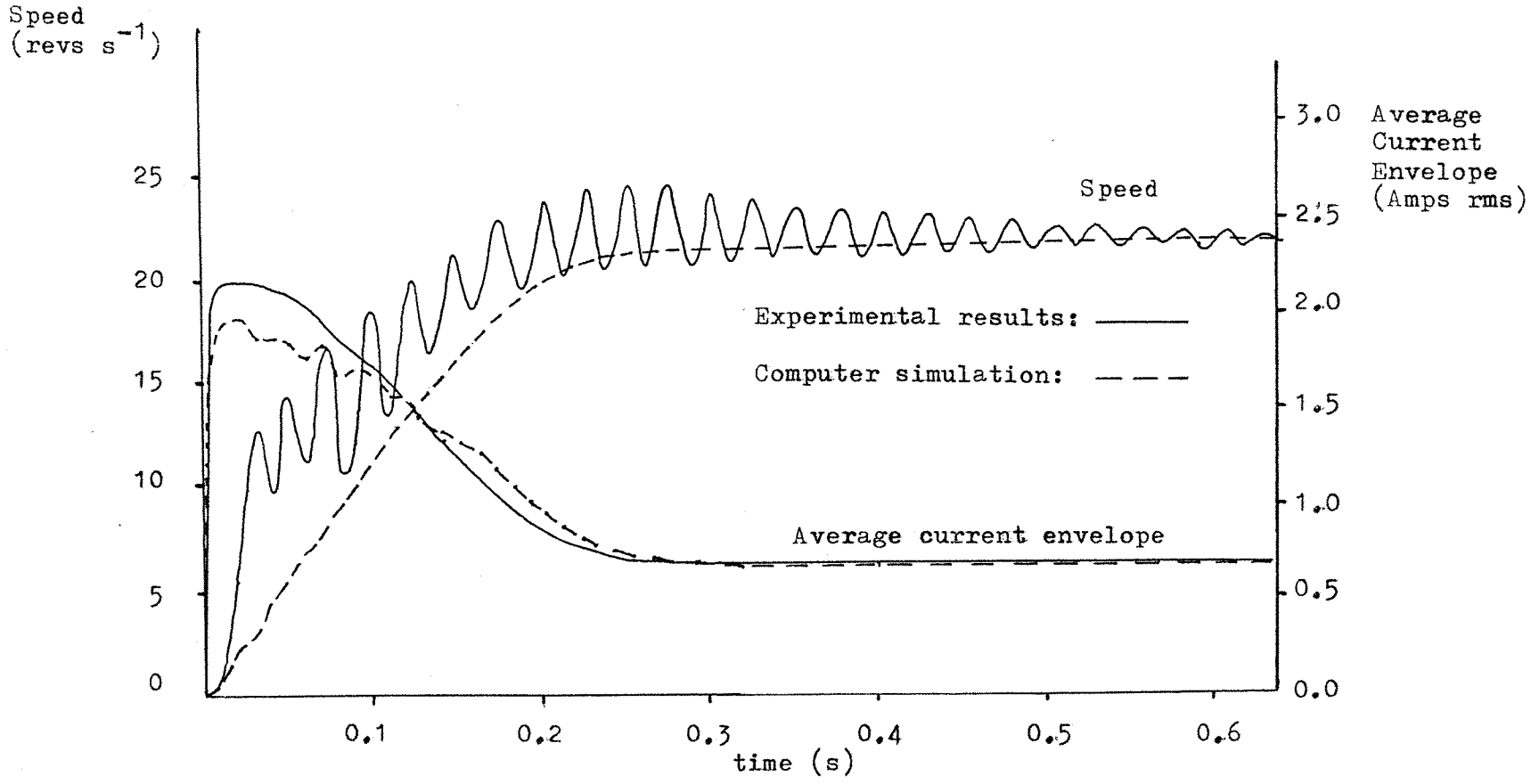

2) Comparison between graphs of speed against time produced by a test and its computer simulation

Figure 5.1, which shows the experimental results and computer simulationof acceleration test 1 shows the best agreement between the two graphs of speed against time. Figures 5.2 and 5.3 which refer, respectively, to acceleration tests 2 and 3 show that the computer simulation tends to under estimate the speed during the early stages of the test, suggesting that the induction motor produces a greater torque than predicted by the mathematical model. If so, this would be consistent with the "deep bar effect", mentioned by Say [5] in which the "skin-effect" causes the impedance of the rotor circuit to be higher at starting than at normal running speed because the currents in the rotor bars have a higher frequency. This in turn causes greater starting torque than would be predicted from the computer simulation which used values of impedance based upon low-frequency rotor bar currents.

Correspondence with the manufacturers of the induction motor confirmed that the deep bar effect was slight for this particular induction motor, and there is little change in rotor resistance R_2. However, the high starting currents cause the magnetic material of the motor to saturate, altering the distribution of flux in the machine, reducing some of the leakage reactances. The reduction in impedance is small and its effect on the drive is masked by the resistance of the stator winding and the impedance of the transformers (assumed constant). It is estimated that this reduction in impedance would cause an approximate increase in starting torque of 5%, which is insufficient to account for the discrepancy between the test and its computer simulation.

The large starting current also causes a large current to flow through the transformers used in the drive. Should saturation occur in these circumstances this could reduce the impedance of the transformers and also increase the starting torque.

Computer simulations of acceleration tests 1 and 3, tests which used a 240 volts 50.3 Hz supply, show a small ripple at the start of the speed against time graph. The frequency of the ripple is about 40 Hz and if this is a feature of the real motor-generator set it could contribute to the torsional oscillations observed as it is close to the 39 Hz resonant frequency of the oscillations. However, the ripples in the speed against time graphs of both test and computer simulation were studied no further.

3) Comparison between graphs of average current envelope against time produced by a test and its computer simulation.

As in the case of speed against time, acceleration test 1 produced the best agreement between graphs of average current envelope against time produced by the test and its computer simulation.

Acceleration tests 2 and 3 showed that the computer simulation tended to underestimate the current during the early stages of the test. This is consistent with the high starting currents causing saturation of the transformers and the induction motor and reducing the leakage reactances of these items. However, the changes, described previously, in the leakage reactances of the induction motor would only result in an increase in starting current of about 3% which is insufficient to account for the observed discrepancy between results from the test and its computer simulation.

During the three tests the highest starting current recorded corresponded to 2.14 amps r.m.s. and was recorded during acceleration test 3 in which the motor-generator set operated from a 240v. 50.3 Hz supply and the D.C. generator was loaded. This starting current corresponded to an amplifier output current of 13.3 amps r.m.s., within the 14 amp maximum rated output current, but above the rated current, 5.7 amps, of the transformers. This overload was tolerated as it was of short duration. As the overload was of short duration, there was no "nuisance" operation of the fuses or circuit breakers used to protect the drive.

5.3.5 The sources of discrepancy between the experimental results and the computer simulation

These arise from three main sources : limitations of the mathematical model, inaccuracies of the electrical and mechanical parameters of the drive (see Appendix C) and experimental error. These three sources of discrepancy are discussed in greater detail below:

Limitations of the mathematical model

1) The effects of magnetic saturation: The mathematical model does not attempt to model magnetic saturation. As described previously, magnetic saturation affects the leakage reactances of the induction motor and the transformers. Magnetic saturation also affects the distribution of m.m.f. and the magnetic flux in the induction motor, causing a non-sinusoidal distribution. This also affects the accuracy of the mathematical model since the

transformations between two and three-phase systems described by Adkins and Harley [32] and quoted in Chapter 4 of this thesis, assume a sinusoidal distributiuon of flux and m.m.f.

2) The modelling of the transformers: The mathematical model represents the transformers by their winding resistances and leakage reactances referred to their H.V. windings. A better way would be to represent the transformers by their equivalent circuits. When designing such a representation it must be remembered that the transformers are energised from their L.V. windings by the amplifiers. Therefore the connection of the induction motor to the H.V. terminals of the transformers results in large currents flowing during starting but does not cause a sudden increase from zero of the magnetic flux in the transformers.

3) Step length. In iterative methods of numerical solution, such as the one used in the compluter simulation, accuracy depends upon step-length and tends to improve as the step-length decreases. Consequently step-length could affect the discrepancy between the experimental results and the computer simulation. The simulation of each test was repeated using a step length of 0.2 ms instead of 0.5 ms but this made little difference to the results produced. It was therefore concluded that step length was not a major source of discrepancy.

4) Point-of-wave switching angle. Another possible source of discrepancy is the choice of point-of-wave switching angle used in the computer simulation. The computer simulations of the acceleration tests were repeated using different point-of-wave switching angles but this had little effect upon the results produced. It was therefore concluded that point-of-wave swithcing angle had little effect upon performance of the induction motor.

5) Non-linearity of the amplifiers. The amplifiers were of "hi-fi" quality and it is therefore assumed that the output waveform was a faithful reproduction of the input waveform and so the amplifier channels were represented by an equivalent Thevevin voltage source using linear elements. However this representation may be inadequate since the amplifier channels contain non-linear semiconductor devices which could cause the amplifier

channels to act in a non-linear manner during current surges during the starting of the induction motor. This would result in changes in output waveform purity and change in the internal impedance of the amplifier, affecting the quality of the supply to the induction motor and therefore its performance. The behaviour of the amplifiers during sudden large changes in output current was not studied.

Inaccuracies in the electrical and mechanical parameters of the drive (see Appendix C)

The tests which were used to find the electrical and mechanical parameters of the equipment used in the drive are capable of good accuracy. Appendix C describes these tests. The major sources of error were considered to be the following:-

1) Inaccuracies in the electrical parameters of the transformers

The drive used three single-phase transformers to step up the output voltage of the amplifier channels to a suitable voltage to supply the induction motor. Only one transformer was tested and it was assumed that the three transformers had identical properties since each was made to the same specification by the same manufacturer. It is possible that the properties of the transformers were different but this was not investigated.

2) Inaccuracies in the electrical parameters of the induction motor: Appendix C has discussed the main sources of discrepancy between the manufacturer's data and data derived from experimental tests on the induction motor, and has also described the main sources of discrepancy. The computer simulations of the acceleration test were repeated using data derived from experimental tests but there was no significant difference between simulations using manufacturers' data and those using experimental data.

It is also possible that the electrical properties of each winding of the induction motor would not be the same, leading to errors in the electrical parameters.

3) Phase unbalance: Dissimilar electrical properties of the transformers and dissimilar electrical properties of the windings of the induction motor would cause unbalanced currents to flow in the induction motor, affecting its performance. Such unbalance was noticed but was not considered serious as it was small.

4) Electrical parameters of the D.C. generator. It was considered that the methods used to find these parameters were capable of good accuracy and any errors in these parameters were small. Such errors would affect only acceleration test 3 in which the D.C. generator was loaded and excited.

5) Mechanical parameters (including excitation losses) of the motor-generator set: The losses of the motor-generator set and the way they varied with speed and excitation were found from the Swinburne test which is capable of accurate results. However the electrical parameters of the D.C. generator were used in the calculation of the losses and so errors in the parameters of the D.C. generator test would affect the parameters describing the loses of the motor-generator set. Likewise, calculations of the polar moment of inertia of the motor-generator set would be affected by errors in the parameters describing the losses of the motor-generator set. The measurement of the polar moment of inertia involved measuring the time taken for the motor-generator set to decelerate from a known speed to rest and as such timing was done using a stopwatch, the personal equation of the observer can lead to an error of about 4% in the estimate of polar moment of inertia.

Inaccuracies in experimental technique

Since graphs of speed and current are being compared the relevant inaccuracies of experiemntal technique may be divided into three parts : inaccuracies in measurement of speed, of current, and of time.

Inaccuracies in measurement of speed : These would be caused by the three items of equipment used to measure speed and plot graphs of speed against time, namely the encoder, the frequency to voltage conversion circuit, and the chart recorder. Both the encoder and the chart recorder were precision instruments and were therefore assumed to cause little error. It was also assumed that the frequency to voltage conversion circuit produced a linear response over the whole range of speeds met during the tests.

Another source of error lies in scaling the speed against time graphs against theoretical estimates of steady-state speed rather than experimental readings. The accuracy of the steady-state representation used to produce these theoretical estimates was confirmed by comparing speeds estimated by the representation with experimental readings of speed. When the induction

motor was operatng from supplies with voltages and frequences similar to, but not identical with those used in the tests, and the D.C. generator was unloaded, the differences between the estimated and the experimental readings was less than one per cent.

Inaccuracies in measurement of current. Graphs of current were drawn using a current transformer to measure phase current and the chart recorder to plot the output of the current transformer. The current transformers used were designed for use in measuring instruments and experimental tests confirmed that they were accurate and linear over the range of currents and frequencies used in the tests. As the chart recorder was a precision instrument it was assumed that it caused little error in the current against time graph. Similarly the error produced by scaling the current against time graph was assumed to be small as the graph was scaled against a measured deflection of the trace produced by a known current flowing through the current transformer. The error in the measurement of this current was assumed to be small as it was measured by a good quality ammeter.

Inaccuracies in measurement of time. These would be caused by errors in the speed of the paper upon which the graphs were plotted. The nominal paper speeds indicated by the controls of the chart recorder were checked against the graph of the motor phase current when the motor had reached steady state. The frequency of the current equalled that of the supply and therefore the three-phase digital oscillator, whose frequency was known. The difference between the nominal and actual paper speeds was small, about four per cent, but was allowed for when drawing the time axis on the graphs.

5.3.6 Conclusions

The mathematical model of the induction motor drive is a good model of behaviour during acceleration from rest. Some of the discrepancies between experimental results and computer simulation result from torsional oscillations and vibrations and also the change in induction motor parameters caused by conditions during the start of the acceleration.

5.4 Deceleration test

5.4.1 Experimental procedure

During this test the V.V.V.F. supply was set initially to produce a supply having a particular voltage and frequency and the motor-generator set was run with the induction motor running from this supply. Deceleration of the motor-generator set was achieved by altering the setting of the switches on the front of the three-phase digital oscillator so that both the supply voltage and frequency suddenly decreased. Graphs of speed and the current in one phase were recorded just before, during and just after the period of deceleration. These graphs, therefore, not only showed the behaviour of the motor-generator set during deceleration but also allowed comparison between this behaviour and steady-state behaviour at both the initial and the lower values of supply voltage and frequency that were used in this test. During the test the D.C. generator was unloaded and not excited.

The decleration test was repeated twice using the same initial values but different lower values of supply voltage and frequency. Before each repetition of the test the motor-generator set was run with the induction motor running from the V.V.V.F. supply having voltage and frequency equal to the initial values and then having voltage and frequency equal to the lower values to be used in the test. With the paper-feed mechanism of the chart recorder disengaged, adjustments were made to the chart recorder so that the changes in speed and phase current amplitude resulting from changes in supply voltage and frequency would produce graphs of suitable size and position on the paper.

During the deceleration test the supply frequency would change faster than the motor-generator set would be able to respond and for a brief period the sudden decrease in the supply frequency would cause the induction motor to operate supersynchronously, generating power back into the V.V.V.F. supply and therefore into the amplifer channels. Although the manufacturers of the amplifiers warn against feeding power back into one or more amplifier channels, the amplifiers were able to cope with the deceleration caused by the decrease in supply frequency. The ability of the amplifier channels to cope will be discussed later in this section.

5.4.2 Computer simulation of the decleration test.

Aim of the simulation

The deceleration test studied the behaviour of the motor-generator set during deceleration from steady-state operation at a higher speed to

steady-state operation at a lower speed: the changes in speed resulting from changes in the voltage and frequency of the supply to the induction motor. Accordingly, the aim of the computer simulation of the deceleration test was to simulate not only the behaviour during deceleration but also the steady-state operation before and after deceleration.

The basic principle of the simulation

The computer program used to simulate the acceleration of the motor-generator set was also used to simulate the deceleration. The simulation was divided into two parts:

1) Simulation of steady state behavour at the higher speed

The computer programme was run as if simulating an acceleration test. The supply voltage and frequency used were the initial values used in the decleration test. After sufficient simulation time had been allowed for the computer programme to reach a steady state and produce sufficient results to describe the steady-state operation, the iteration of the computer programme was stopped. The computer programme printed out the values of the state space variables x_1 to x_6 and the simulation time at which the iteration was stopped.

2) Simulation of the deceleration of the motor-generator set

This was done by restarting the computer programme and using a supply voltage and frequency corresponding to the lower values used in the deceleration test. The intitial conditions at simulation time $t = 0$ were as follows: The initial values of the state space variables x_1 to x_6 were made equal to the final values reached when simulating the steady-state behavour of the motor-generator set at the higher speed - consequently the second part of the simulation described the behaviour during and after deceleration: time $t = 0$ representing the instant at which the supply to the induction motor changed.

Sufficient simulation time was allowed for the computer programme to reach a steady state and produce sufficient results to describe steady-state operation at the lower speed.

During the deceleration tests, the D.C. generator was unloaded and unexcited and so both parts of the simulation used zero D.C. generator excitation. Throughout both parts of the simulation of the deceleration test the computer programme printed results of speed against simulation time and also printed results from which the average envelope of the red phase current could be plotted.

The effect of point-of-wave phase angle upon the simulation of the deceleration test

Appendix C describes the operation of the three-phase digital oscillator and states that during a change in output frequency or voltage or both, the oscillator maintains phase angle continuity of its output voltages. It may be assumed that a phase angle continuity is also maintained during change in voltage or frequency of V.V.V.F. supply provided that the amplifier channels and the transformers used in the V.V.V.F. supply do not cause transients in phase angle during changes in supply voltage or frequency.

Equation 4.28 of Chapter 4 shows that phase angle continuity of the three phase supply may be simulated by phase angle continuity of the equivalent d and q-axis supply voltages to the Kron primitive machine used to represent the induction motor. If ω_i is the intitial supply frequency used in the deceleration test and α_i is the point-of-wave phase angle used in the first part of the simulation, then the phase angle of the d-axis voltage at the end of the first part of the simulation is

$$\omega_i t_i + \alpha_i$$

Where t_i is the simulation time reached at the end of the first part of the simulation.

Let α_1 be the phase angle of the d-axis voltage at the start of the second part of the simulation. Therefore for phase angle continuity the phase angle of the d-axis at the end of the first part of the simulation must equal that at the start of the second part, and so:

$$\alpha_1 = \omega_i t_i + \alpha_i \qquad (5.5)$$

Sufficient multiples of 2π were subtracted from α_1 so that it fell within the range 2π to -2π. Unlike α_i which is described as the point-of-wave phase angle (that is the point on red phase voltage waveform at which the induction motor is connected to the supply), α_1 is more accurately described not as a point-of-wave phase angle but as the frequency change phase angle: that is, the phase angle of the supply voltage when the frequency changes.

The choice of α_i is not crucial to the simulation of the steady-state behaviour of the motor-generator set when the induction motor operates from a supply having voltage and frequency equal to the initial values used in the test. This is because all transients due to point-of-wave switching will have

died away once the simulation reaches a steady state. However, the choice of α_i, ω_i and t_i will affect α_l.

It is likely that the change in frequency and voltage of the supply will cause transients whose nature will depend upon α_l, the frequency change phase angle. However the change in supply voltage and frequency during the deceleration test was produced by manually altering the setting of the switches which controlled the output voltage and frequency fo the three phase digital oscillator. As described in Appendix B this method of changing the output voltage and frequency would give no control over the phase angle of the output waveform when these changes took place and so α_l would have a random value. Consequently it is not possible to use values of α_l in the simulation that were produced during the test.

However, it is likely that transients produced by the change in supply voltage and frequency during the deceleration test are not likely to be as severe as those at the start of the deceleration test. This is because changes in supply frequency during the deceleration test were accompanied by proportional changes in the supply voltage in order to avoid magnetic saturation of the induction motor, so tending to keep the magnetic flux in the induction motor approximately constant during changes in supply voltage and frequency. This contrasts with the acceleration test which involves sudden magnetisation of the induction motor. During the simulation of the acceleration test it was found that the value of α_i had little effect on the behaviour of the motor-generator set after about 0.02 seconds of simulation time. Consequently, it was assumed that the value of α_l would have little effect on the deceleration of the motor-generator set but computer simulations were done to check this.

The power flow between the induction motor and the supply during deceleration

As mentioned previously in this section, one problem that could have occurred during the deceleration test was that the sudden decrease in supply frequency would cause brief supersynchronous operation of the induction motor. This would cause the induction motor to generate, feeding power back into the supply and therefore damaging the amplifier channels. No damage was noted, possibly because generation did not occur. To verify this, the computer programme used in the simulation was altered so that it calculated the power flow into the induction motor. Power flow was calculated during

both parts of the simulation. Power flow was calculated during the first part of the simulation to check whether the computer programme produced a suitable estimate of the size and direction of the power flow during steady-state operation of the motor generator set at the initial value of supply voltage and frequency used in the deceleration test. Power flow was calculated during the second part of the simulation to check whether generation occurred during deceleration and also to check the size and direction of power flow during steady-state operation of the motor-generator set at the lower values of supply voltage and frequency used in the test.

The power flow P_{e3} into the induction motor is the sum of the power flow into all three phases and is given by

$$P_{e3} = v_R i_R + v_Y i_Y + v_B i_B \tag{5.6}$$

Using equations 4.27, 4.29, 4.34, 4.35, 4.72 and 4.75 P_{e3} may be expressed in terms of the supply voltage and frequency, and the state-space variables x_1 and x_4 which represent the d and q-axis stator currents, respectively of the Kron primitive machine:

$$P_{e3} = \frac{3V}{\sqrt{2}}(x_1 \cos(\omega t + \alpha) + x_4 \sin(\omega t + \alpha)) \tag{5.7}$$

where α is either the point-of-wave phase angle or the frequency change phase angle, depending upon the part of the simulation in question. A negative value of P_{e3} implies power flow from the induction motor to the supply and therefore generation.

5.4.3 The comparison between experimental results and computer simulation of the deceleration tests

Two deceleration tests were performed and the experimental results and the computer simulation of each test are compared in figures 5.4 and 5.5. The conditions of each test are listed below.

Deceleration test 1:

Initial supply voltage and frequency : 200 volts 50.2 Hz

Final supply voltage and frequency : 158 volts 39.6 Hz

Figure 5.4 compares the experimental results and computer simulations of this test.

Figure 5.4: Deceleration test 1: Graphs of speed and average current envelope against time.

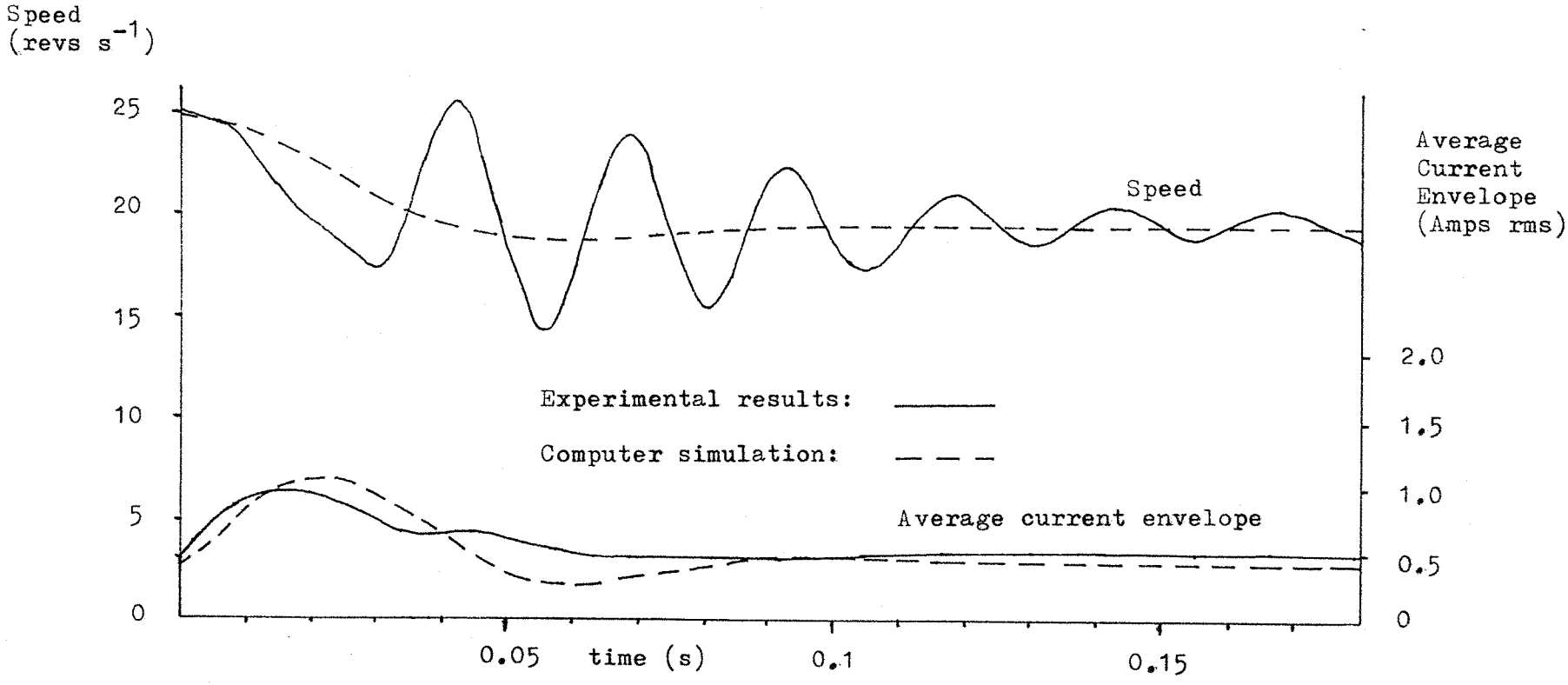

Figure 5.5: Deoeleration test 2: Graphs of speed and average current envelope against time.

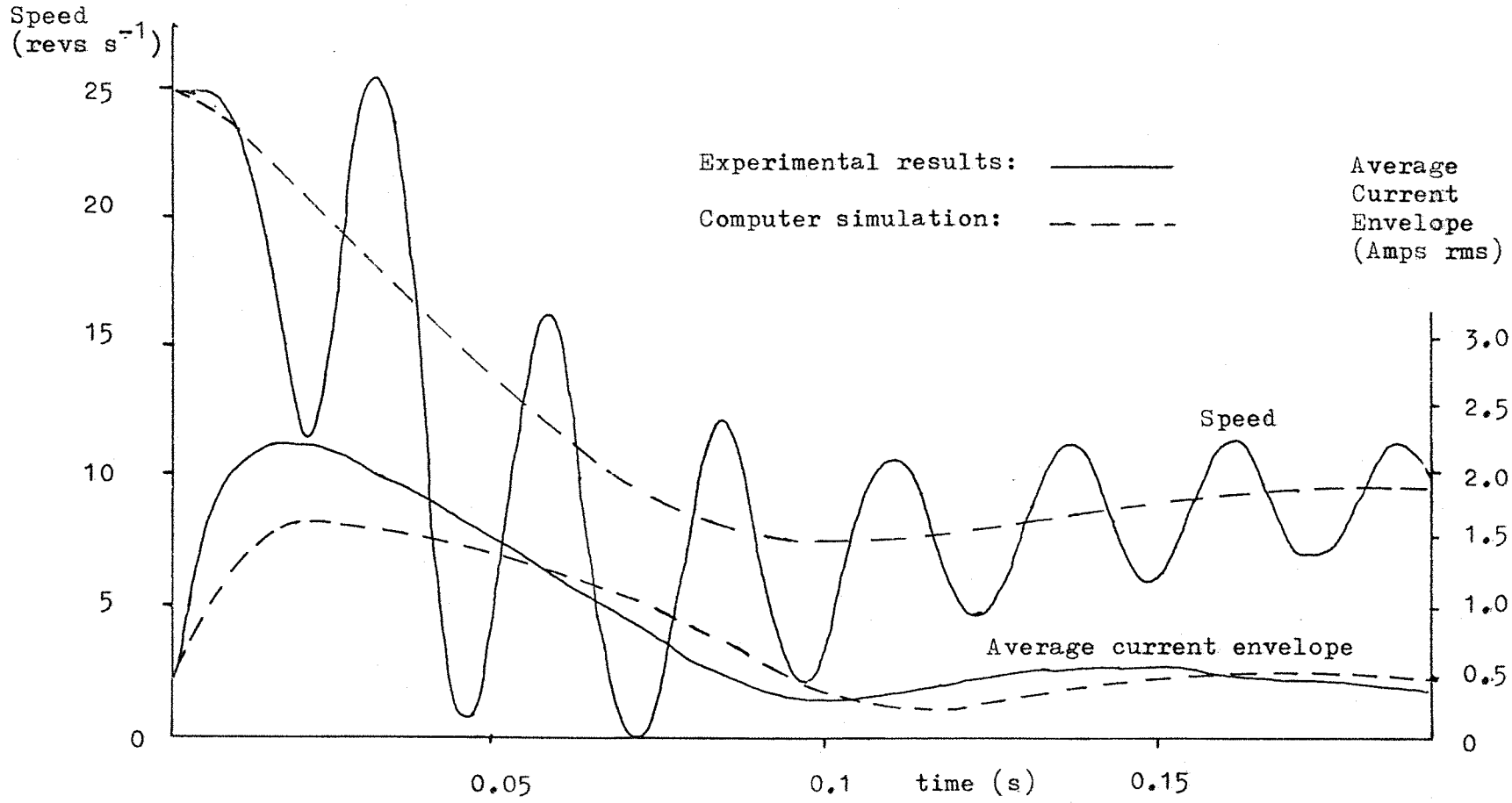

Deceleration test 2:

Initial supply voltage and frequency = 200 volts 50.2 Hz

Final supply voltage and frequency = 80 volts 20.0 Hz

Figure 5.5 compares the experimental results and computer simulation of this test.

During these tests reduced supply voltage (200 volts) instead of rated supply voltage (240v) was used as the initial supply voltage in order to avoid large current surges during deceleration which would overload the amplifiers.

Comparison of graphs of speed against time

Figures 5.4 and 5.5 both show a ripple superimposed upon the graphs of experimental results of speed against time. This ripple was due to vibration and torsional oscillations and was assumed to be similar to that met during the acceleration tests.

Figure 5.4 shows a good agreement between the experimental results and the computer simulation of deceleration test 1. Repeats of the simulation using different point-of-wave angles at which the supply frequency changed showed that different values of this angle had little effect upon the results of the simulation.

Figure 5.5 shows that the agreement between experimental results and the computer simulation is not as good as in deceleration test 1. In a similar manner to deceleration test 1 the choice of point of wave phase angle at which the frequency changed had little effect upon the results of the computer simulation.

An interesting feature of both tests was that the final speed was not the minimum speed reached during a particular test. Instead the motor-generator set rapidly decelerated from the higher speed to a minimum speed and then accelerated more slowly to the final speed. Figures 5.4 and 5.5 show this feature to be present in both the experimental results and the computer simulations of both tests.

Comparison between graphs of average current envelope against time

Figures 5.4 and 5.5 show that there is fair agreement between experimental results and the computer simulation of a test. Again, the point of wave phase angle at which the frequency changed had little effect upon the results of the computer simulation.

Sources of discrepancy between experimental results and the computer simulation of a test

The sources of discrepancy relevant to the acceleration test and described in section 5.3.3 are also relevant to the deceleration test. Altering the step-length of the iteration used in the computer simulation had little effect upon the simulation, neither did substituting experimental values of the electrical parameters of the induction motor for manufacturers data. The effects of point-of-wave angle were studied and were shown to have little effect upon the results of the computer simulation. This was expected as it had assumed for reasons stated in subsection 5.4.2 that the point of wave angle would have little effect upon the performance of the induction motor or, indeed upon the simulation of its behaviour.

Another source of discrepancy is the behaviour of the drive during "regeneration", that is, operation of the induction motor as a generator.

The effects of regeneration

Say [5] states that an induction motor will act as a generator if it operates at a speed above its synchronous speed. These conditions occur during the deceleration test as the sudden reduction in supply frequency results in operation of the induction motor above the synchronous speed corresponding to the new supply frequency. It is reasonable to suppose that regeneration would occur and this was confirmed by computer simulations of both tests. Equation 5.7 of section 5.43 describes the calculation of power flow between the supply and the induction motor. Regeneration was predicted by the computer simulation regardless of the point-of-wave angle at which the supply frequency changed. The experimental results also suggest that regeneration occurred since the time taken to reach the minimum speed achieved during a test was about 100 ms. This was a much shorter time than would be expected if the motor-generator set decelerated under the influence of bearing friction and fluid friction alone, implying that the kinetic energy of the motor-generator set was being converted to electrical energy in the induction motor.

During regeneration the flow of induction motor current is in a reverse direction to that during motoring. This reversal is resisted by the output transistors of the amplifier channels because of their semiconducting nature. In other words, an output transistor which would be conducting during motoring action during a particular point in the output voltage waveform would be reverse-biased by a current attempting to flow in the reverse

direction. This could cause damage and is the reason why the maufacturers of the amplifiers warn against attempting to feed power into one or more amplifier channels.

A reason why damage did not occur during deceleration tests was probably the "free-wheeling" diodes across the output transistors. Such diodes would conduct when the associated transistors were reverse-biased and could provide a path for any current flow during regeneration. Under these circumstances the behaviour of an amplifier channel would alter considerably accounting for the discrepancy between the experimental results and the computer simulation. This would also explain why the discrepancy was most marked during deceleration from the highest speed to the minimum speed since this situation, according to the computer simulation, corresponded to regeneration.

However, the amplifer channels are unable to return power to the mains supply as they derive their D.C. power from a diode bridge rectifier which only allows power flow from the mains into the amplifier. Thus any power flow into the amplifier channels must be absorbed internally in the amplifiers. Examination of the circuit diagram of an amplifier shows that each amplifier has a 15,000 μF smoothing capacitor to smooth the output of the bridge rectifier and it is likely that this capacitor absorbs the energy produced during regeneration. The test likely to produce the greatest regeneration was test 2 as the loss in kinetic energy was greatest. Consequently problems caused by regeneration are likely to be more acute during this test than during test 1. These problems are discussed below:

The kinetic energy lost by the motor-generator set during deceleration from the highest speed to the minimum speed during deceleration test 2 can be calculated knowing the change in speed and the moment of inertia of the motor generator set and is 28.9 Joules. Manufacturer's data states that the smoothing capacitor in question is normally charged to about 63 volts by the bridge rectifier. If all the kinetic energy lost by the motor generator set was stored as electrical energy in such a capacitor its voltage would rise to about 89 volts. In practice the voltage rise would be much less because of ohmic losses in the induction motor, transformers and free-wheeling diodes and also because frictional losses would contribute to the deceleration. Furthermore, any such electrical energy stored would be divided between two such capacitors since two amplifiers were needed to obtain three amplifier channels necessary for a three-phase supply. It is likely that the

amplifier channels could stand a resulting small rise in D.C. supply rail voltage and could therefore tolerate small amounts of regeneration of short duration. It is unlikely they could withstand prolonged regeneration because of the high voltages produced across the capacitors and components in the amplifer channels.

Phillips [20] describes how constant-current source inverters achieve regeneration. In order to preserve the same direction of current during regeneration as during motoring, the inverter achieves reverse power flow by reversing the polarity of the voltage of each phase of the induction motor rather than by reversing the current flow. This avoids problems of reverse - biasing the semiconductors in the inverter. The rectifier which normally converts mains A.C to D.C. for the inverter now becomes an inverter, and delivers the power from the induction motor to the mains. Such behaviour is only possible if the rectifier uses controlled semiconductors, such as thyristors.

5.4.4 Conclusion

The experimental results and the computer simulations of the deceleration tests have shown that the mathematical model developed in Chapter 4 to describe the motor-generator set is able to describe the behaviour resulting from a sudden reduction in supply voltage and frequency. Discrepancies between the experimental results and the computer simulation occur mainly during deceleration of the motor-generator set causing regeneration and consequent changes in the performance of the amplifier channels. The deceleration tests and their computer simulations have suggested how the amplifiers are able to cope with limited regeneration.

5.5 Load Variation Test

5.5.1 The purpose of the test

The purpose of this test was the study of the behaviour of the induction motor drive when the induction motor was subject to small sinusoidal changes in load torque about a mean value of torque. The test used the D.C. generator to apply load torques to the induction motor. Measurements were made of the ratio between the magnitude of the changes in load torque and the resulting changes in speed of the motor-generator set and measurements were also made of the phase shift between the changes in load torque and speed. In other words, the test was a frequency response test, in which gain and phase shift were measured. In this case, "gain" was defined as the change in speed divided by the change in load torque.

The test used small changes in load torque in order that the induction motor torque speed characteristic could be asumed to be linear over the small range of speeds and load torques likely to be met during the test. It was also assumed that this linearity of the torque-speed characteristic would ensure that small sinusoidal changes in load torque would produce small sinusoidal changes in speed and so it would be meaningful to refer to a phase shift between changes in speed and load torque.

The validity of the mathematical model was studied by comparing the values of gain and phase shift obtained by experiment with values predicted by the mathematical model. The use of sinusoidal changes in speed and load torque meant that experimental data and the results of predictions based upon the mathematical model would be suitable for display on Bode diagrams.

5.5.2 The method of producing small sinusoidal changes in load torque about a mean value of torque

The D.C. generator provided a convenient way of applying a controlled torque to the induction motor - an electrical load on the D.C. generator results in the D.C. generator exerting a torque upon the induction motor. It must be remembered that this torque forms only part of the load torque upon the induction motor. The remainder is the sum of torques produced by the inertia and various losses of the motor-generator set (see previous Chapter).

The load variation test required small sinusoidal changes in load torque, which implied variations with time of the electrical load upon the armature of the D.C. generator. Two methods of producing an electrical load which varied with time were considered and are outlined below:

1) The use of a load resistance of fixed value connected to the armature of the D.C. generator and the use of variable excitation. Changes in the excitation would produce changes in the voltage across the load resistance and therefore changes in the load upon the D.C. generator.

2) The use of a fixed generator excitation and a load resistance whose value changes with time and so produces changes in the load upon the D.C. generator.

The chief advantage of the use of variable excitation and a fixed load resistance to produce changes in load is that these changes can be achieved by control circuitry rated to cope with the power needed for excitation, rather than the much larger power of the load upon the D.C. generator. However, this method suffers from the non-linear relationship between the excitation of the D.C. generator and the torque exerted by the D.C. generator upon the induction motor. The non linearity arises for the following reasons: At a given speed of the motor-generator set, the output voltage of the D.C. generator is proportional to the excitation and therefore if the load resistance is fixed, the armature current of the D.C. generator is proportional to the excitation. However, as stated in equation 4.58 the torque produced by the conversion of mechanical power into electrical power in the armature is proportional to the product of the excitation and the armature current and therefore in this case, the torque produced by the conversion of power in the armature is proportional to the square of the excitation. Consequently the torque exerted by the D.C. generator upon the induction motor bears a non-linear relationship to the excitation.

Altering the field current of the D.C. generator alters the excitation. In view of the square-law relationship between the torque produced by power conversion and the excitation it was considered difficult to control the field current in such a way that produced small sinusoidal changes in torque. Control would be made more difficult because of the following effects:-

1) The torque-speed characteristic of the induction motor would cause changes in speed with load and spoil the linear relationship between excitation and output voltage of the D.C. generator.

2) Magnetic saturation would spoil the linear relationship between field current and excitation.

Consequently it was decided to use constant excitation and a load resistance whose value changes with time in order to produce sinusoidal changes in load torque. Figure 5.6 shows the circuit which was used: the signal generator, the two transistors and the 2.2 Ohm resistor controlled the armature current of the D.C. generator. The signal generator was able to

Figure 5.6: Load variation test: Circuit used to produce variations in load torque

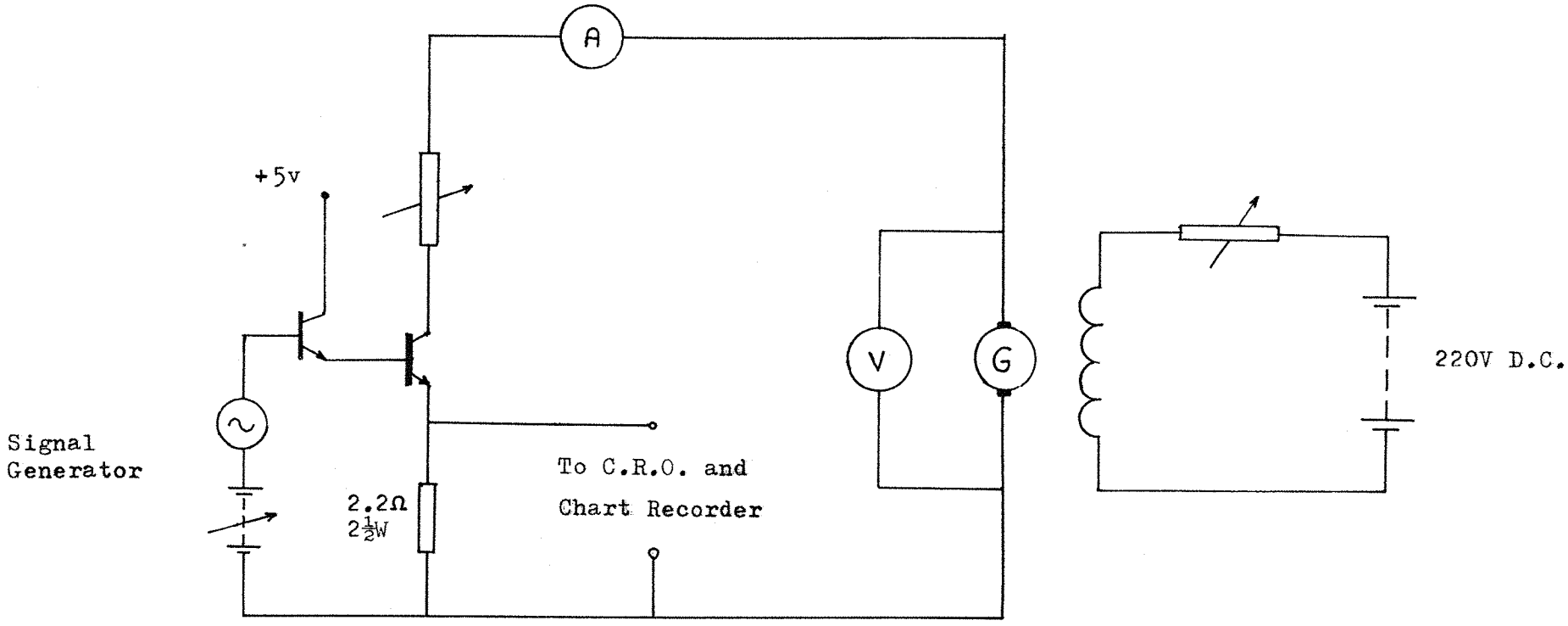

produce sine waves having a D.C. offset and this offset was used to bias the transistors. Because the transistors were connected in emitter follower mode the changes in armature current exactly followed changes in the voltage of the signal generator. This, of course, assumes that changes in the voltage of the signal generator did not cause incorrect biasing of the transistors. A small sinusoidal signal, therefore, produced a small sinusoidal change in armature current and therefore if the excitation of the D.C. generator remained constant this change in armature current produced a sinusoidal change in load torque upon the induction motor. Of the two transistors shown in Figure 5.6 the one which directly controlled the armature current acted as a variable resistance whose value altered in such a way that the changes in resistance caused changes in armature current which followed, and were proportional to, changes in the output voltage of the signal generator. This transistor was mounted on a substantial heat-sink to cope with the power dissipated in the transistor as it acted as a variable resistance. Two transistors were needed in the circuit in order to produce sufficient current gain.

The current flowing in the 2.2 ohm resistor is the sum of the armature current and the base current of the transistor which directly controls the armature current. Assuming that the current gain of this transistor is large, then the current in the 2.2 Ohm resistor is approximately equal to the armature current. Consequently the voltage across the 2.2 Ohm resistor describes, approximately, the armature current and therefore the torque exerted upon the induction motor by the conversion of power in the armature of the D.C. generator. This voltage was measured by a C.R.O. and a channel of a chart recorder in order to measure and record changes in armature current and therfore load torque upon the induction motor. The output current and voltage of the D.C. generator were measured by meters connected as shown in Figure 5.6.

It is important to note that the use of constant excitation and variable load resistance to produce sinusoidal changes in load torque is unaffected by changes in the D.C. generator voltage caused by changes in speed with load, provided that at all times the voltage is able to circulate the required current through the load. This is because the torque resulting from power conversion in the armature is proportional to the product of the excitation and the armature current.

5.5.3 Experimental procedure

The purpose of this test was to study the behaviour of the motor-generator set when the induction motor was subject to small changes in load torque about a mean value of torque. The magnitude of the changes in load torque used in the test was a compromise between two conflicting requirements:

1) Changes in load torque small enough to allow the assumption that the torque-speed characterisitic of the induction motor was linear over the range of the small changes in load torque and resulting small changes in speed.
2) Changes in load torque large enough to produce changes of speed large enough to be measured accurately. This was of particular concern since the vibration of the motor-generator set produced changes in speed which could mask changes in speed due to changes in load torque.

It was decided to set excitation of the D.C. generator to produce an armature voltage of 50 volts when the D.C. generator was unloaded, and to produce an armature current that varied sinusoidally from zero to 1 ampere about a mean value of 0.5 ampere. This subjected the induction motor to a load whose power varied with an approximate amplitude of 25 watts about a mean value of approximately 25 watts plus the rotational losses. These figures are only approximate due to the effects of losses, and the change in losses and D.C. generator voltage with changes in speed due to changes in load. The change in load upon the induction motor was therefore about 50 watts which is about a fifth of the rated output power, 250 watts, of the induction motor. This change in load power was considered an acceptable compromise between the two conflicting requirements described previously.

The use of 50v for the voltage of the D.C. generator when unloaded arose because 50v was the maximum rated voltage of power transistors conveniently at hand. The use of an armature current that varied between 0 - 1.0 amps resulted in an overload during a small part of the waveform of the armature current. However, this overload was not considered dangerous because it was small, of short duration, and the R.M.S. value of the current waveform, 0.612 amps was less than 0.82 amps, the rated armature current, indicating that the armature was unlikely to overheat.

Before the test the motor-generator set was run with the V.V.V.F. supply adjusted to deliver the voltage and frequency to be used in the test. In order to unload the D.C. generator, the signal generator was switched off thus

switching off the transistors used to control the armature current. The excitation of the D.C. generator was adjusted to produce an output voltage of 50 volts, and the resulting speed of the motor-generator set was measured by a frequency meter connected to the output of the shaft encoder. While the motor-generator set was operating as described above, the chart recorder channels used to plot graphs of speed and armature current against time were calibrated in the following way:

The signal generator was switched on and adjusted to produce a D.C. output that caused the transistors to conduct causing a steady armature current to flow. This in turn produced a deflection of the spot of light used by the chart recorder channel to draw a graph of armature current against time. The size of deflection could be altered by altering the sensitivity of the chart recorder channel. This was sometimes needed in order to produce a graph of suitable size for measurement. The sensitivity was altered by a variable resistor in series with the chart recorder channel. The chart recorder channel was calibrated by comparing the size of deflection of the spot of light with the change in armature current indicated by an ammeter measuring armature current. In a similar way, the C.R.O. could be calibrated to display changes in armature currents although the sensitivity of the C.R.O. was adjusted by altering the gain of its input amplifier. The trace displayed by the C.R.O. was unaffected by changes in the resistance used to alter the sensitivity of the chart recorder channel used to record the armature current, since this resistance and the impedance of the chart recorder channel were in parallel with, and very much larger than the 2.2 ohm resistor.

The change in armature current from zero to a steady value increased the load upon the induction motor and caused a fall in speed. This in turn caused a deflection in the spot of light used by the appropriate chart recorder channel to draw a graph of speed against time. This chart recorder channel was calibrated by comparing the size of the deflection against the change in speed indicated by the frequency meter used to measure the output frequency of the shaft encoder. If necessary, the sensitivity of this chart recorder channel could be altered by methods described in Chapter 3.

The positions on the chart recorder paper of the graphs of speed and armature current against time could be altered by altering the zero setting of the appropriate channel of the chart recorder.

All the above adjustments and calibrations were carried out with the paper feed mechanism disengaged in order to save paper. Once these

adjustments and calibrations were made, the equipment was ready for the test to begin.

At the start of the test the V.V.V.F. supply was set to deliver the supply voltage and frequency to be used in the test and the motor-generator set was run from this supply. The signal generator was adjusted to give zero output voltage, so preventing any armature current from flowing, and the excitation of the D.C. generator was adjusted so that the output voltage of the D.C. generator was 50 volts when unloaded.

The signal generator was adjusted to generate a frequency of 0.1 Hz. The amplitude of the A.C. signal and the D.C. offset produced by the signal generator were adjusted in conjunction with adjustments to the load resistance, to produce an armature current which varied from zero to 1 amp in a sinusoidal manner. At such a low frequency the moving coil meter used to measure the armature current was assumed to give an accurate indication of the maximum and minimum values of armature current. At higher frequencies the C.R.O. was used to measure the maximum and minimum values since the moving coil meter would be unlikely to follow the faster changes in armature current.

Once the armature current was controlled to vary in the manner described, the paper feed mechanism of the chart recorder was engaged and graphs of armature current and speed against time were recorded. From these graphs, change in speed and the phase shift between the change in speed and the change in armature current (and therefore load torque upon the induction motor) can be found from drawing and measurement.

The vibration of the motor generator set did affect the graph of speed against time as the ripple in speed produced by the vibration was of significant size compared to the change in speed produced by changes in armature current. This superimposed a high frequency ripple upon the much lower frequency speed change resulting from changes in speed due to changes in load torque. Measurements of speed change and of phase shift between the change in speed and change in armature current were made from a curve drawn on the graph of speed against time. This curve was drawn in such a way that it "averaged out" the effects of the high frequency speed change caused by vibration yet showed the overall change in speed due to change in load torque.

This test was repeated using different frequencies of change in armature current in the range of 0.1 Hz to 14 Hz. Above 14 Hz the frequency

of the change in speed approached that of the frequency of vibration and it was not possible to distinguish between changes in speed due to vibration and changes in speed due to changes in load. Consequently no frequencies higher than 14 Hz were used.

5.5.4 Measurement of changes in induction motor current

The acceleration test and the deceleration test described in this chapter both took recordings of induction motor current for comparison with predictions made using the mathematical model. During the load variation test an attempt was made to study the changes in induction motor current caused by changes in load torque upon the induction motor. These changes in induction motor current caused amplitude modulation of the induction motor current and consequent changes in the envelope of the waveform of the current. An attempt was made to measure the size of the changes in the envelope and their phase shift with respect to changes in load torque upon the induction motor. The object of the attempt was to make measurements that could be compared with estimates produced from the mathematical model, and so test the validity of the model. However, the following difficulties were met:

1) The percentage change in induction motor current with the size of load used in the test was small, making detection of change difficult. The small percentage change results from the tendency of small induction motors, such as the one used in the test, to draw a current having a large magnetising current component which shows little change with load. An attempt was made to solve this problem using power factor correction capacitors which reduced the magnetising current taken from the supply and so increased the percentage change in current taken from the V.V.V.F. supply. The changes in current taken from the supply could be related to actual changes in induction motor current after allowances were made for the power factor correction capacitors. However, these capacitors reacted to the high frequency components of the digitally-synthesised sine wave and caused the current transformer measuring current to produce a signal containing large amounts of high-frequency noise. This tended to hinder measurement of current.
2) Another problem met was that of plotting the envelope of the induction motor current. As the frequency of variations in the load torque

increases so does the frequency of the changes in envelope of the induction motor current resulting in less peaks of the current waveform available to plot one cycle of change in the envelope. This can lead to considerable uncertainty in plotting the envelope of the current waveform even at quite low frequencies of load torque variation. An attempt was made to solve this problem by using three current transformers and three chart recorder channels to plot the currents in all three phases rather than just one phase as had been done in the acceleration and deceleration tests. Provided that the zero settings of each chart recorder channel were the same and the burdens across the current transformers were adjusted so that the amplitude of each trace was the same when the induction motor was supplying a steady load, then there should be three times as many current waveform peaks available than before to plot the current waveform envelope. In practice the adjustment of the burdens proved too coarse and the resulting differences in amplitude of the traces prevented accurate plotting of the envelope. Adjustments of the burdens was needed to compensate for differences in the current transformers and chart recorder channels, and also slight differences in phase currents. These differences were thought to arise from differences between the impedances of the transformers in the V.V.V.F. supply and differences in the impedances of the induction motor.

A further attempt was made to solve the problem of plotting changes in the induction motor current. A three phase bridge rectifier was used to rectify the voltages across the burdens of the three current transformers used to measure the three phase currents. The output of the bridge rectifier was a D.C. voltage which represented the largest of the magnitudes of the phase currents at a particular point in time. However, this method also suffered from problems of adjusting the burdens of the current transformers to cope with slight unbalance of the phase currents which caused ripple in the D.C. voltage.

In the light of the problems described, no measurements of changes in induction motor current were made during the load variation test.

5.5.5 Computer simulation of the load variation test

Objective of the simulation

The objective of the computer simulation of the load variation test was the simulation of the behaviour of the motor generator set when the induction motor was subject to a varying load torque. The computer programme used in the simulation was designed to calculate the change in speed caused by changes in load torque and the phase shift between the changes in load torque and speed. The computer programme was based upon that used to simulate the acceleration test, but was modified in the following ways:

Simulation of changes in load torque

As described previously, changes in load torque were produced by sinusoidal changes in D.C. generator armature current from zero to a maximum value. Consequently it was not necesary to calculate x_6, the state-space variable representing armature current, from the state space equation 4.86. Instead x_6 was calculated from the much simpler equation

$$x_6 = \tfrac{1}{2} I_{AM} (1 + \sin \omega_{AM} t) \tag{5.8}$$

where

I_{AM} is the maximum value of the armature current.

ω_{AM} is the frequency of the changes in the armature current (rad s^{-1}).

Equation 5.8 was substituted for x_6 in equation 4.85 to yield

$$f_5(\underline{x}, \underline{u}) = \frac{1}{J}\left(\frac{3}{2} n_p^2 M (x_2 x_4 - x_1 x_3) - n_p T_b - k_{ff} x_5 - k_x (E_x)^q n_p^{(2-\gamma)} x_5^{(\gamma-1)} - \tfrac{1}{2} n_p E_x I_{AM} (1 + \sin \omega_{AM} t)\right) \tag{5.9}$$

This substitution allowed the removal of all references to x_6 in the fifth-order Kutta-Merson algorithm, and consequently $\underline{x}_o$, $\underline{x}_n$, $\underline{x}_{n+1}$ and the fifth-order Kutta Merson coefficients $\underline{K}_1$ to $\underline{K}_5$ were all converted to five-element column matrices.

As described previously, before each load variation test the excitation of the D.C. generator was adjusted so that the armature voltage of the D.C. generator was 50 volts when the armature was unloaded. The excitation used in the test cannot be known exactly as, owing to an oversight of the author, the speed of the motor-generator set was not recorded. However, the speed can be estimated using the method of calculation described in section 4.8 of Chapter 4 and the excitation can be estimated from this estimate of speed.

Calculation of the change in speed due to changes in load torque

The changes in load torque would cause changes in speed about an average value of speed. This average value was crucial to the calculation of the change in speed and also the phase shift between changes in speed and load torque. The average value of speed was defined as the steady-state speed of the motor-generator set when the armature current of the D.C. generator equalled the average value of armature current used in the particular test in question and the excitation of the D.C. generator equalled the value of excitation used in the particular test in question. The average speed can be calculated from these values of excitation and armature current using the method described in Section 4.8. Since the excitation is known, equation 4.97 may be used instead of equation 4.100 in the calculations.

The change in speed due to change in load torque was calculated by finding the difference tetween the maximum and minimum speeds obtained during the simulation. The maximum and minimum speeds were found in the following way:

At the start of the simulation, stores in the memory of the computer were reserved for the maximum and minimum values of speed obtained during the simulation. The maximum and minimum values of speed were found in the following way:

Maximum speed: At the end of each step in the iteration, the speed was calculated and if the speed was greater than both the average speed and the maximum speed obtained so far the store containing the maximum speed was updated with the speed calculated during the step in question.

Minimum speed: If the speed calculated at the end of a step in the iteration was less than both the average speed and the minimum value of speed obtained so far, the store containing the minimum speed was updated with the speed calculated during the step in question.

Calculation of the phase shift by which changes in speed lag changes in load torque

The computer programme calculated the phase shift from the interval of simulation time separating similar points on the waveforms of armature current and speed.

Equation 5.8 shows that the armature current is at its average value $\frac{I_{AM}}{2}$ at time t equals zero, and is increasing. A similar point on the speed waveform occurs when the speed reaches its average value and is increasing. If t' is the simulation time at which this point occurs on the speed waveform,

then the separation in time between similar points on the speed and current waveforms is t_a. The phase shift ϕ_s by which changes in speed lag changes in armature current is given by

$$\phi_s = \omega_{AM} t \qquad (5.10)$$

where ϕ_s is in radians if ω_{AM} is in radians per second.

It is most unlikely that at some step in the iteration the calculated speed will equal exactly the average speed. Instead it is more likely that at some stage during the simulation two consecutive steps in the iteration will produce values of speed that lie either side of the average value, implying that at some point between the two steps the speed equalled the average value. Consequently the following method was used to estimate t_a, the time at which the speed equalled the average speed and was also increasing:

At each step in the iteration the speed of the motor-generator set was calculated and both this value of speed and the value calculated during the previous iteration were compared with the average speed.

If ω_{ra} is the speed calculated at the end of the present step in the iteration, ω_{rb} is the speed calculated at the end of the previous step in the iteration, and ω_{AV} is the average speed then the following inequality:

$$\omega_{rb} \leq \omega_{AV} \leq \omega_{ra} \qquad (5.11)$$

implies that the speed is increasing and that at some point between the two steps in the iteration, the speed equalled the average value. If t_c is the simulation time at which inequality 5.11 applied then if ω_{ra} occurred at time t_c, ω_{rb} occurred at time t_c - h since the steps in the iteration are spaced h seconds apart. Figure 5.7 shows the relationship between t_c, h, ω_{ra}, ω_{rb}, ω_{AV} and the speed waveform.

Since in all cases considered the step length h (0.5 ms) was much smaller than the periodic time of the speed and armature current waveforms (71ms in the case of 14Hz : the highest frequency of changes in speed and armature current studied) the portion of the speed waveform between successive iterations may be assumed to be linear. From Figure 5.7 it may be seen that from the triangle formed by points A, B and D, the triangle formed by points A,C and E and the properties of similar triangles, the following relationship links t , t_c, h, ω_{ra},ω_{rb} and ω_{AV}:

$$\frac{\omega_{rb} - \omega_{ra}}{h} = \frac{\omega_{AV} - \omega_{ra}}{t + h - t_c} \qquad (5.12)$$

Figure 5.7: Diagram showing the relationship between t_c, ω_{ra}, ω_{rb}, ω_{AV}, t', h, and the graph of speed against time.

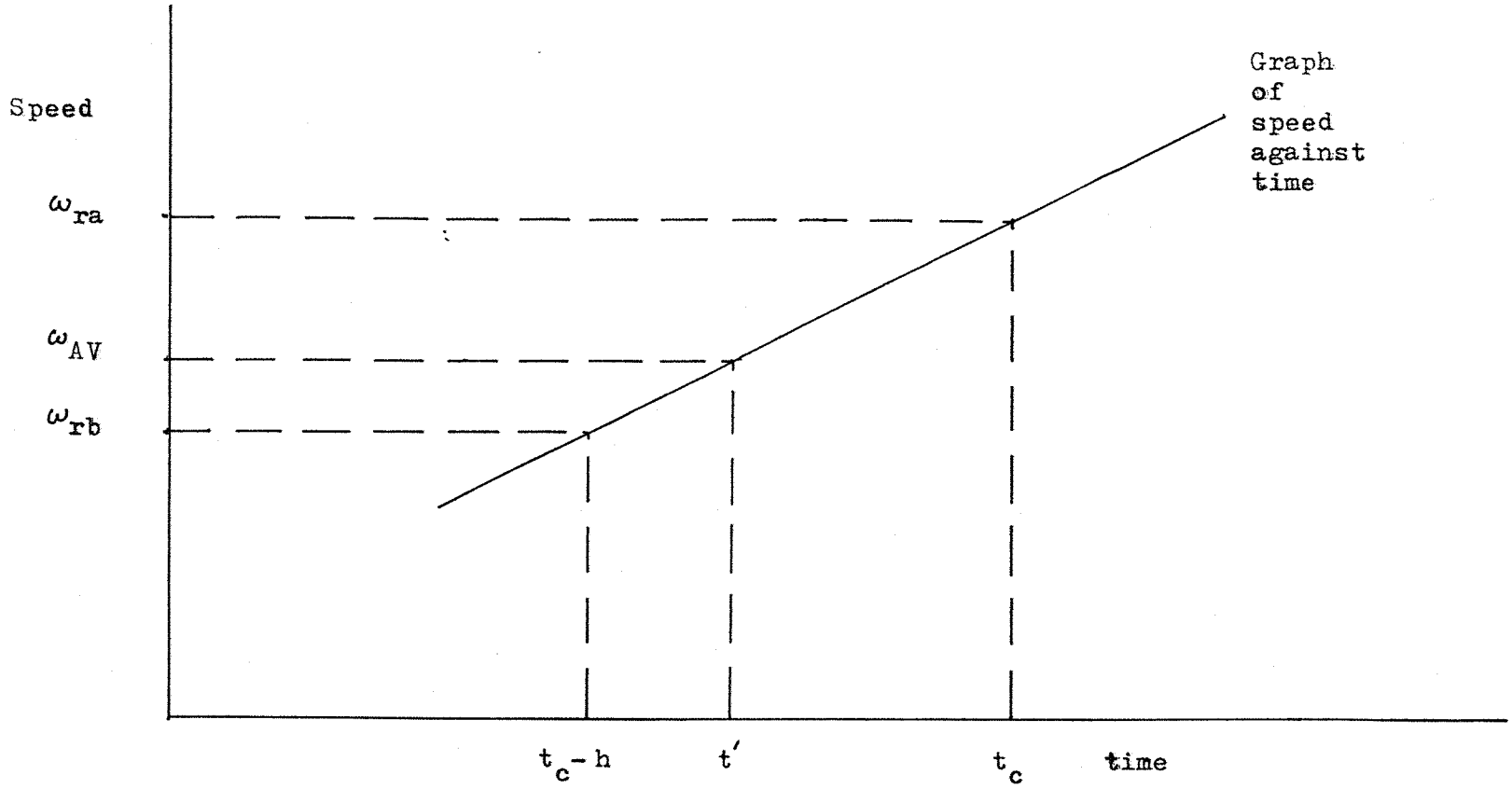

This equation may be rearranged in order to calculate t_a:

$$t' = t_c + h \frac{(\omega_{AV} - \omega_{rb})}{\omega_{rb} - \omega_{ra}} \tag{5.13}$$

During the simulation of the load variation test, it is possible that the true average speed, that is the average of the maximum speed ω_{max} and the minimum speed ω_{min}, may not be quite equal to ω_{AV}, the value predicted by assuming that the excitation of the D.C. generator is equal to that used in the test and that the armature current of the D.C. generator equals the average value used in the test. This difference between ω_{AV} and the true average speed results in a phase error ϕ_e in determining the phase shift between the changes in speed and armature current. Consequently equation 5.10 may be modified to include this phase error:

$$\phi_s = \omega_{AM} t + \phi_e \tag{5.14}$$

ϕ_e may be calculated in the following way:

If the speed ω_r of the motor-generator set varies sinuosidally between ω_{max} and ω_{min} then its amplitude is $\frac{1}{2}(\omega_{max} - \omega_{min})$ and its average value equals $\frac{1}{2}(\omega_{max} + \omega_{min})$

Also, if the speed varies with the same frequency ω_{AM} as the armature current, then since ϕ_s is the phase shift between the armature current waveform which is described by

$$x_6 = \tfrac{1}{2} I_{AM} (1 + \sin \omega_{AM} t) \tag{5.12}$$

the following equation therefore describes ω_r:

$$\omega_r = \tfrac{1}{2} ((\omega_{max} + \omega_{min}) + (\omega_{max} - \omega_{min}) \sin (\omega_{AM} t - \phi_s)) \tag{5.15}$$

As described previously, $\omega_r = \omega_{AV}$ at $t = t'$ and therefore substituting these values into equations 5.15 and 5.15 and combining the resultant expressions yields

$$\phi_e = \arcsin \left(\frac{2\omega_{AV} - (\omega_{max} + \omega_{min})}{\omega_{max} - \omega_{min}} \right) \tag{5.16}$$

Consequently ϕ_s, the phase shift by which changes in speed lag the changes in current may be calculated from the following equation, obtained by substituting equation 5.16 for ϕ_e in equation 5.14 and as stated above, putting $t = t'$

$$\phi_s = \omega_{AM} t' + \arcsin \left(\frac{2\omega_{AV} - (\omega_{max} + \omega_{min})}{\omega_{max} - \omega_{min}} \right) \tag{5.17}$$

The effects of initial conditions and transients at the start of the simulation

These affect calculations of the change in speed and the phase shift between changes in speed and changes in armature current of the D.C. generator.

As stated previously, the computer programme used to simulate the load variation test was developed from the computer programme used to simulate the acceleration test. Like the simulation of the acceleration test the simulation of the load variation test started by simulating the sudden connection of the induction motor. In such circumstances it is pointless to calculate the maximum and minimum speed and the phase shift between changes in speed and changes in armature current,since changes in speed due to changes in armature current will be masked by the acceleration of the motor generator set. Also, the simulation of the sudden connection of the supply to the induction motor will cause transients in the phase currents of Kron's primitive machine used to represent the induction motor, and these transients could also cause changes in speed which would mask changes due to changes in the armature current.

Consequently before the computer programme calculated the maximum and minimum speeds and the phase shift between changes in speed and armature current, sufficient time was allowed for the decay of changes in speed due to effects caused by the sudden connection of the supply to the induction motor. In order to reduce the length of time required, the initial condition used at $t = 0$ at the start of the simulation were modified so that x_5 equalled $n_p \omega_{AV}$ rather than zero as in the simulation of the acceleration. The other state space variables x_1 to x_4 were set equal to zero at $t = 0$, as was the case in the simulation of the acceleration test. The initial conditions used in the simulation of the load variation test corresponded to the motor generator set running at speed ω_{AV} but with no currents in the phases of the induction motor. Although this situation was never realized in practice it was assumed that using $n_p \omega_{AV}$ instead of zero as the initial value of x_5 in the simulation would result in less time needed for the decay of changes in speed due to effects caused by the simulation of the sudden connection of the supply to the induction motor. The validity of this assumption was checked by running a simulation of the load variation test using the supply voltage and frequency used in the experimental test but with the armature current set a constant value of 0.5 amps (the average value of armature current used in the test). In other words, the simulated load upon the D.C. generator was

constant and would result in the computer simulation reaching an eventual steady-state speed.

It was found that for a given simulation, the steady-state speed was reached more quickly using $n_p \omega_{AV}$ as the initial value of x_5 rather than zero, but the value of the steady-state speed did not depend upon which of the two initial values were chosen. In all cases involving $n_p \omega_{AV}$ as the initial value of x_5 a steady-state speed was reached by 0.4 seconds of simulation time.

Accordingly, the computer time allowed 0.7 seconds of simulation time to elapse before calculating the maximum and minimum values of speed and the phase shift between changes of armature current and changes in speed. The choice of 0.7 seconds rather than 0.4 seconds indicated by the simulations involving a steady armature current allowed a safety margin of 0.3 seconds for the complete decay of changes in speed resulting from the effects of the simulation of the sudden connection of the supply to the induction motor.

5.5.6 Experimental results

The test was performed using a 240v 50.2 Hz supply and adjusting the excitation of the D.C. generator to produce an output voltage of 50 volts when unloaded. Under these conditions the excitation of the D.C. generator was 0.3186 volts rad^{-1} (estimated from the steady-state representation of the induction motor drive). The armature current varied sinusoidally from zero to one ampere producing a load torque which varied from zero to 0.3186 Nm in a similar manner. Figure 5.8 shows graphs of $\log_{10}$ (speed change) and phase shift between the torque and speed changes against the frequency of load torque variations. Graphs derived from experimental results and computer simulations are shown.

The graphs of speed change and phase shift produced by the computer simulation of the load variation test show results that would be expected intuitively from such a test. These graphs show that at low frequencies (below about 2.0 Hz) of load variation, the speed change and phase shift are approximately constant as the changes in speed follow the changes in torque. The changes are in anti-phase as an increase in load torque produces a decrease in speed and vice-versa. Above 2.0 Hz the change in speed decreases and the phase shift increases as the inertia of the motor generator set affects its response to faster changes in load torque.

To an extent, the experimental results reflect the computer simulation, both showing that at low frequencies of load variation the speed

Figure 5·8 : Load Variation Test: Graphs of $\log_{10}$(Speed Change) and Phase Shift against Frequency of Load Variation.

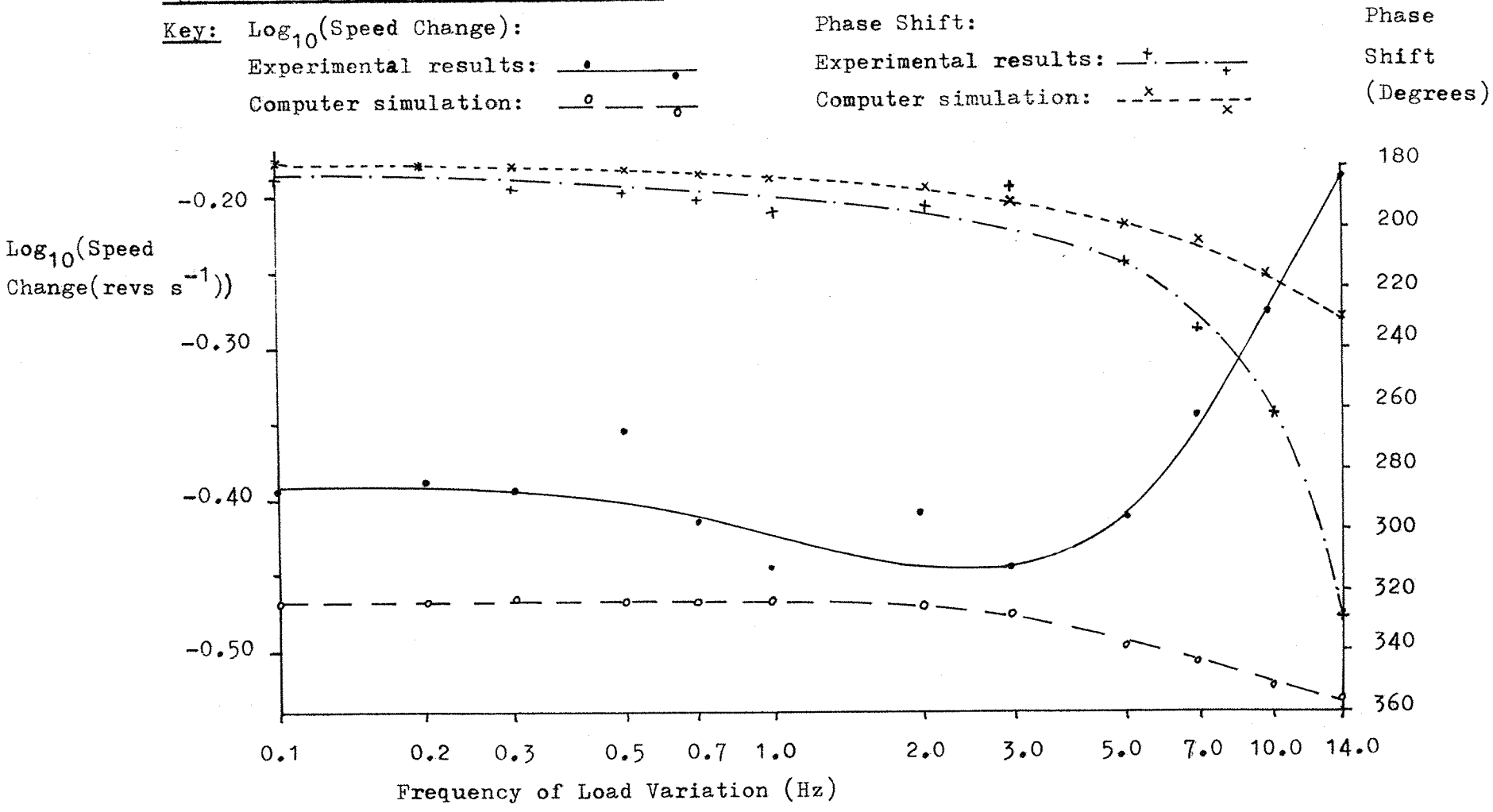

change and phase shift are constant, the phase shifts both being about 180 degrees. The experimental results suggest a possible decrease in speed change with increase in frequency of load variation, but the effects of vibration and torsional oscillations could easily mask such an effect.

Above 3.0 Hz the experimental results show that the speed change increases with frequency of load torque variation. The maximum change in speed produced during the test was at 14 Hz, the maximum frequency of load torque variation used in the test. A likely explanation for this unexpected result is torsional oscillations. Chapter 3 describes how investigations during the commissioning of the drive showed it to have a natural frequency of about 39Hz at which torsional oscillations produced by vibration can become large. Similarly, Figures 5.1 to 5.5 show that forces produced during acceleration and deceleration can produce such oscillations at a similar frequency. Half of this frequency, 39Hz is 19.5Hz which is close to 14Hz, the frequency at which maximum change in speed was produced during the test. Furthermore Figure 5.8 indicates that greater changes in speed may occur above 14Hz.

It is concluded, therefore, that at frequencies of load torque variation between 3.0 and 14Hz these changes in load torque begin to excite a mode of torsional oscillation. Support for this explanation is provided by the experimental results of phase shift which show a greater increase in phase shift with frequency than is shown by the phase shifts predicted by the computer simulation.

As described previously, vibration is a major source of error in this test as, in many case, it produces a change in speed comparable to that produced by changes in load torque. This was assumed to be the reason why the results of speed change at 0.5Hz and 2.0Hz departed from the smooth curve drawn in Figure 5.8. It was assumed that these departures were not due to resonance with modes of torsional oscillation as they were not matched by similar abnormalities in the results of phase shift.

Another source of discrepancy between experimental results and the computer simulation of the test is the amplitude modulation of the induction motor phase current waveform. Measurements described previously showed that changes in load of a size equal to that used in the test produced a measurable change in induction motor phase current. During the test these changes in phase current would result in amplitude modulation causing the phase current to be composed of a "carrier" frequency equal to the supply frequency, and "sideband" frequencies whose number and frequency would

depend upon the exact nature of the change in phase current due to changes in load torque. Although this modulation is common to both the test and its computer simulation the mathematical model of the induction motor makes no provision for modelling the effects of these sideband frequencies upon the magnetisation of the iron in the transformers and the induction motor. Similarly the sideband frequencies could cause the air-gap m.m.f. waveform to be non-sinusoidal, affecting the validity of the transformations described in Chapter 4 and used to convert between two- and three-phase quantities. The effects of these sideband frequencies is likely to increase as the frequency of load torque variation increased since this would cause the differences between the sideband and carrier frequencies to increase. However, these effects were not studied further.

Figure 5.8 shows that the computer simulation tends to underestimate the speed change resulting from low frequency changes in load torque. The reason for this is not obvious but the presence of vibration could account for some of the difference.

5.5.7 Summary

The load variation test and its computer simulation indicated that the mathematical model of the induction motor drive is unsuitable for representing the drive when subject to rapid changes in load torque. This is because the mathematical model has no facilities for dealing with vibration or possible modes of torsional oscillations which can result from such changes in load torque.

5.6 Comparison between steady-state conditions predicted by the mathematical model with those predicted by the steady-state representation

During computer simulations of the acceleration and deceleration tests it was found that once a simulation had reached a steady-state it produced results of speed and current that agreed very closely with such results obtained using the steady-state representation. It was therefore concluded that the mathematical model was a good description of the induction motor drive during steady-state operation.

5.7 An overall assessment of the validity of the mathematical model

The three tests described in this chapter - the acceleration test, the deceleration test and the load variation test - studied the induction motor drive under a variety of conditions. The acceleration and deceleration tests showed

that after allowing for the effects of vibration and torsional oscillations the mathematical model developed in Chapter 4 was a good description of the behaviour of the induction motor drive during acceleration and deceleration. The validity of the mathematical model is also supported by the agreement of the model with the steady-state representation, also described in Chapter 4.

However, the tests described in this chapter indicated that a major shortcoming of the mathematical model was its inability to model vibration and torsional oscillations of the motor-generator set. Consequently any further work aimed at improving the mathematical model should concentrate upon modelling vibration and torsional oscillations. The validity of the resulting mathematical model could be studied by tests similar to those described in this chapter and, or alternatively, by a test which used a varying supply frequency to cause small changes in speed of the motor-generator set.

5.8 Conclusions

This chapter has tested the validity of the mathematical model, described in Chapter 4, of the induction motor drive. After allowing for the inability of the mathematical model to describe vibration and torsional oscillations, the model is a good description of the behaviour of the induction motor drive during steady-state and transient conditions. The results of the tests described in this Chapter have shown that the mathematical model needs improvement so that it is able to model vibration and torsional oscillations.

6 THE CONTROL OF THE INDUCTION MOTOR DRIVE

6.1 Introduction

This chapter describes a control system which was used to control the induction motor drive and describes practical tests and computer simulations used to study the controlled induction motor drive.

6.2 The control strategy

6.2.1 Aim of the control strategy

As stated at the start of this thesis, the initial aim of this research was to develop a cage induction motor drive capable of four-quadrant control over a wide range of speed. However, the time available did not permit the development of such a drive and so a more simple control strategy was chosen instead. The aim of the control strategy was, therefore, to control the induction motor, so that it would run at a "target" speed, irrespective of changes in load provided the load did not exceed the rated load of the induction motor. No attempt was made to achieve changes in the direction of rotation of the induction motor.

6.2.2 Basic principle of the control strategy

The control strategy used speed-feedback to achieve closed-loop speed control of the induction motor. Differences between the actual speed of the induction motor and the target speed ω_{rc} caused the control strategy to reduce this difference in speed, called the "speed error," in the following way:

Consider an induction motor operating from a supply of voltage V and frequency ω_1 running at a speed ω_r, and supplying a load whose torque was constant with speed. The gross electrical torque T developed in the induction motor may be estimated from equations 2.1, 2.2 and 2.3 listed in Chapter 2. This torque equals the sum of the load torque and torques due to frictional losses.

Upon detection of speed error, the control strategy calculates T and then estimates from equations 2.1, 2.2 and 2.3 the supply frequency ω_2 at which the induction motor can develop the same gross electrical torque needed to drive the load at the target speed. This assumes that the frictional losses do not change with speed.

Although the estimation of ω_2 assumes that both the load torque and the frictional losses are constant with speed, the control strategy is able to cope with changes with speed of these quantities. This is because changes in frictional losses and changes in load torque with speed will result in the

induction motor running at a speed different to the target speed when the supply frequency changes to ω_2. This difference in speed will result in a new estimate of the load torque and consequently new estimates of and change in supply frequency in an attempt to reduce the speed error. Thus the induction motor speed reaches the target speed iteratively, with each estimation of the load torque at the target speed being better than the last.

6.3 Factors affecting the control strategy

6.3.1 Equipment used to control the drive

The control system was based around an "Apple II" micro-computer which used a speed-measuring circuit and a shaft encoder to measure the speed of the induction motor-D.C. generator set. The Apple II micro-computer used a machine-code programme based upon the control strategy described above and altered the frequency of the three-phase digital oscillator and therefore the frequency of the V.V.V.F. supply according to the requirements of the control strategy. Chapter 3 describes the equipment used in greater detail.

6.3.2 Range of supply frequencies used in the control of the drive

It was decided to study the control of the drive using speeds and supply voltages and frequencies close to those for which the induction motor was designed, since this would avoid possible problems of poor performance due to the induction motor being unsuitable for operation greatly above or below its rated supply voltage or frequency. Accordingly it was decided to study the ability of the control system to maintain a chosen speed whose value was near to 25 revs s^{-1}, the synchronous speed corresponding to a 50Hz supply. Likewise all studies of the control of the drive used a 240v supply - the rated voltage of the induction motor.

The loads used in the study were restricted to a range between zero and rated full load in order to avoid overloading the induction motor.

Manufacturer's data indicated that the speed regulation of the induction motor was 2.33 revs s^{-1} when operating from a 240v 50Hz supply and delivering full load power (250W). Since the induction motor was a four-pole machine, the regulation indicated that the supply frequency needed to increase by about 4.7 Hz in order to maintain the speed at 25 revs s^{-1} while the induction motor delivered full load and operated from a 240v supply. Consequently it was decided to use supply frequencies in the range 50 to 60Hz in order to maintain the speed at 25 revs s^{-1} at all loads used in the study.

This range of frequencies, 10 Hz, was larger than the necessary increase in supply frequency of 4.7Hz indicated by the regulation, in order to provide an adequate margin available for change in frequency. The frequencies available from the three-phase digital oscillator in this range were: 50.3, 51.4, 52.7, 53.9, 55.3, 56.6, 57.9 and 59.8 Hz, giving eight available frequencies. Since all these frequencies were above 50Hz, the three phase digital oscillator maintained constant output voltage at these frequencies.

6.3.3 Range of speeds likely to be met during the control of the drive

The lowest steady-state speed likely to be met using the loads, supply voltages and frequencies described previously corresponds to operation at full load from a 240v 50.3Hz supply and, from equation 4.101 was estimated to be 22.7 revs s^{-1}. Similarly, the highest steady-state speed likely to be met corresponds to unloaded operation at 240v 59.8Hz and was estimated to be 29.9 revs s^{-1}.

6.3.4 The effects of speed measurement resolution

The speed measuring circuit, mentioned in Section 3.10 of Chapter 3 measured the speed of the motor by counting the number of encoder pulses during a 15.5 ms, counting period and expressing this number as an eight-bit number which was sent to the computer. The maximum number of pulses that could be counted was, therefore 255.

The encoder produced 250 pulses per revolution and the maximum speed that could be measured by the speed measuring circuit was that speed that produced 255 pulses in 15.5ms, namely 65.81 revolutions per second. Consequently, the speed measuring circuit was able to measure the speeds likely to be met during the control of the drive.

Since the output of the speed measuring circuit is digital its output must be integer and consequently the resolution of the counting of the output pulses of the encoder is one pulse in the 15.5 ms counting period. Since the encoder produces 250 pulses per revolution, the speed measurement resolution is therefore 0.2581 revs. per second.

Consequently the speed measuring circuit can measure speeds between zero and 65.81 revs per second with a resolution of 0.2581 revs per second. The decimal number corresponding to the eight-bit binary number produced by the speed measuring circuit is called the "speed number" and is denoted by N_S. N_S is the nearest integer given by the expression:

$$N_s = \text{nearest integer to } \left(\frac{\omega_r \, t_m \, N_e}{2\pi} \right) \qquad (6.1)$$

Where:

t_m is the counting period (15.5 ms)

N_e is the number of pulses produced by the encoder (250)

Likewise, the speed corresponding to a particular speed number, N_s is given by rearranging expression 6.1 to yield

$$\omega_r = \frac{2\pi N_s}{t_m \, N_e} \qquad (6.2)$$

6.3.5 Range of speed numbers used in the control strategy

It was decided to design the control strategy to deal with a speed range corresponding to speed numbers between 77 and 116 inclusive. The resulting speed range, 19.87 to 29.94 revs per second was slightly larger than the estimated range of steady-state speeds likely to be met during the control of the drive in order to allow for errors in estimation and the effects of transients.

6.4 The control strategy algorithm

6.4.1 The main stages of the control strategy algorithm

As described in Section 6.2 the aim of the control strategy is to improve the regulation of the induction motor. This is achieved by sensing speed error and altering the supply frequency accordingly. If speed error is present the control strategy estimates the torque developed by the induction motor to drive the load and overcome frictional losses, and then estimates the supply frequency needed for the induction motor to develop the same torque while driving the load at the target speed. The control strategy algorithm divides into three main stages:

1) Detection of speed error.
2) Estimation of the torque developed by the induction motor.
3) Estimation of the supply frequency needed for the induction motor to drive the load at the target speed.

6.4.2 Detection of speed error

The target speed was entered into the computer memory as a corresponding speed number given by expression 6.1. The computer detected speed error by comparing this speed number, call the "target speed number" with the speed number produced by the speed measuring circuit. If speed error was detected the control strategy algorithm acted to reduce the error.

It was possible to arrange for the control strategy algorithm not to respond to speed error below a threshhold value. This facility proved useful in combatting problems due to vibration of the motor generator set affecting the output frequency of the encoder and therefore the speed number produced by the speed measuring circuit.

6.4.3 Estimation of the torque developed by the induction motor

A possible method of estimation would be the real-time calculation based on equations 2.1, 2.2 and 2.3. However such calculation would be slow and would therefore hinder the effectiveness of the control strategy. Instead, the limited number of supply frequencies used in the control of the drive and the limited range of speed numbers likely to be met during the control of the drive suggested an alternative method of estimation, described below:

Each of the eight supply frequencies was represented by a number, called the "frequency number" N_F. For 50.3 Hz, $N_F = 1$, for 51.4 Hz, $N_F = 2$ and so on up to 59.8 Hz, $N_F = 8$. These supply freqencies and the 39 speed numbers in the range 77 to 116 likely to be met gave 312 combinations of supply frequency and speed number. Equations 2.1, 2.2 and 2.3 were used to calculate the torque developed at the speed and the supply frequency corresponding to each combination of supply frequency and speed number. The values of torque so calculated were stored in a look-up table as a matrix with each element having the form $T(N_F, N_S)$ where $T(N_F, N_S)$ is the torque developed when the induction motor operates from a 240v supply having a frequency corresponding to N_F and runs at a speed corresponding to N_S.

The control strategy estimated in the following manner the torque developed by the induction motor when operating from a 240v supply of particular frequency and running at a particular speed. Firstly the computer read the speed number produced by the speed measuring circuit, and secondly, the control strategy algorithm selected the look-up table entry which corresponded to the supply frequency and speed number in question.

If the speed number was lower than 77, the lowest speed number for which entries in the look-up table existed, then the control strategy algorithm chose the entry corresponding to speed number 77 and the supply frequency. This entry was an estimate of the torque developed by the induction motor. Likewise if the speed number was above 116 the entry corresponding to speed number 116 and the supply frequency was selected.

6.4.4 Estimation of the supply fequency needed for the induction motor to drive the load at the target speed

Having found the torque T developed by the induction motor the control strategy algorithm estimated the supply frequency needed for the induction motor to drive the load at the target speed. This was done in the following way:

If N_{ST} is the target speed number then the following entries in the look-up table: T (1, N_{ST}), T(2, N_{ST}), T (3, N_{ST}), T (4, N_{ST}), T (5, N_{ST}), T(6, N_{ST}), T(7, N_{ST}) and T (8, N_{ST}) describe eight possible values of torque produced by the induction motor running at the target speed. The values depend upon the supply frequency corresponding to the entries and the control strategy algorithm estimated the supply frequency needed for the induction motor by finding which of the values is equal or closest to T, the torque being developed by the induction motor at present. When this value had been found the control strategy selected the supply frequency corresponding to the value as the supply frequency needed for the induction motor to drive the load at the target speed.

It is possible that two of the eight possible values of torque described by entries T (1, N_{ST}) to T(8, N_{ST}) would not only be closest to T but would also be equally close to T. In such a case the control strategy algorithm selected the higher of the two frequencies corresponding to the two closest values of torque. The choice between the higher or lower value of frequency was arbitrary.

The possibility of more than two of the eight possible values of torque described by entries T(1,N_{ST}) to T(8, N_{ST}) being equally close to T would not arise since amongst the entries in the look up table, at any given value of N_{ST}, T(N_F, N_{ST}) becomes more positive as N_F increases. This is because increasing values of N_F at a given value of N_{ST} implies operation at increasing supply frequency whilst the speed remains the same, in turn implying increasing slip and therefore torque.

Once the control strategy algorithm had selected the required supply frequency the computer sent the appropriate frequency control number to the three-phase digital oscillator to achieve the required supply frequency.

6.4.5 The language of the control strategy algorithm

In order to achieve a quick response control system the control strategy algorithm was written in the assembly language of the 6502 microprocessor used in the Apple II computer rather than "BASIC" the high-level language available on the Apple II computer. The assembly language used 8-bit arithmetic.

6.4.6 Storage of the entries in the look-up table

The values of induction motor torque at different speeds and supply frequencies are real numbers which may be positive or negative depending on sub - or super-synchronous operation. A look-up table containing such numbers representing induction motor torque at different supply voltages and frequencies would be unsuitable for a control strategy algorithm using 8-bit assembly language because the arithmetic uses positive integers between 0 and 255.

However, the control strategy algorithm bases its selection of a suitable supply frequency upon comparison of the values of induction motor torque relative to one another and not upon absolute values of torque. Consequently if the values of induction motor torque are stored in the look-up table in such a way that the arithmetic difference between any two entries in the look-up table is proportional to the arithmetic difference between the two values of torque which they represent, then selection of the appropriate supply frequency may be based upon entries which are 8-bit numbers suitable for the 8-bit assembly language.

Each value of induction motor torque was converted to an equivalent 8-bit number in the following way:

Of all the values of torque calculated for the different combinations of speed number and supply frequency described previously, the most positive value was represented by 255 and the most negative value by zero. The most positive value of torque occurred at the highest supply frequency (59.8Hz) and at the lowest speed number (77) represented in the look-up table. Likewise, the most negative value of torque occurred at the lowest frequency (50.3Hz) and highest speed number (116) represented in the look up table. In other words, the most positive value of torque was T(8,77) and the most negative value was T(1,116).

Each value of torque $T(N_F, N_{ST})$ was represented by an equivalent integer $T_i(N_F, N_{ST})$ given by the expression:

$$T_i(N_F, N_{ST}) = \text{nearest integer to } \left(\frac{255\,(T(N_F, N_{ST}) - T(1,116))}{T(8,77) - T(1,116)} \right) \qquad (6.3)$$

This relationship ensured that the difference between any two entries in the look up table was proportional to the difference between the two values of torque they represent, subject to small errors due to rounding real numbers up or down to the nearest integer.

Such rounding could affect the selection, described earlier, of supply frequency since it is then more likely that of the eight values of torque selected for comparison with the estimated torque, two such values, though different from each other, would be equally close to the estimated torque. This could result in an incorrect estimate of the supply frequency since, as described previously, the control strategy algorithm would select the higher of the two supply frequencies corresponding to the two closest values of torque.

6.5 Experimental tests of the closed-loop controlled induction motor drive.

6.5.1 The Objective of these tests

The objective of these tests was the study of the closed-loop control of the induction motor drive using the control strategy described previously. In particular these tests studied the stability of the drive and its ability to maintain constant speed regardless of load upon the D.C. generator, provided that the load upon the induction motor did not exceed its rated value (250 watts).

6.5.2 Equipment used in these tests

The drive was constructed as shown in Figure 3.1 with the computer measuring the speed of the motor-generator set using the encoder and the speed-measuring circuit. The computer was connected to the three-phase digital oscillator and a changeover switch allowed control of the output frequency by either the computer or the switches on the front panel of the three-phase digital oscillator. A variable resistance was connected to the armature of the D.C. generator to load the generator. Moving-coil meters measured the phase currents and voltages of the induction motor and also the armature voltage and current of the D.C. generator.

Throughout these tests, chart recordings of speed were made in order to study changes in speed during the test. The method of recording was similar to that described in Chapter 5. As previously mentioned, due to an oversight of the author the graphs of speed against time were not calibrated against readings of speed measured by a frequency counter connected to the encoder. However, the graphs have been calibrated against theoretical estimates of steady-state speed using the theory described in Section 4.8 of Chapter 4.

6.5.3 Experimental procedure

At the start of each test the target speed was entered into the computer in the form of the equivalent speed number, and the control strategy algorithm was started. Only speed numbers in the range 77 to 116, the range for which the control strategy had been designed, were entered.

In order to meet the objective described previously each test comprised the following four stages:

Stage 1 Open-loop control: unloaded operation

The motor-generator set was run with the D.C. generator set unloaded. The changeover switch on the three-phase digital oscillator was set so that the switches on the front of the three-phase digital oscillator controlled the frequency of the V.V.V.F. supply, producing open-loop control of the motor generator set. The supply frequency chosen was that which produced a speed closest to the target speed.

Stage 2 Open-loop control: loaded operation

After the motor-generator set had been running steadily whilst subject to open-loop control and no load, a resistance was connected to the armature of the D.C. generator, loading the generator and causing the motor-generator set to decelerate. The value of the resistance was maintained constant during any particular test.

Stage 3 Closed loop control: loaded operation

After the motor-generator set had been running steadily whilst subject to open loop control and load, the changeover switch on the three-phase digital oscillator was set so that the computer controlled the frequency of the V.V.V.F. supply in response to the speed of the motor generator set and also in response to the control strategy algorithm.

This stage of the test studied the ability of the control strategy to restore the speed of the motor-generator set to the target speed. The effectiveness of the control strategy could be judged by comparing the difference between the speeds obtained during stages 1 and 2 with the difference in speeds obtained during stages 1 and 3 of the test.

Before the final stage of the test, sufficient time was allowed for the control strategy to take effect and for the chart recorder to produce a sufficient record of speed against time.

Stage 4 Closed-loop control: unloaded operation

Without closed-loop speed control, removal of the load upon the D.C. generator would normally cause acceleration of the motor-generator set. This stage of the test involved disconnecting the load upon the D.C. generator and studying the ability of the control strategy to maintain the target speed.

A successful control strategy would produce speeds during stages 3 and 4 that are close to the speed during stage 1.

Test Procedure

Before each test, the motor-generator set was run with open loop control from the V.V.V.F. supply of frequency equal to that which would be used during stage 1 of the test. The load resistance was connected to the armature of the D.C. generator and the load resistance and the excitation of the D.C. generator were adjusted to produce the load required for stage 2 of the test. The load chosen varied between tests but was sufficient to produce a large change of speed between stages 1 and 2 of the test. Such a large change of speed could be more clearly shown by the chart recorder than a small change in speed. More importantly, a large change in speed would be more readily detected and corrected than a small change in speed because of the fairly coarse measurement of speed, 0.258 revs s^{-1}, resulting from the resolution of the encoder and the measuring time of the speed measuring circuit, and the coarse supply frequency adjustment: eight different frequencies spaced about 1Hz apart.

In order to relate graphs of speed against time drawn by the chart recorder to the application and removal of load from the D.C. generator, the lead connecting the load resistance to the armature of the D.C. generator was passed through a current transformer. The output of the current transformer was connected to a spare channel of the chart recorder. The application and

removal of load from the D.C. generator caused a sudden change in current through the lead upon which the current transformer was threaded, and caused a spike in the trace produced by the channel measuring the output of the current transformer. This spike was distinct from the much smaller spikes produced by changes in armature current due to changes in armature voltage resulting from changes in speed during the test.

In the graphs of speed against time produced during each test, the change from open-loop control to closed-loop control was marked by a change in speed which took place some time after the motor-generator set had reached a steady speed in response to open loop control and the application of load to the armature of the D.C. generator.

6.6 The effects of vibration and torsional oscillations upon the closed-loop control of the induction motor drive

6.6.1 The behaviour of the induction motor drive under closed-loop control

When attempts were made to control the drive using the closed-loop control system described earlier the speed of the motor-generator set fluctuated wildly. This occurred during both loaded and unloaded operation of the D.C. generator.

It was suspected that vibration and torsional oscillations similar to those described in Chapters 3 and 5 were responsible for this behaviour as they would cause rapid changes in the speed number produced by the encoder and the speed-measuring circuit. The control strategy would interpret these changes as being due to changes in speed due to changes in load and would alter the supply frequency accordingly, producing changes in speed. Furthermore, the mechanical forces produced by these changes in supply frequency would produce more torsional oscillations, contributing to the problem. The production of torsional oscillations in this manner was noted during the decleration tests described in Chapter 5.

The cause of the problem of fluctuations in speed was confirmed by programming the computer to print successive speed numbers produced by the speed measuring circuit. The wide range of speed numbers produced whilst the motor-generator set ran steadily, supposedly, was comparable to that which would be caused by large changes in load and would therefore certainly affect the operation of the control system.

Further support for the theory that vibration and torsional oscillations were responsible for wild variations in speed during computer control comes from the computer simulation of these tests. The results of these computer simulations will be described later.

In order to avoid possible difficulties in trying to locate and cure the problems of vibration and torsional oscillations it was decided to tackle these problems by using appropriate software methods to minimise the effects of a fluctuating speed number. Two complementary methods were adopted:

6.6.2 Use of an average speed number

This is, perhaps, the most obvious solution to the problem. The speed number tended to vary about a mean value and so the control strategy algorithm was modified so that the speed number used to determine the supply frequency was the average of several successive speed numbers produced by the speed measuring circuit.

However, in order to produce an average speed number that did not vary too greatly for the purpose of the control strategy algorithm, sufficient successive speed numbers had to be read. The time required to do this significantly slowed the response of the control system to changes in speed. For example, sixteen successive speed numbers were insufficient and yet about a quarter of a second was needed to read these numbers, since the speed measuring circuit produced a speed number every 15.5 milliseconds. Consequently another method was also used to tackle the problem of vibration and torsional oscillations.

6.6.3 Use of a dead-band

In order to minimise the effects of fluctuations in the average speed number the control strategy algorithm was modified so that it did not change the supply frequency unless the speed was outside a certain limit called the "dead-band". This was done by comparing the average speed number with the target speed number and attempting to control the speed only if the absolute value of the difference between these two numbers was above a certain limit.

It is apparent that the size of the dead-band affects the accuracy of the final steady-state reached by the control system. Too large a dead-band can result in a large speed error.

6.6.4 The compromise involved in the use of an average speed number and a dead-band

From the preceding discussion it is apparent that the use of an average speed number and a dead-band involves compromise between accuracy

and speed of response of the closed-loop control system. If it is required to produce a quick-acting control system, this can be achieved by using few successive speed numbers to produce the average speed number. However a wide dead-band would be needed to contain the resultant fluctuations in the average speed number, and the accuracy of the closed loop control system would deteriorate. Conversely, if an accurate control system was needed this would require a narrow dead-band but would also require many speed numbers to produce an average speed number that did not vary greatly due to vibration and torsional oscillations. The time needed to produce such an average speed number would slow down the response of the closed-loop control system.

It was found that an acceptable compromise used sixteen successive speed numbers to form an average speed number and also used a dead-band of 3, corresponding to a dead-band of 0.774 revs s^{-1}. However this compromise did not completely eliminate speed fluctuations due to torsional oscillations and vibrations, but did contain these fluctuations within manageable limits.

Accordingly, the computer simulation of these tests also simulated the use of a dead-band and an average speed number to produce an accurate simulation of the tests.

6.7 Computer simulation of the closed-loop control of the induction motor drive

6.7.1 The purpose of the computer simulation

The purpose of the computer simulation was to check whether the problems of instability of the closed-loop controlled induction motor drive were due to vibration causing spurious speed measurement or were caused by an inherent flaw in the control strategy.

6.7.2 The general form of the computer simulation

In order to simulate each test upon the closed-loop controlled induction motor drive, the computer simulation had four parts:

1) The computer simulation of the induction motor drive.
2) The computer simulation of speed measurement
3) The computer simulation of the control strategy algorithm
4) The computer simulation of each of the four stages of a test.

These four parts are described in turn below.

6.7.3 The computer simulation of the induction motor drive

Chapter 5 has shown that the mathematical model developed in Chapter 4 gives a good description of the speed of the motor-generator set during transients and steady-state operation and so this mathematical model was used to simulate the induction motor drive. Consequently the computer simulation was based upon the computer simulation of the acceleration test: both the acceleration test and its computer simulation are described in Chapter 5. The computer simulation of the acceleration test was modified to describe the closed-loop control of the induction motor drive by including subroutines which described the computer simulation of speed measurement, the control strategy algorithm, and the computer simulation of each of the four stages of a test.

The iteration used in the computer simulation of the closed loop control of the induction motor drive used a step length of 0.5ms: the same as that used in the computer simulation of the acceleration test.

6.7.4 The computer simulation of speed measurement

As described previously, the speed-measuring circuit counted the number of encoder pulses during 15.5ms and expressed the result as an 8-bit binary number. This was simulated in the following way:

At intervals of 15.5ms of simulation time the computer calculated the average speed during the past 15.5ms and used equation 6.1 to produce the equivalent speed number. Since the step length of the iteration used in the computer simulation was 0.5 ms, 15.5 ms of simulation time represented 31 steps in the iteration and so the computer calculated the average speed every 15.5 ms by calculating the average of all the speeds reached during the previous 31 steps.

6.7.5 The computer simulation of the control strategy algorithm

The computer simulation of the control strategy algorithm was a subroutine that contained a "translation" of the control strategy algorithm from assembly language to BASIC, the language of the computer simulation. In other words, the computer simulation used the same principles as the control strategy algorithm for detecting speed error, estimating the torque exerted on the induction motor and selecting the supply frequency needed for the motor-generator set to run at the target speed.

The same eight different supply frequencies available for speed control of the induction motor drive were also available for control during the computer simulation, and so the computer simulation included facilities for changing the supply frequency during the simulation to simulate changes in supply frequency. This was achieved by altering . However, Appendix C and Chapter 5 state that during a change in frequency of the three phase digital oscillator, phase continuity is maintained. The simulation of phase continuity during a change in frequency is described in subsection 5.4.2 and equation 5.5. The computer simulation of the control strategy algorithm used a similar method.

The computer simulation of the control strategy algorithm used a look-up table of torque similar to that used in the closed-loop control of the induction motor-drive. A separate subroutine which operated at the start of the computer simulation of the closed-loop control of the induction motor drive calculated the induction motor torque at all combinations of supply frequency and speed numbers that were present in the look-up table used for the closed-loop control. These values of induction motor torque were calculated from the equivalent circuit of the induction motor and were converted to integer numbers between 0 and 255 using equation 6.3. These integer numbers were stored in a manner similar to that used in the look-up table used for closed-loop control. Such calculation, conversion and storage produced a look-up table that was similar to the one used for closed loop control.

6.7.6 The computer simulation of each of the four stages of a test

The four parts of each test are distinguished by the connection or disconnection of load from the armature of the D.C. generator and the change between open- and closed-loop control of the induction motor drive. Table 6.1 lists the conditions of load and of type of control relevant to each stage of a test.

Table 6.1 The conditions of load and type of control relevant to each stage of a test

	Load	
	Disconnected	Connected
Open-loop control	Stage 1	Stage 2
Closed-loop control	Stage 3	Stage 4

Consequently the task of simulating each stage becomes one of simulating the connection and disconnection of load and of simulating changes in types of control according to the table above.

Simulating the connection and disconnection of load.

In the computer simulation, the load upon the armature of the D.C. generator was expressed as the load resistance connected to the armature, and the excitation of the D.C. generator. Both the excitation and the load resistance used in a particular test can be calculated from the steady-stage representation of the induction motor drive, described in Section 4.8 of Chapter 4, and the supply voltage and frequency and the armature voltage and current used in Stage 2 of the test in question. Connection of load was simulated by allowing the computer to use equation 4.86 and equations 4.87 to 4.92 to calculate x_6, the state-space variable representing the armature current of the D.C. generator.

Disconnection of load was simulated by setting x_6 to zero and also ensuring that in the matrices $\underline{K}_1$ to $\underline{K}_5$ (which are the coefficients of the 5th Order Kutta-Merson algorithm), all elements corresponding to x_6 were set to zero and the computer program by-passed equation 4.86. This ensured that the 5th Order Kutta-Merson algorithm proceeded on the basis of no armature current and therefore no load. Reconnection of load was simulated by using equation 4.86 in the computer program and allowing x_6 and the corresponding elements of the coefficients of the 5th Order Kutta-Merson algorithm to reach values calculated by that algorithm.

During the simulation of the connection and disconnection of load, the excitation of the D.C. generator was constant, as was the case during any particular test.

Simulation of the change between open and closed loop control

This was simulated by omitting or including the subroutine which simulated the control strategy algorithm.

6.7.7 Input data required by the computer simulation of the closed loop control of the induction motor drive.

The following data was required: The supply voltage and frequency used during stages 1 and 2 of the test, the excitation of the D.C. generator and the load resistance, the initial conditions, the point-of-wave switching angle and the target speed.

The target speed was entered as an equivalent speed number, described by expression 6.1. The initial conditions were defined by making the state variables x_1 to x_6 equal zero at time t = 0, corresponding to the motor-generator set at rest and isolated from all supplies. The point-of-wave switching angle was set equal to zero at the start of the simulation though, as will be described later, the nature of the simulation allowed any possible value of point-of-wave switching angle.

6.7.8. The order and duration of the simulation of each stage of a test

To achieve an accurate simulation of a test, each stage was simulated in the order in which it occurred in the test and, apart from stages 1 and 2, the simulation time used to simulate a given stage was the same as the duration of that stage during the test. Since stages 1 and 2 correspond to steady state open loop-controlled operation of the drive it was considered unnecessary to simulate these stages for longer than was needed for the computer simulation to reach a steady state. Further simulation time would not have yielded any more useful information about the speed of the motor-generator set during stages 1 and 2. One second of simulation time was allowed for each of stages 1 and 2. The initial conditions used in the computer simulation meant that the simulation of stage 1 included the simulation of the motor-generator set accelerating from rest. The study of this acceleration was not relevant to the study of the closed-loop control system and was therefore ignored, and the steady state speed attained during the simulation of stage 1 was assumed to apply to the whole of the simulation of this stage.

6.7.9 Errors in the look-up table of induction motor torque at different speeds and supply frequencies

A misinterpretation of manufacturers data concerning the induction motor resulted in the look-up table used during the experimental tests of the closed loop control system being based upon incorrect values of R_1, R_2, L_1, L_2

and M, of the induction motor. Table 6.2 compares these values with those based upon data listed in Appendix C.

Table 6.2 Differences in values of elements of the equivalent circuit of the induction motor.

Element	Value based on data in Appendix C	Value used to calculate the look-up table	% difference
R_1	69.13	69.2	0.10
R_2	33.49	33.5	0.03
M	1.264	1.262	0.16
L_1	1.4258	1.295	9.17
L_2	1.3147	1.351	2.76

Although these differences are small, for accurate simulation the values used to calculate the look-up table used in the experimental test were used to calculate the look-up table used in the computer simulation. However, in common with other simulations described in this thesis the mathematical model of the induction motor was based upon the values quoted in Appendix C.

6.8 The experimental conditions of each test

Two tests were performed:

6.8.1 Test 1

The purpose of this test was to study the result of applying a load that would cause a speed error that could be reduced to almost zero by changing the supply frequency to a value within the range of frequencies available to the closed-loop control system (50.3 to 59.6Hz). It was realized that the closed-loop control system was unlikely to achieve zero change in speed because of the coarse frequency control: eight frequencies were available. Consequently some steady-state speed error was anticipated or possibly some "hunting" about a mean value as the closed-loop control system switched between two or more supply frequencies in an attempt to produce an average supply frequency near the value needed for zero speed error.

In this test, the initial supply voltage and frequency were chosen to be 240 volts 50.3Hz and the generator excitation was adjusted to give an armature voltage of 230 volts when unloaded. According to the steady state representation of the induction motor drive, this corresponds to an excitation of 1.4668 volts s rad^{-1} and steady-state speed 24.956 revs s^{-1}. The target speed number used was 95, corresponding to 24.774 revs s^{-1} which was close to the steady state speed of the motor generator set with the D.C. generator excited as described and the induction motor operating from a 240 volts 50.3 Hz supply. Thus the effectiveness of the closed-loop control system could be judged by comparing the speed during closed-loop control with the steady-state speed described above which occurred at the start of the test. The load resistance was adjusted to give an armature current of 1 amp. After allowing for the armature resistance and fall in speed with load, these conditions correspond to a load resistance of 211.5 Ohms, and a steady-state speed of 22.948 rev s^{-1} according to the steady-state representation of the induction motor drive. Under these conditions the load upon the armature of the D.C. generator was 211.5 watts. The speed error resulting from the application of this load was 2.008 revs s^{-1} which, since the induction motor was a four-pole machine could be corrected by an increase in supply frequency of about 4 Hz to 54.3 Hz: within the range of available frequencies. This neglects the slight increase in load with speed caused by the increase in D.C. generator voltage and increase in excitation and fluid friction losses with increasing speed.

6.8.2 Test 2

The purpose of this test was to study the effects of applying a load which would cause a speed error too great to be corrected by the closed-loop control system using the limited range of frequencies available. It was anticipated that the closed-loop control system would respond by selecting the highest available supply frequency in an attempt to achieve the least possible speed error under the circumstances, so reducing but not eliminating the speed error.

Accordingly, the initial supply frequency used was 55.3Hz and the excitation of the D.C. generator was adjusted to give an armature voltage of 245 volts when unloaded. This corresponds to a steady-state speed of 27.415 revs s^{-1} and an excitation of 1.4223 volts s rad^{-1}, according to the steady-state representation of the induction motor drive. The target speed number

used was 106, corresponding to a speed of 27.355 revs s^{-1} and was chosen for reasons similar to those behind the choice of the target speed number used in test 1.

The load resistance was adjusted to produce an armature current of 1.12 amps. According to the steady-state representation of the induction motor drive, these conditions correspond to a load resistance of 195.7 ohms and a steady-state speed of 24.531 revs s^{-1}. Under these circumstances the speed error is 2.824 revs s^{-1} and an increase in supply frequency of about 5.65 Hz to 60.948 Hz would be needed to correct the speed error since the induction motor was a four-pole machine. The required supply frequency is above the range of frequencies available to the closed-loop control system. Again, the slight increase in load with speed has been neglected.

The conditions of each test are summarised in Table 6.3 below:

Table 6.3 Summary of test conditions

Condition	Test 1	Test 2
Initial supply frequency (Hz)	50.300	55.300
Target speed (revs s^{-1})	24.744	27.355
Target speed number	97	106
D.C. generator excitation (volts s rad^{-1})	1.4668	1.4223
D.C. generator load resistance (Ohms)	221.50	195.70
Load upon the D.C. generator during Stage 2 of the test (Watts)	211.50	245.50
Dead band (revs s^{-1})	$\pm$ 0.774	$\pm$ 0.774
Number of speed numbers comprising the average speed number	16	16

6.9 Comparison of experimental results and computer simulations of tests upon the closed-loop controlled induction motor drive.

6.9.1 Experimental results

Figures 6.1 and 6.2 show respectively the results of tests 1 and 2. Each figure compares the experimental results with the computer simulation.

From Figure 6.1 it may be seen that the control system was able to keep the speed of the motor-generator set at or about the target speed of 24.774 revs s^{-1} whilst the D.C. generator was loaded and whilst it was unloaded. The changes in speed during closed-loop control were assumed to result from vibration affecting the measurement of speed used by the control strategy.

From Figure 6.2 it may be seen that the control system was unable to keep the speed of the motor generator set at the target value, 27.355 revs s^{-1}. This was expected as the conditions of the test were designed to see how the control system coped with a load and a target speed that together could not be achieved using the frequencies available to the control system. Whilst the D.C. generator was loaded the control system responded by selecting the highest available frequency, 59.8 Hz, which produced some improvement in the speed error. When the load was removed, the control system attempted to restore the speed of the motor-generator set to the target speed, though such restoration was poor because of the problems of vibration described previously.

6.9.2 Computer simulation of the tests

Figures 6.1 and 6.2 illustrate the results of the computer simulations of tests 1 and 2. These results show that once transients have decayed the speed during closed loop control shows none of the fluctuations caused by vibration. It may therefore be concluded that the control system using a dead-band and average speed number as described would have produced a steady speed but for the problems caused by vibration.

An interesting feature of the graphs of speed against time produced by the experimental results and computer simulations of both tests is the "spike" that occurs immediately after the end of stage 3 when the load is removed from the D.C. generator. This is caused by the sudden increase in speed resulting from the removal of load and the delay in response of the control system resulting from the time taken to take 16 speed measurements and produce their average before correcting the change in speed.

After allowing for the effects of vibration, there is good agreement between the experimental results and the computer simulations of the tests.

Figure 6.1: Closed-loop control test 1: Graphs of speed against time.

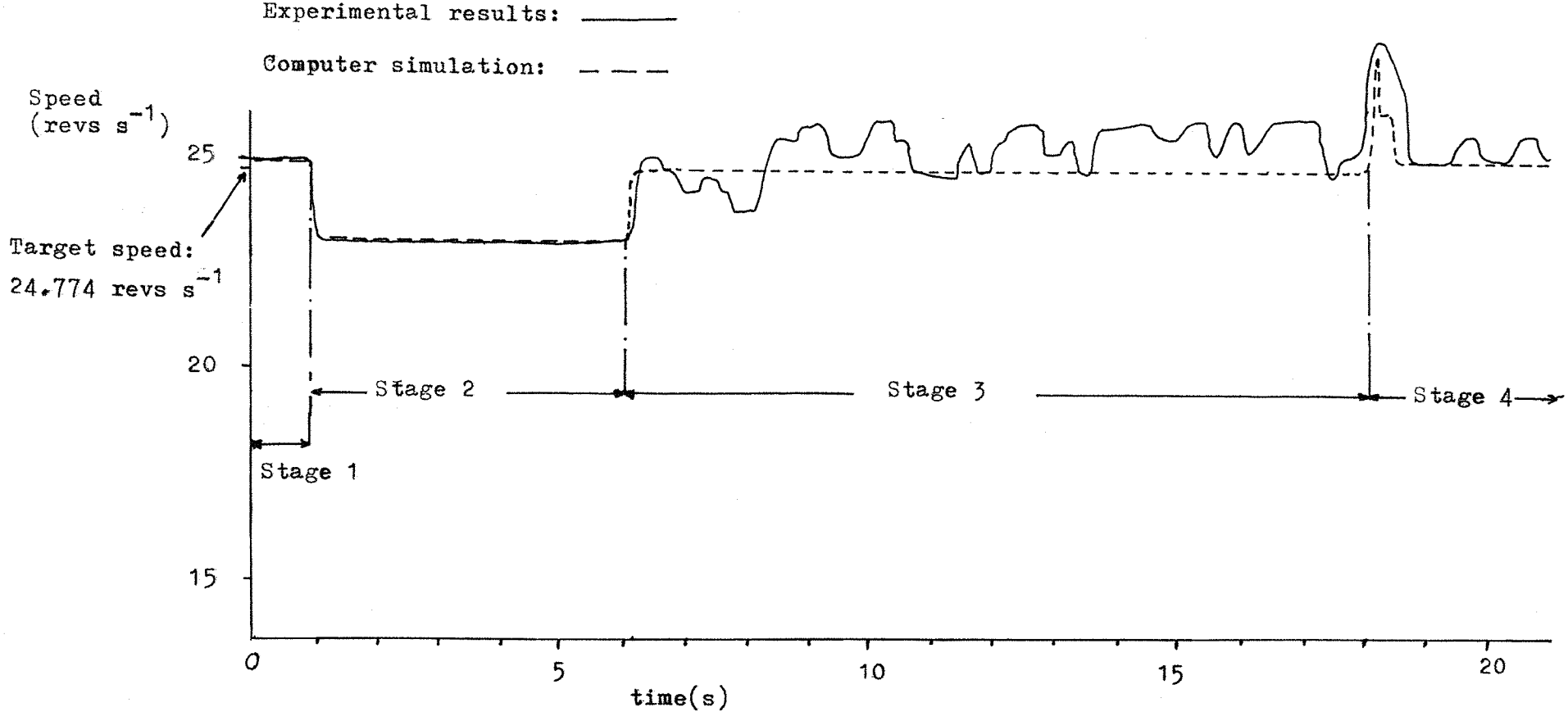

Figure 6.2: Closed-loop control test 2: Graphs of speed against time.

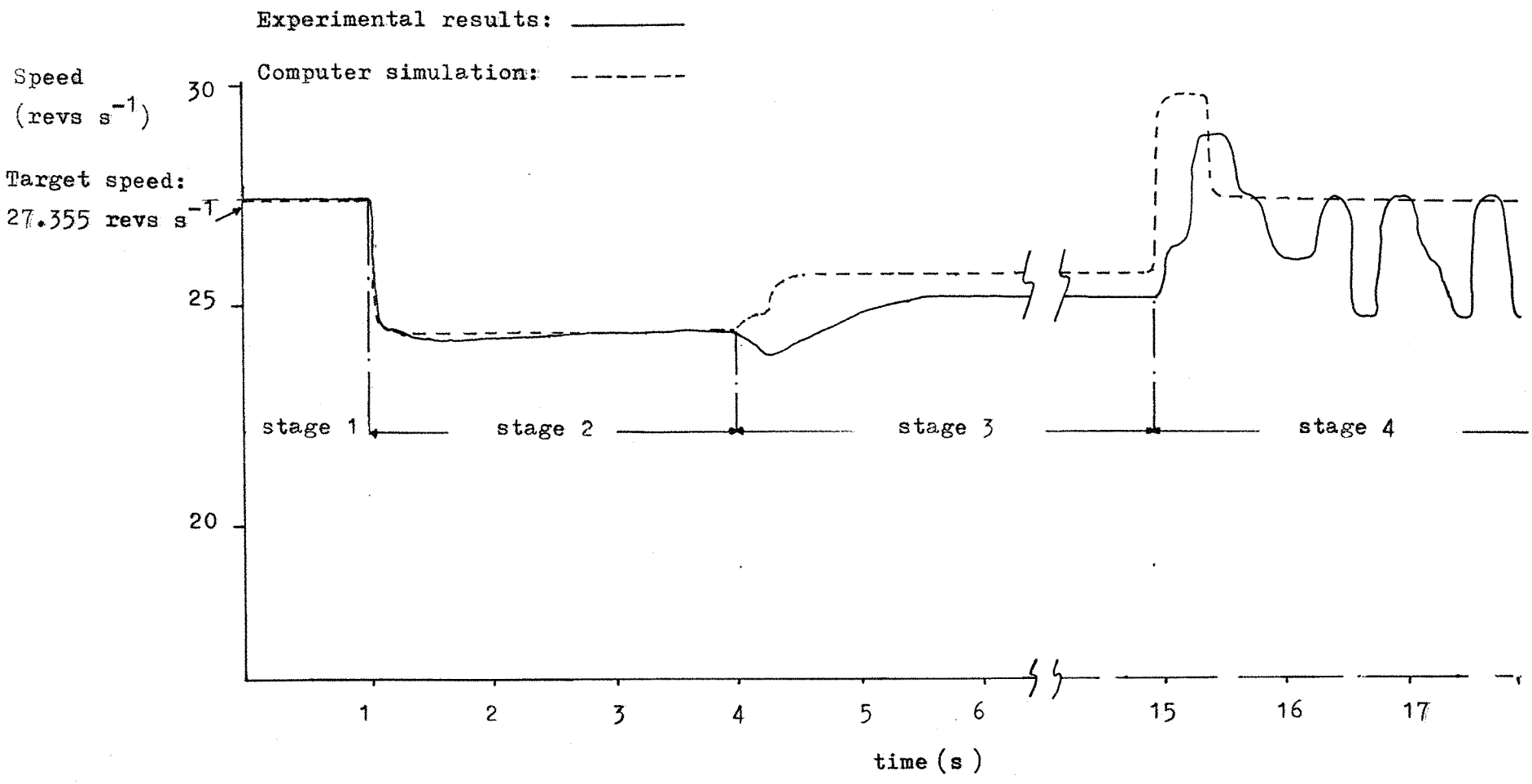

6.9.3 Further study of variations in speed during closed loop control

Although vibration was a likely cause of variations in speed it is possible that there is an inherent characteristic of the control strategy that causes, or at least encourages, variations in speed during closed loop control. Accordingly, the computer simulations of tests 1 and 2 were repeated but without using an average speed number or a dead-band. Each speed number produced during the computer simulation was used individually by the control strategy to control the supply frequency. Figures 6.3 and 6.4 show the results, respectively of such a simulation of tests 1 and 2. These results show that "hunting" can occur during closed loop control and can occur whether or not the D.C. generator was loaded.

A possible explanation of the hunting shown by the computer simulation and of the variation of speed during the test itself were the differences between the parameters upon which the look-up table of torque was based, and the actual parameters of the induction motor was listed in Appendix C. The reason for this difference has been described earlier. Such differences would cause the control strategy to select an unsuitable supply frequency in response to speed error. This in turn would result in the motor generator set not reaching the target speed, causing speed error which the control strategy would attempt to correct in a similar manner, leading to hunting.

Accordingly, this explanation was tested by repeating the computer simulations of tests 1 and 2 and basing both the look-up table and the model of the drive upon the parameters listed in Appendix C. The computer simulations were repeated using the dead band and average speed number described previously and also using neither. However, there was little difference between the results obtained using these simulations and the results described in Figures 6.1 and 6.4. It was therefore concluded that the differences between the parameters used to model the drive and those used to calculate the look-up table were not responsible for the hunting and variations in speed observed.

Another possible explanation of the hunting observed during the computer simulations was the speed of the response of the motor-generator set compared to the time interval between successive speed numbers. This time interval was 15.5 ms, determined by the speed-measuring circuit. Because of the nature of the encoder and the speed-measuring circuit the speed number produced would be proportional to the average speed of the

Figure 6.3: The computer simulation of closed-loop control test 1 (simulating the absence of an average speed number and the absence of a dead-band in the control strategy).

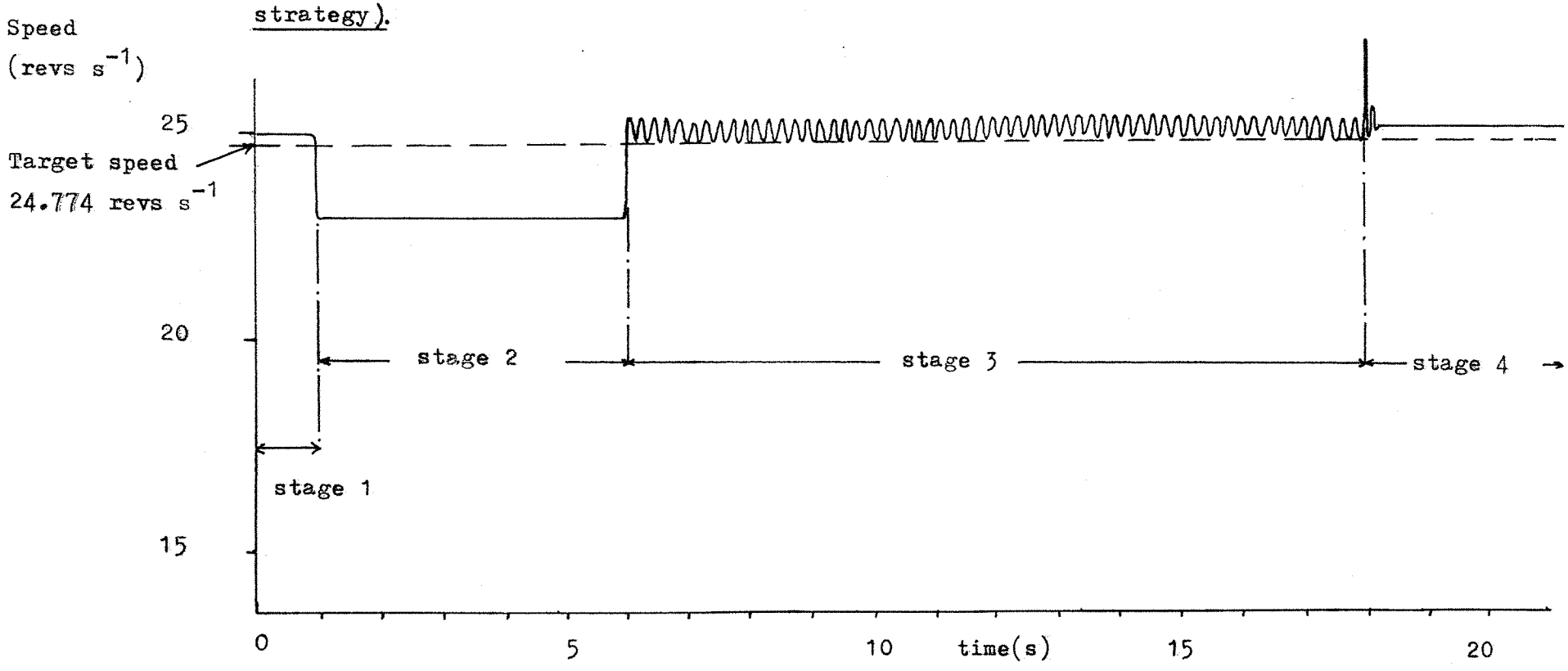

Figure 6.4: The computer simulation of closed-loop control test 2 (simulating the absence of an average speed number and the absence of a dead-band im the control strategy.).

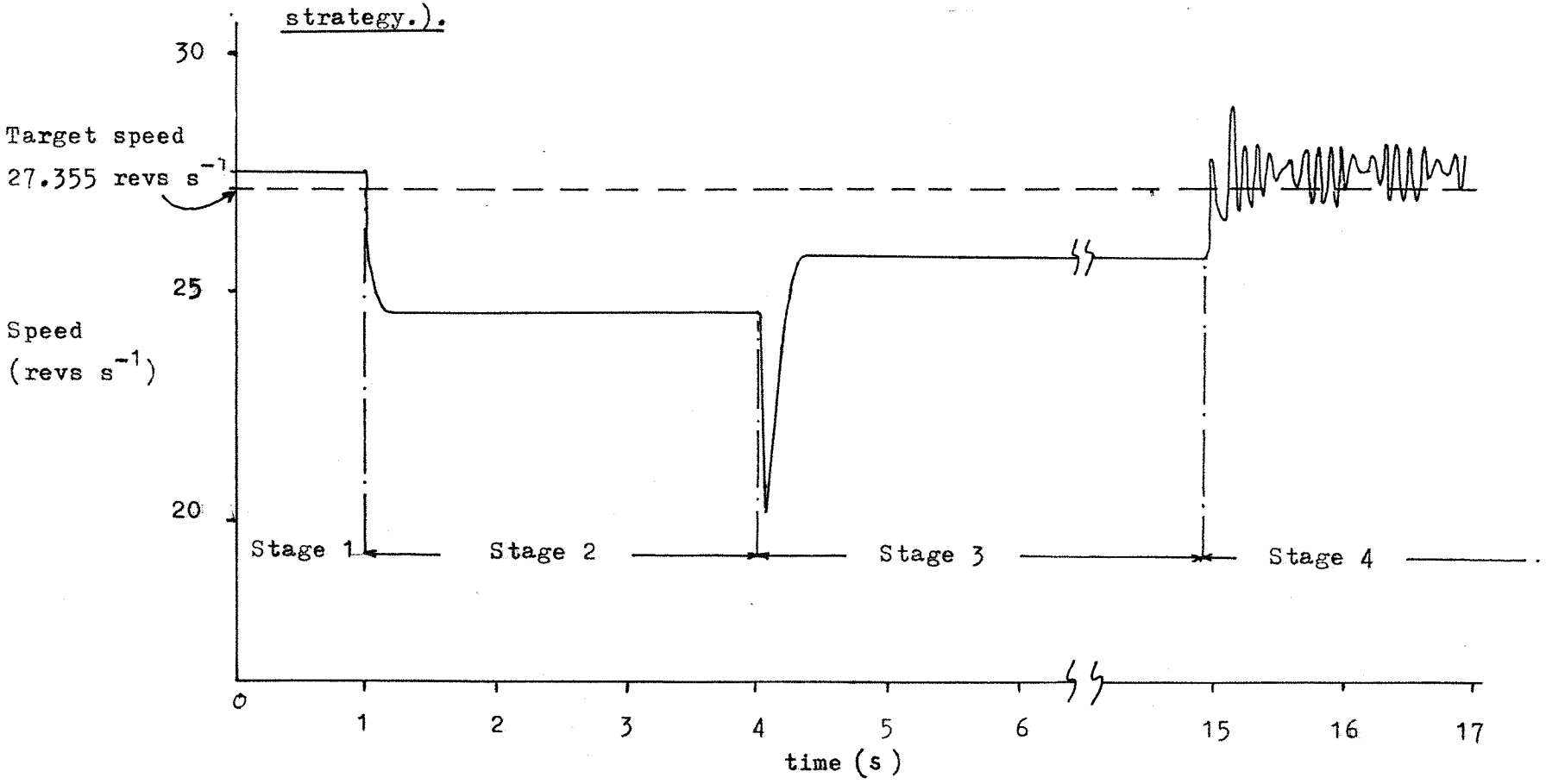

motor-generator set during this 15.5 ms period (this average speed should not be confused with the average speed number described earlier). Consequently even if the motor generator set reaches the target speed at the end of the 15.5 ms time interval, the speed number produced may not equal the target speed number. The control system would respond to the apparent speed error by causing a further change in supply frequency. This behaviour could produce over-correction and account for the hunting observed during the computer simulation.

This explanation was verified by repeating the simulations of tests 1 and 2 with a subroutine that simulated a 10ms delay between the end of one 15.5 ms speed-measuring period and the start of another. No dead-band or average speed number was used and, as in previous simulations, the parameters used to calculate the look-up table in the computer simulation were the same as those used to calculate the look-up table used in the experimental test. The delay allowed more time for the motor-generator set to respond to changes in supply frequency and hunting was eliminated.

It may therefore by concluded that the closed-loop control system is prone to hunting but the small oscillations indicated by the computer simulations are insufficient to account for the large variations in speed observed during experimental tests. It is therefore likely that the main cause of these variations was vibration affecting the value of speed used by the control system, although the tendency of the control system to hunt could contribute to these variations.

6.9.4 Temporary decrease in speed following the application of closed-loop control during test 2.

Figure 6.2 shows a temporary decrease in speed following the application of closed-loop control during test 2. Although this is not featured in the corresponding computer simulation it does feature in Figure 6.4 which shows the results of a similar computer simulation which does not use a dead-band or use an average speed number.

It is likely that this temporary decrease in speed results from an increase in the supply frequency at the start of the closed-loop control. These changes would cause transients which may temporarily affect the torque developed by the induction motor, accounting for the decrease in speed observed. However, this phenomenon was not studied further.

6.10 Conclusions

As stated at the start of this Chapter, the aim of the closed loop control system was to keep the speed of the motor generator set constant at a particular target speed regardless of changes in load provided the load on the induction motor was within the rating of the induction motor.

Computer simulations showed that the control strategy used was viable although some hunting could occur. However experimental tests and further computer simulation showed that the control strategy used was vulnerable to the effects of vibration and torsional oscillations upon the measurement of speed. The problems caused by these effects can be minimised by using an average speed number and a dead-band but at the expense of accuracy and speed of response of the resulting control system. Nevertheless the resulting control system shows an overall tendency to keep the speed of the motor-generator set close to the target speed regardless of changes in load.

6.11 Suggestions for further work on the closed loop control system

6.11.1 Suggested main areas for futher work

These are:-

1) Solving the problems caused by vibration and torsional oscillations
2) Improving the accuracy of speed control
3) Extending the available range of speeds.

6.11.2 Solving the problems caused by vibration and torsional oscillations

Experimental tests upon the computer simulations of the closed-loop control of the induction motor drive have highlighted the problems caused by vibration and torsional oscillations. A solution to these problems is necessary should a similar control system be used to control this or a similar induction motor drive where it may not be possible to eliminate the vibrations or torsional oscillations themselves. Two possible solutions are described below:

1) Suitable design of the encoder and its mounting and coupling so that variations in speed due to torsional oscillations and vibration are damped out.
2) Suitable mathematical operations performed upon the output of the speed-measuring circuit. This chapter has discussed the use of an average speed number and a dead-band and has noted the effects of each upon the accuracy and speed of response of the drive. It is possible that

suitable mathematical treatment of the output of the speed-measuring circuit could solve the problems caused by vibration and torsional oscillations: in other words the problems could be solved by computer software rather than solved by the "hardware" of suitably-designed encoders and couplings.

6.11.3 Improving the accuracy of speed control

The accuracy of speed control is limited ultimately by three main factors : resolution of the encoder and speed measuring circuit, control of supply frequency, and accuracy of the 8-bit arithmetic used by the computer to execute the control strategy. These factors are discussed below:

1) Resolution of the encoder and the speed measuring circuit: As described in Chapter 5 the resolution is equivalent to plus or minus 0.258 revs s^{-1} which imposes a limit of similar size upon the accuracy of speed control. The resolution, and therefore the accuracy may be improved by using an encoder of greater resolution (e.g. a 1000 pulse rev^{-1} encoder instead of the 250 pulse rev^{-1} encoder used) or a longer counting period of the speed-measuring circuit or a combination of both.

2) Control of supply frequency. The frequency of the V.V.V.F. supply was not continuously variable but was limited to eight frequencies spaced about 1 Hz apart. Such coarse frequency control would inevitably lead to coarse frequency control. The solution to this problem would be to design the three-phase digital oscillator so that it produced output frequencies that were spaced closer together.

3) Accuracy of the 8-bit arithmetic used. The accuracy of 8-bit arithmetic is limited to "rounding" errors. These errors were most important in the look-up table in which values of torque were represented as eight bit numbers in which the rounding error, corresponding to changes in the least significant bit, were about $\frac{1}{4}$ per cent. In order to reduce significantly the rounding errors during calculation of the average speed number, 16-bit arithmetic was used. The rest of the control strategy algorithm was based upon comparison between values of torque in the look-up table and therefore involved no further rounding used in the look-up table to represent values of torque.

Therefore, the accuracy of the closed-loop control system could be improved by using 16-bit arithmetic and by using 16-bit numbers in the look-up table.

3) Extending the available range of speeds

As stated at the start of this chapter only a limited range of speeds was considered necessary to study the proposed system of closed-loop control. The range of speeds could be extended by extending the range of frequencies available from the three-phase digital oscillator, subject to the following restrictions: the safe maximum speed of the motor-generator set and the need to reduce the output voltage at low frequencies to avoid magnetic saturation of the induction motor.

However, a greater range of speeds means a greater scope for regeneration during deceleration because of the available change in speed. The deceleration tests described in Chapter 5 show the amplifiers used in the V.V.V.F. supply can cope with limited regeneration, but if any problem is met it may be solved using one or more of the following methods:

1) Temporary disconnection of the induction motor during deceleration until the required speed has been reached.
2) Limiting the value of negative slip of the induction motor so that regeneration is reduced.
3) Modifications of existing amplifiers or use of amplifiers of different design to accommodate regeneration.

CHAPTER 7 CONCLUSIONS

7.1 The objective of the research

The original objective of the research was to produce a variable speed induction motor drive based upon a cage motor and capable of four-quadrant speed control over a wide range of speeds. Owing to the limited time available to complete the research it was not possible to meet this objective. Instead the research concentrated upon producing a variable speed drive based upon a cage motor that was able to maintain a target speed regardless of load provided the load did not exceed the rating of the induction motor. No attempt was made to achieve regeneration or reversal of direction of rotation during closed loop control. The conclusions reached during the research are described below:

7.2 The main parts of the research described in this thesis

The task of developing a variable-speed induction motor drive capable of maintaining a target speed may be divided into three main parts:

1) The development of a variable-speed induction motor drive.
2) The development of a suitable closed-loop control system.
3) The development of a suitable mathematical model of the induction motor drive upon which to base the closed-loop system.

The conclusions reached during each of the above parts are described below:

7.3 The development of the variable speed induction motor drive

Many variable speed induction motor drives use inverters of the switching and filtering type to produce a V.V.V.F. supply for the induction motor to achieve variable speed operation. Such inverters produce harmonics and in order to avoid problems caused by harmonics the V.V.V.F. supply used in the induction motor drive described in this thesis was based upon digital waveform synthesis and linear amplication. The V.V.V.F. supply used a high efficiency waveform and a suitable transformer connection to improve the efficiency of the amplification. The resulting waveform of the V.V.V.F. supply had little distortion and the distortion that was present had no noticeable effect upon the performance of the drive.

Tests upon the drive showed it was capable of operating over a wide range of speeds limited only by the maximum safe speed of the motor-

generator set and the range of frequencies available from the three-phase digital oscillator controlling the V.V.V.F. supply. Within such a range of frequencies, the control of speed is limited by the three phase digital oscillator which produces a large number of discrete frequencies rather than a continuous range. However the output frequencies are very stable since they are derived from a crystal oscillator of excellent stability.

Although no attempt was made to achieve regeneration or reversal of rotation during closed-loop control, tests upon the drive showed that reversal of rotation could be changed by suitable steps in the algorithm used for digital waveform synthesis. This achieved reversal of rotation by reversing the sense of phase rotation of the outputs of the three-phase digital oscillator. Tests also showed the drive to be capable of limited regeneration. It is possible that the use of suitable amplifiers could achieve full regeneration.

It is therefore concluded that the drive described above was a practical and successful way of producing a variable speed drive based upon an induction motor. The drive produced a wide range of speeds in both directions of rotation and was also capable of limited regeneration. It is also concluded that this drive could form the basis of a drive capable of full four-quadrant operation provided it used amplifiers capable of handling regeneration.

7.4 The development of a suitable mathematical model of the induction motor drive

The mathematical model of the induction motor drive was based around Kron's primitive machine. This thesis describes tests used to verify the accuracy of the model. It was concluded that the mathematical model was a good description of the drive under steady-state and transient conditions except for the inability of the mathematical model to describe vibration and torsional oscillations of the motor-generator set. It was therefore concluded that further work intended to improve the mathematical model should concentrate upon modelling vibration and torsional oscillations.

7.5 The development of a suitable closed-loop control system

It was considered that a closed-loop control system based upon the mathematical model described previously would have too slow a speed of response because of the complexity of the mathematical model. Accordingly a closed-loop control system was developed based upon a table of values of torque at different speeds and supply frequencies. These values of torque

were calculated using steady-state analysis. Although the mathematical model was not used in the closed-loop control system it was used successfully to model the closed-loop control system.

Experimental tests upon and computer simulations of the closed-loop control system showed that vibration and torsional oscillations seriously affected the performance of the control system. Suitable modifications to the strategy used in the control system allowed the drive to approach the objective of maintaining a constant speed regardless of load, provided the load did not exceed the rating of the induction motor. Computer simulations showed that the basic principles of the control strategy were sound and that apart from slight hunting under certain conditions the closed-loop control system would have been capable of good speed control.

7.6 Summary

This thesis has described the construction of a variable speed induction motor drive able to operate in forward and reverse over a wide range of speeds, though not under closed-loop control. Although the drive was capable of limited regeneration it was not capable of full four-quadrant control and therefore did not meet the original objectives of the research.

A mathematical model of the induction motor drive has been developed which is a good description of the performance of the drive, although studies have shown that improvements need to be made in order for the mathematical model to describe vibrations and torsional oscillations in the motor-generator set.

This thesis has concluded by describing a closed-loop control system which achieved reasonable speed control of the drive. Studies identified vibration and torsional oscillations as the main limitation to the performance of the control system. A computer simulation of the induction motor drive under closed-loop control was developed and proved useful in analysing the performance of the drive.

CHAPTER 8 SUGGESTIONS FOR FURTHER WORK

Introduction

The research described in this thesis has suggested further work. Such suggestions for further work may be divided into three categories:

1) Improvements to the mathematical model of the induction motor drive.
2) Improvements to the induction motor drive itself.
3) Improvements to the control strategy.

These are described in greater detail below:

8.1 Improvements to the mathematical model of the induction motor drive

A significant improvement could be made by modelling the effects of vibration and torsional oscillations of the motor-generator set. The nature of the vibrations and torsional oscillations could be studied using the following methods:-

1) A load variation test similar to the one described in this thesis. The variation in load excites torsional oscillations.
2) Acceleration and deceleration tests similar to those described in this thesis. The mechanical forces during such changes in speed excite torsional oscillations.
3) Frequency modulation of the V.V.V.F. supply. Such modulation would cause changes in speed which would excite torsional oscillations. A test based on this principle would be an interesting "dual" of the load variation test in which changes in speed result from changes in load rather than supply frequency.
4) Running the motor-generator set at a range of steady speeds in order to study how the vibration was affected by speed.

8.2 Improvements to the induction motor drive

The original objective of this research was to develop an induction motor drive capable of four-quadrant control over a wide range of speeds. In order to meet this objective the following improvements need to be made to the induction motor drive.

1) The drive should be capable of continuous regeneration. This would require modification to or replacement of the existing amplifiers or, alternatively, a method of dissipating regenerated power without damaging the amplifier channels.

2) The drive should be capable of a wide range of speeds. This can be achieved by increasing the range of available frequencies from the three-phase digital oscillator. Appropriate voltage control would be needed at low frequencies to avoid magnetic saturation and it would also be necessary to impose a maximum frequency limit to avoid overspeeding. Good speed control would also require fine control of the output frequency of the three-phase digital oscillator.

8.3 Improvements to the control system

As described above, good speed control requires fine frequency control of the output frequency of the three-phase digital oscillator. Similarly good speed control also requires accurate speed measurement which in turn requires good resolution of the encoder and speed-measuring circuit. The resolution can be improved by using an encoder of greater resolution (i.e. 1000 pulses per second) or a speed measuring circuit which uses a longer time period to count the encoder pulses, or the resolution could be improved by a combination of both methods.

A major problem was that of distinguishing between genuine changes in speed due to changes in load and apparent changes in speed due to vibration and torsional oscillations. The problem can be viewed as separating a wanted "signal" (the change in speed due to change in load) from the unwanted "noise" (the changes in speed due to vibration and torsional oscillations). This separation could be achieved by suitable statistical analysis of the successive speed numbers produced by the speed measuring circuit.

The control strategy described in this thesis was based upon a steady-state representation of the induction motor. It is possible that advances in the speed and power of micro-electronics could allow the development of a real-time control system based upon the mathematical model described in this thesis. Such a control system would be better equipped to cope with transients, especially if the mathematical model could describe vibration and torsional oscillations.

REFERENCES

[1] Converter Propulsion Systems with Three-Phase Induction Motors for Electric Traction Vehicles.
H. Keilgas, R.Nill.
IEEE Transactions on Industry Applications. Vol IA-16 No. 2 March/April 1980. pp 222-233.

[2] An A.C. Electric Drive Vehicle.
E.H. Wakefield.
IEEE Transactions on Industry Applications. Vol IA 10 No. 5 September/October 1974 pp. 544-552.

[3] Energy-Saving Motor Controllers-Background and Update.
L. Holmes.
Electronics and Power March 1982 Vol. 28 No. 3. pp 232-235.

[4] The Choice in A.C. Variable-Speed Drives.
P.D. Shilston.
Electronics and Power October 1981. Vol. 27, No. 10. pp 739-741.

[5] Alternating Current Machines.
M.G. Say.
Pitman.

[6] Electric Machiney (2nd Edition).
A.E. Fitzgerald and C. Kingsley Jr.
Mc Graw-Hill/Kogakusha.

[7] Electromechanics and Machines.
R.E. Steven.
Chapman and Hall.

[8] Electric Machinery.
H. Cotton.
Pitman.

[9] Four Quadrant D.C. Variable-Speed Drives - Design Considerations
G. Joos and T. H. Barton.
Proc. IEEE Vol. 63, No.12 December 1975. pp 1160-1168.

[10] A Variable-Speed Drive that took a Century and a Half to Develop.
R.M. Davies.
Pg 6, Electrical Times May 27th 1983.

[11] Eddy Current Coupling as an Industrial Variable Speed Drive.
D.A. Bloxham and M T Wright.
Proc. IEE Vol 119 No. 8 August 1972. pp 1149-1154.

[12] Adjustable-Speed A.C. Drives - A Technology Status Review.
B.K. Bose.
Proc. IEEE Vol 70 No. 2 February 1982, pp 116-131.

[13] Three-Phase Three-Thyristor Voltage Control Scheme.
E.D. Spooner.
IEEE Transactions on Industry Applications, Vol IA-11 No. 5.
September/October 1975. pp 478- 482.

[14] Induction Motor Speed-Changing by Pole-Amplitude Modulation.
Prof G.H. Rawcliffe, R.F. Burbidge, W.Fong.
Proc. IEE Vol 105A 1958. pp 411-419.

[15] The Development of a New 3:1 Pole-Changing Motor.
Prof G.H. Rawcliffe, B.V. Jayawant.
Proc IEE Vol 103A 1956, pp 306-316.

[16] Recent Developments in A.C. Drive Technology.
E.W.G. Kirk and M.A. Leppard.
Electronics and Power October 1980, pp 805-807.

[17] Analysis and Comparison of Two Types of Square - Wave Inverter Drives.
T.A. Lipo , F.G. Turnbull.
IEEE Transactions on Industrial Applications Vol IA-11 No. 2 March/April 1975, pp 137-147.

[18] Electronics TEC Level IV.
D.C. Green.
Pitman.

[19] G.T.O. Thyristor Device Design.
P.D.Taylor.
Electronics and Power June 1984, Vol 30 No. 6, pp 463-466.

[20] Current Source Converter for A.C. Motor Drives.
K.P. Phillips.
IEEE Transactions on Industry Applications Vol IA-8 No. 6 November/December 1972 pp 679-683.

[21] Optimizing the P.W.M. Waveform of a Thyristor Inverter.
P.H. Nayak and R.G. Hoft.
IEEE Transactions on Industry Applications September/October 1975. pp 526-530.

[22] Control Strategies for P.W.M. Drives.
T.L. Grant and T. H. Barton.
IEEE Transactions on Industry Applications Vol. IA-16 No. 2 March/April 1980, pp 211-215.

[23] Electric Power Systems.
B.M. Weedy.
Wiley.

[24] Inverter-Induction Motor Drive for Transit Cars.
A.B. Plunkett and D.L. Plette.
IEEE Transactions on Industry Applications Vol IA-13 No. 1
January/February 1977 pp 26-37.

[25] Digital Phase-Locked Loop for Induction Motor Speed Control.
R. Moffat, P.C. Sen, R. Younker, M.M. Bayoumi.
IEEE Transactions on Industry Applications Vol IA-15 No. 2
March/April 1979, pp 176-182.

[26] New Methods of Induction Motor Torque Regulation.
A.B. Plunkett, T.A. Lipo.
IEEE Transactions on Industry Applications Vol IA-12 No. 1
January/February 1976, pp 47-55.

[27] Variable Speed Induction Motor Drives use Electronic Slip Calculator Based on Motor Voltages and Currents.
A. Abbondanti and M.B. Brennan.
IEEE Transactions on Industry Applications Vol. IA-11 No. 5
September/October 1975, pp 483-487.

[28] Direct Flux and Torque Regulation in a P.W.M. Inverter-Induction Motor Drive.
A.B. Plunkett.
IEEE Transactions on Industry Applications Vol IA-13 No. 2
March/April 1977. pp 139-146.

[29] Microprocessor Control of an Induction Motor with Flux Regulation.
P.C. Sen, J.C. Tresize, M. Sack.
IEEE Transactions on Industrial Electronics and Control Instrumentation Vol IECI-28 No. 1 February 1981, pp 17-21.

[30] A Microprocessor-Based Phase-Locked Loop Control System of Inverter-Fed Induction Motor Drive [Sic].
F. Harashima and T. Haneyoshi.
IECI '78 Proceedings - Industrial Applications of Microprocessors
March 20-22 1978, pp 187-193.

[31] A Three-Phase Transistor Class B Inverter with Sine-Wave Output and High Efficiency.
K.G. King.
International Conference on Power Semi-Conductors and their Applications. London, England. 3-5th December 1974
(London, England: IEE 1974) pp 20-25.

[32] The General Theory of Alternating Current Machines.
B. Adkins and R.G. Harley.
Science Paperbacks.

APPENDIX A: THE HIGH EFFICIENCY WAVE FORM : A WAY OF IMPROVING THE EFFICIENCY OF CLASS B AMPLIFICATION OF A SINE WAVE

A.1 Class B Amplification

Figure A.1 shows two complementary pair transistors connected in a "push-pull" circuit. The resistance R_{b1} and R_{b2} and diodes Di1 and Di2 correctly bias transistors Tr1 and Tr2 so that Tr1 conducts during the positive half cycle of the input waveform and Tr2 conducts during the negative half cycle. If the diodes are made of the same semiconductor material as the transistors the voltage drop across each forward biased diodes equals the voltage drop across the base-omitter junction of a transistor when it is conducting. Consequently the output voltage across the load follows the input voltage. The voltage of the supply rails limits the output voltage of the push-pull circuit.

This method of amplification is known as "Class B" amplification and results in current gain but not voltage gain.

A.2 The efficiency of Class B amplification

Figure A.2 shows the positive half cycle of a sine wave produced across the load of the push-pull circuit of Figure A.1. The amplitude of the sine wave equals the voltage of the positive supply rail. At points in the cycle when the output voltage is less than the voltage of the positive supply rail, the difference in voltages appears across transistor Tr1 and causes a power loss in that transistor. The shaded area of Figure A.2 represents the voltage drop and power loss. King [31] shows that the maximum efficiency η_B of a Class B amplifier is given by

$$\eta_B = \frac{F_f V_{AC} \cos \phi}{2 V_{DC}} \qquad \text{(A.1.1.)}$$

Where:

V_{AC} is the r.m.s. voltage of the A.C. output waveform.

F_f is the "form factor" of the A.C. output current waveform. The form factor is the average value of the waveform during a half cycle divided by the r.m.s. value. For a sine wave, the form factor is 1.11.

$\cos \phi$ is the power factor of the load.

Figure A.1: "Push - Pull" Circuit used for Class B Amplification.

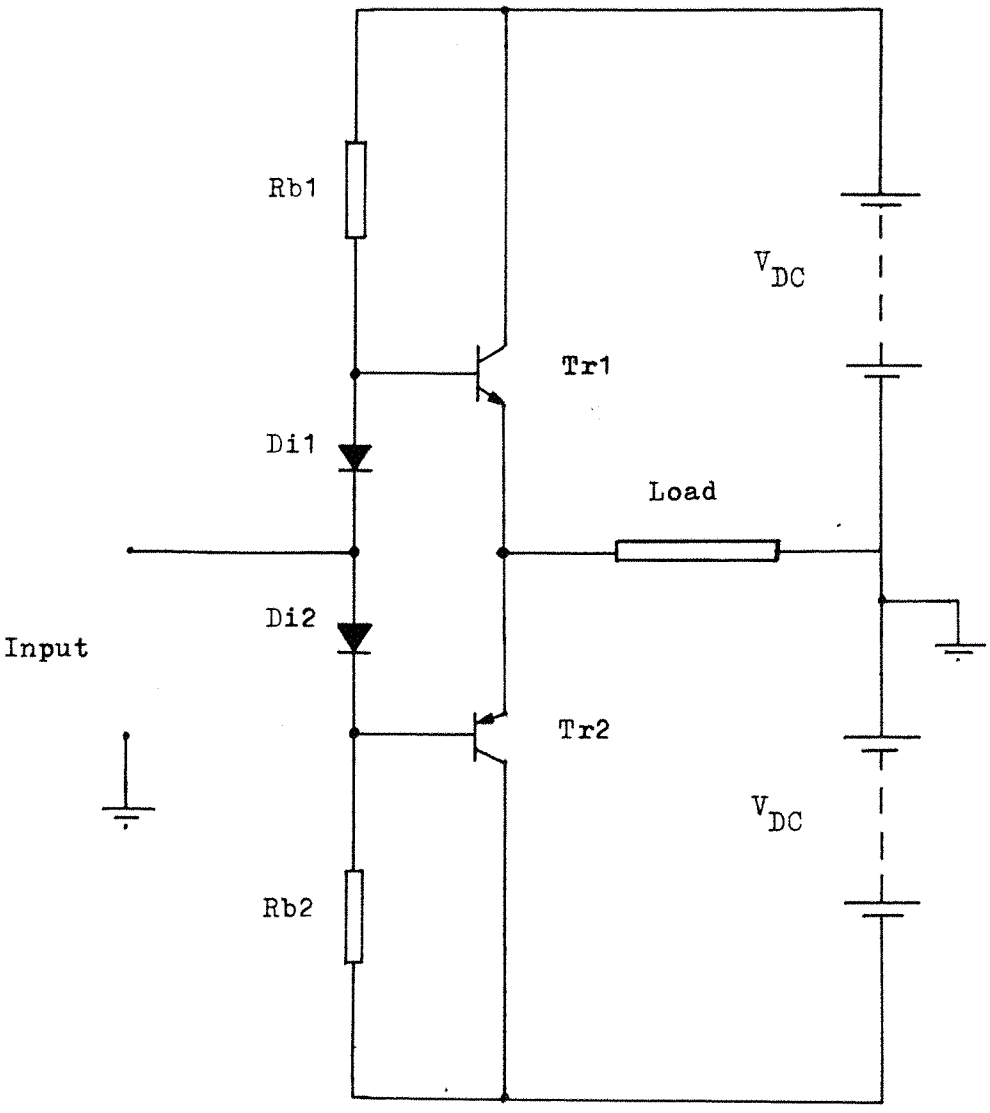

Figure A.2: A graph showing the relationship between the output voltage waveform, the positive D.C. supply rail voltage, and the voltage drop and power loss in Tr1 when the push - pull circuit of Figure A.1 produces a positive half - - cycle of a sinusoidal output voltage waveform whose amplitude equals the positive D.C. supply rail voltage.

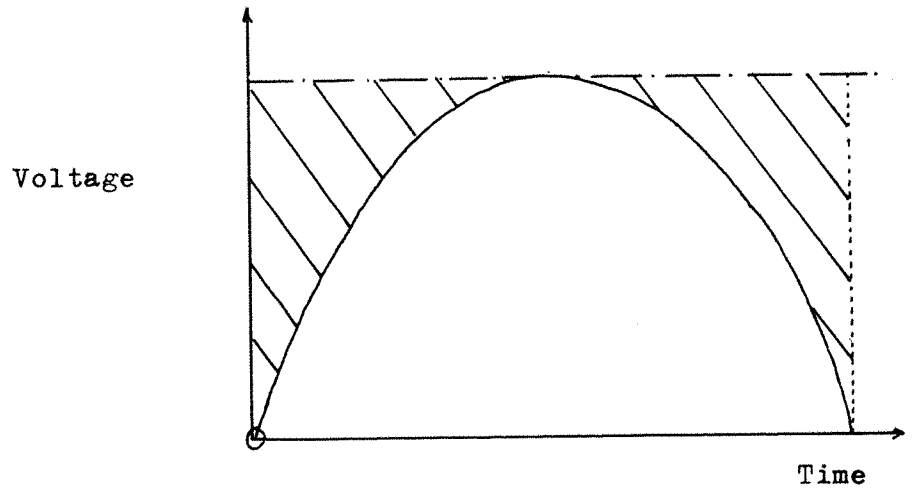

Key:

——— Output voltage.

_.—. Voltage of the positive D.C. supply rail.

 Shaded area representing the voltage drop across Tr1, and the power loss in Tr1.

V_{DC} is the magnitude of the voltage of each supply rail above earth, assuming the magnitudes to be equal.

The maximum theoretical efficiency obtained during Class B, amplification of a sine wave is when its amplitude equals V_{DC}, in other words $\sqrt{2}\ V_{AC} = V_{DC}$. From equation A.1.1 the maximum efficiency on resistive load is 78.5%.

A.3 The efficiency of a Class B amplifier amplifying a sine wave voltage and its third harmonic voltage

King [31] has shown that the efficiency of a three-phase inverter using Class B amplification may be improved by amplifying a special waveform. This waveform contains a sine wave component whose frequency equals the desired output frequency of the inverter, and also a sine wave component which is the third harmonic of the inverter frequency. A suitable output connection removes the third harmonic from the three phase supply to the load.

Figure A.3 shows the effect upon the output voltage waveform of the push-pull circuit when it amplifies a sine wave and its third harmonic. The third harmonic voltage is zero when the fundamental sine wave voltage is zero, and when the fundamental voltage reaches its maximum positive value, the third harmonic voltage reaches its maximum negative value. The third harmonic reduces the amplitude of the output waveform and allows the use of lower supply rail voltages whilst the amplitude of the fundmental component of the output voltage remains the same. Figure A.3 also shows that the change in shape of the output waveform and also the reduction in the D.C. supply rail voltage reduces the voltage drop and power loss in Tr1 and improves the efficiency of the amplification.

King [31] shows that if the amplitude of the third harmonic component of the waveform illustrated in Figure A.3 is $(1 - \frac{\sqrt{3}}{2})$ times the amplitude of the fundamental component then the maximum theoretical efficiency of amplification is 90.8%. This is an improvement on 78.5%, the maximum theoretical efficiency of Class B amplifcation of a sine wave.

In this thesis, the type of waveform which has been described above and which improves the efficiency of Class B amplification is called the "high efficiency" waveform. Appendix B describes the generation of this waveform.

Figure A.3: A graph showing the effect of the amplification by the push-pull circuit of Figure A.1 of a sine-wave and its third harmonic upon the relationship between the output voltage waveform, the positive D.C. supply rail voltage and the voltage drop and power loss in Tr1. The amplitude of the positive half-cycle of the output waveform equals the positive D.C. supply rail voltage.

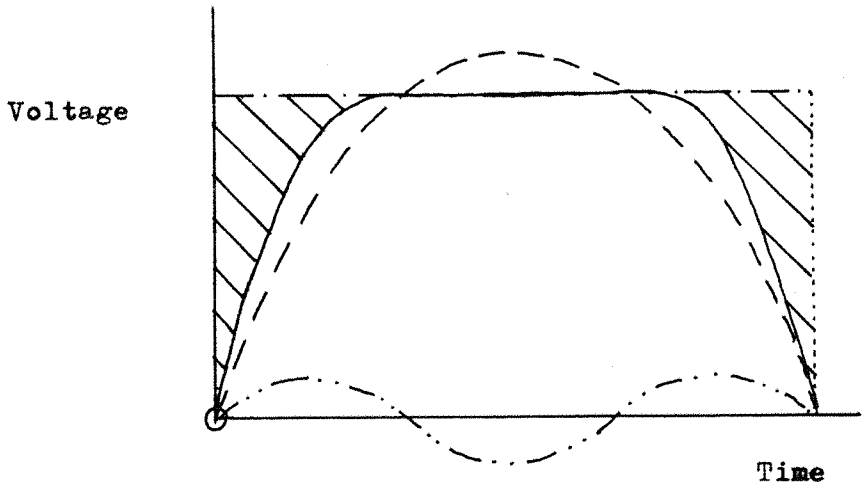

Key:

——— Output voltage.

—.— Voltage of the positive D.C. Supply rail.

— — — Fundamental component of the output waveform.

—..— Third harmonic component of the output wave-form.

 Shaded area representing the voltage drop across Tr1, and the power loss in Tr1.

A.4 Removal of the third harmonic from three phase loads

Although the high efficiency waveform improves the efficiency of class B amplification, many loads require a pure sine wave supply. If three amplifiers use Class B amplification of the high efficiency waveform to produce a three phase supply then a suitable load connection or the use of transformers can prevent the third harmonic component of the high efficiency waveform from affecting the load.

The fundamental components of the phase voltages of a three phase supply are each separated by a 120 degrees phase shift with respect to the other two phases. If the supply contains third harmonic components they will each be separated from the third harmonic components of the other phases by a phase shift three times that separating the fundamental components from each other. Therefore the each third harmonic component will be separated from the others by a 360 degree phase shift, which means they are effectively in phase. Although the phase voltages of a three phase supply main contain third harmonic voltages, the line voltages will not as the third harmonic voltages of each phase are in phase and will cancel each other in the line voltages. Consequently any load connected between two or more phases and disconnected from the neutral will be unaffected by any third harmonic voltage. Such loads include loads connected in delta or isolated star.

The induction motor drive described in Chapter 3 used three single-phase step-up transformers to transform the output of each channel of the power amplifiers to a voltage large enough to drive the motor. Because of reasons discussed in Section 3.8 of Chapter 3 the low voltage windings were connected in earthed star formation across the outputs of the channels. Each amplifier channel produced an output having the high efficiency waveform described previously and each output was separated by a phase shift of 120° from the other outputs to produce a three-phase supply. The earthed star connection caused the amplifiers to apply the high efficiency waveform to the low voltage windings of the transformers which then transformed the high efficiency waveform so that it appeared at the terminals of the high voltage winding. The prescence of the high efficiency waveform at the terminals of the high voltage winding was confirmed using an oscilloscope and a step-down transformer to measure the voltage at those terminals.

The induction motor was connected in isolated star to the terminals of the high voltage winding, and was therefore unaffected by the third harmonic voltages of the high efficiency waveform. Measurements made using

a current transformer and an oscilloscope showed that the motor phase currents were sinusoidal and had the same frequency as the high efficiency waveform.

Consideration of the ampere-turns balance between the primary and secondary windings suggested that the currents in the low voltage windings would be sinusoidal if the motor phase currents were sinusoidal. Measurements made using a current transformer and an oscilloscope showed the currents in the low voltage windings to be almost sinusoidal, but containing a small third harmonic component. The small third harmonic component remained even if the motor was disconnected from the transformers, and was a component of the magnetising current produced in the transformer by the high efficiency waveform.

A.5 Summary

This appendix has descirbed some of the work done by King [31] to improve the efficiency of V.V.V.F. supplies which use Class B linear amplification to produce a three phase supply. This appendix has also described the relevance of King's work to the induction motor drive used in this thesis. The improvement in efficiency results from amplifying a waveform containing both the fundamental and the third harmonic of the desired output frequency of the waveform. Although the phase voltages produced contained third harmonic components the line voltages do not and so a suitable transformer connection used in the induction motor drive prevents the third harmonic components affecting the motor. Appendix B describes the generation of the high efficiency waveform.

APPENDIX B: THE GENERATION OF THE HIGH EFFICIENCY WAVEFORM

B.1 The choice of method of generating the high efficiency waveform

King [31] used a circuit based upon a three-phase bridge rectifier to generate three high efficiency waveforms each separted by a 120° phase shift to serve as inputs to the Class B amplifiers used in each phase of the inverter output. The circuit needed a balanced low voltage three-phase supply at the same frequency as the desired output freqency of the inverter.

The inverter built by King [31] converted a 60 Hz three-phase supply to a 400 Hz three-phase supply and therefore operated at constant output freqency. However the induction motor drive built by the author needed a V.V.V.F. three phase supply to drive the motor at different speeds. Therefore if the analogue circuit used by King was used to generate the high efficiency waveforms for use in the induction motor drive, the circuit would need a V.V.V.F. balanced three-phase low voltage supply to achieve variable speed operation of the motor.

A low voltage V.V.V.F. three-phase oscillator based upon analogue principles could have produced a supply suitable for generation of the high efficiency waveforms. However, it would be difficult to design such an oscillator whose voltage, frequency and phase balance would be stable with time and under all operating conditions. Recent advances made in digital circuitry since King's work [31] in 1974 has meant that many waveforms can be generated digitially and also their voltages and frequencies can be controlled accurately using digital techniques. The technique of generating waveforms digitally is called "digital waveform synthesis".

It was decided to use digital waveform synthesis to generate directly the high efficiency waveforms to be used in the induction motor drive. This method of generation avoided the problems described previously when generating the high efficiency waveforms using analogue principles.

B.2 Digital waveform synthesis

Digital waveform synthesis is based upon D to A (digital to analogue) conversion. D to A conversion converts a binary number to a voltage related to the value of that number. The general principles of digital waveform synthesis suitable for a computer program are described below:

A cycle of the waveform to be synthesised is divided into many equal time intervals. The average voltage during each time interval is represented

by a binary number and these numbers are stored in a table in the memory of the computer. Such a table is called a "look-up" table. The order of the numbers in the look-up table corresponds to the order of the time intervals whose average voltages the numbers represent.

During the computer program used for digital waveform synthesis, the computer reads the first entry in the look-up table. The computer sends this number to the D to A converter which produces a voltage related to the number and equal to the original voltage represented by the number. The computer repeats this procedure with each successive number in the look-up table. When the computer reaches the end of the look-up table it returns to the beginning of the table to start synthesising the next cycle of the waveform.

B.3 Changing the frequency of a digitally-synthesised waveform

This is done by including a time delay between each successive reading of the look-up table. The computer produces a time delay by successively decrementing a number by one and then moving on to the next instruction when zero is reached. The initial value of this number is called the "frequency control number". The time taken to decrement the number by 1 is proportional to the frequency of the clock in the computer. Changing the value of the frequency control number alters the length of the time delay, altering the periodic time and therefore the frequency of the digitally-synthesised waveform.

Because the method uses integer arithmetic it cannot produce a continuous range of freqencies but produces a number of discrete frequencies instead. The periodic time of the waveform is aproximately proportional to the length of the time delay between reading successive entries in the look-up table and therefore approximately proportional to the frequency control number. The frequency of the synthesised waveform is, therefore approximately inversely proportional to the frequency control number, and so this method of waveform synthesis produces frequencies which are closely-spaced at low frequencies but widely-spaced at high frequencies. In other words, the spacing of the frequencies produced varies over the range of possible frequencies.

The frequencies produced are very stable since they depend upon the rate of execution of the computer program. The rate depends upon the

frequency of the computer clock which is normally a crystal oscillator having excellent frequency stability.

B.4 Changing the amplitude of a digitally synthesised waveform

One method of changing the amplitude would be to read each entry in the table, multiply (or divide) that entry, and sent the result to the D to A converter. However, the time taken to perform the necessary arithmetic can seriously lengthen the time taken to produce one output cycle of waveform an can lower the frequency of the highest possible waveform frequency.

A quicker method uses several look-up tables in the memory of the computer, each table containing entries corresponding to a particular waveform amplitude. The computer program produces different waveform amplitudes by consulting different look-up tables. Each look-up table has the same number of entries so that the time taken to read all the entries in the look-up table does not depend upon the look-up table read. Therefore the frequency of the output waveform is independent of the look-up table read.

B.5 The generation of three-phase signals

The methods described in the Appendix can be used to generate three phase signals. Three D to A converters are needed, one for each phase, and in order to save computer memory, the numbers required by each D to A converter are taken from the same look-up table. The correct phase shift between the phases is achieved by reading each set of three numbers needed by the three D to A converters from entries which are spaced one third of a the table apart. This method requires the number of entries in the look-up table to be a multiple of three.

B.6 Reversal of the order of phase rotation of the three phase signals

Reversal of the order of phase rotation of the three phase waveforms used as inputs to the amplifier channels causes reversal of phase rotation of the supply to the motor and reverses its direction of rotation.

Reversal of the order of phase rotation may be achieved by changing over the output of any two D to A converters. The changeover is achieved by supplying one D to A converter involved in the changeover with the numbers originally destined for the other D to A converter involved in the changeover.

B.7 The three-phase digital oscillator

The three phase digital oscillator was designed and built by Mr. D. Levitt and Mr. M. Barkhordar. The oscillator was designed around a microprocessor and was, in effect, a small computer dedicted solely to the task of generating digitally-synthesized three-phase waveforms for use in the induction motor drive. The oscillator used the principles of digital waveform synthesis described earlier, but did not have a phase rotation reversal facility.

Figure 3.2 shows a photograph of the box containing the oscillator and figure 3.3 shows a photograph of the components used in the oscillator. The fifty-pence coin is included in the photograph for size comparison purposes.

The oscillator could produce 64 different frequencies from 8.4 Hz to 240.4 Hz and a frequency control number, described earlier, controlled the frequency of the oscillator. The frequency control number came in binary form either from eight switches on the front of the box containing the oscillator, or from a ribbon cable plugged into the back of the box. An eight-pole change-over switch selected input either from the switches or from the ribbon cable.

The oscillator produced three-phase voltages having the high efficiency waveform described earlier. Each waveform had a 5 volts D.C. offset because of the nature of the D to A conversion used. The A.C. component of the waveforms had a maximum amplitude of 10 volts (peak to peak). The amplitude was not independent of output frequency but varied with it in the manner described in Chapter 3.

The method of digital waveform synthesis used in the oscillator used 90 entries in the look-up table representing the waveform and the D to A converters were capable of a resolution of 39.1 mV. The number of entries and the resolution of the D to A converters produced a synthesised waveform which closely approximated the desired high efficiency waveform, but had a slight ripple. The amplitude of the ripple, however, was small. The frequency of the ripple was high, 90 times that of the frequency of the waveform because 90 entries were used in the look-up tbale. At the high frequency of the ripple (900 Hz for a 10 Hz output waveform) the inductive impedances of the transformers and the induction motor are high and these impedances, together with the small amplitude of the ripple, produced very little effect in the induction motor current. Tests using a current transformer and an oscilloscope showed the motor current to be virtually sinusoidal with very

little ripple. It was concluded that the ripple produced by the digital waveform would not produce any observable effect upon the performance of the induction motor.

B.8 Phase continuity during changes in frequency

The microprocessor read the frequency control number between reading successive entries in the look-up table and used that number as the frequency control number to control the time delay between reading the entries. Consequently any change in the frequency control number caused an immediate change in frequency, whatever the point reached in the reading of the look-up table when the frequency change occurred. The microprocessor was programmed so that it maintained phase continuity of the output waveforms, that is the phase angle of the waveform before the frequency change was the same as that after the frequency change.

B.9 Summary

Digital waveform synthesis is a good method of producing non-sinusoidal waveforms such as the high-efficiency waveforms used in the drive. The method is readily extended to the generation of three-phase signals and offers the following advantages over analogue methods:

1) Excellent frequency stability : equal to that of a crystal oscillator.
2) Good control of output voltages.
3) Accurate phase displacement.
4) Phase reversal may be achieved by arithmetic operations in the computer programme used to generate the phase waveforms rather than by using changeover switches.

The excellent frequency stability, good control of output voltage and good phase displacement result from the accuracy of digital techniques. These techniques are not as readily affected as analogue techniques by drift in the values and tolerances of components. However, the output voltages of the waveforms produced by digital waveform synthesis are affected by drift in the values and the tolerances of the components used in the D to A converters.

Provided that the D to A converters are capable of sufficient resolution and there are sufficient entries in the look-up table which represents the waveform, the currents in the induction motor used in the drive will be virtually sinusoidal and the "step-like" nature of the waveform will not affect the performance of the induction motor.

A disadvantage of this method of waveform synthesis is the limited number of available frequencies and the unequal spacing between the frequencies over the whole range of frequencies.

APPENDIX C THE PARAMETERS RELEVANT TO THE MATHEMATICAL MODEL OF THE INDUCTION MOTOR DRIVE

C.1 The equivalent circuit of the induction motor

The mathematical model developed in Chapter 6 needs the values of the circuit elements of the equivalent circuit of the induction motor. The manufacturers, Brook Crompton Parkinson Motors of Huddersfield, supplied these values which were based upon a mathematical analysis of the design and construction of the motor. These values were checked against values estimated by the author from data gathered from light-running and locked-rotor tests performed upon the induction motor, and measurement of the resistance of the stator winding of the motor. Since the stator winding resistance is likely to change with temperature, the resistance was measured while the machine was still warm from the tests, in order to measure the resistance likely during normal operation of the motor. The resistance was measured using D.C. and the difference between the A.C. and D.C. resistances which results from the skin-effect was neglected.

A common assumption made when calculating the values of elements in the equivalent circuit is to assume that R_1 the per-phase resistance of the stator winding is small enough to be neglected in comparison with the large impedance of the magnetising branch of the equivalent circuit. However, inspection of the data suppied by the manufacturers suggested that R_1 would make a significant contribution to the power losses in the motor during the light-running test. Allowances were made for the losses in R_1 when calculating the elements of the magnetising branch from data obtained during the light-running tests. During the light-running tests the D.C. generator was coupled to the induction motor and ran as a motor to overcome frictional losses in the motor generator set and to make the induction motor run at synchronous speed. This eliminated the effects of frictional losses upon the results of the light-running tests.

The light-running and locked-rotor tests used the V.V.V.F. power supply of the drive and used a supply frequency of 50.2 Hz, the nearest available frequency to 50Hz upon which the manufacturer's data was based. The effects of this difference in frequencies was considered small.

The light running and locked rotor tests were repeated using a supply frequency of 30.2 Hz to see if the values of elements in the equivalent circuit changed with a large change in supply frequency.

Table C.1 below lists values of the elements of the equivalent circuit of the induction motor. The values listed are those obtained from manufacturers data and from light running and locked rotor tests performed at 50.2 Hz and 30.2 Hz.

Table C.1 Values of the elements of the equivalent circuit of the induction motor.

Element	Value		
	Obtained from Manufacturer	Obtained from experimental tests at	
		50.2 Hz	30.2 Hz
R_1	52.88 Ohms	56.2 Ohms	56.2 Ohms
R_2	33.49 Ohms	32.7 Ohms	36.8 Ohms
L_1	1.327 H	1.458 H	1.840 H
L_2	1.315 H	1.458 H	1.840 H
R_m	8891 Ohms	1527.60 Ohms	4755.9 Ohms
M	1.264 H	1.4064 H	1.7775 H

From Table C.1 it may be seen that in the cases of most elements, the data obtained from the manufacturers is in good agreement with that obtained from experimental tests at 50.2 Hz and 30.2 Hz. The large differences in R_m result because of the following reasons:

1) The magnetising losses are the difference between the total power taken by the induction motor during the light-running test and the ohmic losses in the stator winding during the test.
2) During the light-running test the magnetising losses of this induction motor are much smaller than the ohmic losses in the stator winding.

Consequently small errors in measuring the power taken by the induction motor and the ohmic losses in the stator winding can result in large percentage changes in the estimates of the magnetising losses and large changes in R_m.

In table C.1, $L_1 = L_2$ for each set of experimental results. This results from assuming that the leakage reactance of rotor and stator circuits are the same. Steven [7] states this to be a common assumption made when

deriving the equivalent circuit of the induction motor from the light-running and locked-rotor test.

The differences between the manufacturer's data and the data obtained from experimental tests result from the following reasons:

1) The limitations of the equivalent circuit as a representation of the induction motor.
2) Experimental error.
3) Manufacturing tolerances causing the induction motor used in this study to differ from the manufacturer's specifications.

It was decided that the manufacturer's data was likely to be the most reliable and was therefore used in the mathematical model of the induction motor drive.

C.2 The resistance and leakage inductance of the windings of the transformers used in the induction motor drive

These impedances were found from open and short-circuit tests on one transformer and referred to the high voltage windings of the transformers. The tests were performed at 50 Hz and it was assumed that the characteristic of all three transformers were the same. The impedances of the windings referred to the high voltage winding are quoted below:

Resistance of the winding = 13.5 Ω

Leakage inductance of the winding = 98.7 mH.

The turns ratio of the transformers was 6.2. This ratio produced rated induction motor voltage from the maximum amplifier channel voltages at full induction motor load. Allowances were made for the effects of the third harmonic component of the high efficiency waveform, namely that the transformers transformed the fundamental component but blocked the third harmonic component.

C.3 The internal impedances of the amplifier channels

These were estimated from the voltage regulation of an amplifier channel from no load to full load of a channel when subject to an A.C. load test at maximum rated output voltage. The regulation suggested an output impedance of 0.0714 Ω, which equals 2.7 Ω when referred to the high voltage windings of the transformers.

C.4 The resistance and self inductance of the armature of the D.C. generator

The resistance of the armature of the D.C. generator was found by applying a D.C. voltage to the armature and measuring the current through the armature. The resistance varied from 26Ω when the armature was cold to 28Ω when the armature was warm after the generator armature had carried current for a while. The self-inductance of the generator armature was estimated using the following test: A 50 Hz A.C. voltage was applied to the armature and measurements were taken of the current flowing in the armature and the power dissipated in the armature. In such circumstances the armature was assumed to behave as circuit containing the following elements in series:

R_{AG}, the D.C. resistance of the armature

L_{AG}, the self inductance of the generator

r_{mg}, a resistance representing the magnetic losses caused by 50 Hz A.C. flowing in the armature. These losses are different to the magnetic losses produced by rotation of the armature in the magnetic field of the D.C. generator.

The current I_{AG} flowing in the armature winding during this test is given by

$$I_{AG} = \frac{\text{Voltage applied to the winding}}{((R_{AG} + r_{mg})^2 + (\omega L_{AG})^2)^{\frac{1}{2}}} \qquad (C.1)$$

The power dissipated in the armature winding during this test is given by

$$\text{Power dissipated} = I_{AG}^2 (R_{AG} + r_{mg}) \qquad (C.2)$$

It was assumed that the armature remained warm during this test and so $R_{AG} = 28\Omega$. Applying the above equations to the readings of voltage, current and power dissipation in this test yields:

$r_{mg} = 12.63$

$L_{AG} = 0.215H.$

In order to prevent movement of the armature during measurements made to find the resistance and the self-inductance of the armature winding, the generator excitation was turned off.

However, r_{mg} represents the magnetic losses produced in the D.C. generator when 50 Hz flows through the armature. If the armature current is constant D.C., these losses are zero and r_{mg} is also zero. Likewise, if the armature current varies much more slowly than 50 Hz then the magnetic losses produced will be less than those produced by 50Hz A.C. in the armature and they may be neglected and r_{mg} assumed to be zero. During the Swinburne test (described in the next section) or tests involving loading of the D.C. generator, the armature current was either constant or varied at a frequency much less than 50 Hz. Therefore, throughout this study, the effects of magnetic losses caused by changes in armature current were ignored and r_{mg} was assumed to be zero.

To summarise

$R_{AG} = 28.0\ \Omega$

$L_{AG} = 0.215\ H$

r_{mg} assumed to be zero.

C.5 The rotational losses of the motor-generator set

C.5.1 The Swinburne test

A Swinburne test, described by Cotton [8], was performed on the motor-generator set with the D.C. generator operated as a motor. The purpose of this test was to separate the rotational losses into losses caused by bearing and brush friction, losses caused by fluid friction and excitation losses (losses caused by hysterisis and eddy currents in the armature as it rotates in the magnetic field of the D.C. generator). The bearing and brush torque T_b, the fluid friction constant k_{ff}, and the relationship between excitation losses, excitation and shaft speed of the motor-generator set may be found from the separated losses.

The induction motor was switched off and the D.C. generator was run as a D.C. motor. Different field currents were used and different voltages were applied to the armature in order to produce the following speeds : 8, 12, 16, 20, 24, 28 and 32 revolutions per second. Readings of armature voltage and current were taken.

During these tests the mechanical power P_{MG} developed in the armature of the D.C. generator when acting as a motor is given by

$$P_{MG} = V_{AM} I_{AG} - I_{AG}^2 R_{AG} \qquad (C.3)$$

Where V_{AM} is the voltage supplied to the armature of a D.C. generator when acting as a motor.

During the Swinburne test P_{MG} equals the rotational losses as there are no other loads.

The excitation E'_x of the generator acting as a motor is defined as

$$E'_x = \frac{Em}{\omega_r} \tag{C.4}$$

in an analogous manner to the definition of E_x given by equation 4.56. E_m is the back E.M.F. of the D.C. generator when acting as a motor and is given by

$$E_m = V_{AM} - I_{AG} R_{AG} \tag{C.5}$$

C.5.2 Separation of the rotational losses

The rotational losses are power losses due to :

1) Bearing and brush friction torque T_b. The magnitude of this torque is assumed to be constant irrespective of speed.
2) The fluid friction torque T_{ff}. This torque is assumed to be proportional to speed and obeys the equation 4.52 quoted in Chapter 4:

$$T_{ff} = k_{ff} \omega_r \tag{4.52}$$

3) The magnetic losses. Equation 4.53 describes the relationship between the magnetic losses P_{MAG} and ω_r during the Swinburne Test:

$$P_{MAG} = k_{MAG} (\omega_r) \tag{4.53}$$

The rotational losses can be separated by drawing a graph of rotational losses versus excitation at the different speeds used in the Swinburne test. Figure C.1 shows the general form of a graph of rotational losses versus excitation at a particular speed. The solid line represents readings taken during the test and the broken line represents extrapolation from those readings. The graph shows that the rotational losses increase with excitation.

Figure C.1: The Swinburne Test: The General Form of a Graph of Rotational Losses against Excitation for a D.C. Generator operating as a D.C. Motor at Constant Speed.

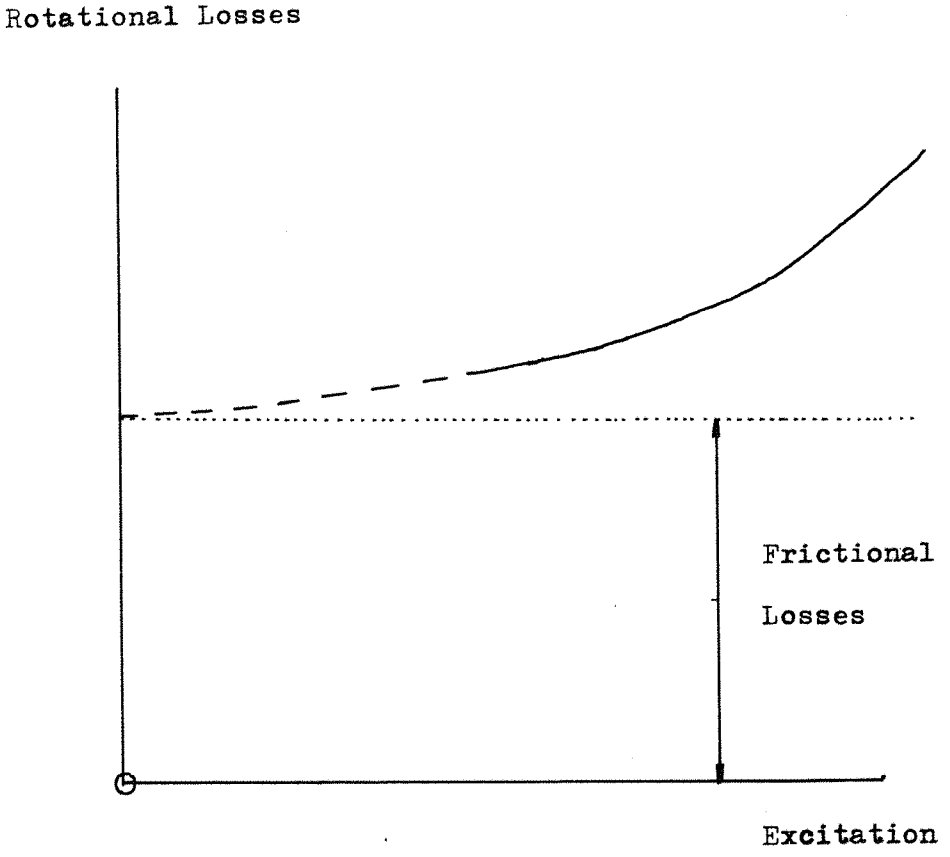

Key:

_____ Curve produced from experimental results

_ _ _ Extrapolation from experimental results

..... Frictional losses

Taking logarithms of both sides of equation C.7 yields

$$\log_{10}(k_{MAG}) = \log_{10}(k_x) + q \log_{10}(E'_x) \qquad (C.8)$$

This relationship suggests that a graph of $\log_{10}(k_{MAG})$ plotted vertically and $\log_{10}(E'_x)$ plotted horizontally will be linear, having a gradient of q and an intercept $\log_{10}(k_x)$ on the $\log_{10}(k_{MAG})$ axis. Such a graph was plotted with E'_x expressed in volts s rad^{-1} and was linear.
The graph gave the following values:
$q = 2.75$
$k_x = 4.37 \times 10^{-3}$

Substituting these values into equations C.7 means that k_{MAG} may be expressed by the following relationship.

$$k_{MAG} = 4.37 \times 10^{-3} (E'_x)^{2.75} \qquad (C.9)$$

The dimensions of k_{MAG} are found from equation 4.53 and are watts second radians^{-}

Although k_{MAG}, k_x and E'_x and the relationships between them have been based on the operation of the D.C. generator as a motor, the definitions of k_{MAG} and k_x are still valid for the D.C. generator operating as a motor since the back e.m.f. of a D.C. motor is produced in the same way as the generated e.m.f. of a D.C. generator. Also the definition of excitation for both types of operation is similar, and therefore k_{MAG} may be defined as

$$k_{MAG} = 4.37 \times 10^{-3} (E_x)^{2.75} \qquad (C.10)$$

where E_x is the excitation of the D.C. generator acting as a generator and is defined in Equation 4.56.

Determination of the dynamic bearing and brush friction torque T_{bd} and the fluid friction constant k_{ff}

The frictional losses found when separating the magnetic and frictional losses from the rotational losses at a particular speed may be converted to an equivalent frictional torque by dividing the frictional losses by the speed in question. The frictional torque T_F is the sum of the bearing and brush friction torque T_b and the fluid friction torque T_{ff}. Therefore, from equation 4.52

Separation of magnetic losses and frictional losses

The intercept of the broken line with the rotational loss axis of the graph in Figure C.1 represents the rotational losses that would be produced if the D.C. generator were able to run as a D.C. motor with no excitation (clearly a ficticious situation). These losses are due to friction alone and are the frictional losses.

The height of the curve of the graph above the dotted line representing the frictional losses represents the magnetic losses at particualar excitations at the speed to which the graph refers. k_{MAG} and γ may be found in the following way:

If logarithms of both sides of equation 4.53 are taken then

$$\log_{10}(P_{MAG}) = \gamma \log_{10}(\omega_r) + \log_{10}(k_{MAG}) \qquad (C.6)$$

This has the form of an equation of a straight line. If a series of graphs of rotational losses versus excitation are plotted for each speed used in the Swinburne test, and the excitation losses at different excitations are found from these graphs, then a graph of $\log_{10}(P_{MAG})$ on the vertical axis and $\log_{10}(\omega_r)$ on the horizontal axis will have a gradient of γ and an intercept of $\log_{10}(k_{MAG})$ on the $\log_{10}(P_{MAG})$ axis.

Such graphs were plotted for the following excitations 4, 5, 6, 7, 8 and 9 volts s rev^{-1} (which correspond to 0.64, 0.80, 0.95, 1.11, 1.27 and 1.43 volts s rad^{-1} respectively). P_{MAG} was measured in watts and in order to preserve consistency with the analysis of Chapter 4 which assumes an induction motor speed measured in radians per second, ω_{AG} was expressed in radians per second. The average value of γ found from the gradients of the graphs was 1.34 and the intercepts of the graphs on their $\log_{10} P_{MAG}$ axes gave values of k_{MAG} for different excitations.

When analysing the induction motor drive using the mathematical model developed in Chapter 4 it would be useful to obtain an expression relating k_{MAG} to the excitation of the D.C. generator. It was assumed that k_{MAG} obeyed the following power law:

$$k_{MAG} = k_x (E'_x)^q \qquad (C.7)$$

where q is an index and k_x is a constant which both describe the relationship between the magnetic loss factor k_{MAG} and E_x, the excitation of the D.C. generator.

$$T_F = T_b + k_{ff}\,\omega_r \qquad (C.11)$$

If values of frictional torque are found for each speed used in the Swinburne test, a graph of frictional torque on the vertical axis and speed on the horizontal axis will, according to equation C.11 have a gradient of k_{ff} and an intercept of T_b on the vertical axis. Such a graph was plotted and was linear (within the limits of experiment error) and gave

$k_{ff} = 2.33 \times 10^{-4}$ Nms rad^{-1}

$T_b = 0.0826$ Nm

As described in section 4.3 of Chapter 4 this value of T_b is also that of T_{bd}, the dynamic bearing and brush frictional torque.

C.6 The moment of inertia of the motor-generator set

The moment of inertia of the motor-generator set was found by running the D.C. generator as a D.C. motor at a speed of 50 revs s^{-1}, and with the induction motor switched off. While the motor-generator set was running at this speed, the supplies to the field and the armature of the D.C. generator were switched off and the time taken for the motor-generator set to come to rest after switching off the supplies was noted. During the deceleration, the frictional torques of the motor generator set slow down the set according to the differential equation.

$$J\,\frac{d\omega_r}{dt} = -(T_b + k_{ff}\,\omega_r) \qquad (C.12)$$

There are no magnetic losses to slow down the machine set as there was no field current during deceleration.

Define

ω_{GD} as the speed of the motor-generator set before the supplies were switched off, and

t_{GD} as the time taken for the motor-generator set to come to rest after the supplies were switched off.

The initial conditions relevant to equation (C.12) are

$$\omega_r = \omega_{GD} \text{ at } t = 0$$

which can be used to solve equation (C.12) to give

$$\omega_r = \left(\left(\frac{T_b}{k_{ff}} + \omega_{GD}\right) e^{-\frac{k_{ff}t}{J}}\right) - \frac{T_b}{k_{ff}} \qquad (C.13)$$

which gives the speed of the motor generator set at any time during the deceleration.

At the instant the motor generator set comes to rest, $\omega_r = 0$ and $t = t_{GD}$. Substituting these values for ω_r and t and rearranging yields the moment of inertia J of the motor-generator set in terms of ω_{GD}, t_{GD}, k_{ff} and T_b:

$$J = \frac{k_{ff}\, t_{GD}}{\ln\left(\frac{T_b + k_{ff}\omega_{GD}}{T_b}\right)} \qquad (C.14)$$

The motor-generator set took 7.5 seconds to decelerate from 50 revolutions per second after all supplies to the D.C. generator were switched off. Therefore ω_{AG} equals 314.16 radians per second and t_{GD} equals 7.5 seconds for this set of results. Substituting these values for ω_{GD} and t_{GD} into equation C.13 gives the following value for J:

Moment of inertia

$J = 1.75 \times 10^{-3}$ kg m^2.

Table C.2 lists the values of the parameters needed by the mathematical model:-

Table C.2 Parameters of the induction motor drive

Elements of the equivalent circuit of the induction motor

R_1	52.88 Ohms
R_2	33.49 Ohms
L_1	1.327 H
L_1	1.315 H
R_m	8891 Ohms
M	1.264 H

The turns ratio, resistance and leakage inductance of the windings of the transformers used in the drive

Resistance	13.5 Ohms
Leakage Inductance	98.7 mH
(Both are referred to the high-voltage winding)	
Turns ratio	6.20

The internal impedance of each amplifier channel

Internal impedance (assumed entirely resistive)	0.0714 Ohms
Internal impedance referred to the high-voltage winding of a transformer used in the drive	2.75 Ohms

The resistance and self-inductance of the armature of the D.C. Generator

R_{AG}	when the armature is cold	26.0 Ohms
R_{AG}	when the armature is warm	28.0 Ohms
L_{AG}		0.215 H

The moment of Inertia of the Motor - Generator Set

J 2.75×10^{-3} kg m^2

Rotational losses of the Motor - Generator Set

Parameters describing these losses

T_{bd}	0.0826 Nm
k_{ff}	2.33×10^{-4} Nms rad^{-1}
γ	1.34
k_x	4.37×10^{-3}
q	2.75

Table C.3 lists the ratings of the induction motor and the D.C. generator.

Table C.3: Ratings of the induction motor and the D.C. Generator

The Induction Motor

Three phase, four pole, rating	=	MCR
Rated supply voltage	=	415 v (corresponding to a phase voltage of 240v)

Rated supply frequency	=	50 Hz
Full load output power	=	0.25 kW
Speed on full load	=	1360 r.p.m.
Full load current	=	0.77 amps
Efficiency at full load	=	57.2%
Power factor at full load	=	0.789

The D.C. generator

Rated output voltage	=	220v
Rated output current	=	0.82 A
Full load efficiency	=	70%
Rated Speed	=	1400 r.p.m.

C.7 Conclusions

The mathematical model of the induction motor drive needs the values of certain parameters of equipment in the drive. This Appendix has described tests which may be readily performed in order to obtain these values, and has also described the underlying mathematical principles of the tests.